REFERENCE ONLY

UNIVERSITY OF LONDON THESIS

Degree PhD Year 2006 Name of Author FRIEDMANN, B-J

Modulation of Chemotherapy by Inhibition of the Epidermal Growth Factor Receptor

by

Benjamin Jacob Friedmann

A thesis submitted to the University of London for the degree of Doctor of Philosophy

November 2005

Department of Oncology
Royal Free and University College Medical School
University College London
91 Riding House Street, London W1W 7BS

ProQuest LLC
789 East Eisenhower Parkway
P.O. Box 1346
Ann Arbor, MI 48106-1346

To my parents, who will always guide me

and

To Dina, who will always inspire me

ABSTRACT

Purpose The epidermal growth factor receptor (EGFR) is commonly expressed in human tumours and provides an important target for therapy. Several classes of agents including small molecule inhibitors and antibodies are currently under clinical development. These agents have shown interaction with chemotherapeutic agents *in vitro* and *in vivo*. However, the mechanisms of these interactions are not clearly understood. The purpose of this study was to investigate mechanisms for this modulation.

Experimental Design The synergistic effects of the EGFR inhibitor gefitinib (Iressa^{TM}, ZD1839) in combination with a variety of chemotherapeutic agents was determined in several cancer cell lines and analysed pharmacologically. Using the alkaline single-cell gel electrophoresis (comet) assay, the kinetics of DNA damage and repair following treatment with the chemotherapeutic drugs combined with gefitinib were investigated. The modulation of DNA-PK activity by gefitinib was quantitated using a variety of techniques including immunoprecipitations, immunoblotting, cellular fraction extractions and immunohistochemistry. The effects of inhibiting the DNA repair protein DNA-PK, with LY294002, wortmannin and siRNA to its catalytic subunit (DNA-PK$_{CS}$) were investigated in the same cancer cell lines and compared with the effects of gefitinib.

Results Synergistic effects of EGFR inhibitors and chemotherapy were found with a variety of cell lines. The synergy was found with etoposide, doxorubicin and cisplatin but interestingly not with melphalan. Experiments on DNA repair using the comet assay demonstrated delay in repair of DNA strand breaks and inter-strand cross-links (ICLs) by gefitinib following treatment with etoposide and cisplatin respectively. The mechanism of this interaction was investigated and found that interference with the DNA-PK pathway mimicked the effects of EGFR inhibition. Additionally, gefitinib treatment induced a physical interaction between EGFR and DNA-PK and a cellular re-distribution of DNA-PK was associated with a fall in DNA-PK activity.

Conclusions These results highlight the important effects EGFR inhibitors have on DNA repair and its associated machinery when added in combination with certain chemotherapeutic agents. These results will form the design of further clinical schedules combining these classes of agents and point the way to further studies to investigate the molecular mechanisms of these interactions.

ACKNOWLEDGEMENTS

The work carried out in this thesis was completed under the supervision of Dr Daniel Hochhauser and Professor John Hartley at the Department of Oncology, UCL and was generously funded by the 'Quiet Cancer Appeal' of The Times Newspaper.

First and foremost I would like to thank Daniel for all his help, guidance and encouragement and for giving me the opportunity to parasite off his great and creative mind. Above all, I would like to thank him for being a great friend – long may it continue.

Thank you to John for all his incisive contributions, for letting me pick his brain regularly and for ensuring a level of normality when his abovementioned colleague ventured frequently into a world of stupidity. Thank you also to Dr Martyn Caplin for his additional supervision and mentoring.

I am immensely indebted to a number of great allies in the lab. A special thank you to Dr Minal Kotecha for all her help and advice along the way and for her superb proofreading skills. The immunohistochemistry experiments were carried out by Dr Tahir Shah, for which I am eternally grateful. Thank you also to Boris Savic for his assistance with experiments during the final few months.

Life in the lab would not have been the same without Ali Hazrati. He has been a superb colleague and will always be a very special friend.

I am deeply grateful to my family and in particular my parents, Rachel and Michael, who have, as usual, been a tower of strength, warmth and support.

Finally and above all, I would like to thank my utterly devoted wife, Dina. There are no words to explain how much I love you. I would not have been able to complete this thesis without your encouragement, support and most importantly, your patience. You are my inspiration, my rock and my soul mate.

COMMUNICATIONS

PRESENTATIONS

September 2005: Ludwig Institute for Cancer Research – Modulation of chemotherapy by inhibition of the epidermal growth factor receptor.

PUBLICATIONS

Friedmann B, Caplin M, Hartley J, Hochhauser D. Modulation of DNA repair *in vitro* after treatment with chemotherapeutic agents by the epidermal growth factor receptor inhibitor gefitinib (Iressa™, ZD1839). *Clin Cancer Res.* 2004 Oct 1; 10 (19): 6476-86.

Friedmann BJ, Caplin M, Shah T, Savic B, Lord CJ, Ashworth A, Hartley JA, Hochhauser D. Interaction of the epidermal growth factor receptor and the DNA-dependent protein kinase pathway following gefitinib treatment. *Mol Cancer Ther.* 2005 Submitted.

Friedmann B, Caplin M, Hartley J, Hochhauser D. *Proc. Mol Targets & Cancer Ther, AACR, Boston MA.* 2003 Nov. A104: 75.

Friedmann B, Caplin M, Hartley J, Hochhauser D. *Proc. ISC Conference, Florence.* 2004 Feb.

Friedmann BJ, Savic B, Caplin M, Hartley JA, Hochhauser D. *Proc. Genes & Cancer Conference, Warwick.* 2004 Dec. C7: 52.

Kotecha MT, **Friedmann BJ**, Morris P, Henry JA, Le NM, Price C, Lee M, Hartley JA, Hochhauser D. *Proc. NCRI Cancer Conference.* 2005 Oct. P179: 94.

Friedmann BJ, Caplin M, Savic B, Lord CJ, Ashworth A, Hartley J, Hochhauser D. *Proc. NCRI Cancer Conference.* 2005 Oct. P363: 186.

TABLE OF CONTENTS

INDEX OF FIGURES

INDEX OF TABLES

ABBREVIATIONS

5-FU	5-Fluorouracil
ATP	Adenosine Triphosphate
BER	Base Excision Repair
BSA	Bovine Serum Albumin
CDK	Cyclin-Dependent Kinase
CHO	Chinese Hamster Ovary
cHCl	concentrated Hydrochloric Acid
CML	Chronic Myelogenous Leukaemia
DHFR	Dihydrofolate Reductase
DMSO	Dimethylsulphoxide
DNA	Deoxyribonucleic Acid
DNA-PK	DNA Protein Kinase
DNA-PK_{CS}	DNA Protein Kinase Catalytic Subunit
DSB	Double Strand Break
DTT	Dithiothreitol
ECACC	European Collection of Cell Cultures
ECL	Enhanced Chemoilluminescence
EDTA	Ethylenediaminesulphate Tetra-acetic acid
EGF	Epidermal Growth Factor
EGFR	Epidermal Growth Factor Receptor
EtBr	Ethidium Bromide
FACS	Fluorescent activated cell sorting
FCS	Foetal Calf Serum
FITC	Fluorescein Iothiocyanate
HR	Homologous Recombination
ICL	Interstrand Crosslink
IGEPAL	(octylphenoxy) Polyethoxyethanol
IMS	Industrial methylated spirit
kDa	kiloDaltons
MAb	Monoclonal antibody
MAPK	Mitogen Activated Protein Kinase
MDM2	Murine double minute chromosome number 2

MMR	Mismatch Repair
MOPS	(3-[N-morpholino]) propanesulfonic acid
NER	Nucleotide Excision Repair
NHEJ	Non-Homologous End Joining
NSCLC	Non Small Cell Lung Cancer
OD	Optical Density
OTK	Oncogenic Tyrosine Kinase
PBS	Phosphate Buffered Saline
PCR	Polymerase Chain Reaction
PI	Propidium Iodide
PI3K	Phosphatidylinositol 3-Kinase
PKC	Protein Kinase C
ROS	Reactive Oxygen Species
PS	Phosphatidyl Serine
RT	Room Temperature
RTK	Receptor Tyrosine Kinase
SCCHN	Squamous Cell Carcinoma of the Head and Neck
SDS	Sodium Dodecylsulphate
SRB	Sulphorhodamine B
SSB	Single Strand Break
STAT	Signal Transducer and Activator of Transcription
TBE	Tris-borate-EDTA
TBS	Tris buffered saline
TBS-T	Tris buffered saline Tween
TCR	Transcription Coupled Repair
TE	Tris-EDTA
TEMED	Tetramethylethylenediamine
TKI	Tyrosine Kinase Inhibitor
TM	Tail Moment
UCL	University College London
UK	United Kingdom
UV	Ultra Violet
VEGF	Vascular Endothelial Growth Factor

CHAPTER 1

INTRODUCTION

1.1 Cancer

Cancer is a disease involving dynamic changes in the human genome. The molecular basis of cancer involves mutations which produce oncogenes with dominant gain of function and tumour suppressor genes with recessive loss of function. Mutations vary from specific point mutations to alterations in whole chromosomes; these differences can affect the genes governing the normal regulatory mechanisms of cell growth and proliferation (Vogelstein & Kinzler, 1993). Uncontrolled cell proliferation or inefficient mechanisms of programmed cell death can result in tumour growth. There are well over 200 different forms of tumour subtypes arising in different organs.

As summarised by Hanahan & Weinberg, (2000), the vast majority of malignant tumours can be identified by six fundamental changes; self-sufficient growth signals, insensitivity to anti-growth signals, evading programmed cell death (apoptosis), limitless replicating potential (immortality), sustained angiogenesis and tissue invasion and metastasis. These characteristics can be acquired during the course of tumour development through a series of genetic changes culminating in the uncontrolled and eventual malignant transformation of a clonal cell population. This multi-step process initiating from a normal cell population, develops through a series of pre-cancerous lesions into a metastatic tumour.

Once transformed, a malignant tumour can become invasive and can spread into surrounding tissue. In some cases cancerous cells migrate away from the primary tumour often via the lymphatic system. These micro-metastases can attach to new tissue elsewhere in the body and can form secondary tumours (Hanahan & Weinberg, 2000).

1.1.1 Incidence and Mortality

Each year more than a quarter of a million people are newly diagnosed with cancer in the UK. Overall it is estimated that more than one in three people will develop some form of cancer during their lifetime. Of the different types of cancer, four of them - breast, lung, large bowel (colorectal) and prostate - account for over half of all new cases. Breast cancer is the most common cancer in the UK despite the fact that it is rare in men. The latest available mortality statistics for the United Kingdom (UK) are for 2002. In that year 155,180 people were registered as dying from a malignant neoplasm. Cancer is the cause of approximately a quarter of all deaths in the UK of which over one fifth (22%) are caused by lung cancer. Colorectal cancer was the second most common

cause of death from cancer (10%). Although breast cancer is very rare in men, high rates among women place it as the third most common cause of death from cancer in all persons (8%).

1.2 Chemotherapy

The systematic treatment of cancer has become an important part of cancer management. In some uncommon tumours such as childhood cancers, lymphomas and teratomas, great progress has been made with the use of cytotoxic drugs. In other more common tumours such as lung and pancreatic carcinoma, the results have been less impressive, although modest improvements in survival have been obtained with chemotherapy and endocrine therapy in breast and colorectal cancer (DeVita *et al.*, 2005).

Most anti-cancer agents serve to inhibit tumour cell growth and division although there is considerable potential for the development of agents which affect invasion, vascularisation and metastasis. Cytotoxic agents can reduce tumour cell growth and division by binding to DNA bases or impairing DNA synthesis to inhibit DNA replication, by damaging the mechanisms of cell division, or by blocking the pathways involved in cell growth.

To review all the chemotherapeutic agents is beyond the scope of this discussion. However, some of the key agents used in this study are outlined in detail below.

1.2.1 Antimetabolites

These can be divided into four classes; folate antagonists, pyrimidine analogues, purine analogues and sugar-modified analogues. They all interfere with the production of nucleic acids by inhibiting specific enzymes needed for nucleoside triphosphate synthesis or substituting for normal purine or pyrimidine bases. They are usually cell cycle dependent.

Folate antagonists include the folic acid analogue methotrexate, an indirect inhibitor of thymidine nucleotide production. It does this by competitively inhibiting dihydrofolate reductase (DHFR), a key enzyme of the pathway and so RNA and protein synthesis is inhibited during G_1 to S phase.

Pyrimidine analogues are incorporated into nucleic acids and directly inhibit thymidine nucleotide production. An example is 5-Fluorouracil (5-FU) which contains a fluorine

atom in place of hydrogen on a uracil molecule. Its incorporation into RNA inhibits processing of rRNA and mRNA and subsequent transcription errors. 5-FU can also irreversibly inhibit thymidylate synthase which is needed for DNA synthesis. It has activity against adenocarcinoma of the gut, breast and ovary, but responses are infrequent and can be transient. In colorectal cancer, 5-FU can be used as adjuvant therapy alone or in combination with folinic acid (DeVita *et al.*, 2005). The sugar-modified analogue cytabarine is a sugar moiety altered analogue of cytidine and is a substrate for DNA polymerases thus altering DNA function killing cells in S phase. It is mainly used against acute myeloblastic leukaemia (AML) as well as in acute lymphoblastic leukaemia (ALL) and poor prognosis lymphomas.

There are several cytotoxic agents which are analogues of natural purine bases or nucleotides. These include 6-Mercaptopurine and thioguanine which are derivates of hypoxanthine and guanine respectively. They contain a thiol group (-SH) in place of a hydroxyl group (-OH), inhibit purine nucleotide synthesis and are incorporated into nucleic acids themselves.

1.2.2 Mitotic Inhibitors

Microtubule inhibitor drugs work by disrupting the equilibrium between polymerised and free tubule dimers. They include the vinca alkaloids (vinblastine, vincristine) which bind and inhibit microtubule and mitotic spindle formation thus arresting cells in metaphase. They are used in combination with prednisone for Hodgkins disease and childhood leukaemia. Taxanes such as paclitaxel (Taxol) stabilise microtubules and allow for abnormal bundles to form. It is effective against carcinomas of breast, lung, head and neck and is also used in combination with cisplatin.

1.2.3 DNA-Interactive Chemotherapeutic Agents

Anti-cancer agents that target DNA both directly and indirectly are some of the most effective agents in clinical use. They have increased the survival of cancer patients when used in combination with drugs that have different molecular mechanisms. However, they have significant toxicities and so effort has been made into designing more selective, less toxic alternatives (Hurley, 2002).

DNA-interacting chemotherapeutic agents can be classed based on the nature of their molecular interactions with DNA and the subsequent modifications they induce. Figure

1.1 summarises these different interactions namely, DNA strand crosslinking, intercalation, DNA strand breaking and code reading molecules. The figure includes associations with proteins such as the Topoisomerases (Hurley, 2002).

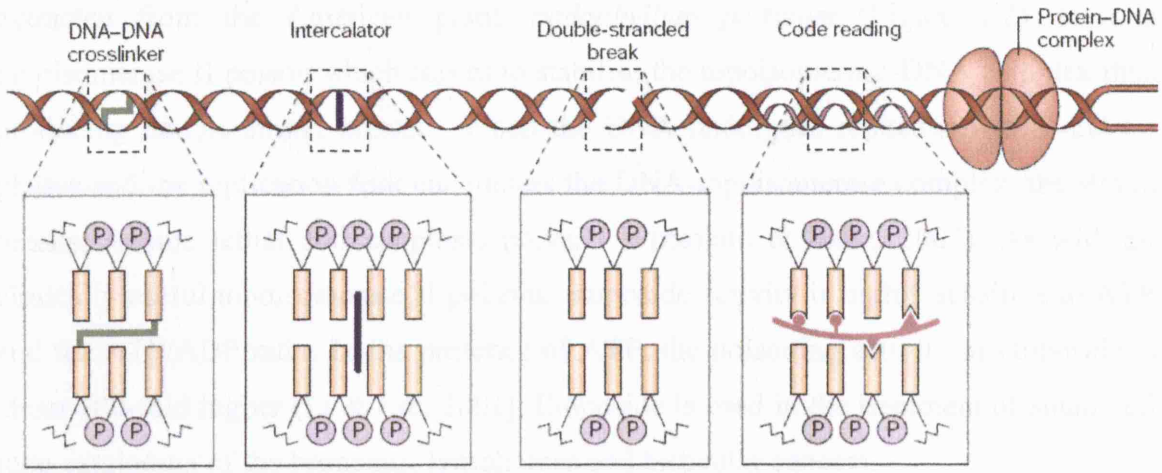

Figure 1.1: Classes of DNA-interactive agents and their molecular interactions with DNA.

Source: Adapted from L. Hurley, Nature Reviews Cancer, 2002.

1.2.3.1 Topoisomerase Poisons

Chromosomal DNA is supercoiled and is unravelled in order for DNA replication to take place. Topoisomerases are responsible for this unwinding as well as causing breakages and rejoining of DNA strands to allow for topological changes and subsequent replication. Topoisomerase I causes transient single strand breaks as opposed to topoisomerase II which produces double strand breaks relieving the tortional stress on the unwound DNA. Both are able to re-anneal the strands and are independent of one another.

Two topoisomerase II isozymes have been identified in human cells namely, topoisomerase IIα (hTOP2α) and topoisomerase IIβ (hTOP2β) (Wang, 1996). hTOP2α is a homodimer which catalyses the ATP-dependent strand-passing reactions and functions in DNA replication and chromosome condensation and segregation (Li & Liu, 2001). It contains two major domains, the N-terminal ATPase domain and the breakage/reunion C-terminal domain (Wang, 1996). hTOP2α is essential for cell growth and is a cell proliferation and tumour marker. Its highest level of expression occurs in the late S/G_2 phase of the cell cycle and is also the major component of the nuclear protein scaffold. hTOP2β is also a homodimer which although exhibits similar enzymatic activities to hTOP2α *in vitro*, is constitutively expressed at a constant level

throughout the cell cycle (Li & Liu, 2001). hTOP2β is involved in diaphragmatic development.

Etoposide (VP-16) is a semi-synthetic derivative of podophyllotoxin originally extracted from the American plant, *podophyllum peltatum* (Figure 1.2). It is a topoisomerase II poison which serves to stabilise the topoisomerase-DNA complex thus producing double strand breaks. When the DNA undergoes replication in S and G_2 phases and the replication fork encounters the DNA-topoisomerase complex, the strand breaks become lethal and apoptosis prevails (Pizzolato & Saltz, 2003). As with all clinically useful topoisomerase II poisons, etoposide activity is highly sensitive to ATP and the ATP/ADP ratio. In the presence of ATP, the poisoning activity of etoposide is about 100-fold higher (Li & Liu, 2001). Etoposide is used in the treatment of small cell lung carcinoma of the bronchus, lymphomas and testicular cancers.

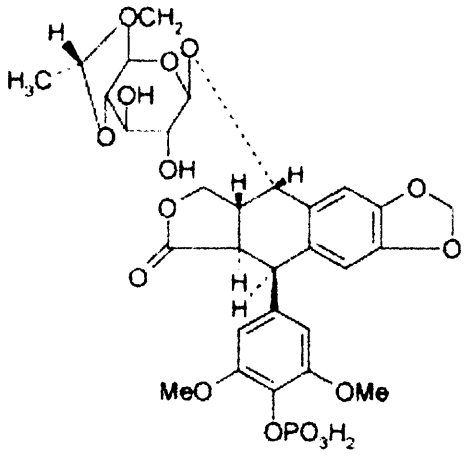

Figure 1.2: Chemical structure of etoposide.

Irinotecan (CPT-11), a topoisomerase I inhibitor is a semi-synthetic soluble derivative of camptothecin, a plant alkaloid present in wood and fruit of the *camptotheca acuminata* tree (Figure 1.3) (Pizzolato & Saltz, 2003).

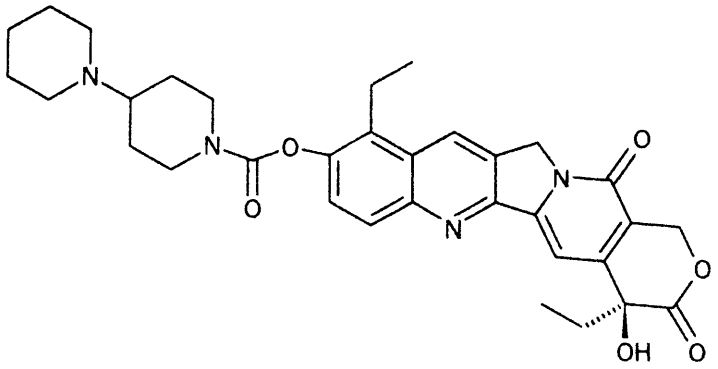

Figure 1.3: Chemical structure of irinotecan.

A unique characteristic of irinotecan is its bulky dipiperidino side-chain linked to the camptothecin molecule via a carboxyl-ester bond. This sidechain, although providing necessary solubility, leads to a substantial reduction in anticancer activity. Cleavage of the side-chain by carboxylesterases - found mainly in the liver and gastrointestinal tract - forms the metabolite SN-38 (7-ethyl-10-hydroxycamptothecin). SN-38 is a much more potent inhibitor of topoisomerase I than irinotecan and is the predominant active form of the drug. Irinotecan has been shown to prolong patient survival when used in the treatment of metastatic colorectal cancer.

1.2.3.2 Non-Covalent DNA Binding Drugs

These are intercalating drugs which have planar regions allowing them to stack between paired DNA bases forming tight drug-DNA interactions. They include the anthracycline antibiotics such as doxorubicin and daunorubicin and the non-anthracyclines such as antinomycin D, bleomycin and mitomycin C.

As an anthracycline, doxorubicin or *adriamycin* has a planar ring system attached to an amino sugar and is produced by *Streptomyces peucetius* (Figure 1.4).

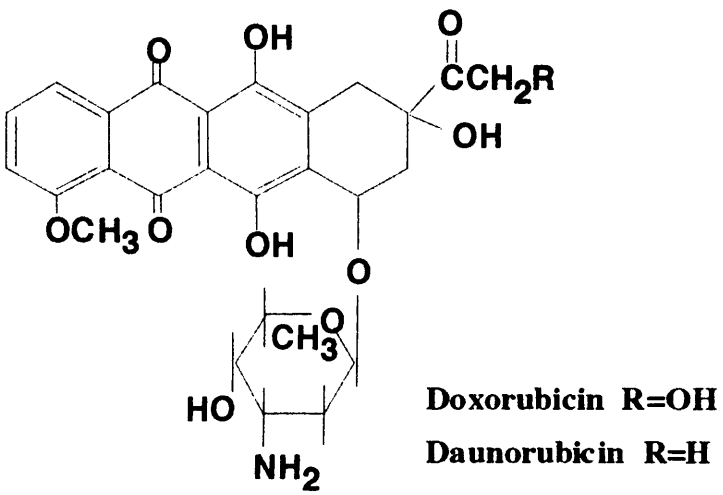

Figure 1.4: Chemical structure of anthracyclines.

Doxorubicin has an enhanced selectivity for cancer cells over normal cells. Insight into the basis of this selectivity was gained when it was discovered that doxorubicin induces protein-associated strand breaks by trapping topoisomerase II that is covalently bound to DNA (Tewey *et al.*, 1984). Given that these processes require protein binding to DNA, the selectivity of agents that target these processes might be dependent on the

level of the associated target protein (for example, topoisomerase I or II), so cells with elevated levels of topoisomerase would be more sensitive to doxorubicin, and a basis for enhanced cancer-cell selectivity arises (Henderson & Hurley, 1995).

Following DNA intercalation, the quinone ring is metabolised producing reactive oxygen species (ROS) and subsequent free radical cleavage damage of DNA. This results in partial unwinding of DNA, impaired DNA and RNA synthesis and single strand breaks in DNA. It is also non-phase specific (Zhong *et al.*, 2001). It is therefore plausible that these multiple mechanisms which also have downstream effects on cell-cycle checkpoints, have a clinical advantage over an agent with a single mechanism of action (Hurley, 2002). It has wide clinical activity for a variety of solid tumours and leukaemia.

1.2.3.3 Covalent DNA Binding Drugs – Alkylating Agents

As the largest group of anti-cancer drugs, the alkylating agents are sub-divided into four groups: nitrosoureas, alkyl sulphonates, nitrogen mustards and platinum compounds. These cell cycle non-specific agents act through covalent bonding of their alkyl groups (e.g. $-CH_2Cl$) which are capable of proton replacement through nucleophilic attack (reviewed in Hartley, 2001). Chlorine serves as a good leaving group to form an imminium ion (R_3N^+) in a strained ring system (Figure 1.5) (Hurley 2002). Given their organic mechanistic capability, alkylating agents are able to react with a variety of biological molecules including nucleic acids, nucleotides, amino acids and proteins. However, cytotoxicity of these agents is due to alkylation of DNA bases, with the consistent observation of DNA synthesis inhibition (Wheeler, 1962). The N^7 position within guanine is the most electronegative species within the four DNA bases and so is usually the most readily alkylated. Other sites of alkylation are the O^6-guanine position and the N^1 and N^3-adenine positions (Hartley, 2001).

If the alkylating agent has two reactive groups, as is shown in Figure 1.5, then following the production of mono-alkylated adducts, this results in formation of crosslinked DNA. These can either be DNA intra- or inter-strand crosslinks (ICL) or DNA-protein cross-links (Figure 1.6).

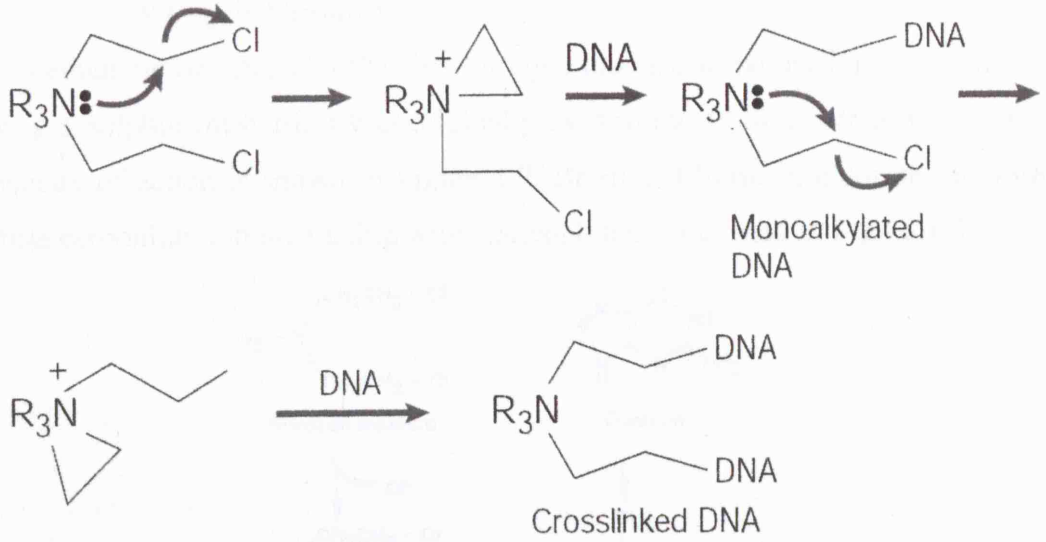

Figure 1.5: Crosslinking chemistry of alkylating agents.
Source: Adapted from L. Hurley, Nature Reviews Cancer, 2002.

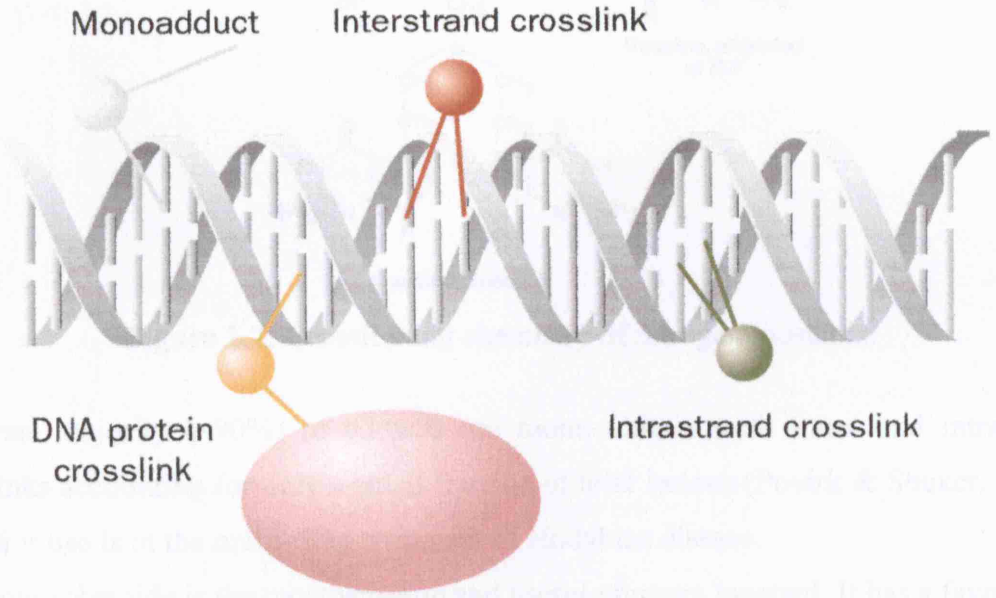

Figure 1.6: Types of DNA adducts formed by alkylating agents.
Source: P.J. McHugh et al., The Lancet Oncology, 2001.

It is the formation of interstrand crosslinking by bi-functional alkylating agents which is considered the major cytotoxic lesion induced. It should be noted that not all mono-adducts form crosslinks and for many the ratio of mono-adducts to crosslinks is at least 20:1 if not much higher (Brendel *et al.*, 1984).

Nitrogen Mustards

Mechlorethamine or HN2 was the first nitrogen mustard to be used and as a derivative of war gas sulphur mustard, it was originally used in the 1940's to treat lymphoma. Its mechanism of action is shown in Figure 1.7. Briefly, it looses a chloride ion with the resulting carbonium ion interacting with nucleophiles as outlined in Figure 1.5.

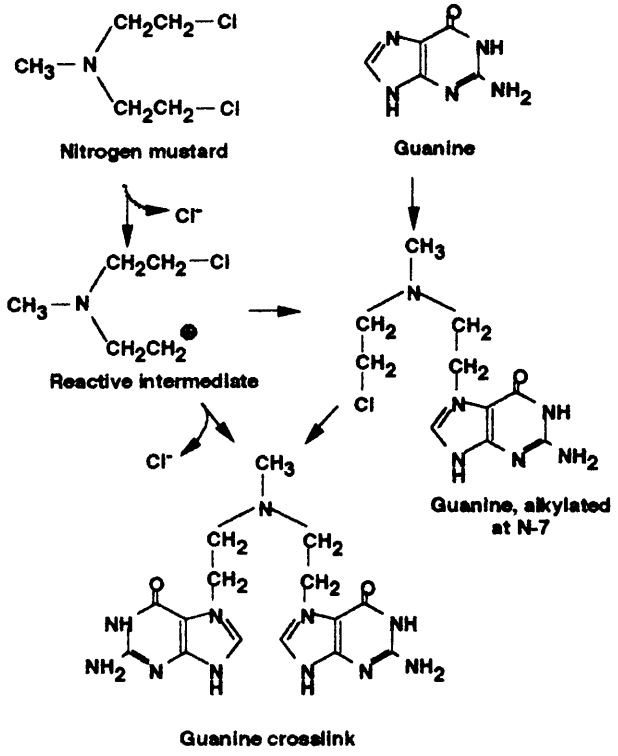

Figure 1.7: Crosslinking chemistry of nitrogen mustards.

The vast majority (~90%) of adducts are mono-adducts with inter- and intrastrand crosslinks accounting for only a small fraction of total lesions (Povirk & Shuker, 1994). Its major use is in the multi-drug treatment of Hodgkins disease.

Cyclophosphamide is the most versatile and useful nitrogen mustard. It has a favourable therapeutic index and the broadest spectrum anti-tumour activity of all alkylating agents. It is activated in the liver by cytochrome P450 enzymes and forms crosslinks via chloroethyl moieties. It is used mainly for non-Hodgkins lymphomas in combination with vincristine and prednisone as well as for ovary, lung and breast carcinomas (Hartley, 2001).

Chlorambucil is an aromatic derivative of HN2 and is the slowest acting and least toxic of all the alkylating agents. It is used to treat chronic lymphocytic leukaemia, lymphoma, Hodgkins disease and multiple myelomas (Hartley, 2001).

Melphalan is the phenylalanine derivative of mechlorethamine and is less reactive due to its slower rate of chloride ionisation (Figure 1.8). In addition to N^7-guanine adducts, melphalan also forms a large amount of adenine adducts with properties consistent with the alkylation at the N^3 position (Povirk & Shuker, 1994). It should be noted that the N^7-guanine atom faces into the major groove of the DNA structure while the N^3-adenine atom faces into the minor groove. Thus, the melphalan-induced adduct exerts much greater demand on DNA conformation than mechlorethamine.

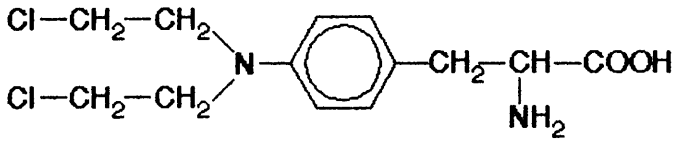

Figure 1.8: Chemical structure of melphalan.

There is variable absorption after oral administration and it is used in the palliative therapy of multiple myeloma, malignant melanoma and ovary and breast carcinomas. There is an increased incidence of secondary malignancies (non-lymphocytic leukaemia) (Tew *et al.*, 1996; Neidle & Thurston, 2005).

Platinum Compounds

Platinum compounds are amongst the most frequently used classes of anti-cancer drugs. As with nitrogen mustards they use chlorine atoms which act as leaving groups binding to N^7-guanine resulting in both inter and intra-strand crosslinks. The rationale for their use was based on the use of electric currents delivered to bacterial culture via platinum electrodes which caused inhibition of bacterial growth (Rosenberg *et al.*, 1985). They found that this inhibition was not due to the electric current but was in fact due to the formation of the platinum complex, cis-diamminedichloroplatinum (cis-DDP or cisplatin) (Figure 1.9).

Platinum compounds have a nomenclature dependent on the platinum oxidation state. They exist either as Pt(II) which forms a four coordination planar complex, or Pt(IV) which forms a six coordination complex. Both are fixed structures and so exist as two distinct isomers namely cis and trans. Transplatin is less cytotoxic with no anti-tumour activity (Chu, 1994).

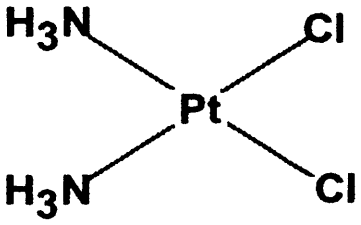

Figure 1.9: Chemical structure of cisplatin.

The cisplatin chloride ions are displaced in aqueous solution rendering it a potent electrophile capable of nucleophilic attack of proteins, RNA and most importantly DNA. As with alkylating agents they are bi-functional and so are capable of forming two covalent crosslinking bonds (Reed *et al.*, 1999). Their DNA interactions can exist in the form of mono-adducts, intra- or interstrand crosslinks or as DNA-protein crosslinks (Trimmer *et al.*, 1999). The major adducts produced are shown in Figure 1.10. Quantitative *in vitro* studies have shown that 1,2-intrastrand d(GpG) adducts account for 65% of the total and 1,2-intrastrand d(ApG) adducts make up 25%. Interstrand crosslinking accounts for only 5-8% of adducts formed however these are considered to be the critical lesions responsible for cytotoxicity (Fichtinger-Schepman *et al.*, 1985; Dronkert & Kanaar, 2001).

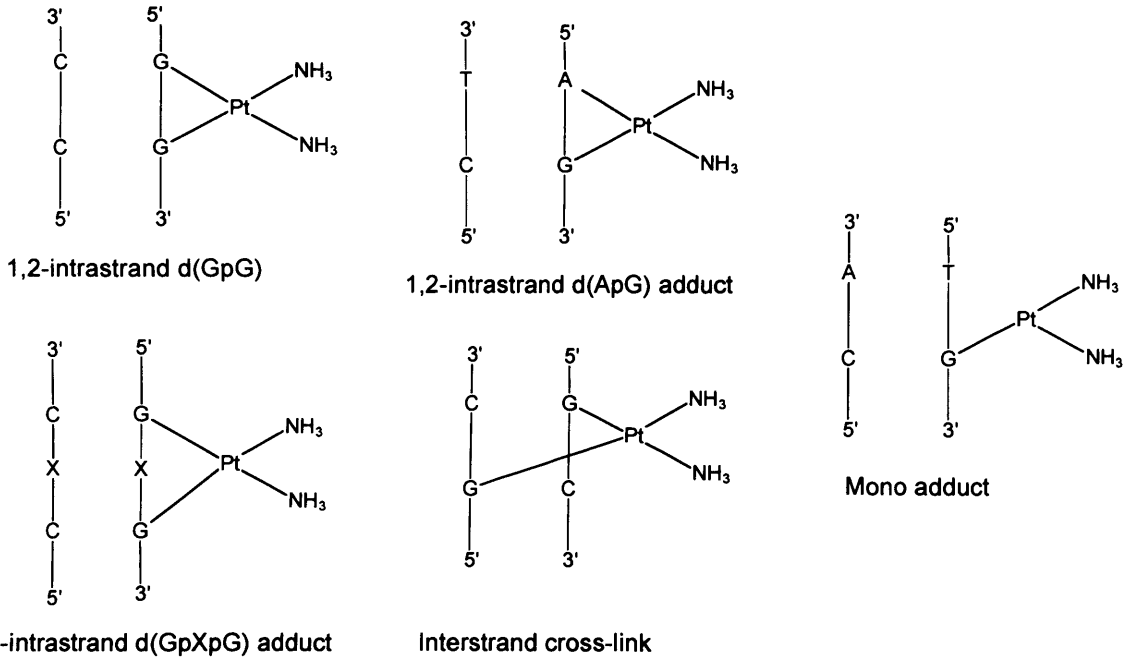

Figure 1.10: Types of bi-functional DNA adducts formed by cisplatin.

The importance of the different intra- or interstrand crosslinks formed by cisplatin (and melphalan) is discussed in more detail in Chapter 4.

Cisplatin is used in a variety of human malignancies including ovary, head and neck, lung, bladder and most strikingly in the treatment of testicular cancer, curing the majority of patients. It is commonly administered in combination with bleomycin and vinblastine. There is minimal marrow toxicity but causes severe nausea and vomiting, nephrotoxicity, neurotoxicity and ototoxicity. Resistance is largely due to a decrease in drug uptake and increased DNA repair. Other platinum analogues include carboplatin and oxaliplatin (Loehrer & Einhorn, 1984).

1.3 DNA Damage and Repair

1.3.1 Causes of DNA Damage

The integrity of genomic DNA is constantly under threat, even in perfectly healthy cells. DNA damage can be the result of a number of consequences. These include the action of endogenous reactive oxygen species (ROS) such as hydroxyl radicals, hydrogen peroxide or superoxide anions. Errors in replication and recombination as well as environmental agents such as ultraviolet (UV) light from the sun, ionising radiation and genotoxins such as cigarette smoke, can all result in DNA damage in the form of single-strand (SSB's) or double-strand breaks (DSB's) (Norbury & Zhivotovsky, 2004). Furthermore, DNA damage can result from the collapse of some chemical bonds in DNA such as hydrolysis of nucleotide residues or deamination of certain bases.

If, for any of these reasons, the DNA cannot be repaired, mutations may result and the risk of cancer increases (Hoeijmakers, 2001).

1.3.2 Cellular Response to DNA Damage and Apoptosis

While unicellular organisms respond to the presence of DNA lesions by activating cell cycle checkpoint and repair mechanisms, multicellular animals have the additional possibility of eliminating the damaged cells by triggering their death.

Initial research in this area was dominated by studies of mammalian systems, but it has since become apparent that DNA damage can also induce apoptosis in diverse experimental model organisms, most notably *Caenorhabditis elegans* and *Drosophila melanogaster*. The combination of data from these genetically amenable models with those from mammalian species has revealed conservation of several key molecular mechanisms, as well as species-specific variations on these themes (Norbury & Zhivotovsky, 2004).

The cell-cycle infrastructure is able to detect DNA damage at specific checkpoints in G_1, S, G_2 and M phases allowing repair of lesions before they become permanent (Zhou & Elledge, 2000). If the damage is too severe, apoptosis will be initiated at the expense of the whole cell.

Common damage detection and signal transduction mechanisms are shared between pathways governing DNA repair, cell cycle checkpoint activation and apoptosis. The consequence of any given level of DNA damage is cell type-specific. By allowing the survival and proliferation of cells with damaged DNA, failure of these processes contributes to tumourigenesis and resistance to cancer therapies (Igney and Krammer 2002).

These mechanisms are different for different types of DNA lesions. Genetic defects perturbing these mechanisms can cause severe syndromes characterised by the degeneration of specific tissues (especially the nervous and immune system) (Rouse and Jackson, 2002).

This finely tuned, multi-branched network of signalling pathways acts in concert to repair the lethal DSB, while temporarily arresting the cell cycle and balancing cellular metabolism accordingly. The complex network is mobilised primarily through the action of a single protein kinase – ATM (Shiloh, 2001; Shiloh, 2003).

Mutations in the ATM gene leading to loss of activity causes the genetic disorder ataxia telangiectasia (A-T) and results in cerebellar degeneration. This leads to severe, progressive neuromotor dysfunction, immunodeficiency, genomic instability, thymic and gonadal atrophy, a striking predisposition to lymphoreticular malignancies and extreme sensitivity to ionising radiation and DSB-inducing agents. ATM belongs to a conserved family of proteins and possesses serine/threonine kinase activity (Shiloh, 2001). Interestingly, all of these proteins contain a domain with motifs that are typical of the lipid kinase phosphatidylinositol 3-kinase (PI3K), so they are referred to as 'PI3K-like protein kinases' (PIKKs). The mammalian members of this family, at present, include five protein kinases namely, ATM, ATR, ATX/SMG-1, mTOR/FRAP, DNA-PK_{CS} and TRRAP (Vanhaesebroeck *et al.*, 2001). These protein kinases, when activated by various stresses, phosphorylate key proteins in the corresponding response pathways. They can therefore simultaneously affect numerous processes, depending on the spectrum of their substrates. Four mammalian PIKKs are known to be involved in the DNA-damage response: the DNA dependent protein kinase (DNA-PK), ATM, ATR

and ATX (Shiloh, 2003). Whereas ATM and DNA-PK respond primarily to DSBs, ATR and ATX respond to both ultraviolet (UV) light damage (possibly UV-light-induced replication arrest) and DSBs, and ATR also responds to stalled replication forks. mTOR/FRAP is the only active kinase in this family not involved in responding to DNA damage (Shiloh, 2003).

An overview of the ATM-mediated network is summarised in Figure 1.11. To fully review all the pathways is beyond the scope of this discussion. However, it is important to highlight the key features. Firstly, ATM works to target the same effector from several different directions. A main component in the G_1-S checkpoint is mediated by the activation and stabilisation of p53, which, in turn, activates transcription of WAF1 (p21, CIP1) which acts as a key inhibitor cyclin/CDK complexes. The main target of ATM in this pathway is p53 and this contributes primarily to enhancing the activity of p53 as a transcription factor (Ashcroft *et al.*, 1999). ATM also activates CHK2, a checkpoint kinase that in turn phosphorylates p53 preventing its interaction with the oncogenic protein MDM2 - a direct and indirect inhibitor of p53. ATM also directly phosphorylates MDM2 thus interfering with nuclear translocation of the p53-MDM2 complex and subsequent degradation of p53 (Maya *et al.*, 2001).

ATM also activates the tumour-suppressor protein, BRCA1 by phosphorylation on a plethora of sites. The differing modes of activation result in different outcomes including regulation of the intra-S-phase checkpoint (Xu *et al.*, 2002) and its involvement in the G_2-M checkpoint (Xu *et al.*, 2001). In addition, ATM also inhibits BRCA1 by activating CtIP. Other effectors controlled by ATM include NBS1, SMC1, CHK1, CHK2, RAD9 and RAD17.

A recently identified downstream effector of ATM in the intra-S checkpoint is the FANCD2 protein, inducing BRCA1-mediated mono-ubiquitylation (Taniguchi *et al.*, 2002). FANCD2 defects lead to the genomic instability syndrome, Fanconi's anaemia – a depletion of bone marrow causing insufficient formation of all types of blood cells.

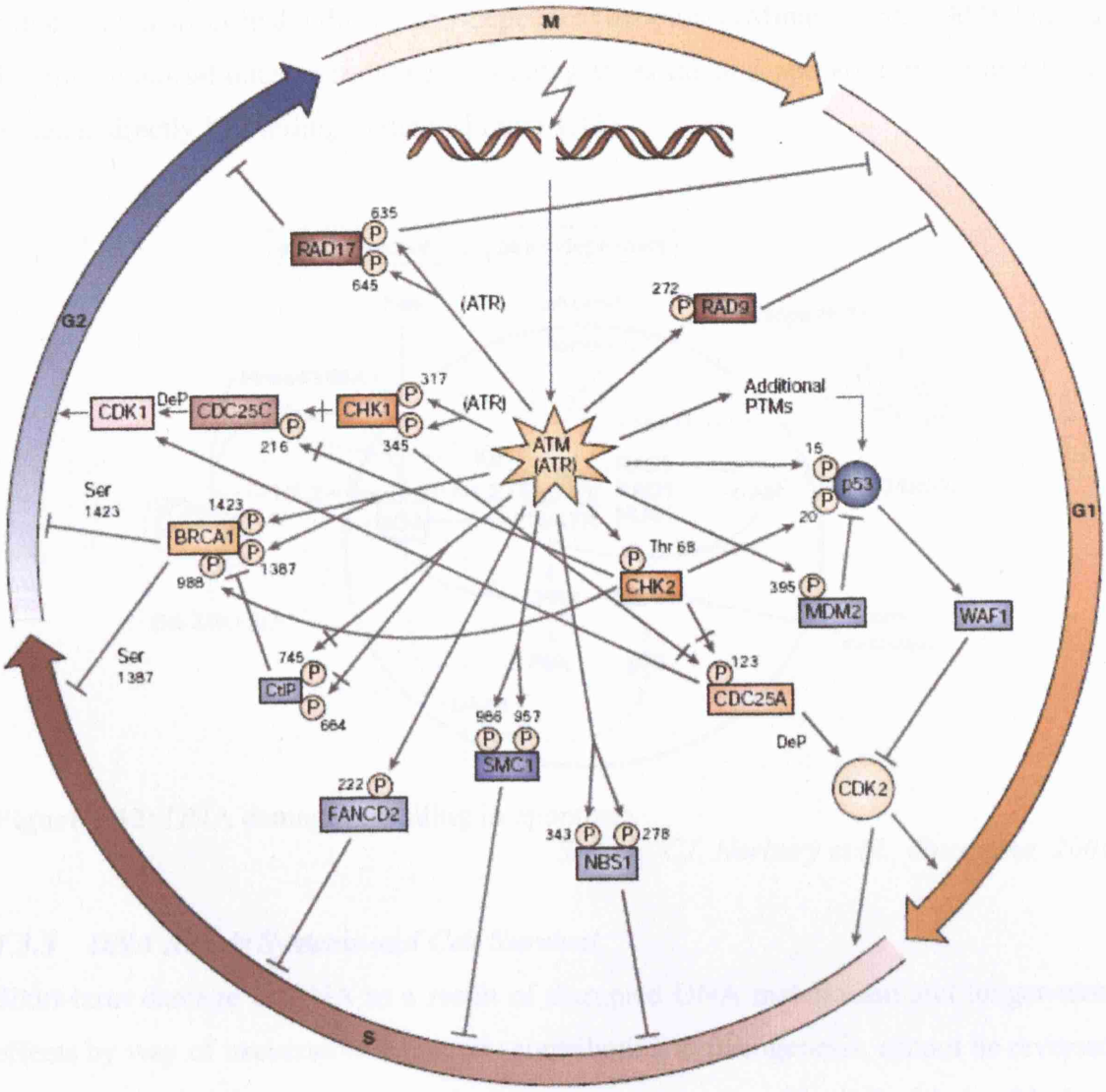

Figure 1.11: ATM-mediated activation of cell-cycle checkpoints in response to DSBs.
Source: Y. Shiloh, Nature Reviews Cancer, 2003.

1.3.2.1 p53-Mediated Apoptosis

The primary physiological role of p53 in response to DNA damage-induced apoptosis is to serve as a transcriptional activator for genes encoding apoptotic effectors (Norbury & Zhivotovsky, 2004). p53 directly activates transcription of several genes encoding members of the Bcl-2 family, most importantly the pro-apoptotic protein Bax. The Bcl-2 family is made up of pro- and anti-apoptotic proteins as well as proteins that regulate mitochondrial permeability (Cory & Adams, 2002). Following DNA damage, p53 also activates Fas allowing for Fas-mediated apoptosis (Reinke and Lozano, 1997).

In addition, p53 itself has been shown to bind to DNA strand breaks (Bakalkin *et al.*, 1994), suggesting a possible role in DNA damage detection, or to translocate to

mitochondria specifically during p53-dependent apoptosis (Mihara *et al.*, 2003). Once at the mitochondrial outer membrane, p53 antagonises the anti-apoptotic Bcl-2 and Bcl_{XL} proteins directly by binding to them (Figure 1.11).

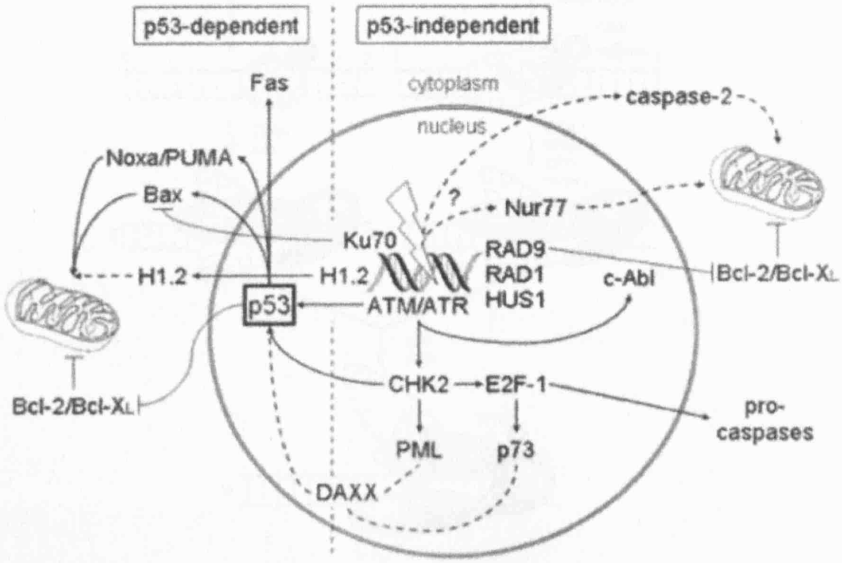

Figure 1.12: DNA damage signalling in apoptosis.
Source: CJ. Norbury et al., Oncogene, 2004

1.3.3 DNA Repair Systems and Cell Survival

Short-term damage to DNA as a result of disrupted DNA metabolism and longer-term effects by way of irreversible mutations contributing to oncogenesis, cannot be reversed by way of a single repair process. No one system can cope with all the kinds of lesions and so at least four main damage repair systems are in place (Hoeijmakers, 2001). These are: Nucleotide Excision Repair, Base Excision Repair, Homologous Recombination and Non-Homologous End Joining.

1.3.3.1 Nucleotide Excision Repair (NER)

Of all repair systems, NER is able to recognise the most diverse array of lesions. Divided into two distinct pathways, this repair mechanism is able to survey the entire genome for distorting injury using the global genome pathway GG-NER. Its alternative transcription-coupled repair (TCR) pathway is able to focus on blocked elongated RNA polymerases (Batty & Wood, 2000). Their mechanisms are illustrated in Figure 1.13.

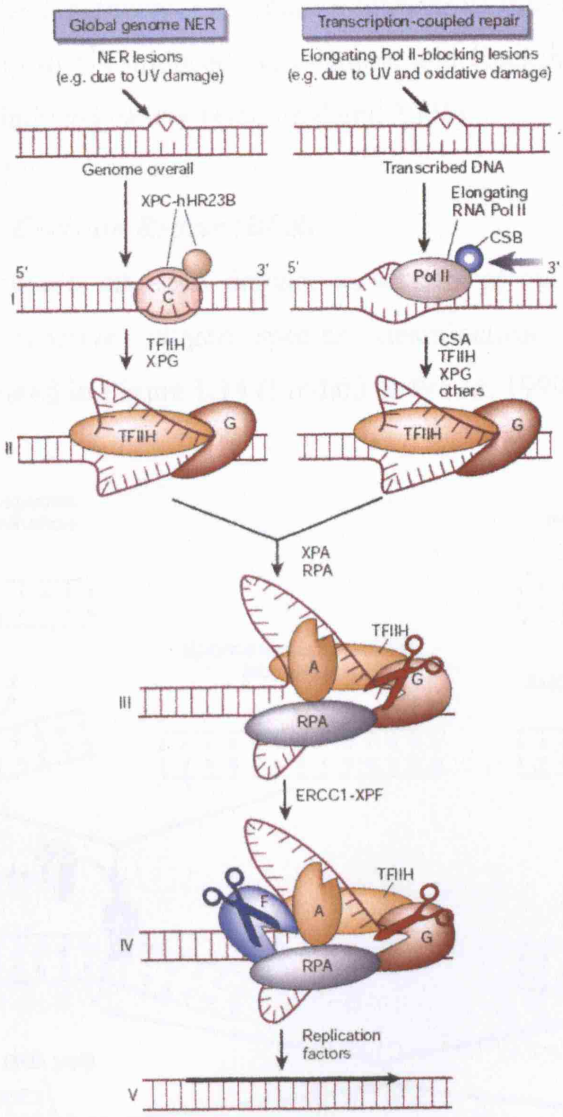

Figure 1.13: Mechanisms of GG-NER and TCR-coupled repair pathways.

Source: JHJ Hoeijmakers, Nature, 2001.

Briefly, the GG-NER-specific complex XPC-hHR23B initially screens for disrupted base pairing. In TCR, the TCR-specific factors CSB and CSA remove the stalled polymerase, exposing the lesion (step one). The subsequent stages for both pathways are then identical. The XPB and XPD helicases of the transcription factor TFIIH open ~30bp of DNA around the damage (step two). Following confirmation of the damage, the single-stranded-binding protein RPA (replication protein A) stabilises the open intermediate by binding to the undamaged strand (step three). On the damaged strand, the endonucleases XPG and ERCC1/XPF cleave the 3' and 5' ends respectively to generate a 24-32 base oligonucleotide (step four). Normal DNA replication then fills the gap and completes the repair pathways.

Genetic defects in these pathways can cause a number of diseases including xeroderma pigmentosum leading to UV-induced skin cancer, and Cockayne syndrome which can protect against UV-induced cancer (Hoeijmakers, 2001).

1.3.3.2 Base Excision Repair (BER)

The BER pathway repairs all DNA damage as a result of cellular metabolism such as the production of reactive oxygen species, deamination and hydroxylation. The mechanism is illustrated in Figure 1.14 (Lindahl & Wood, 1999).

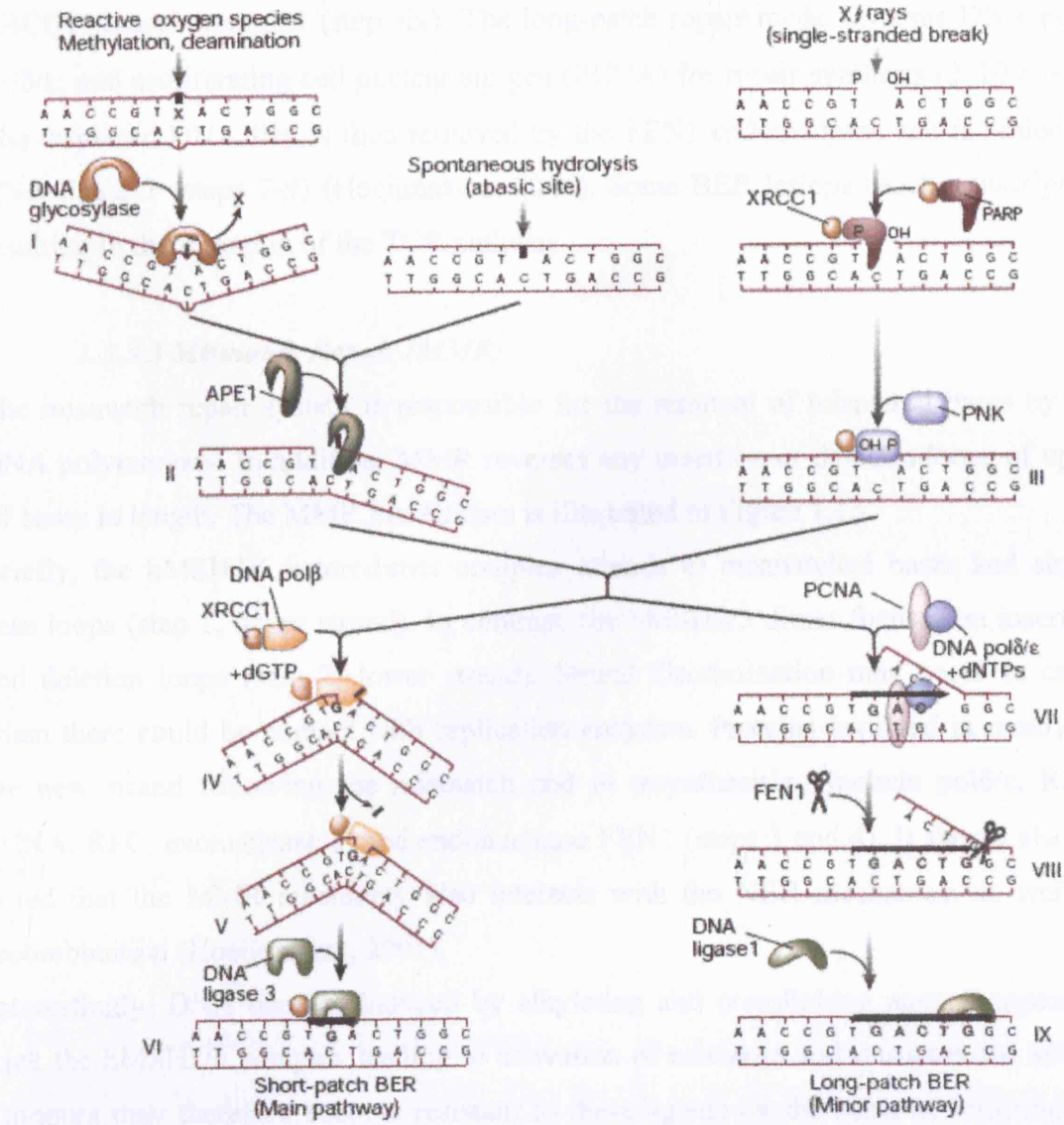

Figure 1.14: Mechanisms of the base excision repair pathway.
Source: JHJ Hoeijmakers, Nature, 2001.

Briefly, the pathway is initiated by DNA glycosylase flipping the damaged base out of the helix so as to accommodate it in an internal cavity of the protein. Inside, the base is then cleaved from the sugar-phosphate backbone (step one). The core pathway then proceeds with strand incisions by the APE1 endonuclease (step two). Poly-ADP-ribose polymerase (PARP), which binds to and is activated by DNA strand breaks, and polynucleotide kinase (PNK) (Whitehouse *et al.*, 2001) may be important when BER is initiated from a SSB to protect and trim the ends for repair synthesis (step three). DNA polβ then fills the one-nucleotide gap (step four) and uses its lyase activity to remove the 5'-terminal baseless residue (step five). The rendered nick is then sealed by the XRCC1–ligase3 complex (step six). The long-patch repair mode involves DNA polβ, polδ/ε; and proliferating cell nuclear antigen (PCNA) for repair synthesis (2–10 bases). The displaced DNA flap is then removed by the FEN1 endonuclease and is sealed by DNA ligase 1 (steps 7-9) (Hoeijmakers, 2001). Some BER lesions block transcription resulting in the initiation of the TCR pathway.

1.3.3.3 Mismatch Repair (MMR)

The mismatch repair system is responsible for the removal of mispaired bases by the DNA polymerases. In addition, MMR reverses any insertion or deletion loops of up to 10 bases in length. The MMR mechanism is illustrated in Figure 1.15.

Briefly, the hMSH2/6 heterodimer complex attends to mismatched bases and single base loops (step 1, upper strand). In contrast, the hMSH2/3 dimer focuses on insertion and deletion loops (step 2, lower strand). Strand discrimination may occur in cases when there could be contact with replication enzymes. Proteins involved in removing the new strand following the mismatch and in resynthesising include polδ/ε, RPA, PCNA, RFC, exonuclease 1, and endonuclease FEN1 (steps 3 and 4). It should also be noted that the MMR machinery also interacts with the NER mechanism as well as recombination (Hoeijmakers, 2001).

Interestingly, DNA damage induced by alkylating and crosslinking agents, appear to trick the hMSH2/6 complex leading to activation of mistaken and unsuccessful MMR. Tumours may therefore become resistant to these agents on the basis of selection for defective MMR, making chemotherapeutic strategies all the more challenging (Karran & Bignami, 1994).

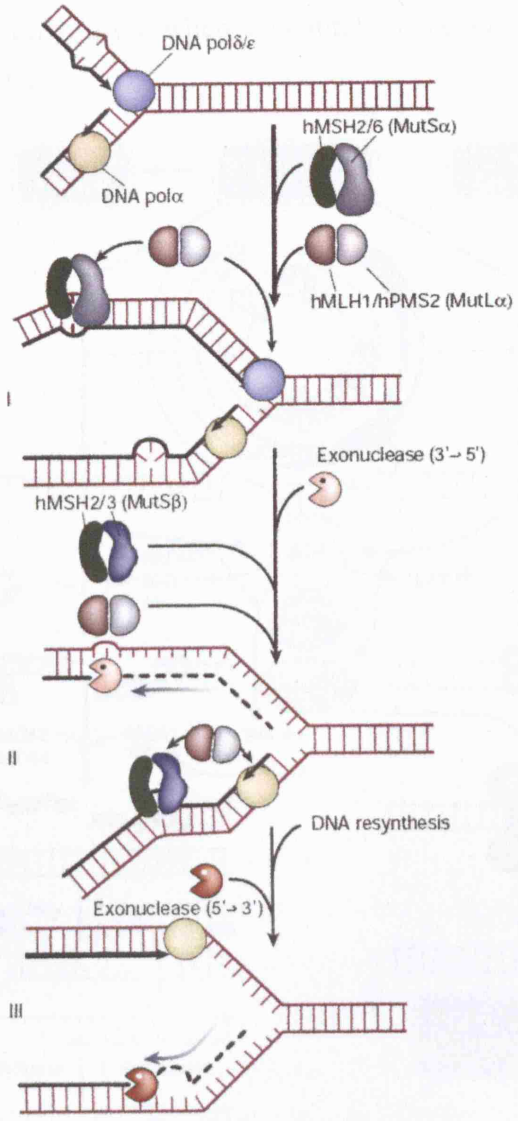

Figure 1.15: Mechanisms of the mismatch repair pathway.
Source: JHJ Hoeijmakers, Nature, 2001.

Defects and instability in MMR can arise in hereditary non-polyposis colorectal cancer (HNPCC) and in a variety of other cancers. These lead to increased mutation rates and subsequent oncogenesis (Hoeijmakers, 2001).

1.3.3.4 Homologous Recombination (HR) and End Joining (NHEJ)

As discussed previously, DNA double-strand breaks arrest the cell cycle and activation of repair proteins. In addition to p53-mediated G_1 arrest, there is the activation of the H2AX histone at the DSB by the ATM/ATR/DNA-PK_{CS} kinases. The repair of DSBs is mediated by the HR and NHEJ systems, the former being the preferred mechanism

when a second identical DNA copy in available (Hoeijmakers, 2001). The latter is more error-prone and so only used when absolutely necessary. Both repair systems are outlined in Figure 1.16.

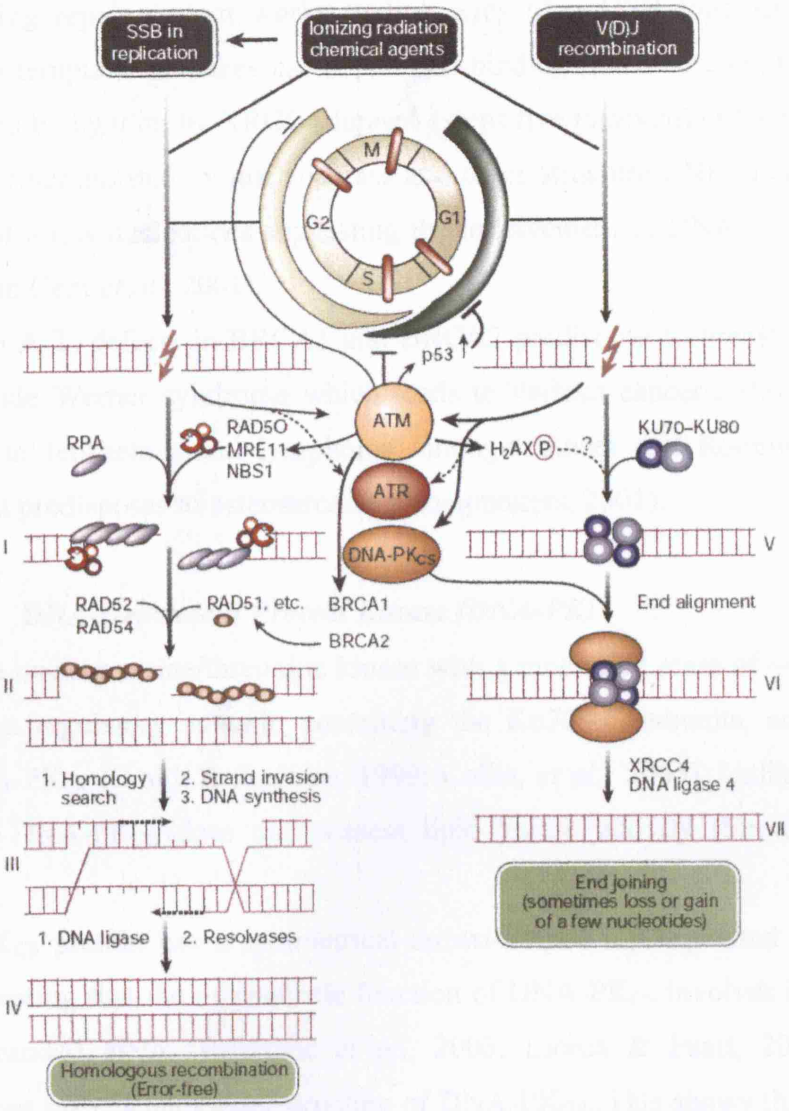

Figure 1.16: Mechanisms of the HR and NHEJ repair pathways.
Source: JHJ Hoeijmakers, Nature, 2001.

HR is initiated by the 5'-3' exonucleases of the abovementioned RAD50/MRE11/NBS1 complexes which are activated by ATM and expose both 3' ends (step one) (Petrini, 2000). RPA then serves as a template for the RAD52 stimulated assembly of the RAD51 nucleoprotein and other related proteins including XRCC2 and XRCC3 (step two). RAD51, the human equivalent of the *E.coli* RecA protein, can exchange the single strand with the same sequence from a double-stranded DNA molecule. Following this, the intact double-stranded copy is used as a template to correctly repair the broken ends

by DNA synthesis (step three). The then formed Holliday junctions are resolved by resolvases (step four) (Haber, 2000; Khanna & Jackson, 2001). BRCA2 has been shown to be involved in the nuclear translocation of RAD51 (Davies *et al.*, 2001; West, 2003).

The end-joining repair system works to link ends of a DSB together, without the assembly of a template. It makes use of the end-binding Ku70/80 complex and DNA-PK_{CS}, followed by ligation by XRCC4-ligase4 (steps five to seven) (Khanna & Jackson, 2001). It is further assisted by nucleosomes and other structures. NHEJ can lead to the gain or loss of a few nucleotides suggesting the involvement of DNA polymerases and nucleases (Van Gent *et al.*, 2001).

In addition to A-T, defects in BRCA1 and BRCA2 predispose to breast cancer. Other diseases include Werner syndrome which leads to various cancers, Bloom syndrome which leads to leukaemia and lymphoma amongst others and Rothmund-Thomson syndrome that predisposes to osteosarcoma (Hoeijmakers, 2001).

DNA-Dependent Protein Kinase (DNA-PK)

DNA-PK is a nuclear serine/threonine kinase with a molecular mass of ~460 kDa. It is made up of a regulatory subunit, containing the Ku70/80 subunits, and a catalytic subunit, DNA-PK_{CS} (Smith & Jackson, 1999; Collis, *et al.*, 2005). Unlike the original PI3-Kinases, DNA-PK_{CS} does not possess lipid kinase activity (Smith & Jackson, 1999).

The DNA-PK_{CS} protein has a symmetrical crown-shaped top separated from a round bottom, suggesting that the mechanistic function of DNA-PK_{CS} involves internalisation of double-stranded DNA (Boskovic *et al.*, 2003; Llorca & Pearl, 2004). Electron microscopy has provided a model structure of DNA-PK_{CS}. This shows that DNA-PK_{CS} is divided into two large regions, labelled as 'head' and 'palm' connected by a third region labelled 'arm' (Figure 1.17B) (Brewerton *et al.*, 2004).

DNA-DNA-PK_{CS} interactions have recently been obtained and show that binding to DNA greatly stimulates DNA-PK_{CS} activity with the phosphorylation of one of its natural substrates, the XRCC4 protein. This indicates that DNA interaction is functionally relevant to DNA-PK_{CS} (Boskovic *et al.*, 2003; Collis, *et al.*, 2005).

Using a multi-model refinement approach, Boskovic and co-workers were able to obtain collections of images of both free and DNA-bound protein (Figure 1.17C-E). Binding induces conformational changes causing the palm domain to bend, coming into contact

with the head and exposing a small channel able to accommodate double-stranded DNA. These structural movements are likely to play a role in the activation of DNA-PK_{CS} kinase activity upon DNA binding (Martensson & Hammarsten, 2002).

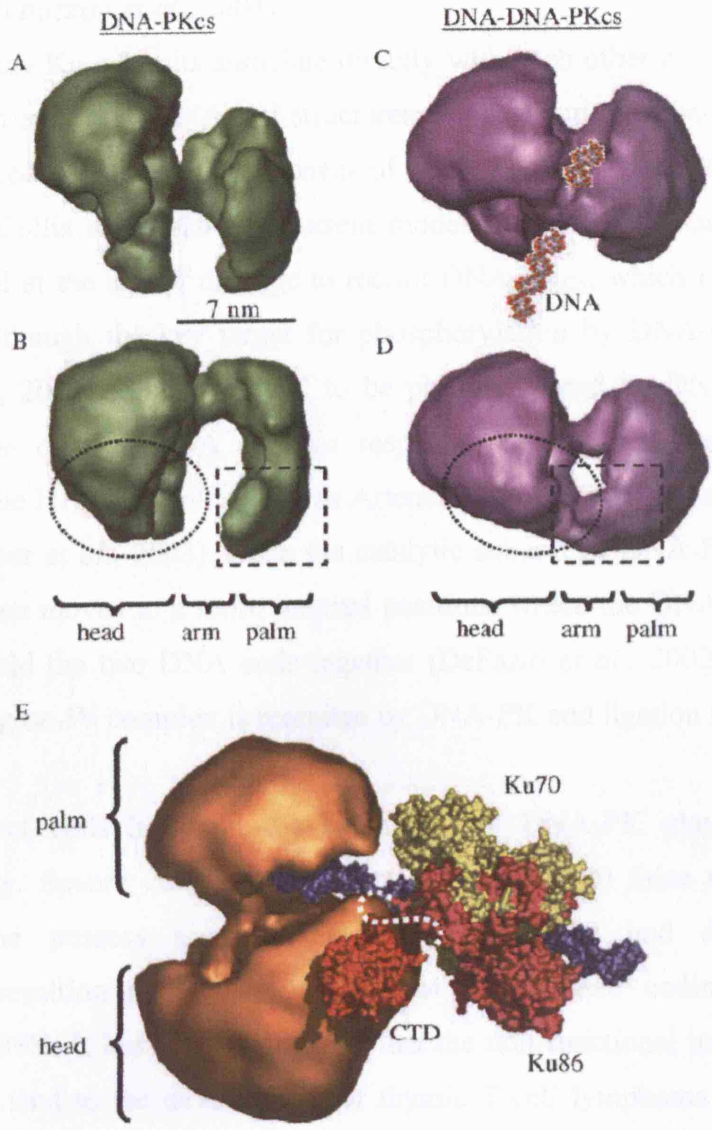

Figure 1.17: 3D structure of DNA-PK_{CS} and its DNA-bound complex.
Source: O. Llorca & L.H. Pearl, Micron, 2004.

Although DNA-PK_{CS} associates with DNA-bound Ku for activation (Chan *et al.*, 2002), DNA-PK_{CS} can also bind to, and is activated by free DNA ends in the absence of Ku (Hammarsten & Chu, 1998). Consistent with this data, crosslinking studies of DNA to DNA-PK_{CS} suggest that DNA can activate DNA-PK_{CS} alone (Lees-Miller *et al.*, 1990; Gottlieb & Jackson, 1993). Given its interactions with other proteins of NHEJ as well as non-NHEJ proteins, DNA-PK_{CS} may also act as a scaffold protein to aid the localisation

of DNA repair proteins to the site of damage (Collis *et al.*, 2005). DNA-PK_{CS}, as well as Ku, is found at the ends of chromosomes, suggesting a further role for DNA-PK_{CS} in the maintenance of telomeric stability and the prevention of chromosomal end fusion (Espejel, 2004; Rebuzzini *et al.*, 2004).

DNA-PK_{CS} and the Ku subunits associate directly with each other even in the absence of DNA, and can each bind DNA end structures independently (Lieber *et al.*, 2003). It has been suggested that the Ku component of DNA-PK is probably the initial DSBs sensor *in vivo* (Collis *et al.*, 2005). Current models propose that Ku binds to DNA termini generated at the site of damage to recruit DNA-PK_{CS}, which is activated upon DNA binding although the key target for phosphorylation by DNA-PK_{CS} is unclear (Llorca & Pearl, 2004). Proteins found to be phosphorylated by DNA-PK_{CS} include regulators of the cellular DNA damage response such as p53, as well as other components of the NHEJ complex such as Artemis, XRCC4 and Ku, as well as DNA-PK_{CS} itself (Lieber *et al.*, 2003). Once the catalytic subunit of DNA-PK is supporting the DNA, Ku then moves to a more internal positions where the DNA-PK_{CS} probably contributes to hold the two DNA ends together (DeFazio *et al.*, 2002). To finish, the XRCC4-DNA-ligase-IV complex is recruited by DNA-PK and ligation is achieved.

DNA-PK-deficient cells highlight the essential role DNA-PK plays in protecting genomic stability. Severe combined immunodeficient (SCID) mice with a defective DNA-PK_{CS} gene possess a premature aging phenotype and defective V(D)J recombination resulting in an accumulation of unprocessed coding intermediates (Bogue *et al.*, 1998). It has also been shown that the non-functional immune system in SCID mice can lead to the development of thymic T-cell lymphoma (Jhappan *et al.*, 1997). In addition, they are of course defective in the repair of chromosomal DSBs. A human DNA-PK_{CS} defective glioma cell line M059J, has been described (Lees-Miller *et al.*, 1995). The radiosensitivity of M059J can be complemented by fusion with murine SCID cells harbouring human chromosome 8 (Hoppe *et al.*, 2000), highlighting the dependence on DNA-PK activity for efficient repair of IR-induced DNA damage.

Ku exists as two subunits of ~70 and 83 kDa (Ku70 and Ku80), with each subunit possessing a leucine zipper motif and binds in a non-sequence-specific manner (Collis *et al.*, 2005). Studies with Ku-negative cells indicate that DNA-PK_{CS} binds to the C-

terminal region of Ku80 (Muller & Salles, 1997). It has been suggested that Ku possesses ATP-dependent helicase activity and that phosphorylation stimulates this activity (Harris *et al.*, 2004).

1.4 Rationally Designed DNA Damaging Agents

Novel chemical approaches have been made in recent years to address the cellular, molecular and genetic basis of cancer in the hope of designing effective therapies (Neidle & Thurston, 2005). They exploit the structure and reactivity of small molecules and macromolecules and the chemical interactions associated with them. An example of this already mentioned, is the application of medicinal chemistry to sulphur mustard gas. This has led to the development of agents that are still in clinical use, from the development of molecules that have progressively decreasing toxicity to normal cells, to a molecule designed to target the oestrogen receptor in tumour cells.

The use of synthetic chemistry on natural products has proved clinically successful, as has been the case for the development of the paclitaxel-related compounds. Structural biology and chemistry represent new approaches for discovering anti-cancer drugs. These are being used to determine the molecular aspects of kinase and protein-protein inhibition. In addition, silicon graphics is in use for screening large virtual libraries of compounds against the known structure of a target. Molecules in development include those that selectively target a unique DNA sequence which inhibit transcription. An example of this is SJG-136, a pyrrolobenzodiazepine (PBD) dimer novel minor-groove ICL agent (Gregson *et al.*, 2001; Hartley *et al.*, 2004).

Inactive compounds or pro-drugs that are converted into active derivatives only in tumour cells are also products of synthetic medicinal chemistry. All these approaches require the optimisation of the distribution, metabolism and excretion properties of a molecule as early as possible in the drug-discovery cycle (Neidle & Thurston, 2005).

1.5 Oncogenic Tyrosine Kinases and DNA Damage

Tyrosine kinases transfer phosphate groups from an ATP molecule to tyrosine residues on specific cellular proteins. As mediators of many signalling processes, tyrosine kinases are tightly controlled by various physiological mechanisms. There are three general mechanisms by which tyrosine kinases become constitutively activated. The first is as a result of chromosomal translocation. Here, reciprocal chromosomal translocations generate fusion proteins, the amino-terminal portion of which is responsible for oligomerisation, allowing constitutive activation of the catalytic activity of a kinase domain that is located on the carboxy-terminal portion. The second is as a result of overexpression of a particular cell-membrane receptor tyrosine kinase which leads to spontaneous (or autocrine ligand-dependent) dimerisation and constitutive kinase activation. Finally, point mutations in the juxtamembrane region of a receptor tyrosine kinase can cause constitutive ligand-independent dimerisation of the receptor and activation of its kinase activity (Skorski, 2002). Changes in more than 30 tyrosine kinases have been implicated in human cancer (Table 1.1) (Blume-Jenson & Hunter, 2001).

In cancer, oncogenic tyrosine kinases (OTKs) play two complementary roles. Firstly, they stimulate certain pathways including growth factor-independent activation of proliferation, protection from apoptosis in the absence of external survival factors, and promotion of invasion and metastasis (Sawyers, 1997; Tatosyan & Mizenina, 2000). Secondly, OTKs render cells resistant to radio- and chemotherapies (Yu & Hung, 2000; Slupianek *et al.*, 2001). Cells that have become malignant as a result of OTK overexpression display early drug resistance (Masumoto *et al.*, 1999). In addition, as tumours progress, the expression of OTKs can increase and contribute to stronger resistance (Cambier *et al.*, 1998). OTK-transformed cells can accumulate additional genetic abnormalities, such as mutations or deletions of p53, p73, MSH2 or (MLH1) which further increase genotoxic resistance (Strano *et al.*, 2001; Skorski, 2002).

OTK	Associated Cancer	Details
ABL, ALK, FGFR, JAK2, PDGFRβ, TRKC	Acute and chronic leukaemias	Dysregulated by fusion with BCR, TEL or NPM causing oligomerisation and activation of the kinase by cross-phosphorylation
ERBB1-4, IGF1R, PDGFRβ, FGFR1-4	Breast and ovarian carcinomas, lung cancer, glioblastomas, gastric and prostate carcinomas	Enhanced expression causes receptor dimerisation and activation of intrinsic kinase activity
SRC, KIT	Gastrointestinal tumours, leukaemias, lung cancers, colon cancer	C-Terminal truncation or gain-of-function point mutations causing increased kinase activity

Table 1.1: Examples of neoplastic disease caused by oncogenic tyrosine kinases.

Four models for OTK-mediated resistance to DNA damage-induced apoptosis are possible:

1. Decreased accumulation of DNA lesions following genotoxic treatment.
2. Increased rate of DNA damage repair.
3. Increased efficiency of DNA-damage-dependent checkpoint activation.
4. Protection from pro-apoptotic signalling pathways normally activated by DNA lesions.

1. Reduced DNA Damage

This is unlikely to be an important factor because OTK-transformed cells tend to accumulate more DNA damage than normal cells (Slupianek, 2002). The reason for this is unknown but it has been proposed that some of the extra DNA damage may represent intermediates in an accelerated process of repair such as the occurrence of DSBs when replication forks encounter DNA lesions (Michel *et al.*, 2001)

2. Increased Rate of Repair

It has been shown that BCR-ABL-like OTK-transformed cells can repair most of the lesions more rapidly than untransformed cells can (Masumoto *et al.*, 1999). This is dependent on the agent used, and the types of DNA damage which results (Skorski, 2002).

Homologous recombination is a crucial component of the drug-resistance machinery in

cells that are transformed by the BCR-ABL-related family of OTKs (Slupianek *et al.*, 2001; Slupianek *et al.*, 2002). HR is upregulated in cells that express these oncogenic fusion proteins through deregulated expression and phosphorylation of RAD51. Increased levels of RAD51 proteins have been observed in many tumours (Raderschall *et al.*, 2002). Importantly, NHEJ appears to be downregulated in BCR-ABL expressing cells (Deutsch *et al.*, 2001).

3. Checkpoint Activation

The Src oncogene can dissociate CDK2 from cyclin A in response to etoposide thus inducing S-phase arrest (Chen & Hitomi, 1999). In addition, BCR-ABL-related OTKs induce pronounced G_2/M-checkpoint activation in response to various agents, including cisplatin (Raderschall *et al.*, 2002). The mechanism of G_2/M-checkpoint arrest in OTK-transformed cells is not known, but probably involves regulation of CDC2 phosphorylation (Slupianek *et al.*, 2002). It is thought that by prolonging the G_2/M phase, OTKs allow for HR to repair more DSBs and allow tumour cells to escape from the apoptotic pathway (Skorski, 2002).

4. Resistance to Apoptosis

OTK-transformed cells are able to modulate expression and post-translational modification of B-cell lymphoma 2 (Bcl-2)-family members to allow protection against apoptosis. To this end, OTKs stimulate anti-apoptotic proteins such as Bcl_{XL} and Bcl-2 and inhibit the pro-apoptotic proteins Bad and Bax (Skorski, 2002).

BCR-ABL can activate STAT5 – a signal transducer and transcriptional activator responsible for Bcl_{XL} overexpression (Gesbert & Griffin, 2000). Additionally, AKT is also activated which, in turn, associates with Bad in a complex away from the mitochondria. AKT can also stimulate the MDM2-dependent, ubiquitin-mediated degradation of p53 and subsequent downregulation of Bax and upregulation of Bcl-2 (Zhou *et al.*, 2001).

1.6 Rationally Designed Cancer Therapies Targeting Tyrosine Kinases

Over the past few years, the number of receptors and in particular tyrosine kinases, being investigated as molecular targets in drug discovery has greatly increased. Screening for low molecular weight therapeutic agents against various cancers has

become an important component of drug discovery (Table 1.2).

General target	Specific Target	Therapeutic Approach
Signal Transduction	Growth Receptors	*- Extracellular antibodies* *- Small molecule inhibitors of tyrosine kinases*
	Ras	*- Small molecule inhibitors of farnesyltransferase* *- Antisense oligonucleotides (K-Ras, N-Ras, H-Ras)*
	Raf	*- Antisense oligonucleotides*
	MAPK	*- Small molecules*
	Rapamycin-Sensitive and PI3K/AKT pathways	*- Rapamycin analogues* *- Small molecule inhibitors*
Malignant Angiogenesis and metastasis	VEGF	*- Antibodies* *- Small molecular inhibitors of VEGFR tyrosine kinases* *- Natural products* *- Ribozymes*
	Matrix metalloproteinases	*Small Molecules*
	Integrins	*- Small Molecules* *- Peptides* *- Peptide cytotoxic conjugates*
Apoptosis Survival	Bcl-2	*- Antisense*
	BCR/ABL	*- Small molecule inhibitors of tyrosine kinases*
	Death Receptors (e.g. TNF)	*- Small molecules*
Tumour Suppressor Gene Function	p53	*- Viral vectors with p53 to restore function* *- Viral vectors that selectively kill mutant p53 cells*
Tumour Differentiation	Polyamines	*- Polyamine inhibitors*
	Retinoid receptors	*- Retinoids*
Cell Cycle checkpoint Control	CDKs	*- Small molecule kinase inhibitors*

Table 1.2: Molecular targeted anti-cancer approaches.

An overview of some of the receptor tyrosine kinases (RTKs) that have been targeted for anti-cancer therapy is summarised in Table 1.3 and in Figure 1.18. Therapies targeting the epidermal growth factor receptor (EGFR) family of tyrosine kinases are not included here, as they will be discussed in detail later (Section 1.7.3).

Drug Names	OTK	Status	Description	Company
Imatinib, Gleevec™, STI561	BCR-ABL, KIT, PDGFR	Approved for CML and GIST	2-Phenylamino-pyrimidine	Novartis
Bevacizumab, Avastin™	VEGF	Approved for colorectal cancer	Humanised anti-VEGF (rhu mAb-VEGF)	Genentech
CDP860	PDGFR	Clinical Development	Anti-PDGFβ-Receptor antibody fragment	Celltech
SU6668	VEGFR2, PDGFR, FGFR	Clinical Development	Indoline-2-one	Sugen/Pfizer
SU11248	VEGFR2, PDGFR, KIT, FLT3	Clinical Development	Indoline-2-one	Sugen/Pfizer
ZD6474	VEGFR2	Clinical Development	Quinazoline	AstraZeneca
PTK-787	VEGFR1/2, PDGFR	Clinical Development	Anilinophthalazine	Novartis/Schering
AG03736	VEGFR2, PDGFR	Clinical Development	-	Pfizer
CP549,632	VEGFR2, FGFR1, TIE2	Clinical Development	-	Pfizer
PKC-412	PKC, VEGFR2, PDGFR, FLT3, KIT	Clinical Development	N-Benzoylstaurosporine	Novartis
CEP-701	FLT3, TRK Kinases	Clinical Development	Indolocarbozole alkaloid	Cephalon
MLN-518	PDGFR, KIT, FLT3	Clinical Development	Quinazoline	Millennium

Table 1.3: Cancer therapies targeted to receptor tyrosine kinases.

Initially, inhibition of RTKs by ATP-directed compounds was considered less advantageous than substrate based inhibitors. This was due to the assumption that the catalytic domain of protein kinases is highly conserved and selectivity with ATP-competitive inhibitors would be difficult to achieve. Nonetheless, progress made in the crystallisation of protein kinases has confirmed that the ATP-binding domain of tyrosine kinases is indeed an attractive target for drug design (Traxler *et al.*, 2001). Numerous reviews cover the design, synthesis and biological evaluation of ATP site-directed inhibitors of RTKs (Traxler, 1998). The first selective RTK inhibitors discovered were the benzene malononitrile tyrphostins which were competitive with the

substrate and non-competitive with ATP. They poorly blocked the insulin receptor kinase and had no measurable activity against cAMP-dependent protein kinase.

Many tyrphostins were found to be ATP-competitive, substrate-competitive, or competitive against both (Levitzki, 2003). Most cyclised tyrphostins, incorporating a nitrile within a second ring, are ATP-competitive. Since 1994 the main focus in the development of inhibitors has been toward the generation of ATP-mimics. Given that the degree of conservation in the ATP binding site is not absolute, one can obtain a high degree of selectivity among closely related ATP binding domains. RTK inhibitors being developed are based on various types of core structures and are shown in Figure 1.18.

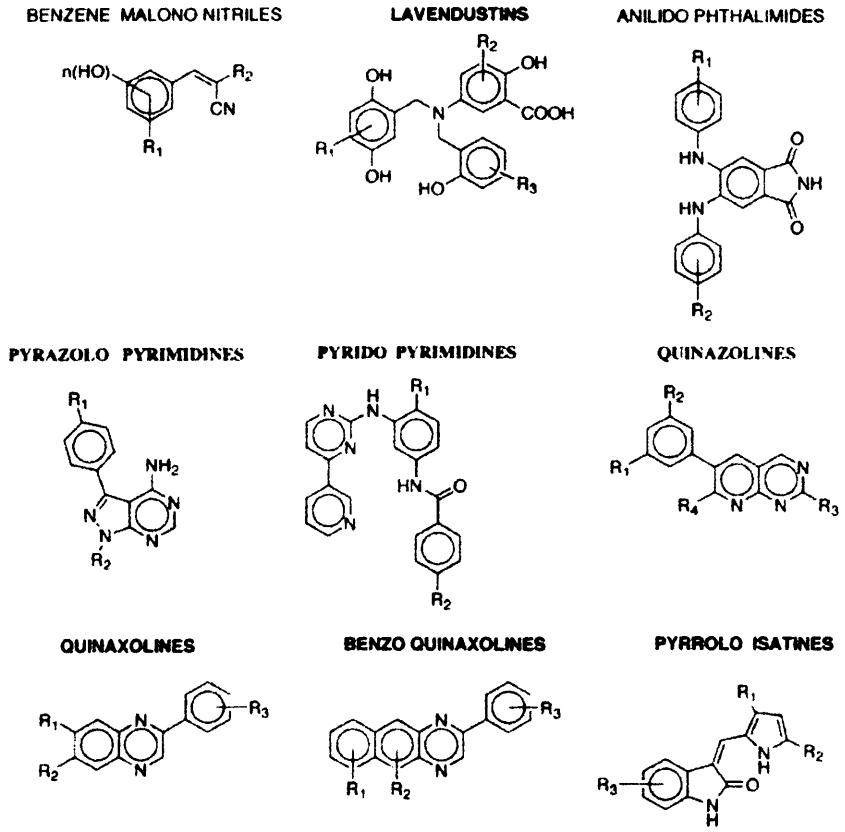

Figure 1.18: Different chemical core structures for development of RTK inhibitors.
Source: A. Levitzki, Accounts of Chem Res, 2003.

Currently, there are more than 20 ATP-competitive inhibitors in various phases of clinical evaluation (Gschwind *et al.*, 2004). To review all of these in detail is beyond the scope of this discussion. However, to allow us to appreciate the full potential of these small molecule inhibitors, the BCR-ABL inhibitor, imatinib is briefly outlined.

1.6.1 Imatinib (Gleevec™, STI561)

Chronic myelogenous leukaemia (CML) is a haematological stem cell disorder and is characterised by excessive myeloid proliferation (Wang, 1993). A reciprocal translocation between chromosomes 9 and 22 occurs resulting in the formation of the Philadelphia chromosome. Consequently, a novel hybrid *BCR* gene exists which produces a BCR-ABL fusion protein with enhanced tyrosine kinase activity (Traxler *et al.*, 2001). This is present in 95% of patients with CML and in about 15% of adults suffering from acute lymphoblastic leukaemia (ALL) (Deisseroth *et al.*, 1994). Imatinib (gleevec™, STI561) is a selective inhibitor of the BCR-ABL kinase (Figure 1.19).

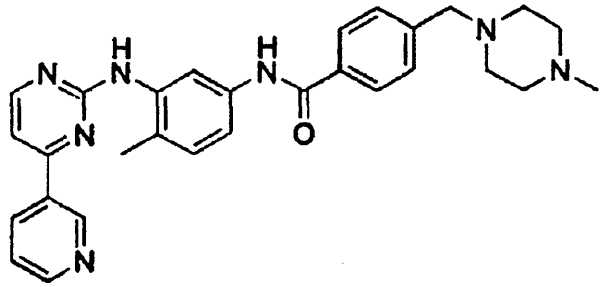

Figure 1.19: Chemical structure of imatinib.

As a 2-phenylaminopyrimidine structure, it has proven to be an excellent lead for the development of selective protein kinase inhibitors with high potency (Traxler, 2001).

Complete molecular remission occurs in only 5% of cases, and even in these cases BCR-ABL cells might be present, below the detection level (Klein *et al.*, 2005). Occasionally, resistance to imatinib can be due to amplification of the BCR-ABL gene (Gorre *et al.*, 2001) although it is usually due to specific mutations in the ABL tyrosine-kinase domain leading to a conformation within the kinase domain that prevents imatinib binding.

Combination therapy is the best approach to avoid selection for cancer cells that are resistant to therapy, and combinations of imatinib with interferon or cytarabine are being investigated (Gardembas *et al.*, 2003; Klein *et al.*, 2005).

Following imatinib treatment, relapse can occur but is not due to mutations since resumed imatinib treatment will control it (Cortes *et al.*, 2004). The cause may be due to CML stem cells as there is evidence that BCR-ABL is present in different haematopoietic lineages. This was first observed in acute myeloid leukaemia (AML) (Warner *et al.*, 2004). In light of this, it is possible that continuous treatment with imatinib can control CML stem cell proliferation (Klein *et al.*, 2005).

1.7 The Epidermal Growth Factor Receptor

1.7.1 HER Structure and Family

RTKs are divided into five subclasses based upon their molecular structure. All have an extracellular ligand-binding region with some containing immunoglobulin-like and leucine-rich domains as well. They possess intracellular tyrosine kinase activity and are capable of dimerisation. A schematic representation of the subclasses is shown in Figure 1.20.

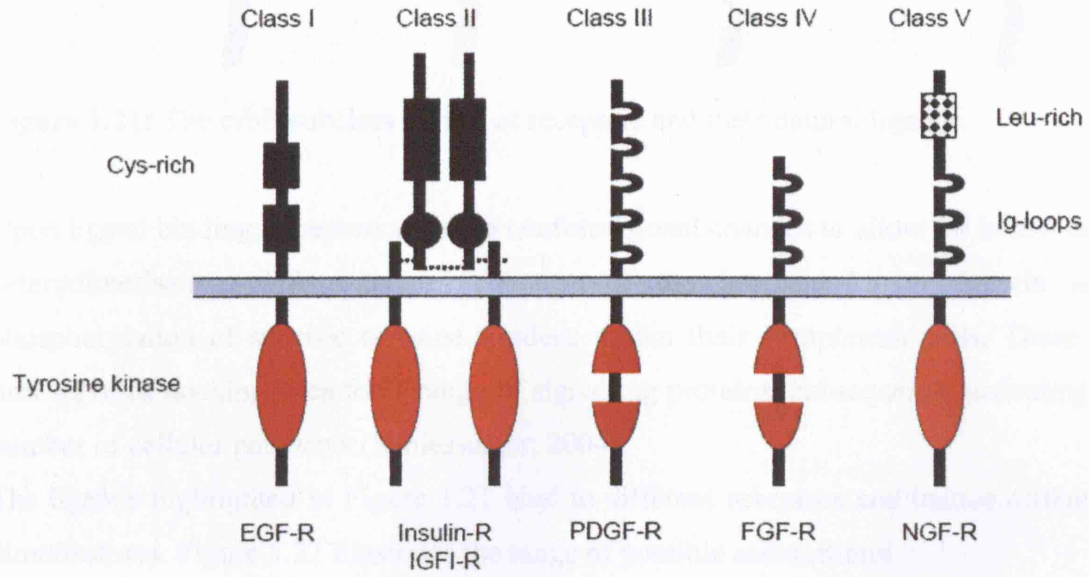

Figure 1.20: Schematic representation of receptor tyrosine kinase subclasses.

Subclass I of the RTK superfamily consists of the epidermal growth factor receptors (EGFR) (also known as the erbB or HER family). It is made up of four family members (EGFR/erbB1, HER-2/neu/erbB2, erbB3 and erbB4) all of which have an extracellular ligand-binding region, a single membrane-spanning region and a cytoplasmic tyrosine-kinase-containing domain (Figure 1.20). They are expressed in a number of tissue types of epithelial, mesenchymal and neuronal origin. Activation of the erbB receptors is controlled by the spatial and temporal binding of their natural ligands. These include EGF, amphiregulin, TGFα, epiregulin, betacellulin, heparin-binding EGF and neuregulins 1-4. They are members of the EGF family of growth factors (Figure 1.21) (Yarden & Sliwkowski, 2001).

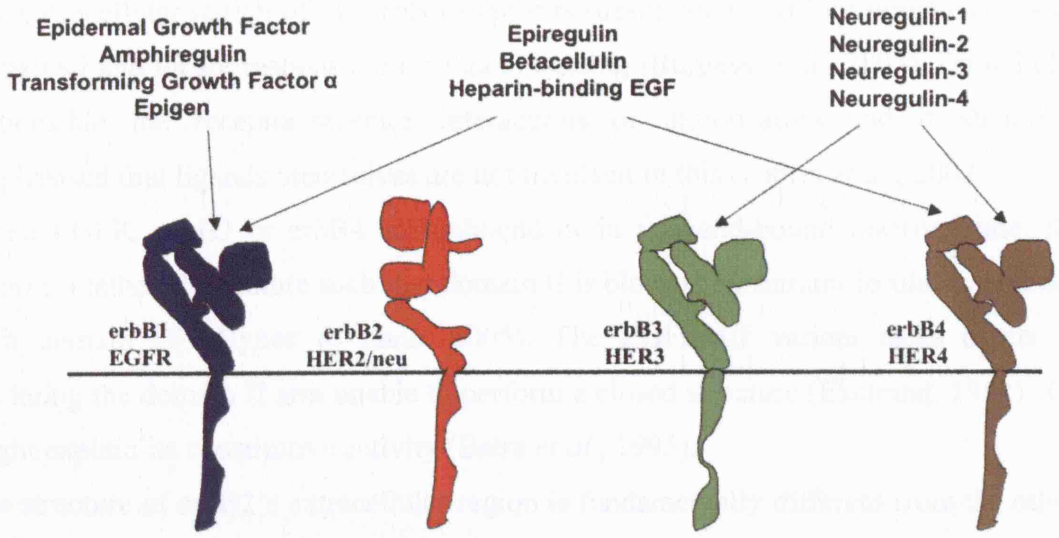

Figure 1.21: The erbB subclass family of receptors and their natural ligands.

Upon ligand binding, receptors undergo conformational changes to allow for homo- and heterodimerisation. This induces activation of the intrinsic kinase domain and phosphorylation of specific tyrosine residues within their cytoplasmic tails. These in turn serve as docking sites for a range of signalling proteins, subsequently activating a number of cellular pathways (Schlessinger, 2004).

The ligands highlighted in Figure 1.21 bind to different receptors and induce different dimerisations. Figure 1.22 illustrates the range of possible associations.

No ligand binds to erbB2. However, erbB2 is an important member of the family as it is the preferred heterodimerisation partner of the other ligand-bound family members (Hynes & Lane, 2005).

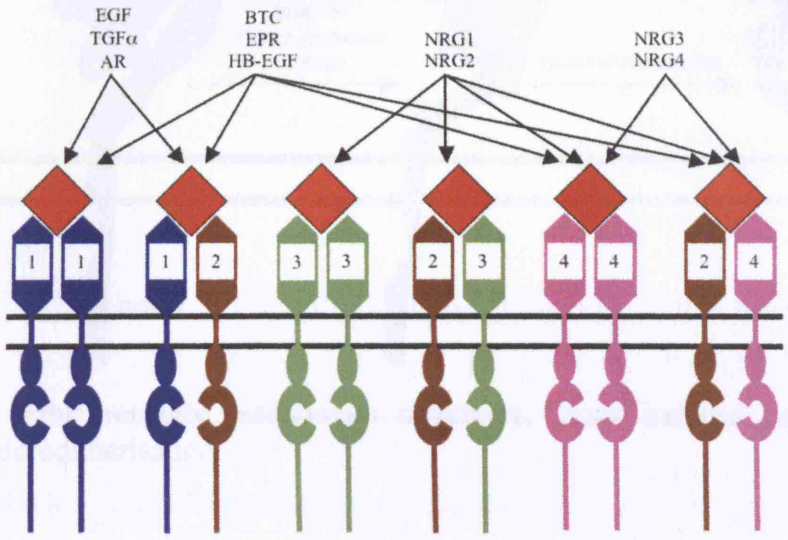

Figure 1.22: ErbB receptor ligands and the dimerisation actions they induce.

The extracellular region of the erbB receptor is sub-divided into four domains of which domains I and III are responsible for ligand binding (Burgess *et al.*, 2003). Domain II is responsible the receptor-receptor interactions of dimerisation and it should be emphasised that ligands themselves are not involved in this (Garret *et al.*, 2002).

When EGFR, erbB3 or erbB4 are unbound or in a ligand-bound inactive state, they assume a tethered structure such that domain II is blocked by intramolecular interactions with domain IV (Hynes & Lane, 2005). The EGFRvIII variant lacks exons 1-7 rendering the domain II arm unable to perform a closed structure (Ekstrand, 1992). This might explain its constitutive activity (Batra *et al.*, 1995).

The structure of erbB2's extracellular region is fundamentally different from the others. It has a fixed conformation in a ligand-active state with no domain II-IV interaction and an exposed domain II dimerisation region (Cho *et al.*, 2003). It possesses a unique domain I-III interaction which buries the binding site making recognition impossible. Given its permanent state of activation, it is the ideal partner for all other active erbB receptors (Hynes & Lane, 2005).

Figure 1.23 shows the extracellular region of erbB1 as a representative and the fixed erbB2 receptor conformation. Upon ligand binding (EGF in this example), erbB1 undergoes conformational change (appears as a mirror image of erbB2) and allows for heterodimerisation.

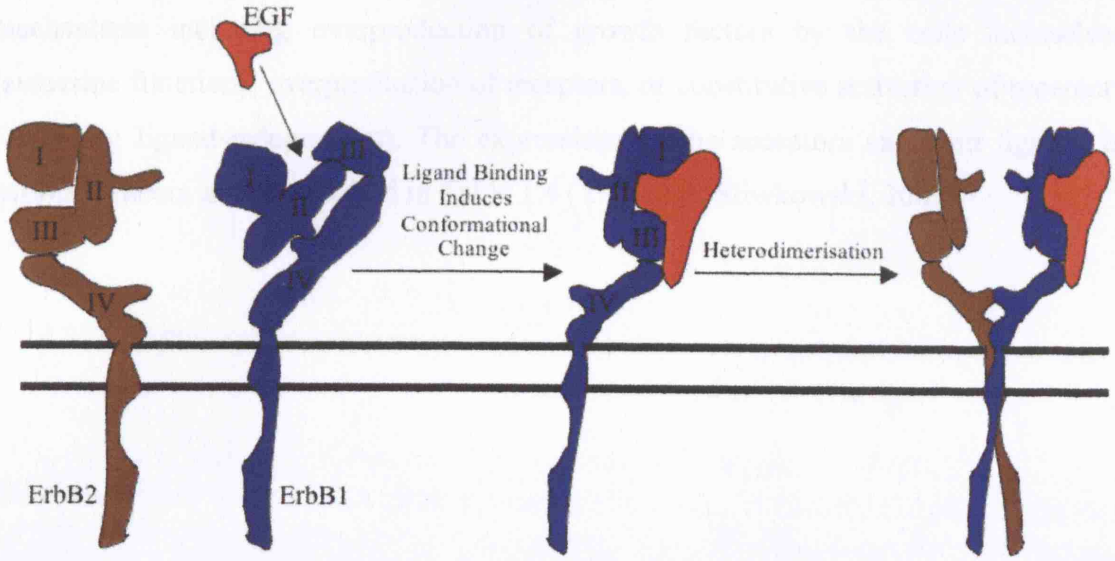

Figure 1.23: ErbB receptor ectodomain structures, ligand-induced conformational change and heterodimerisation.

ATP mediates the phosphorylation of tyrosine residues contained within the cytoplasmic region. This cleft, exposed for ATP accommodation is shown in Figure 1.24 and has been a crucial target region for the development of intracellular receptor inhibitors as will be discussed later.

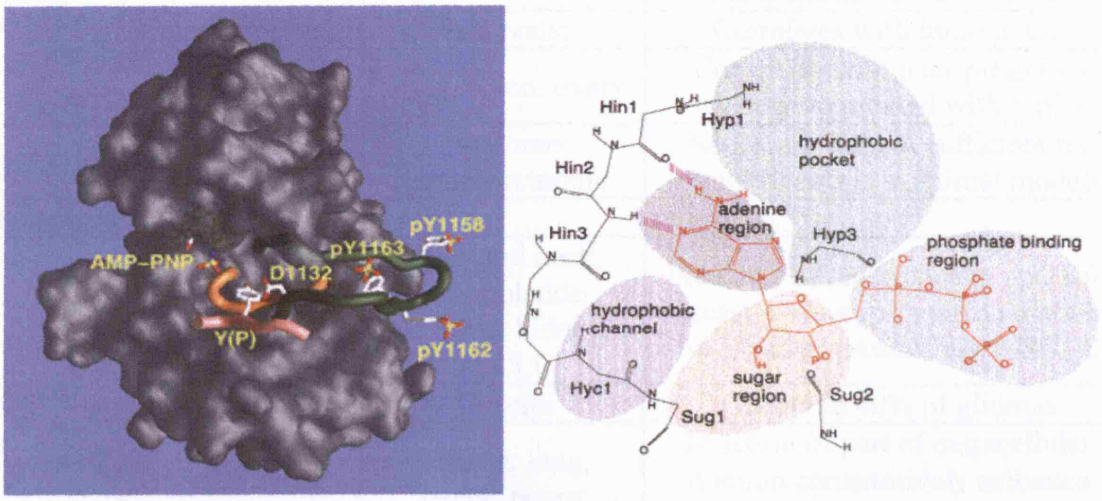

Figure 1.24: The ATP binding pocket contained within erbB RTK domains.
Source: Adapted from K.M. Ferguson, Biochem Soc Trans, 2004.

1.7.2 EGFR Function and Signalling

In many different cancer cells, the erbB pathway is hyperactivated by a range of mechanisms including overproduction of growth factors by the cells themselves (autocrine function), overproduction of receptors, or constitutive activation of receptors (including ligand-independent). The expressions of the receptors and their ligands in various cancers are summarised in Table 1.4 (Yarden & Sliwkowski, 2001).

Molecule	Nature of Dysregulation	Type of Cancer	Comments
Ligands			
TGFα	Overexpression	Prostate	Expressed by stroma in early androgen-dependent and independent prostate cancer
	Overexpression	Pancreatic	Correlates with tumour size
	Overexpression	Lung, colon, ovary	Correlates with poor prognosis when co-expressed with erbB1
NRG1	Overexpression	Mammary adenocarcinoma	Necessary but not sufficient for tumourigenesis in animal models
Receptors			
ErbB1	Overexpression	Head and neck, breast, bladder, prostate, kidney, NSCLC	Indicator of recurrence in operable breast tumour; prognostic marker for bladder, prostate and NSCLC
	Overexpression	Glioma	Occurs in 40% of gliomas
	Mutation	Glioma, lung, ovary, breast	Deletion of part of extracellular domain constitutively activates receptor
ErbB2	Overexpression	Breast, lung, pancreas, colon, oesophagus, cervix, endometrium	Amplification in 15-30% of invasive ductal breast cancers, spread of tumour to lymph nodes. High percentage of S phase cells and lack of steroid hormone receptors
ErbB3	Expression	Breast, colon, gastric, prostate, other carcinomas	Co-expression with erbB1 & erbB2 improves predicting ability
	Overexpression	Oral squamous cell cancer	Correlates with lymph node involvement
ErbB4	Reduced Expression	Breast, prostate	Correlates with differentiated phenotype
	Expression	Childhood medullo-blastoma	Co-expression with erbB2 has a prognostic value

Table 1.4: Expression of erbB receptors and their ligands in cancer.

As receptor tyrosine kinases, their general signalling possibilities are summarised in Figure 1.25.

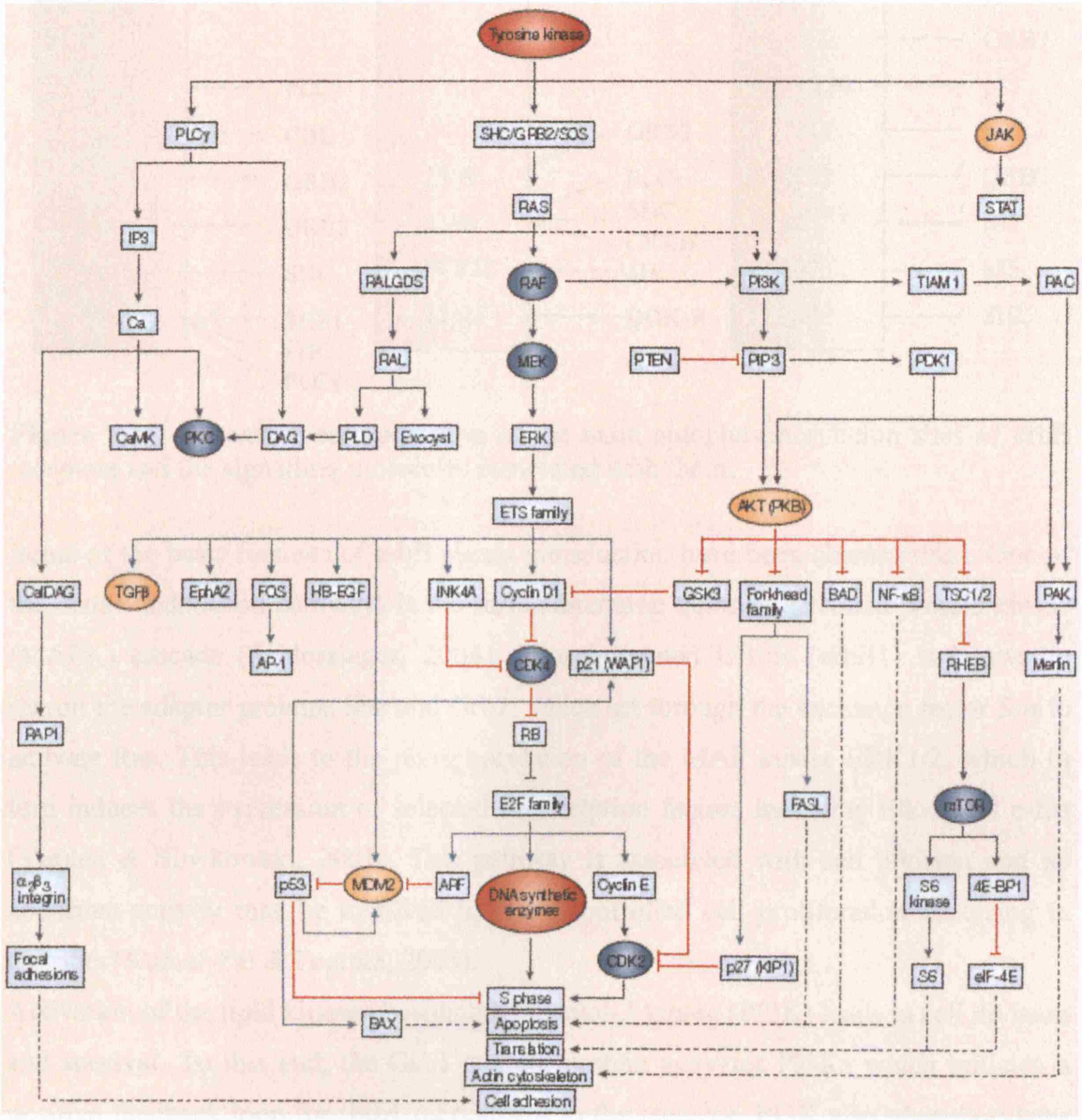

Figure 1.25: ErbB tyrosine kinase signalling pathways.
Black arrows show direct activation events; green arrows denote direct transcriptional targets; red lines show inhibitory pathways and dashed arrows show events that are either indirect or questionable.

Source: S. Klein et al., Nat Rev Cancer, 2005.

Different erbB receptors preferentially modulate certain signalling pathways because of their individual ability to activate specific effector proteins through specific tyrosine residues on their intracellular sites as shown in Figure 1.26 (Hynes & Lane, 2005).

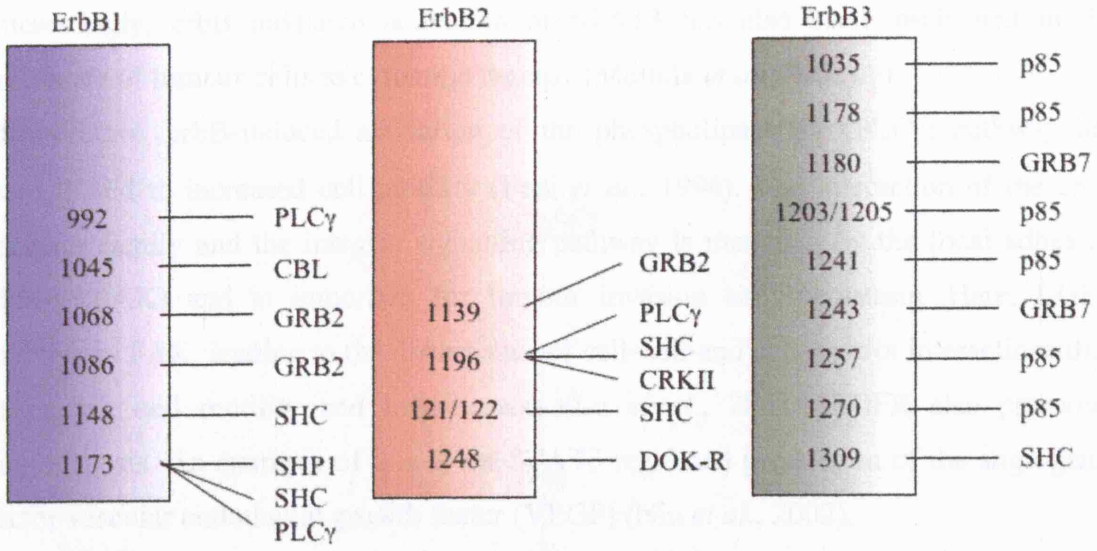

Figure 1.26: Schematic representation of the main autophosphorylation sites of erbB receptors and the signalling molecules associated with them.

Some of the basic features of erbB signal transduction have been characterised. One of the better-understood pathways is the serine/threonine mitogen-activated protein kinase (MAPK) cascade (Schlessinger, 2004). Phosphorylated EGFR (erbB1) is known to recruit the adaptor proteins Shc and Grb2, which act through the exchange factor Sos to activate Ras. This leads to the phosphorylation of the MAP kinase ERK1/2, which in turn induces the expression of selected transcription factors including Elk-1 and c-fos (Yarden & Sliwkowski, 2001). This pathway is associated with cell division and its abnormal activity may be involved in the uncontrolled cell proliferation occurring in tumours (Kumar-Pal & Pegram, 2005).

Activation of the lipid kinase phosphotidylinositol-3 kinase (PI3K) leads to cell division and survival. To this end, the Gab1 adaptor protein activates PI3Ks which initiates a positive feedback loop for Gab1 recruitment to the receptor. PI3K also phosphorylates AKT (PKB) leading to an anti-apoptotic response through the transcription factor nuclear factor (NF)-κB. This is also activated through PKC, a pathway associated with cell cycle progression (Prenzel *et al.*, 2001).

A third pathway is mediated by the cytoplasmic tyrosine kinase c-Src which is involved in a number of cellular processes, including mitogenic signalling (Hynes & Lane, 2005). Amongst the known c-Src substrates, the signal transducer and activator of transcription (STAT) family of transcription factors is known to be of particular importance in the proliferation and survival of cancer cells. In fact, activation of STAT3 initiates a TGF-induced autocrine growth of transformed epithelial cells (Yu & Jove, 2004).

Interestingly, erbB mediated activation of STAT3 has also been implicated in the resistance of tumour cells to cytotoxic therapy (Mesuda *et al.*, 2002).

Furthermore, erbB-induced activation of the phospholipase Cγ (PLCγ) pathway has been linked to increased cell motility (Fedi *et al.*, 1994). The interaction of the erbB receptor family and the integrin signalling pathway is mediated by the focal adhesion kinase (FAK) and is important for tumour invasion and metastasis. Here, EGFR inactivates FAK, leading to the disturbance of cell–cell and cell–matrix interactions thus promoting cell motility and invasiveness (Lu *et al.*, 2001). EGFR also promotes angiogenesis. An example of this is the STAT3 regulated production of the angiogenic factor vascular endothelial growth factor (VEGF) (Niu *et al.*, 2002).

Other proto-oncogenes activated include *fos*, *jun* and *myc* as well as a family of zinc-finger-containing transcription factors such as Sp1, Egr1 and Ets family members (e.g. GA-binding protein (GABP)) (Yarden, 2001).

The principal process responsible for turning off the erbB network is ligand-mediated receptor endocytosis which is dependent on receptor composition (Yarden & Sliwkowski, 2001).

ErbB receptors are often constitutively stimulated in cancer which is often due to the presence of EGF ligands in the tumours. The proteases involved in ligand preparation (by ectodomain shedding) are members of the metalloproteinase family, in particular the ADAM (a disintigrin and metalloprotease) family and matrix metalloproteinases (MMPs) (Hynes & Lane, 2005). ADAMs, have shown to be associated with the shedding of distinct EGF-related ligands in cancer cells. In primary breast tumours, there is a correlation between high EGFR activity and high ADAM17 levels (Borrell-Pages *et al.*, 2003).

For certain cancer types, such as prostate cancer, the deregulated expression of GPCRs and their associated ligands have been linked to tumour development (Daaka, 2004).

Oestradiol (E2), which normally binds to an oestrogen receptor (ER), has been shown to rapidly transactivate erbB receptors (Hynes & Lane, 2005). Tamoxifen, a selective ER modifier was shown to mimic this effect and transactivate erbB1 and erbB2 thus reducing the antiproliferative activity in erbB2-overexpressing breast cancer cells (Shou *et al.*, 2004).

1.7.3 EGFR Tyrosine Kinase as a Target for Anti-Cancer Therapy

The growing realisation that multiple tumourigenic processes are regulated by EGFR signalling pathways has led to research into the mechanisms and effects of EGFR inhibition. Various strategies have been approached to shut down the EGFR pathway, including monoclonal antibodies (mAbs) directed towards EGFR or one of its ligands, bispecific antibodies, immunotoxin conjugates, ligand-EGFR inhibitor conjugates, ligand-toxin conjugates, antisense oligonucleotides and intracellular tyrosine kinase inhibitors (Figure 1.27) (Raymond *et al.*, 2000). Many of these agents are currently undergoing clinical testing and are reviewed in Table 1.5.

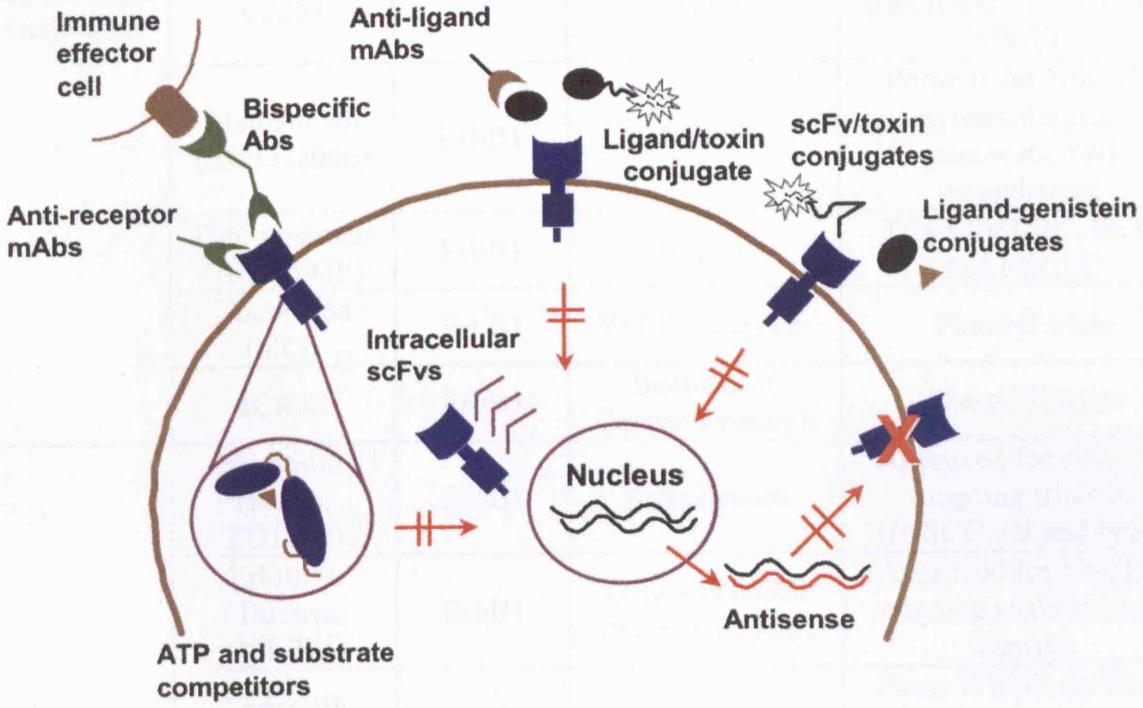

Figure 1.27: Targets for modulating erbB receptor signalling.

Numerous *in vitro* studies and mouse xenograft models of human cancers have shown that EGFR targeted therapy inhibits many mechanisms involved in tumour progression. Preclinical studies inhibited tumour cell proliferation by inducing G_1 cell cycle arrest in a variety of carcinoma cell lines through the inhibition of EGFR-mediated upregulation of cyclin-dependent kinase inhibitors (Peng *et al.*, 1996; Fan *et al.*, 1997; DiGennaro *et al.*, 2003)

Differing agents have different specificity and selectivity for EGFR inhibition. This in turn leads to differing effects in the clinic and will be the focus of discussion later.

Approach	Compound	ErbBR Target	Company	Status
Monoclonal Antibodies	Trastuzumab (Herceptin)	ErbB2	Genentech/ Roche	Approved for ErbB2-overexpressing breast cancer; ongoing trials for use with other drugs
	Pertuzumab (Omnitarg)	ErbB2	Genentech	Phase II for ovarian, breast, prostate and NSCLC – blocks dimerisation
	Cetuximab (Erbitux, C225)	ErbB1	ImClone/Merck/ Bristol Myers Squibb	Approved for CRC; ongoing trials for use with other drugs for pancreatic, HNSCC and NSCLC
	Matuzumab (EMD72000)	ErbB1	Merck	Phase II for NSCLC, gynaecological, pancreatic and oesophageal
	Panitumamab (ABX-EGF)	ErbB1	Abgenix	Trials for CRC, RCC, and NSCLC
	TheraCIM (hR3)	ErbB1	YM Biosciences	Phase II trials
	ICR62	ErbB1	Institute of Cancer Research	Phase I/II trials
Tyrosine Kinase Inhibitors	Gefitinib (Iressa, ZD1839)	ErbB1	AstraZeneca	Approved for NSCLC; ongoing trials in HNSCC, GI and breast
	Erlotinib (Tarceva, OSI-774)	ErbB1	Genentech/OSI Pharmaceuticals	Approved for NSCLC; ongoing trials in many cancers
	Lapatinib (GW-57 2016)	ErbB1 ErbB2	GlaxoSmithKline	Phase II trials on breast with refractory to trastuzumab and chemotherapy
	AEE788 (PKI-166)	ErbB1 ErbB2 VEGFR	Novartis	Phase I underway – first multifunctional inhibitor
	Canertinib (CI-1033)	ErbB1 ErbB2	Pfizer	Phase II trials in breast and NSCLC
	EKB-569	ErbB1 ErbB2	Wyerth-Ayerst	Phase II trials in NSCLC
	EXEL 7647/ EXEL 0999	ErbB1 ErbB2 VEGFR	EXELIXIS	Phase I trials
Ligand-Toxin Conjugate	TP-38	N/A	Duke University/ National Cancer Institute	Phase I/II trials

Table 1.5: ErbB-targeted therapeutics in clinical use.

1.7.3.1 Blocking of the Extracellular Regions of ErbB Receptors

Targeting EGFR (ErbB1, HER-1)

Targeting of the extracellular ligand-binding domain of EGFR with monoclonal antibodies (mAbs) is a rational therapeutic approach for EGFR-expressing cancers. The first and most extensively studied anti-EGFR antibody is cetuximab (erbitux, C225, IMC-225), a chimeric antibody developed by combining the variable regions of the precursor mouse antibody (mAb-225) with human IgG_1 constant regions thus reducing the possibility of an anti-mouse immunological reaction in patients (HAMA) (Herbst & Shin, 2002; Harari, 2004). Cetuximab is highly specific for EGFR, competing for natural ligand-binding sites and causing receptor internalisation and downregulation (Kim *et al.* 2001). It has demonstrated anti-tumour activity against a wide range of tumour cell lines and human xenografts in numerous preclinical studies (Mendelsohn, 2001; Kim *et al.*, 2001). The *in vivo* effects of cetuximab are due to inhibition of proliferation, induction of apoptosis, and disruption of angiogenesis and metastasis (Kumar-Pal & Pegram, 2005). It has recently been approved by the US Food and Drug Administration (FDA) and extensive phase II and III trials for cetuximab either alone or in combination with radio- or chemotherapy are continuing in colorectal carcinoma (Cunningham *et al.*, 2004; Saltz *et al.*, 2004), pancreatic carcinoma (Xiong *et al.*, 2004) and non-small cell lung cancer (NSCLC) (Lynch *et al.*, 2004). Promising results are emerging in the treatment of squamous cell carcinoma of the head and neck (SCCHN) (Baselga and Arteaga, 2005).

Cetuximab was shown to bind to EGFR with a higher affinity (Kd=0.1–0.2 nM, approximately 10 times greater than the natural ligands) with no patients developing anti-chimeric antibodies (Kumar-Pal & Pegram, 2005).

Therapeutic antibodies of the IgG_1 isotype, such as cetuximab, activate immune system effector functions such as antibody-dependent cell-mediated cytotoxicity (ADCC) through the antibody Fc domain (Burton & Woof, 1992). The mAbs matuzumab and ICR62 have also demonstrated strong anti-tumour ADCC *in vitro* (Bier *et al.*, 1998).

Clinically relevant adverse responses to cetuximab include allergic reactions and skin toxicity (Kumar-Pal & Pegram, 2005). It is the first and only anti-EGFR antibody in a phase III randomised, controlled clinical trial to demonstrate a statistically significant increase in survival and locoregional control (Bonner *et al.*, 2004).

Other anti-EGFR mAbs in clinical development include panitumamab. This was

selected from a panel of human IgG_2 anti-EGFR mAbs generated by immunising the xenomouse IgG_2 strain with cells of the human cervical epidermal cancer cell line A431, which express more than 106 EGFR molecules per cell (Davis *et al.*, 1999). *In vitro* studies show it successfully blocks the binding of both EGF and TGFα to the receptor, inhibits EGF-activated EGFR tyrosine phosphorylation and inhibits tumour cell activation and proliferation (Yang *et al.*, 2001, Lynch & Yang 2002). Like cetuximab, panitumamab causes EGFR internalisation in tumour cells thus inhibiting EGFR tyrosine kinase activity (Harari, 2004). Experiments *in vivo* show that antitumor activity mediated by panitumamab correlates with the levels of EGFR expression on the human tumours tested (Harari, 2004). Recent *in vitro* and *in vivo* efficacy has been shown in studies of prostate and renal cell carcinoma (Wang *et al.*, 2003).

The humanised antibodies MDX-447 (Medarex) which has dual activity against EGFR and the Fc receptor, and matuzumab (EMD72000) are also promising agents currently being evaluated in clinical trials for several tumours including head and neck and ovarian cancer respectively (Harari, 2004). Unique antibodies raised against the EGFRvIII mutant form of the EGFR are also in development (Mishima *et al.* 2001).

Targeting ErbB2 (HER-2, Neu)

Trastuzumab (Herceptin) was shown to block overexpressing erbB2 tumour cells but not in tumour cell lines with low levels of the receptor (Sliwkowski *et al.*, 1999).

Clinical studies have shown that the addition of trastuzumab to standard chemotherapy prolonged relapse-free survival, leading to the approval of the drug for treatment of erbB2-overexpressing metastatic breast cancer patients (Hynes & Lane, 2005). It has also been shown to downregulate receptor expression and its mediated pathways (Lane *et al.*, 2000).

The erbB2-overexpressing metastatic breast cancer response rate to trastuzumab is approximately 35%. Possible reasons for this may be due to resistance but also perhaps because the nature of the tumour is not only due to erbB2 overexpression. Clinical studies have led to the proposing of several theories for poor response. One possible explanation is that ligands can bind alternative erbB receptor homo- and heterodimers. Trastuzumab binds to domain IV of the receptor which is not involved in dimerisation. By contrast, pertuzumab binds erbB2 near the centre of the domain II dimerisation arm thus preventing the formation of ligand-induced erbB2-containing heterodimers

(Franklin *et al.*, 2004). This may partly explain why pertuzumab inhibits growth of low-expressing erbB2 tumours whereas trastuzumab does not (Hynes & Lane, 2005).

1.7.3.2 Blocking of the Intracellular Region of EGFR (ErbB1, HER-1)

EGFR tyrosine kinase inhibitors exert their activity intracellularly preventing tyrosine phosphorylation and subsequent signalling shutdown. These small-molecule, low-molecular-weight agents are usually quinazoline- or pyrazolo/pyrrolo/pyrido-pyrimidine derivatives. They work by competing for and inhibiting the Mg^{2+}-dependent ATP binding site of the receptor. These inhibitors differ in their potency, specificity, reversibility of action and bioavailability. The chemical structures of some reversible inhibitors are shown in Figure 1.28 (Levitzki, 2003).

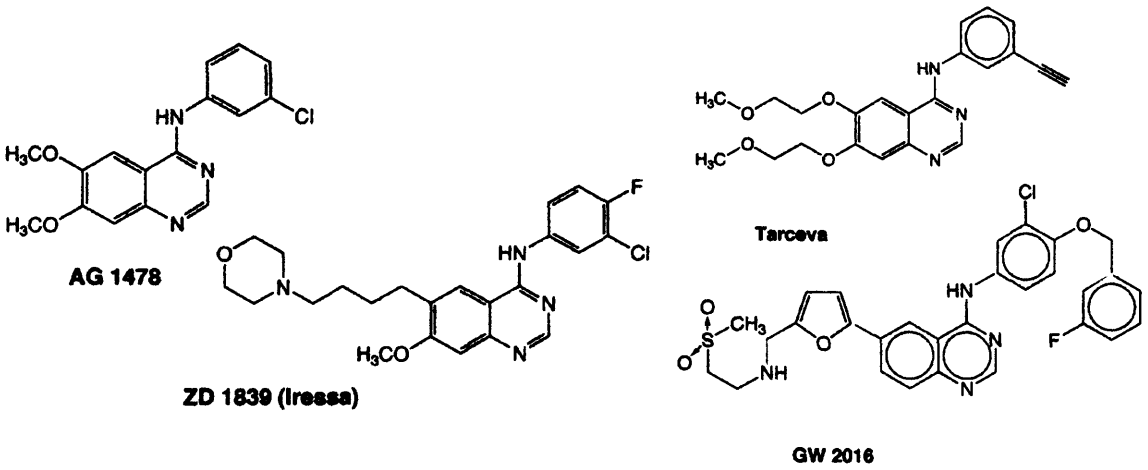

Figure 1.28: Chemical structures of some reversible quinazoline-based EGFR kinase inhibitors.

Source: A. Levitzki, Accounts of Chem Res, 2003.

Irreversible EGFR Kinase Inhibitors

The covalent binding of an irreversible selective inhibitor of the EGFR kinase domain completely removes any catalytic capability and is therefore believed to have better clinical potential (Levitzki, 2003) (Figure 1.29). Canertinib, an EGFR, erbB2 and erbB4 inhibitor is effective in preclinical *in vivo* experiments. However, it is quite toxic in patients. This is most probably due to the high chemical reactivity of its acryloyl group (Wissner *et al.*, 2003). To improve the specificity of irreversible kinase inhibitors the chemical reactivity of the labelling group might have to be reduced. This will limit the unwanted reaction of the inhibitor binding to non-specific targets (Levitzki, 2003).

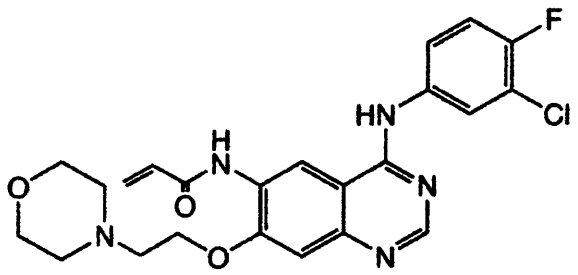

Figure 1.29: Chemical structure of canertinib, an irreversible EGFR kinase inhibitor.
Source: A. Levitzki, Accounts of Chem Res, 2003.

Erlotinib (Tarceva, OSI-774)

Erlotinib is a reversible quinazoline-type inhibitor of the EGFR tyrosine kinase domain. It inhibits proliferation of DiFi human colon tumour cells at submicromolar concentrations, blocks cell cycle progression at the G_1 phase and triggers apoptosis (Moyer *et al.*, 1997). It also completely prevents EGF-induced phosphorylation of EGFR in human HN5 tumour xenografts in athymic mice (Moyer *et al.*, 1997).

Erlotinib given in combination with cisplatin produces a significantly greater response as compared with cisplatin alone, with no detected effects on body weight or lethal toxicity (Harari, 2004). Both *in vitro* and *in vivo* studies have shown that erlotinib is effective in colorectal, head and neck, NSCLC and pancreatic tumour cells (Akita & Sliwkowski, 2003). In addition, erlotinib has recently been shown to have an effect on tumours dependent on erbB2 activity (Harari, 2004). Preclinical combination studies of erlotinib with cisplatin, doxorubicin, gemcitabine or low-dose paclitaxel produced an additive effect with no increase in toxicity (Akita & Sliwkowski, 2003). Interestingly, erlotinib can specifically inhibit mutant EGFRvIII transformed cells which are present in glial tumours (Iwata *et al.*, 2002).

Gefitinib (Iressa^{TM}, ZD1839)

Gefitinib is a novel, low-molecular-weight synthetic anilinoquinazoline (4-(3-chloro-4-fluoroanilino)-7-methoxy-6-(3-morpholinopropoxy)-quinazoline) (Figure 1.30). Its design allows reversible inhibition of the ATP binding domain of the intracellular region of EGFR. Of all TKIs synthesised, it was expected to achieve the strongest clinical success (Herbst *et al.*, 2004). Inhibition of EGFR by gefitinib causes a reduction of the transcription factor, cFOS, mRNA which forms part of the AP1 complex, and a shift of cells from S phase into G_0/G_1 (Raben *et al.*, 2002).

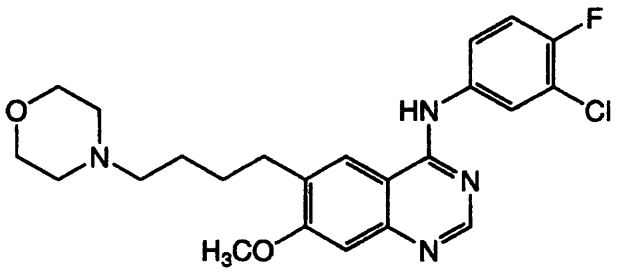

Figure 1.30: Chemical structure of Gefitinib (Iressa™, ZD1839).

Studies have shown that gefitinib is a potent selective inhibitor with high and sustained blood levels over 24 hour periods in bioassays (Barker *et al.*, 2001). It has minimal binding affinity to other RTKs including other EGFR family members, VEGFRs, and all serine/threonine kinases (Wakeling *et al.*, 2002). Gefitinib inhibits the proliferation of several solid tumour cell lines including ovarian, breast, colon, NSCLC and head and neck carcinomas. As with cetuximab and erlotinib, it produces a synergistic increase in inhibition of proliferation of tumour cells in combination with a number of chemotherapeutic agents and will be the subject of much discussion in later chapters (Ciardiello *et al.*, 2000; Sirotnak *et al.*, 2000; Moasser *et al.*, 2001). In addition, gefitinib has shown dose-dependent anti-tumour activity in athymic nude mice bearing a range of xenografts (Herbst *et al.*, 2004).

Early Clinical Developments

Phase I trials were carried out in patients with a range of advanced, refractory, malignant tumours including NSCLC, and were important to the success of the biomarker programme (Baselga *et al.*, 2002; Herbst *et al.*, 2002).

The basal layers of the epidermis express high levels of activated EGFR. Because of this, skin biopsies (pre- and on-therapy) were also included in the studies to evaluate whether gefitinib is successfully blocking EGFR-mediated processes in patients (Albanell *et al.*, 2002). These results confirmed that at sub-toxic doses, gefitinib completely prevented EGFR phosphorylation, decreased MAPK-mediated signalling, increased apoptosis and also increased levels of the cyclin-dependent kinase inhibitor p27 – a precursor to G_1 cell cycle arrest (Herbst *et al.*, 2004). Proliferation was also reduced as measured by a decrease in the proliferation marker Ki67 (Herbst *et al.*, 2004). The most common adverse effects reported in these trials were diarrhoea, nausea,

rash, vomiting and asthenia. Most of these were mild in severity and short-lived, according to National Cancer Institute Common Toxicity Criteria (NCI Evaluation Programme, 1999).

Dose-response studies of gefitinib in solid tumours (mainly in NSCLC) produced promising results across the dose range tested. This highlights a fundamental difference in the dose-toxicity-activity relationships between chemotherapeutic agents and targeted molecular therapies (Herbst *et al.*, 2004). With chemotherapy, dosage used has to be a balance between its anti-tumour activity and its toxicity. This dictates the maximum tolerated dose (MTD) of any given chemotherapeutic agent. Complications can therefore arise if the MTD is lower than the dose needed for effective treatment. Biologically targeted agents like gefitinib, are usually effective well below their MTD and can therefore be administered at their optimal biological dose. It is these molecules that provide the much-needed improvement of risk to benefit ratio (Wolf *et al.*, 2004).

Clinical Developments

Two large Phase II studies – the Iressa Dose Evaluation in Advanced Lung cancer (IDEAL) 1 and IDEAL 2 were undertaken (Fukuoka *et al.*, 2003; Kris *et al.*, 2003). They compared antitumour activity and safety of two doses of gefitinib, 250 and 500 mg/day, in patients with advanced NSCLC who had relapsed following previous treatment with platinum based chemotherapy. Both IDEAL trials reported similar rates of response and disease stability. The 1-year survival rates of pre-treated patients with NSCLC who received 250 mg/day gefitinib was about 31% for each trial with a median overall survival of about seven months (Fukuoka *et al.*, 2003; Kris *et al.*, 2003).

A large Phase III controlled study has very recently been carried out – Iressa Survival Evaluation in Lung cancer (ISEL). It included 1,692 patients with locally advanced or metastatic NSCLC. In this large study patients were randomly assigned to receive gefitinib 250 mg/day versus placebo. Gefitinib failed to statistically prolong survival in comparison to placebo in the overall population or in patients with adenocarcinoma (Thatcher *et al.*, 2005) (www.astrazeneca.com/pressrelease/4245.aspx). In contrast, a similar Phase III trial with erlotinib (BR.21) has also been carried out. 731 patients with NSCLC who received first- or second-line chemotherapy were randomly assigned to receive a lower dose of erlotinib (150 mg/day) or placebo in a 2:1 randomised ratio. Of the patients, 50% had received two prior chemotherapy regimens and 93% had received

platinum. Overall response to erlotinib was 8.9% with median treatment duration of approximately 34 weeks. In comparison with gefitinib which prolonged survival by two weeks (5.6 months versus 5.1 months for placebo), erlotinib prolonged survival by two months (6.7 months versus 4.7 months for placebo) (Baselga & Arteaga, 2005).
Reasons for the differences observed are as yet unknown. However, it is possible that these two agents, by promiscuously cross-reacting with other kinases or by their different molecular interactions with the EGFR kinase domain, may result in different activity profiles. Alternatively, and perhaps in addition, it is possible that they were used at doses with different biochemical potencies against the EGFR (Baselga & Arteaga, 2005). This will be discussed in more detail in a later chapter.

Based on the results of the Phase II IDEAL trials, gefitinib was approved in Japan on July 5, 2002, for the treatment of inoperable or recurrent NSCLC. Subsequently, gefitinib has gained approval for the treatment of previously treated NSCLC in over 30 countries, including the United States (Herbst *et al.*, 2004).
An interesting study was recently carried out to investigate the effects of combining cetuximab with either gefitinib or erlotinib in a variety of human cancer cells (Huang *et al.*, 2004). The combinations enhanced growth inhibition as compared with either agent alone. In addition, phosphorylation inhibition of downstream effector molecules (MAPK and AKT) was also enhanced, as was an increased induction of apoptosis. Furthermore, a more profound tumour regression and regrowth delay was seen in mice treated with the combination.
These studies suggest that combined treatment with distinct EGFR inhibitory agents can augment the potency of EGFR signalling inhibition. This approach suggests potential new strategies to maximise effective target inhibition, which may improve the therapeutic ratio for anti-EGFR-targeted therapies in developing clinical trials.

Other ErbB Receptor Tyrosine Kinase Inhibitors

Other HER receptor family tyrosine kinase inhibitors in clinical development include the GlaxoSmithKline compound lapatinib, EKB-569 (Wyeth Ayerst) and the pyrrolopyrimidine compound, PKI-166 (Novartis). Of these, lapatinib was the first inhibitor specifically designed to inhibit both EGFR and HER-2 (Harari, 2004).

In contrast to the mAbs, TKIs do not induce an immune response but do appear to inhibit internalisation of erbB receptors. A recent study demonstrated that the EGFR specific inhibitor, PD158780, inhibits the recruitment of EGFR to clathrin-coated pits, the first stage in receptor endocytosis (Sorkina *et al.* 2002). TKIs also show activity against other receptors such as HER-2 at higher concentrations (gefitinib and erlotinib) or all four HER (erbB) receptors as in the case of canertinib. The clinical significance of the differences in activity between mAbs and TKI compounds requires further investigation (Harari, 2004).

1.7.4 Resistance to EGFR-Targeted Therapy

Although anti-EGFR targeted therapies are active in some patients, nearly all patients, become refractory to therapy. Therefore, a better understanding of the mechanisms of resistance to anti-EGFR therapies is critical to further improve the efficacy of this class of agents. Mutations in EGFR appear to play a significant role in determining the sensitivity of tumour cells to EGFR inhibitor therapy by altering the conformation and activity of the receptor and will be discussed later. The molecular mechanisms of resistance include:

1.7.4.1 Presence of Redundant Tyrosine Kinase Receptors

Resistance can be due to the activation of alternative RTKs that bypass the EGFR pathway. This will ensure tumour cell survival and proliferation. Other tyrosine kinase receptors capable of this include c-MET (hepatocyte growth factor receptor), Ron (a protein tyrosine kinase related to c-MET), platelet-derived growth factor receptor (PDGFR), and insulin-like growth factor receptor-1 (IGF-1R). Activation of distinct growth factor receptors leads to initiation of pathways that impact multiple cell functions (Camp *et al.*, 2005).

1.7.4.2 Increased Angiogenesis

There is increasing evidence suggesting that EGFR-mediated pathways are intimately involved in tumour angiogenesis through up-regulation of vascular endothelial growth factor (VEGF) and other mediators of angiogenesis. Activation of EGFR by EGF or TGFα has been shown to up-regulate VEGF expression in colorectal cancer, human glioma, prostate cancer, and HNSCC cells *in vitro* (Brancroft *et al.*, 2002).

1.7.4.3 Constitutive Activation of Downstream Mediators

Although EGFR activation stimulates numerous pathways, other potential mechanisms can achieve similar effects. Alterations in genetic mechanisms of signalling mediators leading to their constitutive activation, will no longer require prior signalling via EGFR, thus decreasing the efficacy of EGFR inhibition. One of the most common examples of this potential resistance mechanism is the loss of PTEN/MMAC/TEP (PTEN) phosphatase function through genetic mutation (Camp *et al.*, 2005).

1.7.4.4 EGFR Mutations and Subsequent Sensitivity

Mutations of EGFR have been found in various human malignancies, including gliomas, NSCLC, and breast and ovarian carcinomas. The best characterised is the EGFR variant III (EGFRvIII) seen in up to 40% of glioblastomas as well as in breast and ovarian carcinomas. The EGFRvIII mutation results from an in-frame deletion from exons 2 through 7 in the extracellular domain of EGFR. The mutated gene expresses a constitutively active truncated receptor. In glioma cells this leads to aggressive tumours that are resistant to chemotherapy and show enhanced growth and metastasis (Camp *et al.*, 2005). Their response to EGFR TKIs seems to be diminished relative to that of the wild-type EGFR. In the EGFRvIII-expressing tumours, AKT phosphorylation was not inhibited by gefitinib, suggesting that signalling persisted downstream of the mutated receptor (Learn *et al.*, 2004). No clinical data has been published regarding treatment of EGFRvIII-expressing tumours with EGFR mAbs (Camp *et al.*, 2005).

It is not fully understood why some patient subgroups are more likely to respond to gefitinib than others. However, there have been a number of recent reports about some patients with a marked response to gefitinib. These patients have been shown to express somatic mutations in exons 18-21 in the ATP-binding region of the tyrosine kinase domain in the *EGFR* gene (Figure 1.31) (Lynch *et al.*, 2004; Paez *et al.*, 2004).

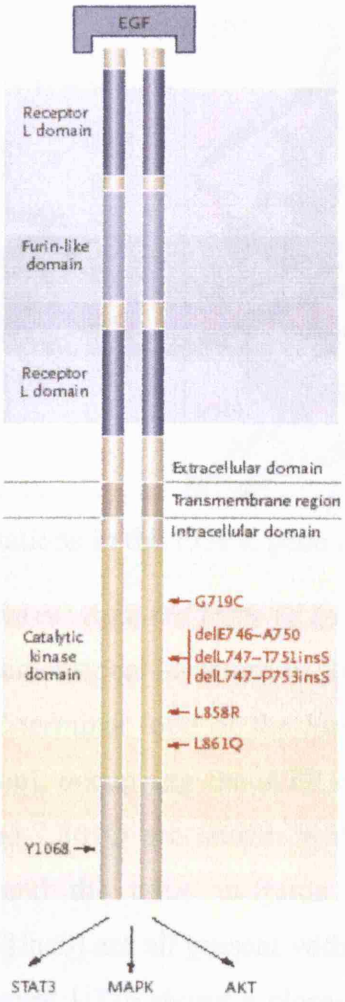

Figure 1.31: Mutations in the EGFR gene in gefitinib-responsive patients.
Source: TJ Lynch et al., N Engl J Med, 2004.

These mutations might therefore predict those patients who are likely to have an objective response to gefitinib. Paez *et al.*, (2004), investigated somatic genetic alterations in NSCLC primary tumour biopsies from 119 unselected patients. In total, 18 different mutations were found in exons 18-21 all clustered around the TK domain of the *EGFR* gene. These mutations were most frequent in adenocarcinomas in Japanese women who were non-smokers (Paez *et al.*, 2004). At the same time in a different study, it was also shown that of nine patients with NSCLC who had achieved an objective response with gefitinib, eight of them expressed somatic mutations in the TK domain of EGFR (Lynch *et al.*, 2004).

Thus far, three classes of EGFR mutations have been identified: missense mutations, deletions and in-frame insertions (Figures 1.31 & 1.32) (Herbst *et al.*, 2004).

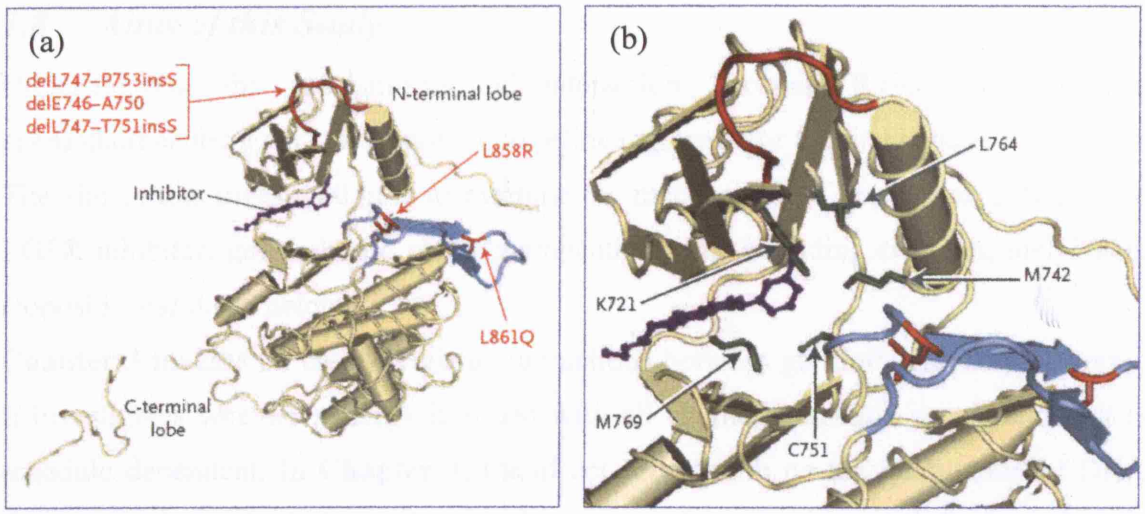

Figure 1.32: Clustering of mutations in the EGFR gene at critical sites within the ATP-binding pocket.

Source: Adapted from TJ Lynch et al., N Engl J Med, 2004.

Figure 1.32a shows the three-dimensional structure of the EGFR ATP cleft flanked by the N-terminal lobe and the C-terminal lobe of the kinase domain with the inhibitor representing gefitinib (dark blue), occupying the ATP cleft. The locations of the two missense mutations L858R and L861Q are shown within the activating loop of the tyrosine kinase (light blue) and the three in-frame deletions (delL747-P753insS, delE746-A750 and del747-T751insS) are all present within another loop (shown in red) which flanks the ATP cleft. Figure 1.32b shows a close-up view of the EGFR tyrosine kinase domain, with the critical amino acids implicated in binding to ATP or gefitinib (Lynch *et al.*, 2004).

The L858R missense mutation and the DelL747-P753insS deletion mutation have provided insight into how these mutations affect the function of gefitinib (Herbst *et al.*, 2004). Activation of mutant EGFR is characteristically more intense and prolonged than that of the activated wild-type receptor, and also requires much lower concentrations of gefitinib for complete receptor inhibition (Lynch *et al.*, 2004). These studies also indicate that these mutations stabilise the interaction between the EGFR-TK domain and ATP or its competitive inhibitor (for example, gefitinib).

1.8 Aims of this Study

Understanding the mechanisms of interaction between RTK inhibitors and chemotherapeutic agents, is important to refine regimens for treating cancer.

The aim of this investigation is to examine the mechanisms of interaction between the EGFR inhibitor, gefitinib and chemotherapeutic agents including cisplatin, melphalan, etoposide and doxorubicin.

Chapter 3 focuses on the synergistic interactions between gefitinib and chemotherapy. It investigates whether synergy is found with all chemotherapeutic agents and if it is schedule dependent. In **Chapter 4**, the effect of gefitinib on the modulation of DNA damage and repair induced by specific chemotherapeutic agents is investigated. **Chapter 5** investigates the effects of cisplatin on EGFR activation and how this is modulated by gefitinib. The effect of gefitinib on DNA-PK expression is also included. In addition, a physical interaction between EGFR and DNA-PK_{CS} and a subcellular redistribution of DNA-PK and EGFR is also assessed following treatment with gefitinib. The effect of gefitinib on DNA-PK functional activity is investigated in **Chapter 6**. Furthermore, inhibition of the PI3-Kinase pathway with LY294002 and wortmannin, and the direct inhibition of DNA-PK_{CS} by RNA interference, is also investigated and compared with the effects of gefitinib. Finally, the effects of gefitinib on chemotherapy-induced DNA damage in cells expressing specific EGFR tyrosine kinase mutations is discussed in **Chapter 7**.

CHAPTER 2

MATERIALS AND METHODS

MATERIALS

2.1 Chemical Reagents and Cytotoxic Drug Source

All reagents and disposables were obtained from Sigma Chemical Co., Poole, UK or VWR International Ltd., Poole, UK unless otherwise stated.

Cytotoxic drugs (Table 2.1) were prepared as stocks in advance, or as fresh prior to individual experiments depending on stability and activity in solution as well as experimental parameters. The concentration ranges used for experiments were modified based on previous personal communications on the cytotoxicity of individual agents where necessary.

Drug	Chemical Structure	Stock Solution	Solvent	Supplier
Gefitinib (Iressa^{TM}, ZD1839)	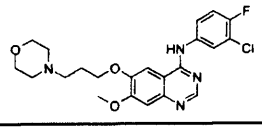	10mM	DMSO	AstraZeneca
Matuzumab (EMD72000)	–	10µg/ml	H_2O	Merck Pharmaceuticals
Cisplatin	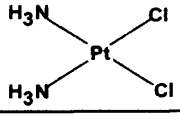	3.3mM	Injection (Sterile Concentrate)	DBL, Warwick, UK
Melphalan	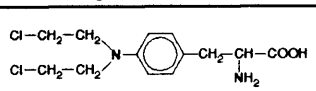	10mM	Ethanol + 1% conc. HCl	Sigma, UK
Etoposide	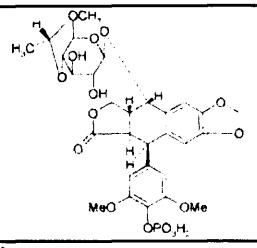	10mM	DMSO	Sigma, UK
Irinotecan	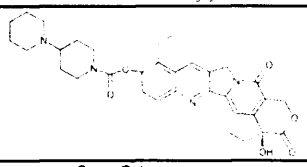	1mM	DMSO	Aventis Pharma, UK
Doxorubicin	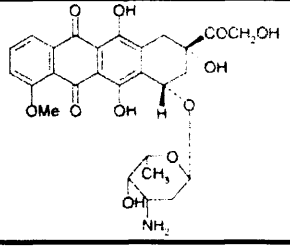	1mM	H_2O	Sigma, UK

Drug	Chemical Structure	Stock Solution	Solvent	Supplier
Biotinylated-Doxorubicin	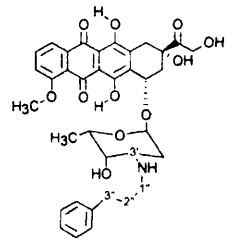	1mM	H_2O	Dr David Selwood, WIBR, UCL, UK
LY294002	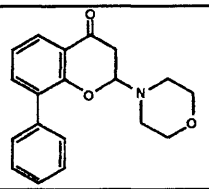	10mM	DMSO	Sigma, UK
Wortmannin	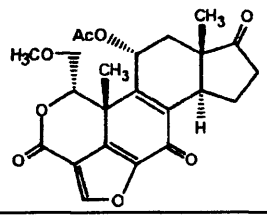	10mM	DMSO	Sigma, UK
Camptothecin	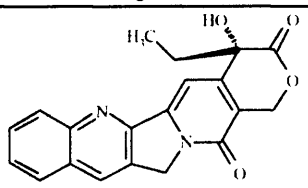	10mM	DMSO	Sigma, UK

Table 2.1: Cytotoxic drugs used in this study.

2.2 Experimental Cell Lines

Human breast cancer cell line, MCF-7 cells were grown in Dulbecco's MEM (DMEM), rat pancreatic AR42J cells were grown in RPMI 1640, human breast cancer MDA-453 cells were grown in Dulbecco's MEM (DMEM), human colon cancer HCT-116 cells were grown in RPMI 1640, human colon cancer CaCo-2 cells were grown in Minimal Essential Medium Eagle (EMEM) and African green monkey kidney cell line Cos-7 cells were grown in Dulbecco's MEM (DMEM).

Cell lines used were obtained as shown in Table 2.2. All tissue culture media were supplied by Autogen Bioclear, Calne, UK and were supplemented with 10% Foetal calf serum (FCS) (previously heat-inactivated for 30 minutes at 57°C) and 1% glutamine. The growth medium described for the routine propagation of exponentially growing cell lines is referred to as complete growth medium throughout.

Cell Line	Origin	Culture Conditions	Supplier
MCF-7	Human Breast Adenocarcinoma – Pleural effusion with hormone receptors. 69 year old Caucasian female.	Dulbecco's Minimal Essential Medium (DMEM)	Cancer Research UK London Research Institute.
AR42J	Rat Exocrine Pancreatic Tumour.	RPMI 1640	Dr Martyn Caplin Department of Gastroenterology, Royal Free Hospital, London.
MDA-453	Human Breast Metastatic Carcinoma – Pleural effusion. 48 year old female.	Dulbecco's Minimal Essential Medium (DMEM)	Cancer Research UK London Research Institute.
HCT-116	Human Colon Carcinoma – Adult Male.	RPMI 1640	Cancer Research UK London Research Institute.
CaCo-2	Primary Colonic Tumour – 72 year old Caucasian male.	Minimal Essential Medium Eagle (EMEM)	Cancer Research UK London Research Institute.
Cos-7	African Green Monkey Kidney – Transformed with sv40. Established from cv-1 Simian cells.	Dulbecco's Minimal Essential Medium (DMEM)	Cancer Research UK London Research Institute.

Table 2.2: Cell lines used in this study.

Plasmids used for different experiments are summarised in Table 2.3 below.

Vector	Insert	Vector	Insert
pSUPER	CFP-115	pUSEamp	None
pSUPER	CFP-117	pUSEamp	Wild Type EGFR
pSUPER	CFP-119	pUSEamp	L858R EGFR
pSUPER	CFP-121	pUSEamp	delL747-P753insS EGFR
pSUPER	CFP-Scrambled		

Table 2.3: Plasmids used in this study.

2.3 Tissue Culture

2.3.1 Maintenance of Cell Lines

All cell lines were grown in 50cm^2 (T50) flasks and maintained at 37°C with 5% CO_2 in dry incubators (Forma Scientific, UK). All procedures were carried out in Class II MDH biological safety cabinet (Intermed MDH, UK) using aseptic techniques. Exponentially growing cells were maintained at a cell concentration according to the European Collection of Cell Cultures (ECACC), Salisbury, UK.

Cells were routinely passaged at 90% confluence (biweekly). To this end, cells were washed with 10ml of 0.01M phosphate buffered saline (PBS) to remove serum. To detach the cells from the flask 5ml of 1X Trypsin/EDTA (Autogen Bioclear, Calne, UK) was then added for 5 minutes at 37°C. 5ml of complete growth medium was then added to inactivate the trypsin and the cell suspension was pelleted by centrifugation at 1,500rpm for 5 minutes at room temperature. Cells were then resuspended in complete growth medium and re-plated at an appropriate passage ratio for the cell line. The passage number was increased by one. Cells were discarded after approximately 25 passages and fresh cells were taken from the initial passage number used.

2.3.2 Cell Count

Trypsinised cells were resuspended in 10ml of complete growth medium and counted using a haemocytometer. To this end, 20µl of cell suspension was mixed with trypan blue (Sigma, UK) to exclude dead cells and the cell number was determined for each of five separate $1mm^2$ fields. The average was multiplied by $1x10^4$ to give the number of cells per ml of suspension.

2.3.3 Determination of Cell Doubling Time

Cells were seeded out at an initial total cell number of $1x10^5$ cells per $25cm^2$ (T25) flask containing 10ml of complete growth medium with an individual flask for every time-point. Cells were trypsinised, centrifuged, resuspended and counted using a haemocytometer as described above and the subsequent concentration used to determine the total cell count per flask. Further samples were taken every 24 hours until confluence. The doubling time of each cell line was calculated by reading off the exponential portion of the growth curve derived by plotting number of hours against total number of cells counted.

2.3.4 Mycoplasma Testing

Cell cultures were routinely tested for *Mycoplasma* contamination every 6 months. The human breast cancer cell line, MCF-7 cells were grown in Dulbecco's MEM (DMEM) supplemented with 10% FCS and 1% glutamine. They were maintained at 37°C with 5% CO_2. A total number of $5x10^4$ MCF-7 cells were seeded onto a sterile coverslip placed in a flat bottom Falcon tube. Cells were allowed to adhere to the coverslips for

24 hours at 37°C with 5% CO_2. Previously, the cell lines to be *Mycoplasma* tested had been set up such that the cells reached confluency concurrently with the set-up of the *Mycoplasma* test. Thus, from a flask containing a confluent cell population to be tested, 500µl of the supernatant growth medium was removed and transferred to the *Mycoplasma* testing tube. The cell-free supernatant must not contain additives such as hydrocortisone, cholera toxin or antibiotics that might interfere with *Mycoplasma* growth. The MCF-7 cells were incubated until they reached confluence after 5 days. The medium was removed and the cells washed once with 0.01M PBS. The cells were then fixed in absolute methanol for 5 minutes and subsequently washed twice with 0.01M PBS and stained with 5µg/ml of Hoechst 33258 dissolved in 0.01M PBS for 10 minutes. Following two more washes with 0.01M PBS, the coverslips were carefully removed from the *Mycoplasma* testing tube, placed cell surface upwards on a glass microscope slide and covered with a coverslip. Analysis was performed under a fluorescent microscope using a x40 objective and ultra-violet (UV) illumination. Control cells showed intense blue-white staining of the nuclei only. *Mycoplasma* infected cells would have been covered in a fine lawn of speckles all over.

2.3.5 Storage and Retrieval of Cells in Liquid Nitrogen

Frozen cell stocks in liquid nitrogen were routinely prepared. Cells were grown in a 175cm^2 (T175) flask to semi-confluency. They were trypsinised and resuspended in media with 20% FCS containing 10% dimethylsulphoxide (DMSO). 1ml aliquots were frozen slowly in cryotubes in a styrofoam box at -80°C overnight before the cryotubes were transferred to a liquid nitrogen tank the next day. Each cryotube contained cells at a 10X higher concentration compared to the concentration at which they were grown.

Cells were recovered from liquid nitrogen by thawing rapidly in a 37°C water bath before being transferred into a T25 flask containing 10ml of growth medium supplemented with 20% FCS. Each cryotube was wiped off with paper towel sprayed with 70% industrial methylated spirit (IMS) to prevent accidental contamination of cell lines through bacteria and other cells stuck to the outer wall of the cryotube. Cells were split after 24 hours to remove any DMSO present in the media.

2.4 In Vitro Cytotoxicity Assay and Pharmacological Analysis

2.4.1 Sulphorhodamine B Growth Inhibition Assay

Cytotoxicity of drugs alone or in combination was determined using the Sulphorhodamine B (SRB) assay in 96-well microtitre plates. As described previously by Skehan *et al.*, (1990), they developed a rapid, sensitive, and inexpensive method for measuring the cellular protein content of adherent and suspension cultures based on the binding of the SRB purple dye to cellular protein. They showed the SRB assay to produce results linear with the number of cells and with values for cellular protein measured by both the Lowry and Bradford assays at densities ranging from sparse sub-confluence to multilayered supra-confluence. The signal-to-noise ratio at 564 nm is favourable and the resolution is 1000-2000 cells/well. In addition, they showed that the sensitivity of the SRB assay compared favourably with sensitivities of several fluorescence assays and was superior to those of both the Lowry and Bradford assays and to those of 20 other visible dyes. The SRB assay provides a colorimetric end point that is non-destructive, indefinitely stable, and visible to the naked eye. It provides a sensitive measure of drug-induced cytotoxicity, is useful in quantitating clonogenicity, and is well suited to high-volume, automated drug screening. SRB fluoresces strongly with laser excitation at 488 nm and can be measured quantitatively at the single-cell level by static fluorescence cytometry (Skehan *et al.*, 1990; Voigt, 2005).

The optimal cell concentrations were determined from the previously calculated doubling times in order to achieve a final cell concentration ideal for accurate optical density (OD) measurement. Cells were plated in 96-well flat-bottomed microtitre plates, each well containing 100µl cell solution ($2.5x10^3$ cells/well or $5x10^3$ cells/well depending on cell doubling time). Prior to drug treatment, cells were allowed to adhere at 37°C with 5% CO_2 for 48 hours.

Following drug treatment, media was carefully removed and the cells subsequently fixed with 100µl 10% trichloroacetic acid solution for 20-30 minutes at 4°C. The fixed cells were washed three times with tap water and any remaining water flicked out of the wells. 100µl SRB stain (0.4% in 1% acetic acid) was then added to each well to allow visualisation of cellular proteins and incubated at room temperature for 20-30 minutes at 4°C. Any excess SRB was removed by washing 4-5 times with 1% acetic acid. Plates

were air-dried overnight. Finally the dye was dissolved in 100µl 10mM Tris/1mM EDTA for 10 minutes on a plate shaker. Plates were read at an absorbance of 540nm on a Tecan Microplate reader and analysed using computer spreadsheet (Microsoft Excel). Growth inhibition was expressed as a percent proliferation of control and was calculated using the following equation:

$$\frac{\text{OD (treated)}}{\text{OD (control)}} \times 100 = \text{Proliferation (\%)}$$

The data shown represents the averages of three different experiments, each performed in triplicate and includes related standard deviations as calculated.

The IC_{50} is defined as the drug concentration needed to produce a 50% growth inhibition. The dose-response curves obtained for each treatment were used to calculate their respective IC_{50} values.

Single Agent Treatments

For single-agent studies, drugs were added at a range of concentrations to triplicate wells. Incubations performed were either acute (2 hours followed by 5 days drug-free medium) or continuous (24 hours followed by 4 days drug-free medium or, 72 hours followed by 2 days drug-free medium). For daily treatment, fresh drug was added after each 24-hour period for 72 hours followed by 2 days drug-free medium. All drugs were diluted in complete growth medium and 100µl of the relevant concentration added to the appropriate wells. One solvent control lane was included in each experiment. The concentration range for each drug was optimised if necessary following analysis of results from the first experiments. For acute drug exposure cells were incubated for 2 hours with the relevant drug prepared in FCS-free medium. Following this, the drug solution was removed and replaced with 200µl drug free complete growth medium. Plates were incubated at 37°C with 5% CO_2.

Dual Agent Treatments

For combination studies, drugs were added sequentially by delivering each drug in turn for 24 hours, followed by 3 days drug-free growth medium. For acute drug exposure, cells were incubated for 2 hours with *Drug A* (in FCS-free medium) followed by 24 hours with *Drug B* followed by 4 days drug-free-medium. Control wells were treated in the same way with aspiration at each period respectively. Again, plates were incubated at 37°C with 5% CO_2.

For determination of synergy, *Drug B* was added at sub-toxic concentrations (e.g. producing 10% or 20% inhibition of proliferation) to a range of concentrations for *Drug A*.

2.4.2 Isobologram Analysis

To assess whether a combination dose of any two given drugs behave in a synergistic or additive fashion; the commonly used isobologram methodology can be applied as has been previously described by Tallarida, (2001). Briefly, a particular effect level is selected, in our case 50% of the maximum (IC_{50}) and doses of each drug alone that give this effect are plotted as axial points in a Cartesian plot. This is illustrated in Figure 2.1 where *Drug A* has an IC_{50} of 20μM and *Drug B* has an IC_{50} of 5μM.

The straight line connecting *A* and *B* in Figure 2.1 is the locus of points (dose pairs or *isoboles*) that will produce this effect in a simply additive combination. This line of additivity allows a comparison with dose pairs that produce this effect level experimentally. Thus, the IC_{50} for two drugs added together lying well above this line have a sub-additive or antagonistic effect (illustrated by the letter *X*). If the IC_{50} for two drugs added lie on or close to the line they are said to have an additive effect (illustrated by the letter *Y*). And if they exist well below the line a super-additive or synergistic effect is achieved (illustrated by the letter *Z*).

It is important to note parenthetically, that the useful visual clarity of the isobologram does not allow for absolute statistical precision. For example, the so-called grey areas such as 'on or *close to* the line' do not provide the conclusive ideal distinctions and so these values would be subject to further pharmacological tests such as regression analysis. To continue with these tests is beyond the aims of this study and the isobologram test provides the necessary pharmacological analysis required.

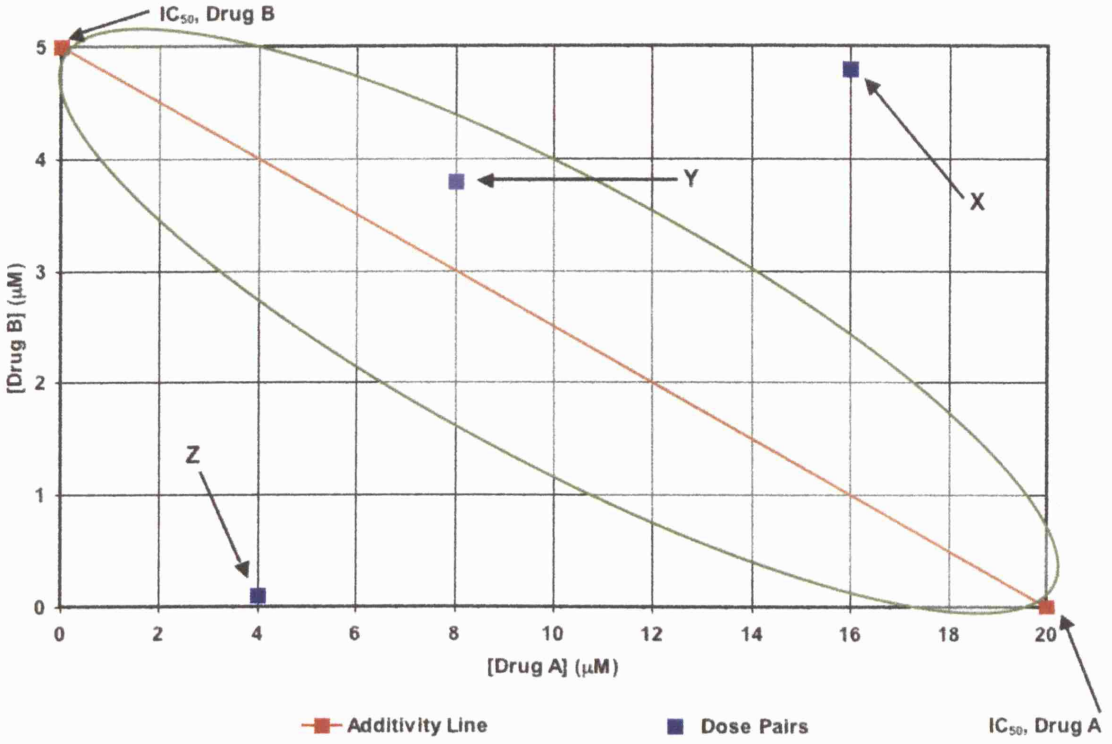

Figure 2.1: Illustrated isobologram for some particular effect.
Adapted from Tallarida RJ, 2001.

2.5 Single Cell Gel Electrophoresis (Comet) Assay

The drug-induced DNA damage in the form of strand breaks and subsequent repair was assessed using the single-cell gel electrophoresis (comet) assay as described previously (Spanswick *et al.*, 1999; Olive, 2002).

The comet assay was originally developed as a method for the detection and visualisation of DNA damage within individual cells and is used extensively for the assessment of strand breaks in a range of applications.

2.5.1 Methodology

Exponentially growing cells were seeded at $5x10^4$ cells in six well plates (Nunclon™, VWR) and incubated for 24h at 37°C in 5% CO_2. To examine the extent of DNA damage and subsequent rate of repair, a short, high chemotherapeutic concentration is ideal. To this end, cells were initially treated with appropriate chemotherapy at a range of concentrations to determine a suitable schedule. Following this, cells were then treated with appropriate chemotherapy at a fixed concentration and replaced with

complete fresh media with or without a second drug. Samples were then taken at suitable intervals to measure the amount of DNA damage and rate of repair.

All procedures were carried out on ice and in subdued lighting. Cells were embedded in 1% Type VII agarose on 1% Type 1-A agarose precoated microscope slides, and lysed for 1 hour in lysis buffer (100mM disodium EDTA, 2.5 M NaCl, 10mM Tris-HCl, pH 10.5) containing 1% Triton X-100 (added immediately before analysis). Following this, they were washed every 15 minutes in distilled water for 1 hour. Slides were then incubated in alkali buffer (50mM NaOH, 1mM disodium EDTA, pH 12.5) for 45 minutes, followed by electrophoresis in the same buffer for 25 minutes at 18 V (0.6 V/cm), 250 mA. The slides were finally rinsed in neutralising buffer (0.5 M Tris-HCl, pH 7.5) followed by saline. After drying, the slides were stained with propidium iodide (2.5 μg/mL) for 30 minutes and then rinsed in distilled water.

2.5.2 Analysis

Images were visualised with the use of a NIKON inverted microscope with a high-pressure mercury light source (NIKON UK Limited, Kingston Upon Thames, UK), 510 to 560 nm excitation filter, and 590 nm barrier filter at x20 magnification. Images were captured by using an on-line charge-couple device (CCD) camera and analysed with Komet Analysis software (Figure 2.2) (Kinetic Imaging, Liverpool, UK).

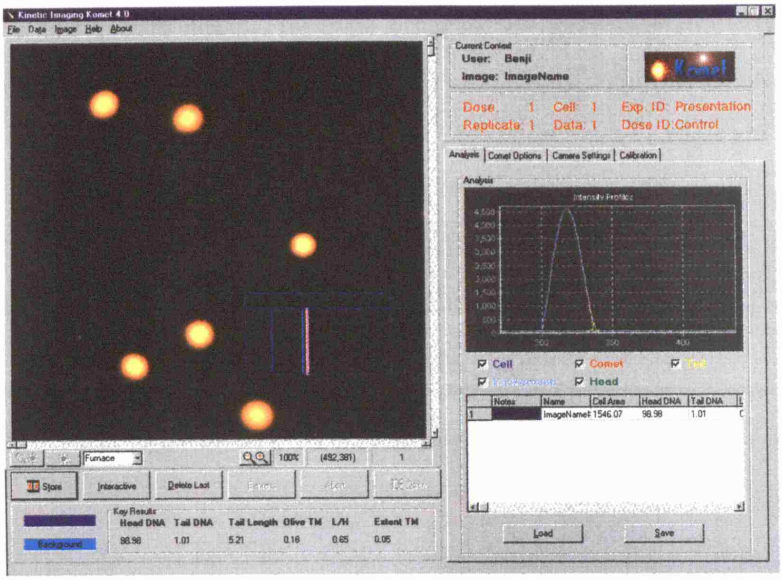

Figure 2.2: Sample screen display of comets (with no tails) as seen using the Komet Analysis Software.

For each duplicate slide 25 cells were analysed. DNA damage and subsequent repair was measured by the increase in the tail moment (measured in μMetres), a function of the amount of DNA in the tail and the length of the tail (Spanswick *et al.*, 1999). Analysis was then achieved using a computer spreadsheet (Microsoft Excel). The data shown is a representation of three independent experiments, and include related standard error bars as calculated.

As can be seen in Figure 2.3, treatment with drugs such as etoposide and doxorubicin which induce strand breaks, produce a tail moment dependent on their dose and length of exposure. A similar effect is achieved by irradiating the cells.

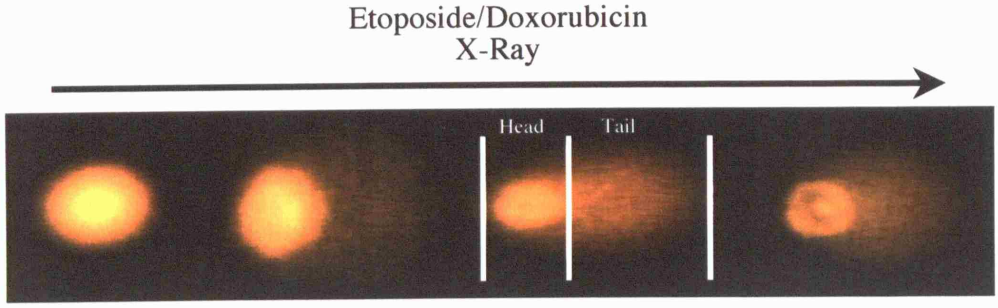

Figure 2.3: Illustration of DNA tail as a result of chemotherapy or irradiation.

2.5.3 Measurement of Drug-Induced DNA Interstrand Crosslinking Using the Comet Assay

Detection and measurement of DNA interstrand crosslinks (ICL) was achieved using a modification of the comet assay (Hartley *et al.*, 1999). Immediately before analysis, cells were irradiated (12 Gy) to deliver a fixed number of random DNA strand breaks. In the presence of strand breaks, ICL's retard migration thus reducing the tail moment compared to the non-crosslinked irradiated control. A simplified illustration of the decrease in DNA tail moment as a result of ICL achieved by chemotherapeutic agents such as cisplatin and melphalan is shown in Figure 2.4.

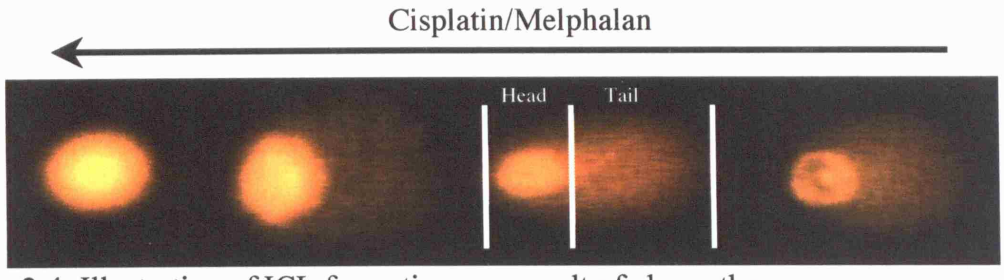

Figure 2.4: Illustration of ICL formation as a result of chemotherapy.

The tail moment for each image was calculated by using the Komet Analysis software as the product of the percentage DNA in the comet tail and the distance between the means of the head and tail distributions, based on the definition of Olive *et al.*, 1990. Crosslinking was expressed as the percentage decrease in tail moment compared with irradiated controls, calculated by the following formula:

Percentage of decrease in tail moment = [1 - (TMdi - TMcu/TMci - TMcu)] x100

Where TMdi equals tail moment of drug-treated irradiated sample, TMcu equals tail moment of untreated unirradiated control, and TMci equals tail moment of untreated irradiated control.

Analysis was then achieved using a computer spreadsheet (Microsoft Excel). The data shown is a representation of three independent experiments, and include related standard error bars as calculated.

2.6 Detection of Apoptosis

To address whether any inhibition in the repair of DNA damage leads to the induction of apoptosis, the Annexin V-FITC assay was performed.

Annexin V-FITC is used to quantitatively determine the percentage of cells within a population that are actively undergoing apoptosis. It relies on the property of cells to lose membrane asymmetry in the early phases of apoptosis. In apoptotic cells, the membrane phospholipid phosphatidylserine (PS) is translocated from the inner surface of the plasma membrane to the outer surface, thereby exposing PS to the external environment.

Annexin V is a Ca^{2+}-dependent phospholipid-binding protein that has a high affinity for PS, and is useful for identifying apoptotic cells with exposed PS. Propidium Iodide (PI) is a standard flow cytometric viability probe and is used to distinguish viable from non-viable cells. Viable cells with intact membranes exclude PI, whereas the membranes of dead and damaged cells are permeable to PI. Cells that stain positive for Annexin V-FITC and negative for PI are undergoing apoptosis. Cells that stain positive for both Annexin V-FITC and PI are either in the end stage of apoptosis, are undergoing necrosis, or are already dead. Cells that stain negative for both Annexin V-FITC and PI are alive and not undergoing measurable apoptosis.

Cells were treated in the same way as in the Comet assay, washed twice with cold saline and then resuspended in 1ml of Annexin binding buffer (10mM Hepes/NaOH pH 7.4, 140mM NaCl, 2.5mM $CaCl_2$) (BD Biosciences). 5.3µl of Annexin V-FITC (Alexa488, PE, Cy3 and Alex647) was then added and each sample was incubated at room temperature for 20 minutes in the dark. PI was then added (5µl) to gate out dead cells and samples were analysed by flow cytometry within 1 hour.

2.7 Protein Extraction

2.7.1 Total Cell Lysis

Cells cultured and treated in $75cm^2$ (T75) flasks were washed twice in PBS at room temperature, drained well and placed in ice. To lyse the cells, 500µl RIPA buffer (1% deoxycholic acid, 1% Triton X-100, 0.1% SDS, 250 mM NaCl, 50 mM Tris pH 7.5, 100 µg/ml AEBSF, 17µg/ml aprotinin, 1µg/ml leupeptin, 1µg/ml pepstatin, 5µM fenvalerate, 5µM potassium bisperoxo (1,10-phenanthroline) oxovanadate (V) (BpVphen) and 1µM okadaic acid) was added to each flask for 10 minutes with occasional rocking. Cells were then scraped into a 1.5ml Eppendorf tube using a cell scraper (VWR International Ltd.) and centrifuged at 13,000rpm for 10 minutes at 4°C. The supernatant (containing total cell protein) was then carefully transferred to a fresh tube and the pellet discarded. This is the total cell lysate and can be stored at -80°C.

2.7.2 Protein Assay

To determine the protein concentration of a particular total cell lysate, the Biorad Protein Assay kit was used. Briefly, 2µl of each lysate is added to 18µl H_2O. In a separate Eppendorf, 20µl *Reagent S* is mixed with 1ml *Reagent A*. 100µl of this is added to each 20µl lysate sample mixed well with a short spin. 800µl *Reagent B* is then added to each and incubated at room temperature for 15 minutes. The optical density (O.D.) for each sample is then read on a spectrophotometer (Beam PU 8600 Series UV/Vis Single, Philips®) at 750nm and the protein concentration determined using the following formula:

$$\text{O.D. x25} = [\ ]/\mu l \text{ (i.e. } \mu g/\mu l)$$

2.7.3 Immunoprecipitation

An immunoprecipitation allows for the partial purification of a specific protein from a complex protein mixture that is present in a total cell lysate. In addition, immunoprecipitations can identify any protein-protein associations that exist in any given circumstance.

Protein G Sepharose™ 4 Fast Flow is protein G immobilised by the CNBr method to Sepharose 4 Fast Flow. Protein G binds to the Fc region of IgG from a variety of mammalian species. Protein G Sepharose 4 Fast Flow may be used to isolate and purify classes, subclasses and fragments of immunoglobulins from any biological fluid or cell culture medium. Since only the Fc region is involved in binding, the Fab region is still available for binding antigen. Hence, Protein G Sepharose 4 Fast Flow is extremely useful for isolation of immune complexes. The potential applications of protein G include almost all of the current and projected applications of protein A. Protein G and protein A, however, have different IgG binding specificities, dependent on the origin of the IgG. Compared to protein A, protein G binds more strongly to polyclonal IgG, for example, from cow, sheep and horse. Furthermore, unlike protein A, protein G binds polyclonal rat IgG, human IgG3 and mouse IgG1 (Table 2.4). In this study, only Protein G Sepharose was used.

Species	Protein G	Protein A
Human IgG_1	++	++
Human IgG_2	++	++
Human IgG_3	++	-
Human IgG_4	++	++
Rabbit	++	++
Cow	++	+
Horse	++	-
Goat	++	+
Guinea Pig	+	++
Sheep	++	-
Dog	+	++
Pig	++	++
Rat	-	-
Mouse	+	+
Chicken	-	-

Table 2.4: Relative binding strength of polyclonal IgG from various species to free protein G and protein A, as measured in a competitive ELISA test.
Source: Amersham Biosciences Instruction Manual 71-7083-00 Edition AF

In order to prepare them, Protein Sepharose G™ 4 Fast Flow (Amersham Biosciences, Sweden) beads were washed as follows: Taking the required volume of Protein Sepharose G™ the supernatant (slurry) was removed by centrifugation at 13,000rpm for 10 minutes at 4°C. The pellet was then resuspended in 100µl PBS and repeated three more times. For each sample, 45µl of Protein Sepharose G™ was then added to 250µg of protein taken from the total cell lysate. (To ensure that the beads themselves were being collected, the nib of the pipette tip was cut off.) The appropriate antibody at a final concentration of 4µg was then added to each sample and then placed on a rotation wheel at 4°C and left overnight. The supernatant was removed by centrifugation at 13,000rpm for 10 minutes at 4°C. This can be stored at -80°C for future analysis as it is still a total cell lysate with the immunoprecipitated protein depleted and is a useful control for confirming that the immunoprecipitation has purified the required protein. The pellet was washed three times by resuspending in 100µl RIPA buffer and centrifuging at 13,000rpm for 10 minutes at 4°C. The pellet contains the Protein Sepharose beads which is attached by the purified proteins and anything associated to them. They can be stored at -80°C for further analysis.

The antibodies used for immunoprecipitations were the rabbit polyclonal anti-EGFR antibody which cross-reacts with human, mouse and rat; and the mouse monoclonal anti-DNA-PK_{CS} antibody which cross-reacts with human and rat. Both were purchased from Abcam Limited, Cambridgeshire, UK (Harlow & Lane, 1999).

Troubleshooting

Whilst the immunoprecipitation technique is well defined and allows for a clear and concise study of specific proteins and their characteristics, optimisation is variable and dependent on a number of factors such as protein of interest and antibodies used. In this study, modifications to the methodology were made to obtain the best results and were as follows:

1. The Protein Sepharose G™ beads were not originally washed in PBS prior to use. Supplied in a preservative this masks the beads activity and thus yields a poor protein binding affinity.
2. The final concentration of antibodies used was increased from 2 to 4µg.

3. Initial rotation time was 2h which did not allow for sufficient antibody-protein binding. This was then increased to overnight.
4. Following rotation, pellets were initially washed once with RIPA buffer. This was increased to three times.
5. Immunoprecipitates were originally resuspended in 50µl RIPA buffer and stored at -80°C for further analysis by immunoblotting. This diluted the protein concentration too much and so samples were stored as pellets.

It should be noted that results for these preliminary experiments are not shown.

2.7.4 Nuclear and Cytosolic Extraction

To separate out nuclear and cytosolic components of total cell lysates, the TransFactor® Extraction Kit (Clontech Laboratories, UK) was used according to the manufacturer's instructions. Briefly, all steps were performed at 4°C unless otherwise specified. Reagents were pre-cooled to 4°C, and not used until fully defrosted. Cells were collected and transferred to an Eppendorf tube centrifuged at 13,000rpm for 10 minutes at 4°C and the supernatant discarded. The pellet was then washed twice in PBS and the pellet size estimated. Lysis buffer was prepared as follows: 150ml 10x Pre-lysis Buffer (Hypotonic) (100mM HEPES pH 7.9, 15mM $MgCl_2$, 100mM KCl), 15ml 0.1M DTT, 15ml Protease Inhibitor Cocktail (Aprotinin, Pepstatin A, Bestatin, trans-Epoxysuccinyl-Lleucylamido (4-guanidino) butane, and 4-(2-aminoethyl) benzenesulfonyl fluoride hydrochloride in DMSO) and 1.32ml ddH_2O. Cells were resuspended in a volume of lysis buffer equal to five times the cell pellet volume and incubated on ice for 15 minutes. Following centrifugation at 13,000rpm for 10 minutes at 4°C, the supernatant was carefully removed and the pellet resuspended in a volume of lysis buffer equal to twice the cell pellet volume.

Suspension was then slowly drawn into a syringe through a narrow-gauge (No. 27) needle and then ejected with a single rapid stroke. This was repeated ten times and centrifuged at 13,000rpm for 10 minutes at 4°C. The supernatant was then transferred to a fresh Eppendorf tube and is the cytosolic fraction. This can be snap-frozen and stored at -70°C.

Extraction Buffer was prepared as follows: 147ml Pre-extraction Buffer (20mM HEPES pH 7.9, 1.5mM $MgCl_2$, 0.42M NaCl, 0.2mM EDTA, 25% (v/v) glycerol), 1.5ml 0.1M DTT and 1.5ml Protease Inhibitor Cocktail. The crude nuclear pellet was resuspended in

a volume of Extraction Buffer equal to two-thirds of the cell pellet volume. To disrupt the nuclei, the suspension was then syringed as before and placed on a shaker at low speed for 30 min at 4°C. The nuclear suspension was then centrifuged at 13,000rpm for 10 minutes at 4°C. The supernatant or nuclear fraction, was transferred to a fresh Eppendorf tube and can be snap-frozen and stored at -80°C.

For determination of the protein concentrations within both the nuclear and cytosolic extractions, the protein assay detailed in Section 2.7.2 was used.

Troubleshooting

A number of obstacles were overcome whilst performing the nuclear and cytosolic extractions:

1. Initial low protein concentrations were due to improper measurement of cell pellet volume.
2. Protein activities were at first not present because some of the proteins of interest are highly susceptible to proteolytic degradation. With practice, work efficiency decreased the time of initial purification steps whilst keeping all reagents on ice at all times.
3. There was difficulty drawing cell lysates into the syringe. This was because of a compact cell pellet and was overcome by using a pipette tip to disperse them.

2.8 Immunoblotting

2.8.1 Electrophoresis

Protein concentrations of total cell lysates were determined using the protein assay outlined in Section 2.7.2. For each sample the required volume containing 30-50μg of protein was transferred to a fresh Eppendorf tube. Loading (Laemmeli) buffer (4% SDS, 10% β-Mercaptoethanol, 20% glycerol, 0.02% bromophenol-blue and 100mM Tris HCl (pH 6.8)) was then added to each lysate before heating at 95°C for 4 minutes to denature the proteins. Samples are then centrifuged at 13,000rpm for 10 minutes at 4°C and the pellet discarded.

For immunoprecipitates, the whole pellet containing 250μg of protein was resuspended in loading buffer and boiled as above. Boiling allows for denaturing of and dissociation between the proteins and the antibodies and beads. Following centrifugation, the pellet

containing beads and antibody was discarded and the supernatant can be loaded for electrophoresis.

The NuPAGE® Electrophoresis System (Invitrogen, UK) was used. For analysis of proteins with a molecular weight of between 120 and 410 KDa, lysates and immunoprecipitates were loaded onto NuPAGE® Novex 3-8% Gradient Tris-Acetate Pre-Cast Gels which were placed in the XCell *SureLock*™ Mini-Cell (two gels per cell) and included an appropriate marker (Kaleidoscope pre-stained standards, BioRad, Hemel-Hempstead, UK) or a positive protein control (A431+EGF cell lysate; BD Biosciences, UK). Upper (200ml) and lower (600ml) buffer chambers were then filled with 1x NuPAGE® Tris-Acetate SDS Running Buffer (diluted from a 20x stock: 50mM Tricine, 50mM Tris base, 0.1% SDS, pH 8.24) and Mini-Cells were run at 150V constant at 4°C for approximately 1h 30min (Expected 40-55 mA/gel at start; 25-40 mA/gel at end).

For analysis of proteins with a molecular weight of between 10 and 180 KDa lysates and immunoprecipitates were loaded onto NuPAGE® Novex 4-12% Gradient Bis-Tris Pre-Cast Gels and placed in Mini-Cells as above. Upper (200ml) and lower (600ml) buffer chambers were then filled with 1x NuPAGE® MOPS SDS Running Buffer (diluted from a 20x stock: 50mM MOPS, 50mM Tris base, 0.1% SDS, pH 7.7) and Mini-Cells were run at 200V constant at 4°C for approximately 50min (Expected 100-125 mA/gel at start; 60-80 mA/gel at end).

2.8.2 Protein Transfer and Immunoblotting

Proteins were electrically transferred to Immobilon™ polyvinylidenedifluoride (PVDF) membranes (Millipore, UK). These extremely hydrophobic membranes will not wet in aqueous solution and so were prepared as follows: blots were immersed in 100% methanol for three seconds and then placed in H_2O for 2 minutes to elute the methanol. To equilibrate, membranes were then soaked in protein transfer buffer (diluted from a 10x stock: 3% TrisBase, 14.4% glycine and 20% methanol). Gels and prepared membranes were then placed into the X-Cell II™ Blot Module (Novex®) as illustrated in Figure 2.5.

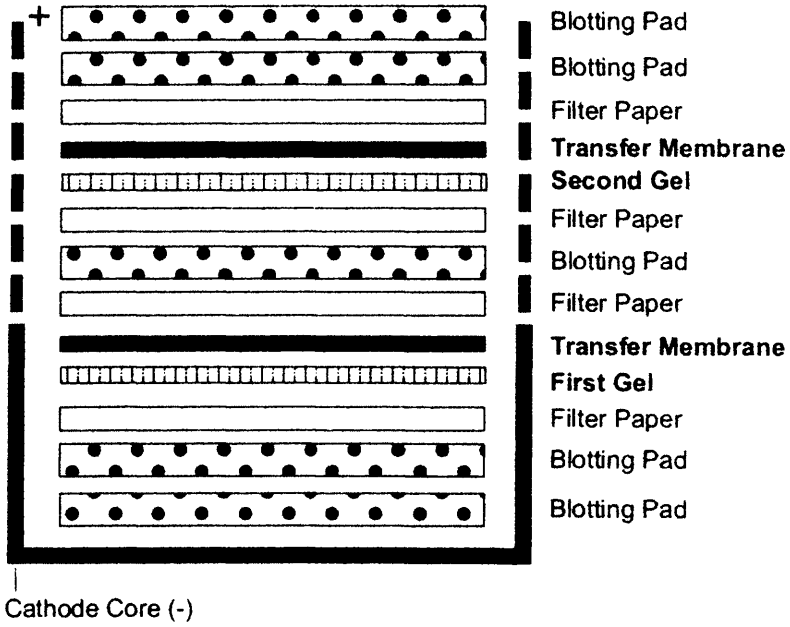

Figure 2.5: Gel/Membrane sandwich for 2 gels.
Source: NuPAGE® Technical Guide, Invitrogen, UK

Transfer was achieved at 40V for 2h using the XCell *SureLock*™ Mini-Cell (two blots per cell) and filled with protein transfer buffer as described in the NuPAGE Novex® protocol.

Membranes were then blocked in 3% casein blocking buffer [(3% skimmed milk powder (Marvel, UK) in TBS-Tween (TBS-T) (20mM TrisBase, 0.15M NaCl pH 7.5 in Elga H_2O with 0.1% Tween-20)] for at least 1 hour on a shaker at 4°C. Membranes being probed for phosphorylated proteins were blocked in 5% Bovine Serum Albumin (BSA) in TBS-T. This is due to the fact that milk contains a number of phosphorylated proteins which interfere with a phosphotyrosine antibody's ability to bind specific proteins of interest.

Blots were then probed with primary antibody against proteins of interest for at least 2h on a roller at room temperature. Antibodies used in this study are detailed in Table 2.5. All were diluted in a 1:1 mix of either Milk-TBS-T or BSA-TBS-T and TBS as necessary. Following this membranes were washed three times for 5 minutes in TBS-T followed by three more washes for 5 minute with TBS. Membranes were then probed with an appropriate horseradish peroxidase conjugated secondary antibody for at least 1h and washed as before.

Immunocomplexes were visualised using the enhanced chemiluminescence (ECL) system (Amersham Pharmacia, Little Chalfont, UK) by incubating the membranes in

the ECL system solution for 1 minute before wrapping the moist blots in cling film and exposing the blots to Kodak X-OMAT™LS film for varying exposure times (two seconds to 24h) (Sambrook *et al.*, 1989).

In order to remove or 'strip' pre-bound antibody, membranes were rehydrated in TBS for 5 minutes and placed in a hybridiser (Techne, UK) with 100ml of stripping buffer (100mM β-Mercaptoethanol, 2% SDS, 62.5mM Tris-HCl, pH 6.7) and left for 30 minutes at 50°C. Membranes were then washed twice in TBS-T for ten minutes each, blocked and reprobed as described above.

Primary Antibodies					
Antibody	**Description**	**Supplier**	**Antibody**	**Description**	**Supplier**
EGFR 170KDa	Mouse, Monoclonal	Santa Cruz, UK	PKBα/ AKT 60KDa	Mouse, Monoclonal	Abcam, UK
EGFR 170KDa	Rabbit, Polyclonal	Abcam, UK	P-AKT (Ser-473) 70KDa	Rabbit, Polyclonal	Abcam, UK
P-EGFR (Tyr-845) 175KDa	Rabbit, Polyclonal	Cell Signaling Technology, USA	MAPK 38KDa	Mouse, Monoclonal	Abcam, UK
P-EGFR (Tyr-1045) 175KDa	Rabbit, Polyclonal	Cell Signaling Technology, USA	P-MAPK 43KDa	Rabbit, Polyclonal	Abcam, UK
P-EGFR (Tyr-1068) 175KDa	Rabbit, Polyclonal	Cell Signaling Technology, USA	Bax 22KDa	Mouse, Monoclonal	BD Biosciences, UK
P-EGFR (PY20) 175KDa	Mouse, Monoclonal	BD Biosciences, UK	Bcl-2 26KDa	Rabbit, Polyclonal	BD Biosciences, UK
DNA-PK_{CS} 460KDa	Mouse, Monoclonal	Sigma, UK	Bcl_{XL} 29KDa	Mouse, Monoclonal	BD Biosciences, UK
Ku70 70KDa	Goat, Monoclonal	Abcam, UK	Lamin B1 67KDa	Mouse Monoclonal	Abcam, UK
Her-2 185KDa	Mouse, Monoclonal	Abcam, UK	α-Tubulin 170KDa	Mouse, Monoclonal	Sigma, UK
Secondary Antibodies					
Antibody		**Supplier**	**Antibody**		**Supplier**
HRP-Conjugated Rabbit Anti-Goat		Abcam, UK	HRP-Conjugated Goat Anti-Mouse		BD Biosciences, UK
HRP-Conjugated Goat Anti-Rabbit		Abcam, UK			

Table 2.5: Primary and secondary antibodies used in this study.

2.9 *Densitometric Analysis*

To mathematically compare the intensity of particular bands produced by immunoblotting, densitometric analysis was used. Briefly, blots were placed in the imaging densitometer (Imaging Densitometer GS-670 BioRad, UK) and the bands of interest selected. Intensity was then measured by computer and the background subtracted. Data is represented as a percentage of control band intensity.

The screen-grab shown in Figure 2.6 illustrates the methodology. In this case V5 serves as a background, V1 is the control and bands V2-4 represent different drug treatments.

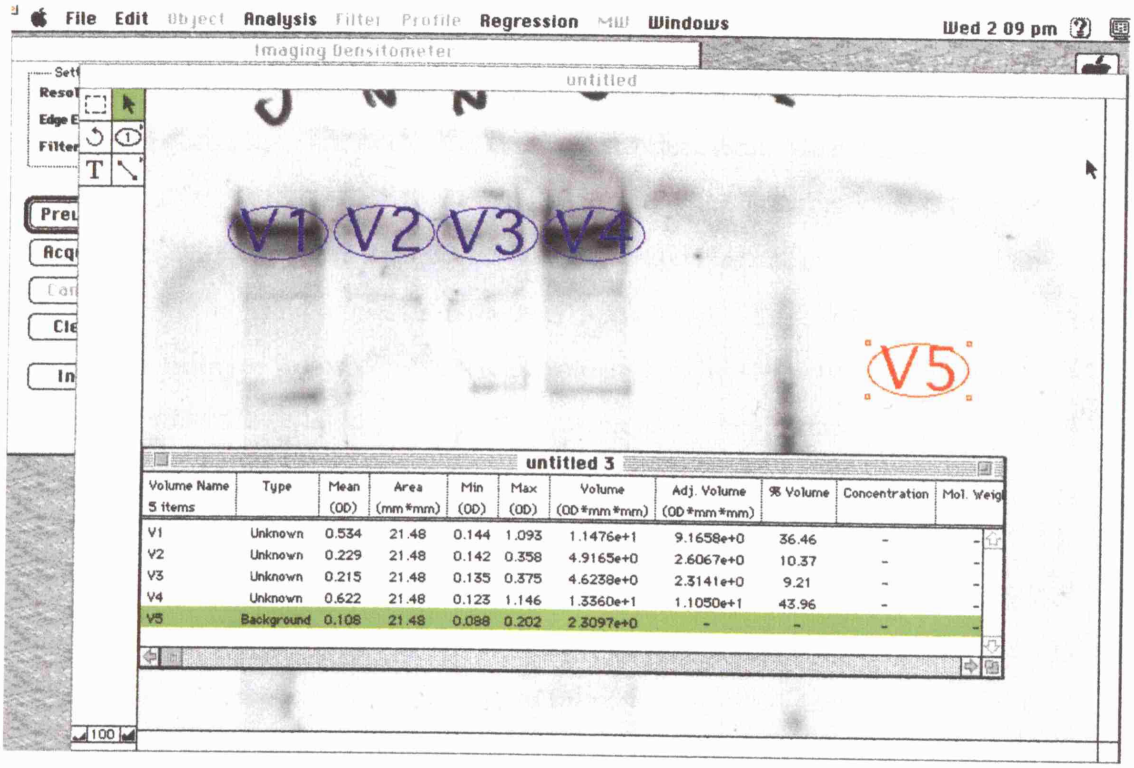

Figure 2.6: Sample screen display of densitometric analysis as seen using the BioRad Imaging Densitometer Software.

2.10 Immunofluorescent Staining

Exponentially growing cells were seeded at $2x10^4$ cells per well on circular glass slides in 12 well plates (Nunclon™, VWR) and incubated for 24h at 37°C in 5% CO_2. Cells were then treated as required, the media subsequently removed and the cells washed twice with cold PBS. Cells were then fixed using 500µL/well of 50% methanol/50% acetone mix at 4°C for 8 minutes. Following this the slides were then washed twice with cold PBS and permeablised using 500µL/well of 0.5% TritonX-100 in PBS. Slides were then blocked in 3% casein blocking buffer [(3% skimmed milk powder (Marvel, UK) in TBS-Tween (TBS-T) (20mM TrisBase, 0.15M NaCl pH 7.5 in Elga H_2O with 0.1% Tween-20)] overnight at 4°C.

Slides were then washed 3 times in cold PBS following which the cells were incubated with anti-DNA-PK_{CS} antibody for 1 hour. Slides were then washed 3 times with washing buffer (0.1% TritonX-100 in PBS) and then incubated for 1 hour at room temperature with FITC-labelled secondary antibody: Alexa fluoro® 488 goat anti-mouse IgG (green). Nuclear counterstaining was performed using 2µg/ml Propidium Iodide (blue) for 3 minutes followed by destaining with distilled water for 20 minutes.

The slides were viewed and photographed using a confocal microscope.

2.11 RNAi Transfection and DNA-PK_{CS} Deletion

The vector system, pSUPER directs the synthesis of small interfering RNAs (siRNAs) in mammalian cells and expression mediated by this vector causes efficient and specific downregulation of gene expression, resulting in functional inactivation of the targeted genes. Stable expression of siRNAs using this vector mediates persistent suppression of gene expression, allowing the analysis of loss-of-function phenotypes that develop over longer periods of time. Therefore, the pSUPER vector constitutes a powerful system to study gene function in a variety of mammalian cell types (Brummelkamp *et al.*, 2002). A map of the pSUPER RNAi system is illustrated in Figure 2.7 with the key sites and vector features highlighted.

We used DNA-directed RNA interference to reduce expression of DNA-PK_{CS}. To this end, we transfected MCF-7 cells with a pSUPER plasmid expressing siRNA directed against DNA-PK_{CS}. To begin with, five different gene-specific pSuper constructs were kindly generated by Alan Ashworth and Chris Lord (Institute of Cancer Research UK,

London, UK) and included a scrambled control which does not recognise anything in the human genome. They expressed the following RNAi target sequences:

115

5'- **ATTCTATGGAGAACTTGCA** -3'

117

5'- **AGTATATGAGCTCCTAGGA** -3'

119

5'- **GATGTTGACTTCATGTACG** -3'

121

5'- **GAGTCTCTGGTGGAACAGT** -3'

Scrambled

5'- **CAUGCCUGAUCCGCUAGUC** -3'

A 1.6 kb fragment containing the *CMV IE* promoter and *eCFP* (enhanced cyan fluorescent protein) was subcloned from pECFP-Mito (Invitrogen) into the *Sap*I site of the resultant pSUPER constructs, generating pSUPER-eCFP-*Parp-1* and pSUPER-eCFP-*control*. The plasmids are all ampicillin resistant to assist transfection. Prior to transfection, 3µl Fugene (Roche, UK) was added to 97µl Opti-MEM (Sigma, UK) and incubated at room temperature for 5 minutes. To this, 1µg DNA was added, mixed well and incubated at room temperature for 15 minutes. For transfection, cells were treated with fresh media and the Fugene/Opti-MEM/DNA mixture. Initially, cells were then incubated with each target sequence and left for varying times (24h-72h). Transient transfection occurred after ~40h and persisted for ~18h. All experiments were therefore performed within this timeframe. Lysates were made as outlined in Section 2.7.1 and immunoblotted as in Section 2.8.

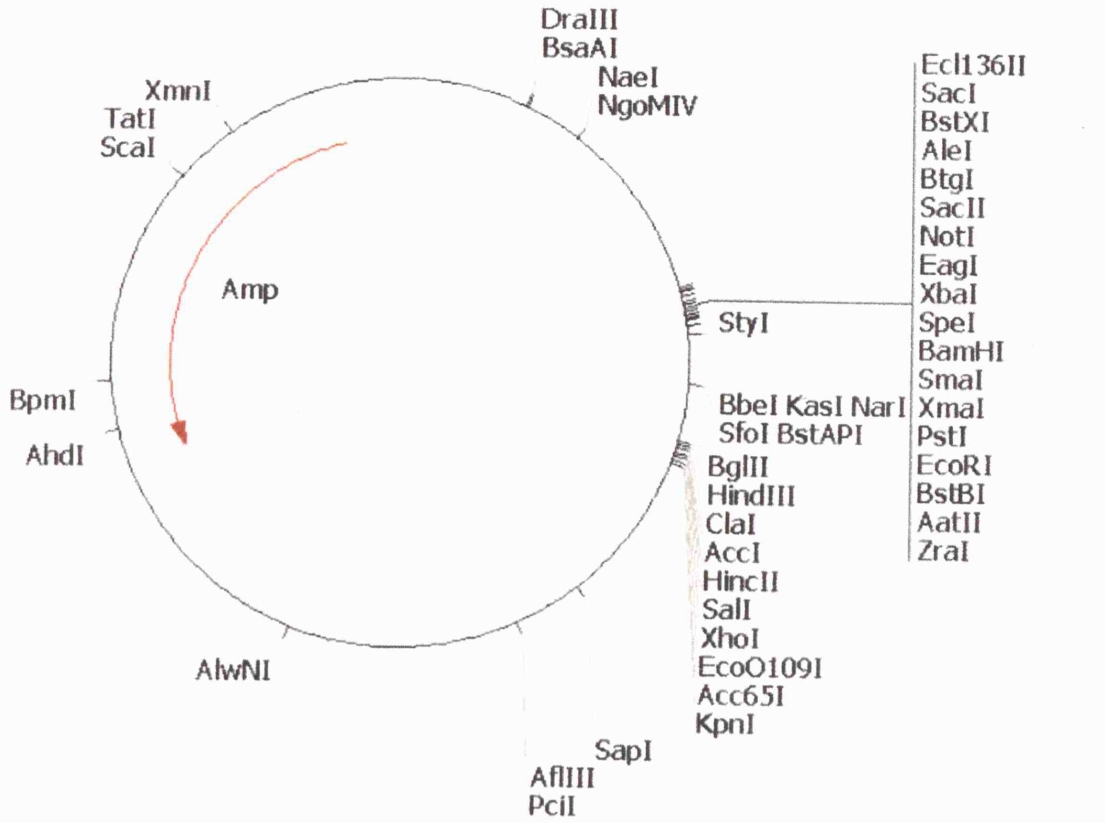

T7 primer binding site (AATACGACTCACTATAG): 627-643
T3 primer binding site (CTTTAGTGAGGGTTAAT): 989-1005
M13(-20) primer binding site (GTAAAACGACGGCCAGT): 600-616
M13 reverse primer binding site (CATGGTCATAGCTGTT): 1023-1038

Key Sites

BglII: 928
HindIII: 934
EcoRI: 707
SalI: 949
XhoI: 955

Vector Features

f1(+) origin: 441-135
H1 promoter: 708 - 934
pUC origin: 1373-2040
Ampicillin resistance ORF: 3048-2191

Figure 2.7: Map of the pSUPER RNAi System used for expressing siRNA directed against DNA-PK_{CS}.

Source: www.Oligoengine.com

2.12 DNA-PK Functional Assay

DNA-PK activity was detected using the SignaTECT® DNA-PK assay system (Promega, UK) according to the manufacturer's instructions. It provides an improved method to quantitate DNA-dependent protein kinase activity, both in purified enzyme preparations and in cell nuclear extracts. The SignaTECT® utilises the unique SAM^{2TM} Biotin Capture Membrane and results in a high density of streptavidin on the membrane matrix. This in turn provides rapid, quantitative capture of biotinylated substrate molecules, based on the strong affinity of biotin for streptavidin (Kd = 10–15M). The SignaTECT® DNA-Dependent Protein Kinase Assay System overcomes the problem of non-specific substrate binding by using a biotinylated DNA-PK p53-derived peptide substrate. The high binding capacity of the SAM^{2TM} Biotin Capture Membrane for the DNA-PK biotinylated peptide substrate and the low backgrounds observed with this system maximises the signal-to-noise ratio. Following phosphorylation of the DNA-PK biotinylated peptide substrate and binding to the SAM^{2TM} Membrane, the excess free [γ-^{32}P]ATP and non-biotinylated proteins are removed via a simple washing procedure. The binding of biotin to streptavidin is rapid and strong. Once formed, the biotin-streptavidin association is unaffected by extremes in pH, temperature, salt concentrations and denaturing agents. Due to the strength of this binding interaction, the ^{32}P-labeled DNA-PK Biotinylated Peptide Substrate is unlikely to be removed during the washing procedure.

The amount of ^{32}P incorporated into the DNA-PK Biotinylated Peptide Substrate is determined by liquid scintillation counting, phosphorimaging analysis or by conventional autoradiography. Figure 2.8 provides a schematic overview of the procedure.

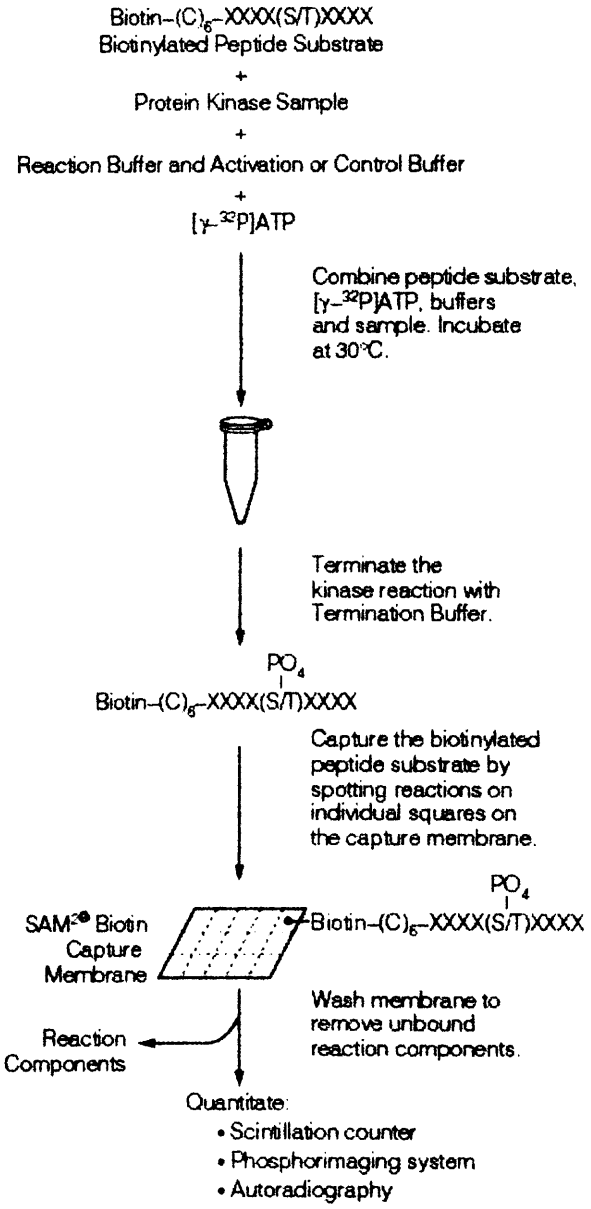

Figure 2.8: Schematic Diagram of the SignaTECT® Protein Kinase Assay protocol.
Source: SignaTECT Assay Technical Bulletin No. 250 (Promega, UK)

2.12.1 Cell Lysis

Treated cells were washed twice with PBS and left on ice. 100µl Lysis Buffer A (50mM NaF, 20mM HEPES pH 7.6, 450mM NaCl, 25% glycerol, 0.2mM EDTA, 0.5mM DTT, protease inhibitor tablet) was added for 10 minutes and cells scraped regularly. The cells were then transferred to an Eppendorf tube, snap-frozen on dry ice and thawed at 30°C. This was repeated three times. Cells were then centrifuged at 13,000rpm for 10 minutes at 4°C and the supernatant transferred to a fresh Eppendorf as a total cell lysate. The protein concentration was then determined using the protein assay detailed in Section 2.7.2.

2.12.2 Enzyme Assay

Calf thymus dsDNA cellulose (Sigma, UK) was prepared by swelling for 24h in Z' Buffer (25mM HEPES KOH pH 7.6, 12.5mM $MgCl_2$, 20% glycerol, 0.1% NP40, 1mM DTT, 50mM KCl) at 4°C. Following this, 200µg of total cell lysate was incubated with 20µl of swollen DNA-cellulose on a rotating wheel for 2h at 4°C. Lysates were then centrifuged at 13,000rpm for 10 minutes at 4°C and the supernatant discarded. Pellets were then washed once with Z' Buffer and resuspended in 60µl Z' Buffer. An ATP mix was then prepared containing 0.5mM ATP and [γ-^{32}P]ATP. The Activation and Control Buffers were prepared as shown in Table 2.6.

Component	Final per Reaction
DNA-PK **Activation Buffer**	2.5µl
DNA-PK 5x Reaction Buffer	5.0µl
DNA-PK Biotinylated Peptide Substrate	2.5µl
BSA (10mg/ml)	0.2µl
[γ-^{32}P]ATP mix	5.0µl
DNA-PK **Control Buffer**	2.5µl
DNA-PK 5x Reaction Buffer	5.0µl
DNA-PK Biotinylated Peptide Substrate	2.5µl
BSA (10mg/ml)	0.2µl
[γ-^{32}P]ATP mix (see step 11)	5.0µl

Table 2.6: Components of the Activation and Control Buffers for the SignaTECT® Protein Kinase Assay.

Buffers were pre-incubated at 30°C for 5 minutes. The reactions were then initiated by mixing an appropriate amount of lysate with Activation or Control Buffer and incubated at 30°C for an additional 5 minutes. It should be noted that each lysate was incubated with Control Buffer as well as Activation Buffer so that the former could provide a background reading.

The reactions were then terminated by adding 12.5µl Termination Buffer to each. These samples can be maintained at 4°C for 24h if necessary. From each, 10µl was removed and spotted onto pre-numbered squares of SAM^{2TM} Membrane and washed several times in salt (2M NaCl, H_3PO_4) on an orbital platform shaker. Membranes were then rinsed with water and left to dry. For a visual, non-mathematical result, the membranes were wrapped in cling film and exposed to Kodak X-OMAT™LS film for 24h. To determine the total counts for calculation of the specific activity of [γ-^{32}P]ATP, 5µl aliquots were removed from each terminated sample and spotted onto SAM^{2TM}

Membrane squares and left to dry without washing. For analysis by scintillation counting, squares were separated and placed into individual scintillation vials and scintillation fluid was added and counted (Wallac 1409 DSA-Based Liquid Scintillation Counter, Turku, Finland). The specific activity of [γ-^{32}P]ATP can then be calculated using the following formula:

$$\textbf{The Specific Activity of [}\gamma\textbf{-}^{32}\textbf{P]ATP in cpm/pmol} = \frac{\textbf{[(37.5/5) X]}}{\textbf{2500}}$$

Where: *37.5 is the sum of the reaction volume (25µl) + Termination Buffer (12.5µl).*
5 is the volume in µl of sample spotted
X is the average counts/minute of the 5µl sample
2500 is the number of picomoles of ATP in the reaction.

From this the DNA-PK Enzyme Activity can be calculated. This can be determined by subtracting the activity of the enzyme in the absence of activator (control buffer) from that of the enzyme in the presence of activator (activation buffer) and is defined by the following formula:

Enzyme specific activity in pmol ATP/minute/µg of protein =

$$\frac{(\textbf{cpm}_{\textbf{reaction with activator}} - \textbf{cpm}_{\textbf{reaction without activator}}) \textbf{ x } 37.5}{\textbf{10 x Time}_{\textbf{min}} \textbf{ x (µg of protein in reaction) x (specific activity of [}\gamma\textbf{-}^{32}\textbf{P]ATP)}}$$

Where: *37.5 is the sum of the reaction volume (25µl) + Termination Buffer (12.5µl).*
10 is the volume in µl of sample mixed with Activation/Control Buffer.

Note: *Time is 1 minute and 10µl of total cell lysate is used i.e. 10 x 1µg/µl from protein assay.*

2.13 Transient Transfection Assay

Wild-type and selected mutant EGFR constructs were transiently transfected into Cos-7 cells using the GeneJuice® transfection reagent (Novagen® EMD Biosciences Darmstadt, Germany). Exponentially growing Cos-7 cells were seeded at 1 x10^5 cells in six well plates (Nunclon™, VWR) and incubated for 24h at 37°C in 5% CO_2 prior to transfection. The optimum amount of Genejuice® reagent recommended for successful transfection of 1μg of DNA is 3μl. This was added to each tube containing 100μl of serum free medium and allowed to incubate at room temperature for 5 minutes. Following this 1μg DNA was added and incubated at room temperature for 15 minutes after which the entire mixture was added slowly over the surface of the appropriate well. Cells were then incubated for 24h allowing both cell recovery and transfection to take place.

The plasmid DNA used was the pUSEamp vector (Upstate Cell Signaling Solutions, NY, USA) and its map is illustrated in Figure 2.9 with the key sites highlighted.

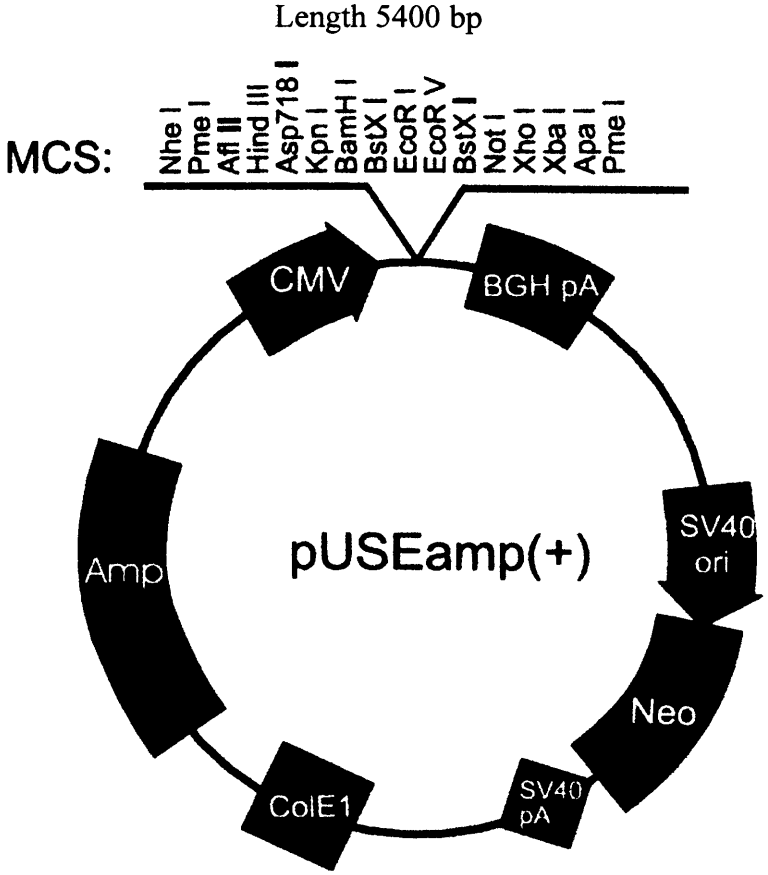

Figure 2.9: Map of the pUSEamp vector used for expressing various EGFR constructs.
Source: Upstate Cell Signaling Solutions (www.upstate.com)

The different EGFR constructs were kindly provided by Daphne Bell and Matthew Myerson from the MGH Cancer Centre, Harvard Medical School, Boston, USA. There were three constructs made in all using the pUSEamp vector and encoded wild-type EGFR as well as L858R and the delL747-P753insS mutant EGFR sequences. In addition to using Cos-7 untransfected cells as a control, cells transfected with the parental pUSEamp vector were also studied.

2.13.1 Drug Treatments

Transiently transfected Cos-7 cells were then serum starved for overnight. Cells were then treated with either cisplatin or gefitinib, or both at a range of concentrations and lengths of exposure. Appropriate schedules were then employed for immunoblotting studies and for the comet assay as outlined above. It should be noted that following treatment, cells were stimulated with EGF for 30 minutes at 100 ng/μl.

CHAPTER 3

INVESTIGATION OF DRUG SYNERGY BETWEEN EGFR INHIBITORS AND CHEMOTHERAPY

3.1 Introduction

The possibility of combining EGFR-targeted therapy with radio- and chemotherapy has been widely studied. This could be a promising therapeutic approach for a number of reasons. Firstly, the differing mechanisms of action of these agents may complement one another. Secondly, since EGFR mediates the expression of mitogenic signals, their inhibition can not only directly cause perturbation of cell growth, but may also affect the sensitivity of cancer cells to conventional chemotherapy and radiotherapy (Melisi *et al.*, 2004).

Both cetuximab and gefitinib as single agents have been shown to inhibit proliferation and increase apoptosis in different cancer cell lines and human tumour xenografts (Ciardiello *et al*, 2000; Ciardiello & Tortora, 2001). Importantly, EGFR expression alone does not determine the sensitivity of specific cell lines or xenografts to gefitinib treatment (Wakeling *et al*, 2002; Blackledge & Averbuch, 2004). Other factors such as the levels of expression of the other HER-family receptors also influence susceptibility to gefitinib treatment (Moasser *et al.*, 2001).

Many studies have demonstrated additive or synergistic antitumour effects when combining EGFR-targeted agents with chemotherapy or ionising radiation (Table 3.1).

Cancer Cell Lines	Anti-EGFR Therapy	Chemotherapy/ Irradiation	Reference
ZR-75-1 (Breast)	Cetuximab	Topotecan	Ciardiello *et al.*, 1999
OVCAR-3 (Ovarian)			
SCC-13Y, SCC-11B (SCCHN)	Cetuximab	Ionising Radiation	Huang *et al.*, 1999
OVCAR-3	Gefitinib	Cisplatin Carboplatin Paclitaxel Docetaxel Oxaliplatin Doxorubicin Topotecan Etoposide Tomudex	Ciardiello *et al.*, 2000
HT29 (Colon)	Gefitinib	Oxaliplatin	Xu *et al.*, 2003
CAL33 (Head and Neck)	Gefitinib	Cisplatin-5'FU	Magné *et al.*, 2002

Cancer Cell Lines	Anti-EGFR Therapy	Chemotherapy/ Irradiation	Reference
DU145, LNCaP (Prostate)	Gefitinib	Flutamide	Sgambato *et al.*, 2004
		Ionising Radiation	
OVCAR-3	Gefitinib	Ionising Radiation	Bianco *et al.*, 2002
A549, Calu-6 (Non Small Cell Lung)			
MCF-7 ADR (Breast)			

Xenografts	Anti-EGFR Therapy	Chemotherapy/ Irradiation	Reference
DLD-1 (Human Colon Carcinoma)	Cetuximab	Irinotecan	Prewett *et al.*, 2002
HT-29 (Human Colon Carcinoma)	Cetuximab	Irinotecan	
A431 (Human Vulvar)	Cetuximab	Doxorubicin	Mendelsohn & Baselga, 2000
A431 (Lung)	Cetuximab	Ionising Radiation	Milas *et al.*, 2003
A431	Gefitinib	Paclitaxel	Sirotnak *et al.*, 2000
A549	Gefitinib	Cisplatin Carboplatin Paclitaxel Docetaxel Doxorubicin Gemcitabine	
SK-LC-16 (Lung)	Gefitinib	Gemcitabine	
LX-1 (Lung)	Gefitinib	Carboplatin Taxol	
PC-3, TCU-PR1 (Prostate)	Gefitinib	Carboplatin Paclitaxel	
GEO (Human Colon Carcinoma)	Gefitinib	Paclitaxel Topotecan Tomudex	Ciardiello *et al.*, 2000
SK-LC-16	Gefitinib	Paclitaxel	Solit *et al.*, 2005
GEO	Gefitinib	Ionising Radiation	Bianco *et al.*, 2002

Table 3.1: Studies of EGFR-targeted agents in combination with radio- or chemotherapy.

3.1.1 Cetuximab Combined Therapies

Studies of cetuximab in combination with various agents indicate dose-dependent additive or synergistic increase in growth inhibition. Several *in vitro* experiments and *in vivo* animal studies have also shown an enhancement of tumour response to radiation by cetuximab in human epidermoid, head and neck, and colon cancer xenografts (Saleh *et al.*, 1999; Milas *et al.*, 2000; Bianco *et al.*, 2000; Prewett *et al.*, 2002). The increased sensitivity to radiotherapy induced by cetuximab may be due to a number of factors including an accumulation of cancer cells in the more radiosensitive cell cycle phases (G_1, G_2-M), a blockade of radiation-induced DNA repair mechanisms, and a reduction of VEGF production by cancer cells with inhibition of tumour angiogenesis (Huang *et al.*, 2000; Ciardiello & Tortora, 2001).

A recent phase III trial in squamous cell carcinoma of the head and neck (SCCHN) showed that the addition of cetuximab to radiotherapy improved survival and enhanced local control as compared with radiation alone (Bonner *et al.*, 2004). Furthermore, in a colorectal cancer model, cetuximab was found to reverse resistance to irinotecan. It was shown that there was activity for the combination of irinotecan and cetuximab in patients who experienced treatment failure with irinotecan alone (Saltz *et al.*, 2001; Prewett *et al.*, 2002; Cunningham *et al.*, 2004).

Studies in patients with advanced disease refractory to cisplatin, showed clinical activity with the addition of cetuximab to the original cisplatin dose (Kim *et al.*, 2002; Baselga *et al.*, 2002). However, the same response rate had been observed with the administration of cetuximab alone (Trigo *et al.*, 2004).

3.1.2 Gefitinib Combined Therapies

The addition of gefitinib increased inhibition of proliferation, induction of apoptosis, and increased antitumor activity *in vitro* and *in vivo* when combined with a variety of chemotherapeutic agents (Table 3.1). Similarly, combination with radiation synergistically increased inhibition of proliferation and pro-apoptotic effects *in vitro* and increased tumour growth delay in the treatment of human tumour xenografts (Bianco *et al.*, 2002; Solomon *et al.*, 2003; Giocanti *et al.*, 2004).

In contrast to the preclinical data, four large phase III clinical trials in patients with either locally advanced stage III disease or stage IV NSCLC failed to show any benefit for combined treatment with cisplatin, carboplatin, gemcitabine and paclitaxel

(Giaccone *et al.*, 2004; Herbst *et al.*, 2004; Gatzemeier *et al.*, 2004; Moore *et al.*, 2005).

3.1.3 Aims

The aims of this chapter are to investigate the features of synergistic inhibition of proliferation between gefitinib and chemotherapy in a variety of cancer cell lines. To this end, the following questions are addressed:

1. Is the synergistic effect of gefitinib and chemotherapeutic agents increased with specific agents?
2. Is synergy with chemotherapy dependent on the administering schedule?
3. Is the processing of chemotherapy-induced DNA damage involved in synergy with gefitinib?
4. Given the positive clinical results, do the same patterns occur with colon cancer cell lines?

These experiments may provide a better understanding leading to further investigations of the mechanisms underlying the interactions between EGFR inhibitors and chemotherapeutic agents to improve therapeutic benefit.

RESULTS

3.2 Gefitinib and Chemotherapy Treatments

Cytotoxicity of drugs alone or in combination was determined by the Sulphorhodamine B (SRB) proliferation assay as described in Section 2.4.1. Experiments were largely carried out on MCF-7 cells. This is a human breast adenocarcinoma cell line established from a pleural effusion from a 69 year female Caucasian (Soule *et al.*, 1973). The line exhibits some features of differentiated mammary epithelium including oestradiol synthesis and may carry B or C type retrovirus (Zhang *et al.*, 1993). Cells express the wild-type and variant oestrogen receptors as well as the progesterone receptor (ECACC, 86012803). MCF-7 cells express functional EGFR of a magnitude of approximately 250,000 EGF binding sites per cell (Ciardiello *et al.*, 1999).

3.2.1 Determination of IC_{50} Values

Before investigating synergistic effects between gefitinib and chemotherapy, single agent treatments were carried out on all cell lines to obtain suitable dose ranges for different exposure times. Figure 3.1 shows the proliferation profile following a 24h exposure to cisplatin, etoposide, melphalan and doxorubicin on MCF-7 cells.

The IC_{50} values for each agent on MCF-7 cells for 24h were: cisplatin, 11.1±0.9μM; etoposide, 3.8±0.3μM; melphalan, 19±1.08μM; and doxorubicin, 62±4.6nM. Single agent treatments were also carried out on the rat pancreatic AR42J cell line and the colon cancer cell lines CaCo-2 and HCT-116 (data not shown).

SRB assays were carried out to assess the anti-proliferative effects of gefitinib under various conditions. Figure 3.2 shows the growth inhibition effects of gefitinib as a single-agent on MCF-7 cells. An acute exposure of cells to gefitinib for 2h showed a dose-dependent inhibition of proliferation with an IC_{50} of 26±1.3μM (Figure 3.2a). Longer exposures of 24h and 72h were also carried out producing IC_{50} values of 17±0.8μM and 16±0.43μM respectively (Figures 3.2b-c). The dose-dependent inhibitory effect of daily gefitinib treatments is shown in Figure 3.2d and the IC_{50} effect is achieved with the significantly lower dose of 0.4±0.007μM. These results highlight some of the cytotoxic effects and pharmacodynamic features of *in vitro* gefitinib treatment as a single agent, and are discussed in more detail in the discussion section of this chapter.

For the purposes of combination studies of gefitinib with chemotherapeutic agents, the IC_{10} and IC_{20} values for gefitinib treatment as a single agent have also been determined and are also shown in Figure 3.2.

Gefitinib single agent treatments were also carried out on the rat pancreatic AR42J cell line which express high levels of EGFR (Ishiyama *et al.*, 1998; Piiper *et al.*, 2003) and are summarised in Table 3.2 below.

AR42J Cells			
Treatment	**IC_{10} (μM)**	**IC_{20} (μM)**	**IC_{50} (μM)**
Gefitinib 72h	3±0.43	6±1.6	15±0.74
Gefitinib 24h	2±0.73	5±0.94	18±0.68
Gefitinib 2h	5±0.88	10±1.67	21±0.97
Gefitinib Daily	0.03±0.007	0.045±0.0066	0.13±0.0042

Table 3.2: IC_{10}, IC_{20} and IC_{50} values for single agent gefitinib treatment on AR42J cells.

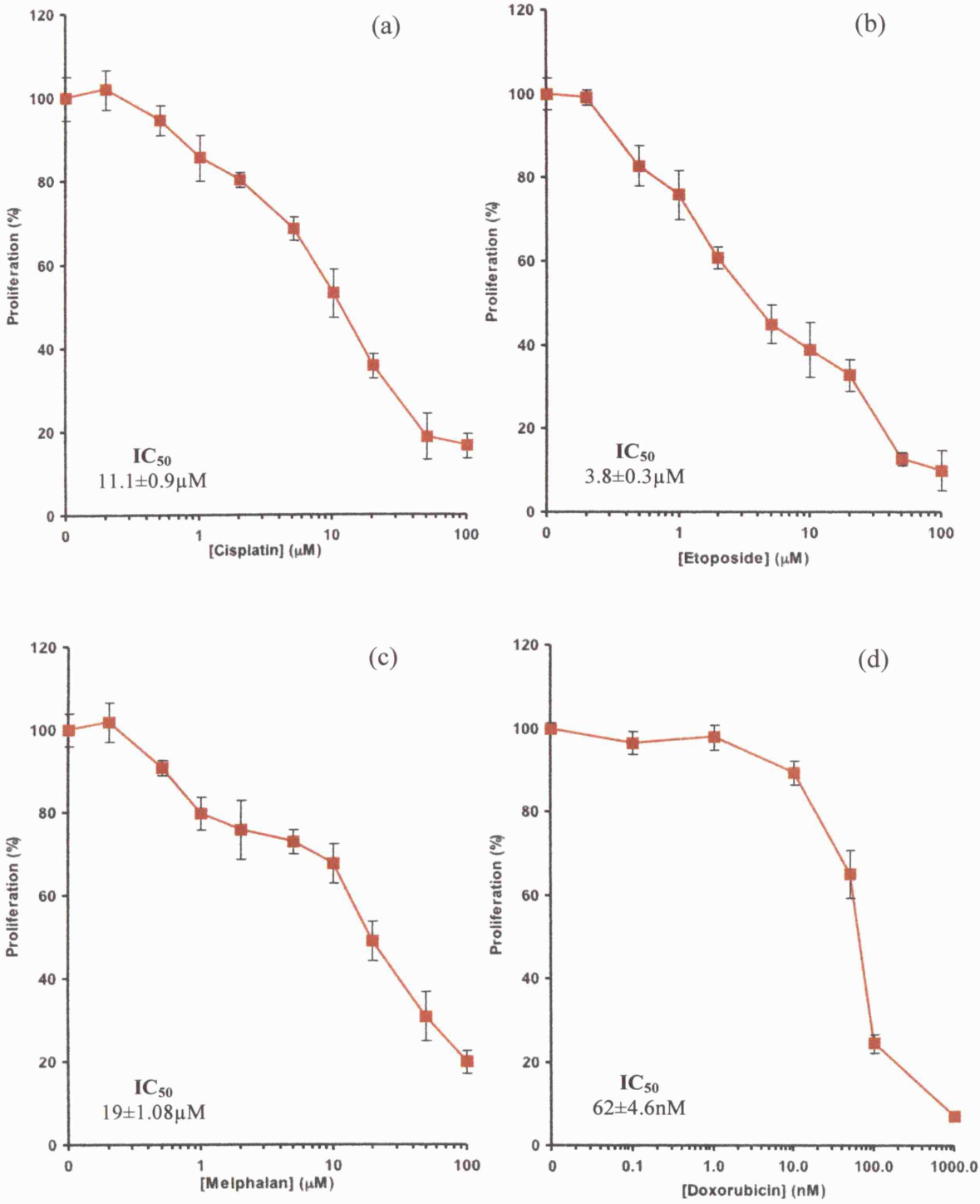

Figure 3.1: *Single agent in vitro growth inhibition by (a) cisplatin (b) etoposide (c) melphalan (d) doxorubicin on MCF-7 cells.* Following 24h exposure to chemotherapy, cells were incubated in drug free medium till Day 6. Data expressed as a percentage of the control untreated well absorbance and represents the averages of three different experiments, each performed in triplicate; *bars,* SD.

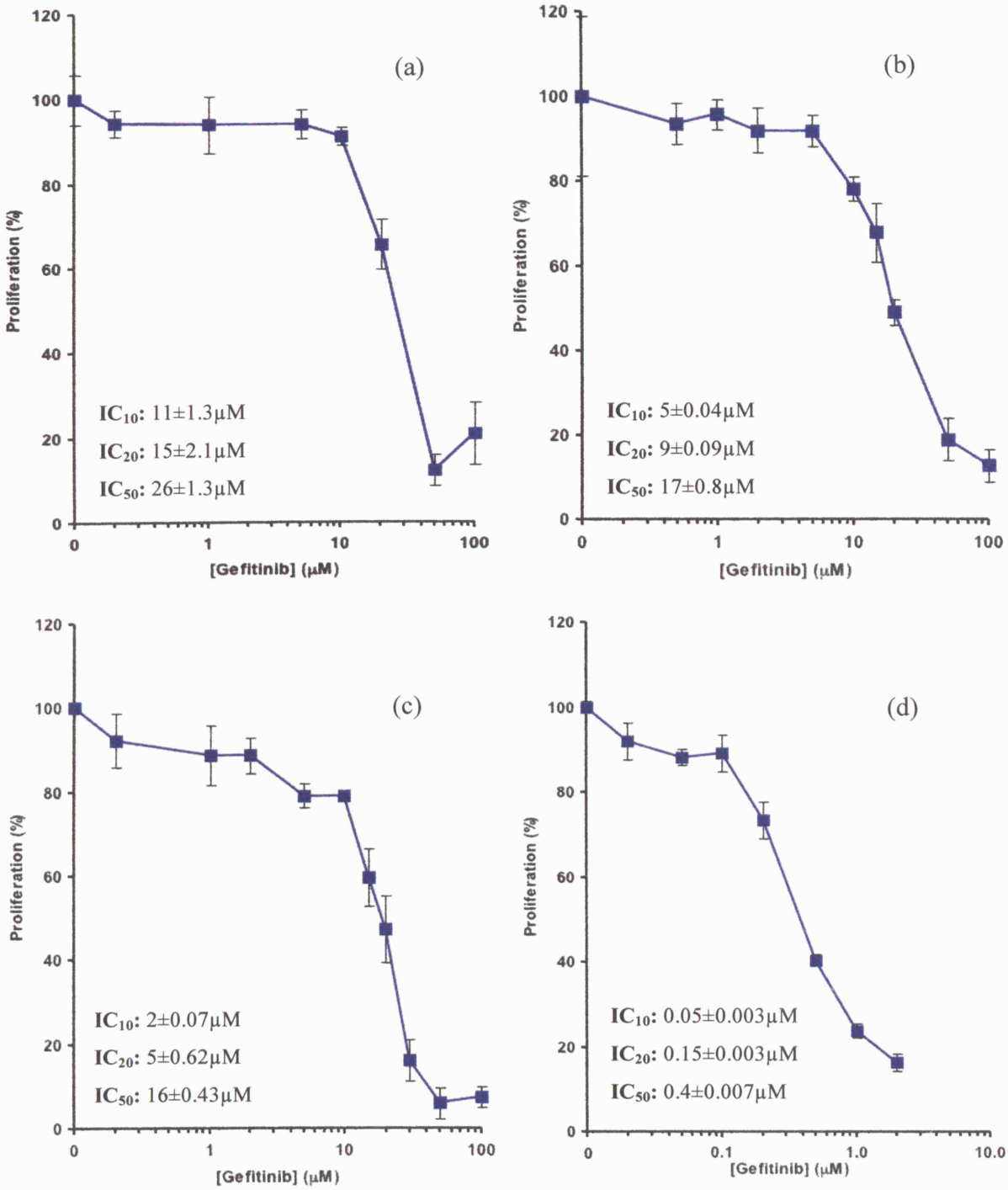

Figure 3.2: *Single agent in vitro growth inhibition by gefitinib for (a) 2h (b) 24h (c) 72h (d) daily treatments on MCF-7 cells.* Following exposure, cells were incubated in drug free medium till Day 6. Data expressed as a percentage of the control untreated well absorbance and represents the averages of three different experiments, each performed in triplicate; *bars,* SD.

3.2.2 Synergistic Effects of Gefitinib with Chemotherapeutic Agents

Combination treatments of gefitinib were carried out on MCF-7 cells with the topoisomerase II poison, etoposide; the topoisomerase II intercalating agent, doxorubicin; the DNA crosslinking platinum based compound, cisplatin and the DNA crosslinking alkylating agent, melphalan (Figures 3.3 to 3.6 respectively).

For combination studies, drugs were added sequentially by delivering each drug in turn for 24 hours. For determination of synergy, gefitinib was added at sub-toxic concentrations (e.g. producing 10% or 20% inhibition of proliferation) to a range of concentrations for chemotherapy. Based on the results shown in Figure 3.2b for gefitinib 24h treatment (IC_{10}: 5±0.04μM; IC_{20}: 9±0.09μM), gefitinib was therefore added at either 5μM or 10μM inhibiting proliferation by 10% or 20% respectively.

The isobologram methodology is used for determining inhibitory, additive or synergistic effects of two drugs in combination. It allows for comparisons of the combined effects with the individual constituents when administered at the same dose (see Section 2.4.2) (Tallarida, 2001).

Etoposide

Figure 3.3a shows the growth inhibition effect of etoposide 24h exposure alone and followed by gefitinib on MCF-7 cells. Cells exposed to etoposide alone demonstrated an IC_{50} of 3.5±0.08μM (Figure 3.1b) whereas when followed by 5μM gefitinib, the IC_{50} was 0.7±0.05μM. Furthermore, etoposide in combination with 10μM gefitinib showed a 10-fold increase in inhibition of proliferation with an IC_{50} of 0.35±0.06μM as compared with etoposide alone.

The isobologram is shown in Figure 3.3b. IC_{50} values for etoposide and gefitinib alone are connected by a straight line or *additivity line* and is the locus of all dose pairs that, based on these potencies, should give the same effect for these two drugs added together. (Note: The IC_{50} value for gefitinib alone is 17μM, see Figure 3.2b). As can be seen in Figure 3.3b, the IC_{50} of both the dose pairs etoposide and 5μM gefitinib and etoposide and 10μM gefitinib, lie well below this line and so confirm a superadditive or synergistic effect.

Doxorubicin

The dual treatment of doxorubicin with gefitinib under the same conditions as for etoposide is shown in Figure 3.4. Doxorubicin alone demonstrates an IC_{50} of 62±4.6nM whereas doxorubicin followed by 5μM gefitinib achieves an IC_{50} with 7±1.1nM and doxorubicin followed by 10μM gefitinib has an IC_{50} of 4±0.5nM. Isobologram analysis shows that doxorubicin combined with both doses of gefitinib lie well below the additivity line confirming a synergistic effect.

Cisplatin

Cells treated with cisplatin alone for 24h produced an IC_{50} of 10±0.9μM. Cells treated with cisplatin for 24h followed by 5μM gefitinib or 10μM gefitinib achieved an IC_{50} with 0.2±0.003μM (Figure 3.5a). Synergistic effects were confirmed by isobologram analysis which places both dose pairs as far within the superadditive region as is possible (Figure 3.5b).

Melphalan

Figure 3.6a shows the growth inhibition effect of melphalan 24h exposure alone and followed by gefitinib on MCF-7 cells. Cells exposed to melphalan alone demonstrated an IC_{50} of 19±1.08μM. In contrast to the results obtained for etoposide, doxorubicin and cisplatin, there was **no** demonstrable synergy with melphalan in combination with 5μM gefitinib (IC_{50} of 18±0.78μM) or with 10μM gefitinib (IC_{50} of 11±0.92). Isobologram analysis confirms this observation displaying both dose pairs close to the additivity line (see Section 2.4.2 and Figure 2.1 for comprehensive pharmacological parameters). It should be noted that the addition of gefitinib following melphalan does not have an inhibitory effect but rather a modest additive effect (Figure 3.6b).

Figures 3.3 to 3.6 therefore illustrate that the effects of gefitinib on cell proliferation in combination with chemotherapy are variable with different DNA-interactive chemotherapeutic agents.

(a)

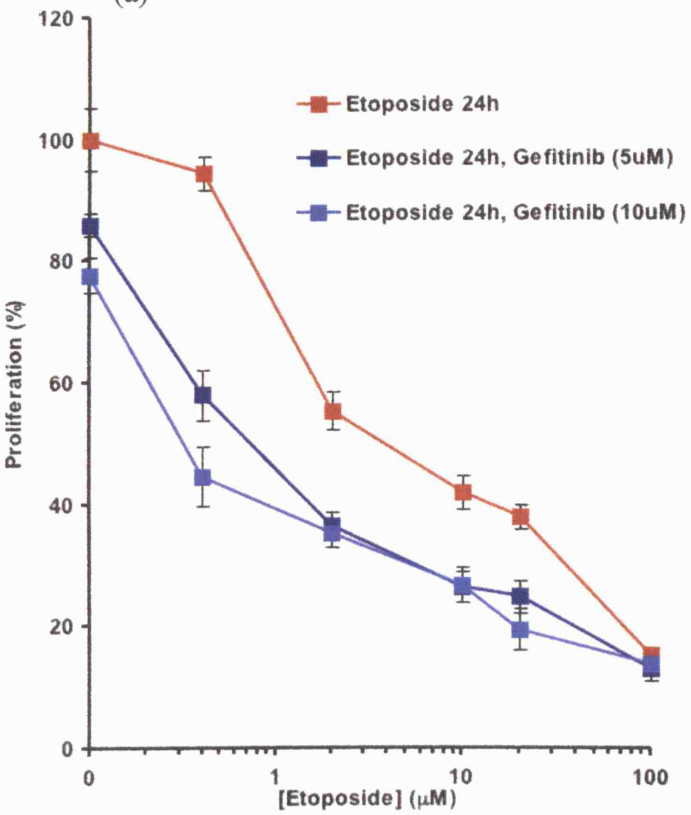

	IC_{50} (μM)
Etoposide 24h:	3.5±0.08
Etoposide 24h & Gefitinib (5μM):	0.7±0.05
Etoposide 24h & Gefitinib (10μM):	0.35±0.06

(b)

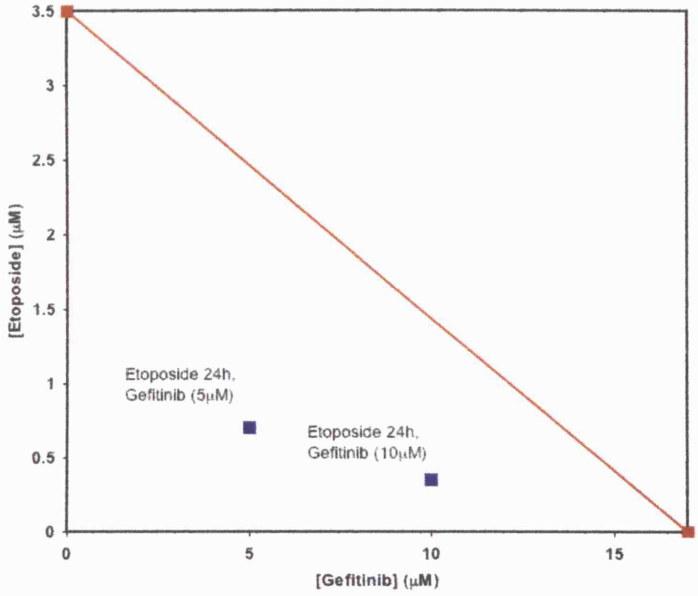

Figure 3.3: *Dual-Agent in vitro growth inhibition and isobologram analysis for etoposide 24h exposure alone and followed by gefitinib on MCF-7 cells.*

(a) Growth inhibition SRB assay: Following 24h exposure to etoposide alone, cells were incubated in drug free medium or gefitinib for 24h and left till Day 6. Data expressed as a percentage of the control untreated well absorbance and represents the averages of three different experiments, each performed in triplicate; *bars,* SD.

(b) Isobologram analysis: The straight line connecting their IC_{50} points (additivity line) (■) is the locus of all dose pairs that, based on these potencies, should give the same effect. A dose pair attaining this effect with lower quantities is superadditive (synergistic), while a point appearing close to the line is additive. Dose pairs (■) IC_{50} of etoposide and gefitinib together.

(a)

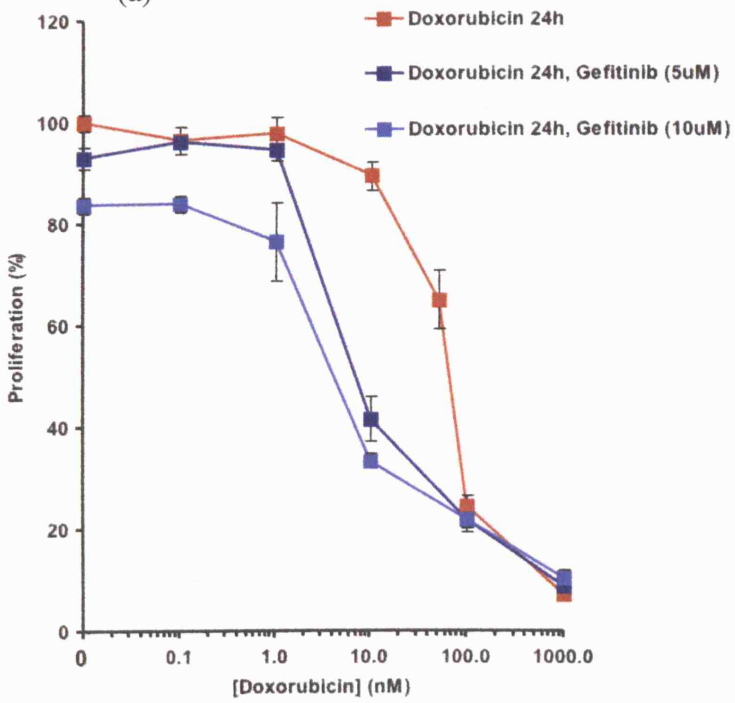

	IC_{50} (nM)
Doxorubicin 24h:	62±4.6
Doxorubicin 24h & Gefitinib (5μM):	7±1.1
Doxorubicin 24h & Gefitinib (10μM):	4±0.5

(b)

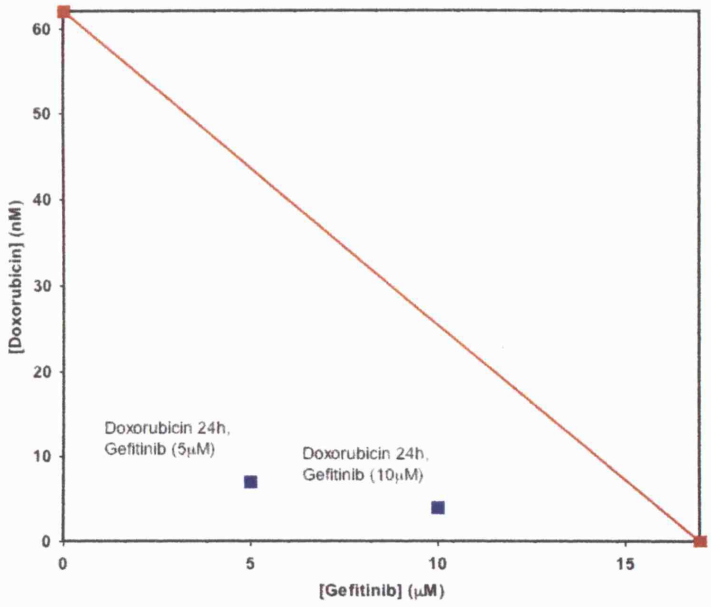

Figure 3.4: *Dual-Agent in vitro growth inhibition and isobologram analysis for doxorubicin 24h exposure alone and followed by gefitinib on MCF-7 cells.*

(a) Growth inhibition SRB assay: Following 24h exposure to doxorubicin alone, cells were incubated in drug free medium or gefitinib for 24h and left till Day 6. Data expressed as a percentage of the control untreated well absorbance and represents the averages of three different experiments, each performed in triplicate; *bars,* SD.

(b) Isobologram analysis: Dose pairs (■) IC_{50} of doxorubicin and gefitinib together.

(a)

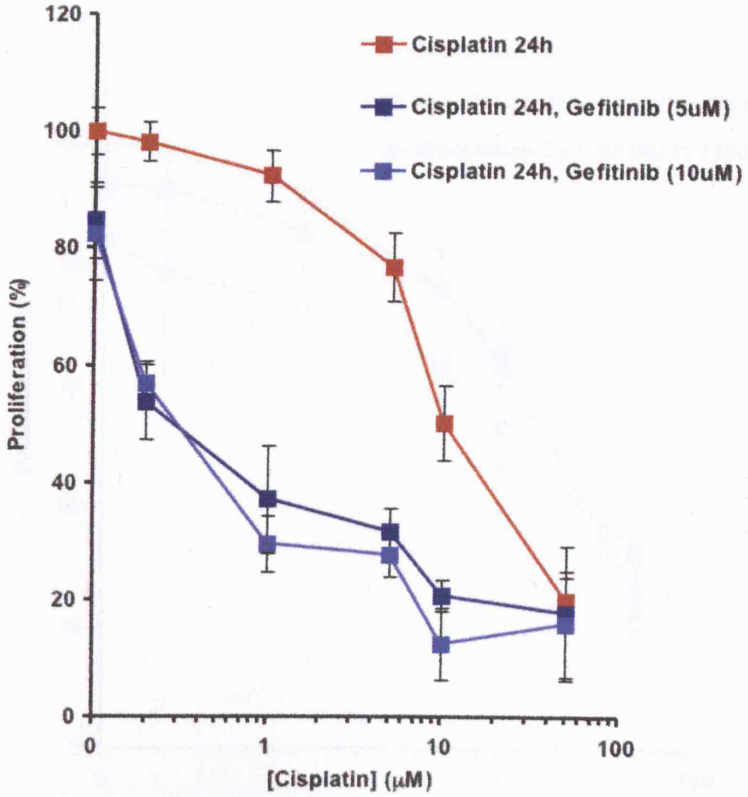

	IC_{50} (μM)
Cisplatin 24h:	10±0.9
Cisplatin 24h & Gefitinib (5μM):	0.2±0.003
Cisplatin 24h & Gefitinib (10μM):	0.2±0.003

(b)

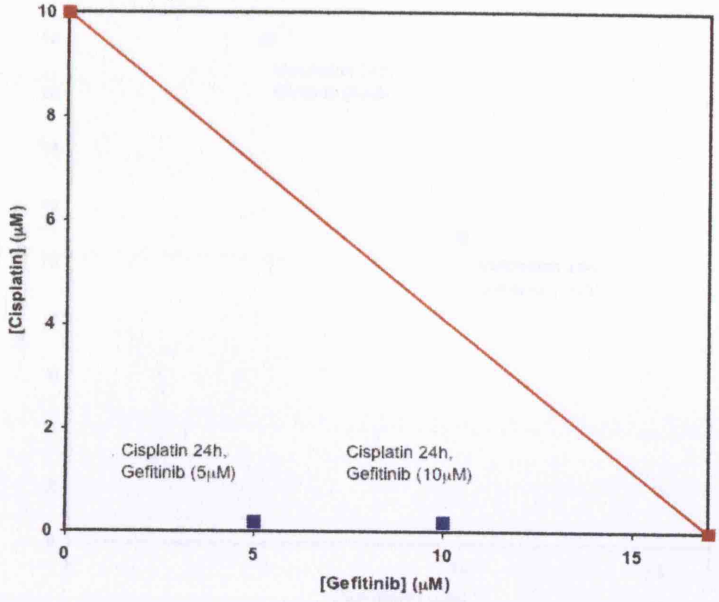

Figure 3.5: *Dual-Agent in vitro growth inhibition and isobologram analysis for cisplatin 24h exposure alone and followed by gefitinib on MCF-7 cells.*

(a) Growth inhibition SRB assay: Following 24h exposure to cisplatin alone, cells were incubated in drug free medium or gefitinib for 24h and left till Day 6. Data expressed as a percentage of the control untreated well absorbance and represents the averages of three different experiments, each performed in triplicate; *bars,* SD.

(b) Isobologram analysis: Dose pairs (■) IC_{50} of cisplatin and gefitinib together.

(a)

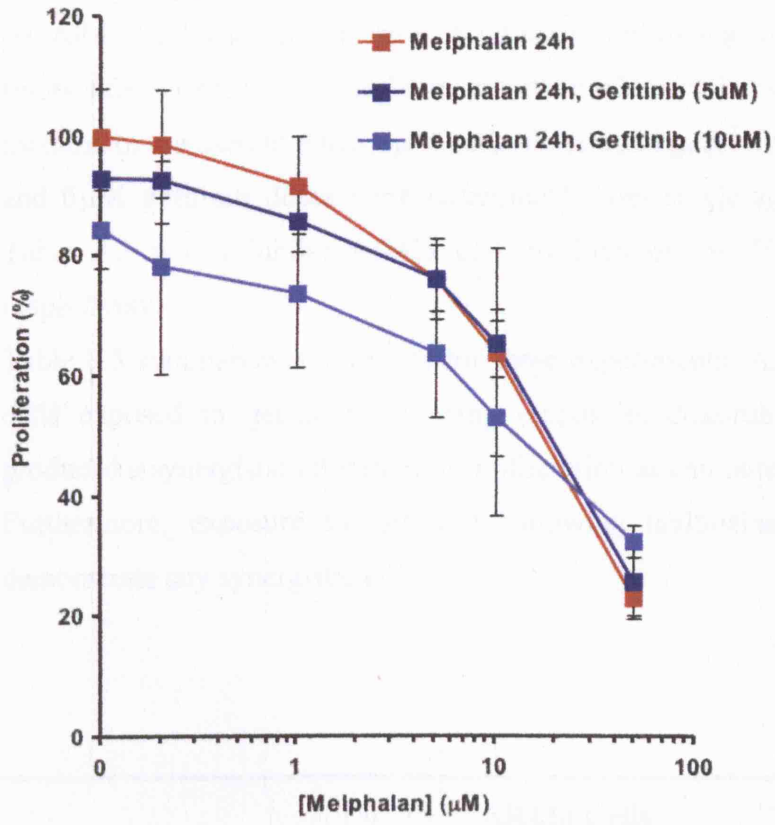

	IC_{50} (μM)
Melphalan 24h:	19±1.08
Melphalan 24h & Gefitinib (5μM):	18±0.78
Melphalan 24h & Gefitinib (10μM):	11±0.92

(b)

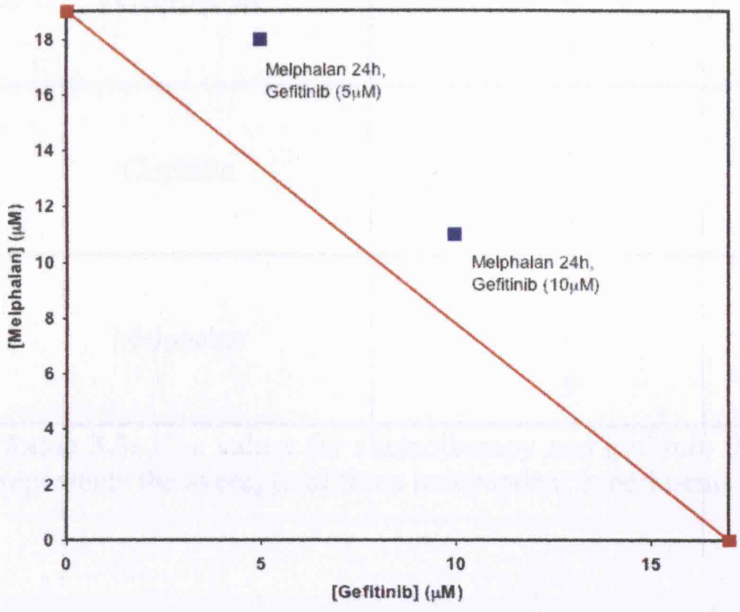

Figure 3.6: *Dual-Agent in vitro growth inhibition and isobologram analysis for melphalan 24h exposure alone and followed by gefitinib on MCF-7 cells.*

(a) Growth inhibition SRB assay: Following 24h exposure to melphalan alone, cells were incubated in drug free medium or gefitinib for 24h and left till Day 6. Data expressed as a percentage of the control untreated well absorbance and represents the averages of three different experiments, each performed in triplicate; *bars,* SD.

(b) Isobologram analysis: Dose pairs (■) IC_{50} of melphalan and gefitinib together.

The synergy studies of gefitinib and chemotherapy outlined above were also carried out on AR42J cells under the same conditions. Following 24h chemotherapy treatment (etoposide, doxorubicin, cisplatin and melphalan) cells were incubated in drug-free medium or exposed to either 2μM gefitinib or 5μM gefitinib for 24h. The 2μM gefitinib and 5μM gefitinib doses were determined from single-agent studies summarised in Table 3.2 which inhibit AR42J cell proliferation by 10% (IC_{10}) and 20% (IC_{20}) respectively.

Table 3.3 summarises the results for these experiments. As with MCF-7 cells, AR42J cells exposed to gefitinib following etoposide, doxorubicin or cisplatin treatment produced a synergistic inhibition of proliferation as compared with chemotherapy alone. Furthermore, exposure to gefitinib following melphalan treatment again did not demonstrate any synergistic effects.

AR42J Cells		
Drug (24h)	**Gefitinib (μM)**	**IC_{50}**
Etoposide	-	1.5±0.04 μM
	2	0.04±0.0031 μM
	5	0.03±0.0089 μM
Doxorubicin	-	58±5.17 nM
	2	8±2.3 nM
	5	8±1.7 nM
Cisplatin	-	1.5±0.07 μM
	2	0.2±0.084 μM
	5	0.05±0.009 μM
Melphalan	-	3.1±0.99 μM
	2	2.2±1.06 μM
	5	1.6±0.57 μM

Table 3.3: IC_{50} values for chemotherapy and gefitinib treatment on AR42J cells. Data represents the averages of three independent experiments each performed in triplicate.

3.3 Schedule-Dependent Synergistic Effects

The synergistic features of gefitinib treatment following etoposide, doxorubicin, cisplatin and melphalan were studied to investigate the effects of schedule of administration on chemosensitisation. Using the SRB assay, inhibitory effects of exposing MCF-7 cells to gefitinib following an acute exposure to chemotherapy were investigated.

Drugs were added sequentially by first exposing cells to the chemotherapeutic agent for 2h followed by gefitinib treatment for 24 hours. Figure 3.7 shows the proliferation profile for a cisplatin 2h exposure. The IC_{50} for cisplatin alone was 24±1.1μM. Cisplatin 2h treatment followed by 5μM gefitinib achieved an IC_{50} of 2.8±0.5μM and cisplatin 2h followed by 10μM gefitinib achieved an IC_{50} of 1.9±0.22μM. Therefore, both doses of gefitinib synergise with around a 10-fold increase in inhibition of proliferation as compared with cisplatin 2h exposure alone. Synergy was again confirmed using isobologram analysis.

The effects of gefitinib treatment following a melphalan 2h exposure are shown in Figure 3.8. Melphalan alone had an IC_{50} of 30.5±3.3μM. As with a 24h exposure, subsequent gefitinib treatment did not demonstrate any synergistic effect on inhibition of proliferation (5μM gefitinib: 28±2.7μM; 10μM gefitinib: 21.9±1.0μM). Isobologram analysis as before indicates a modest additive effect.

Synergy was also seen for gefitinib treatment following acute exposures to etoposide and doxorubicin and are summarised in Table 3.4 below.

MCF-7 Cells		
Drug 2h	**Gefitinib (μM)**	**IC_{50}**
Etoposide	-	22.4±3.3 μM
	5	8.1±0.9 μM
	10	2±0.04 μM
Doxorubicin	-	90.3±7.1 nM
	5	60±3.4 nM
	10	6.2±1.0 nM

Table 3.4: IC_{50} values for gefitinib treatment following etoposide or doxorubicin 2h exposure on MCF-7 cells.

(a)

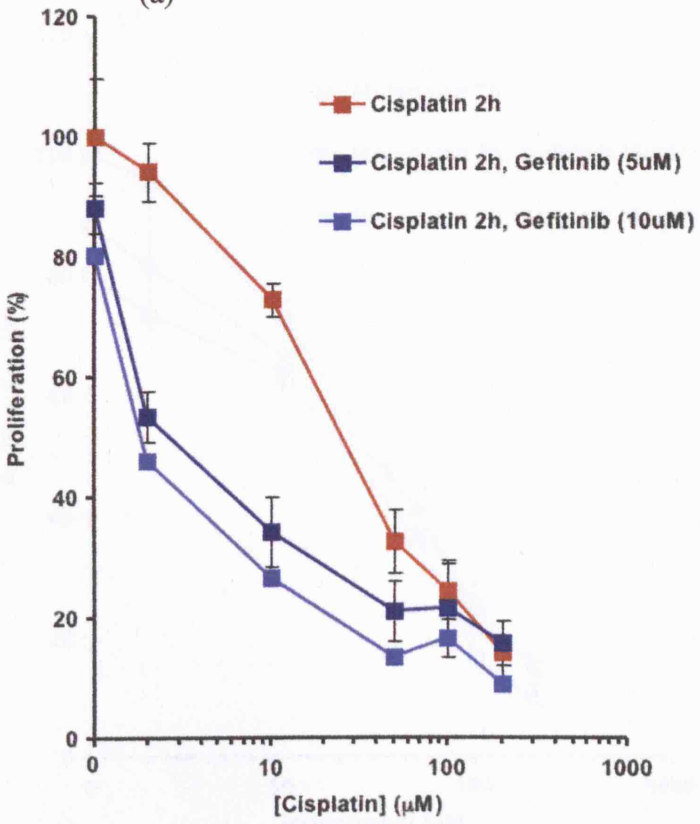

	IC_{50} (μM)
Cisplatin 2h:	24±1.1
Cisplatin 2h & Gefitinib (5μM):	2.8±0.5
Cisplatin 2h & Gefitinib (10μM):	1.9±0.22

(b)

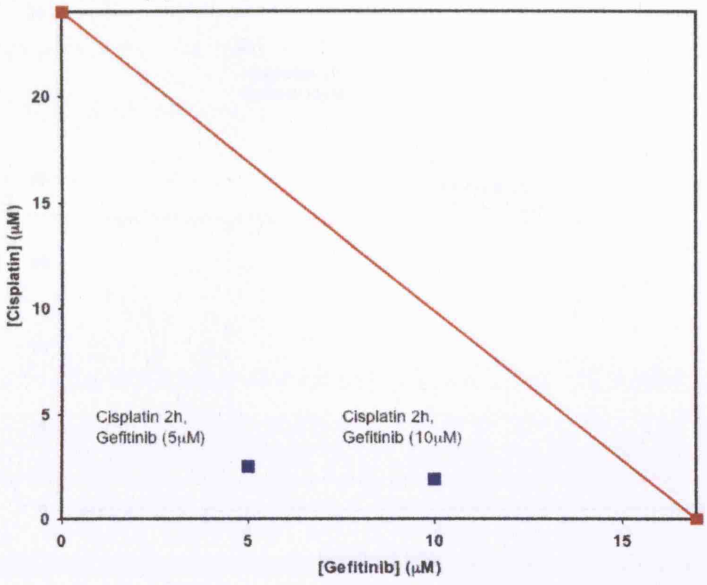

Figure 3.7: *Dual-Agent in vitro growth inhibition and isobologram analysis for cisplatin 2h exposure alone and followed by gefitinib on MCF-7 cells.*

(a) Growth inhibition SRB assay: Following 2h exposure to cisplatin alone, cells were incubated in drug free medium or gefitinib for 24h and left till Day 6. Data expressed as a percentage of the control untreated well absorbance and represents the averages of three different experiments, each performed in triplicate; *bars,* SD.

(b) Isobologram analysis: Dose pairs (■) IC_{50} of cisplatin and gefitinib together.

(a)

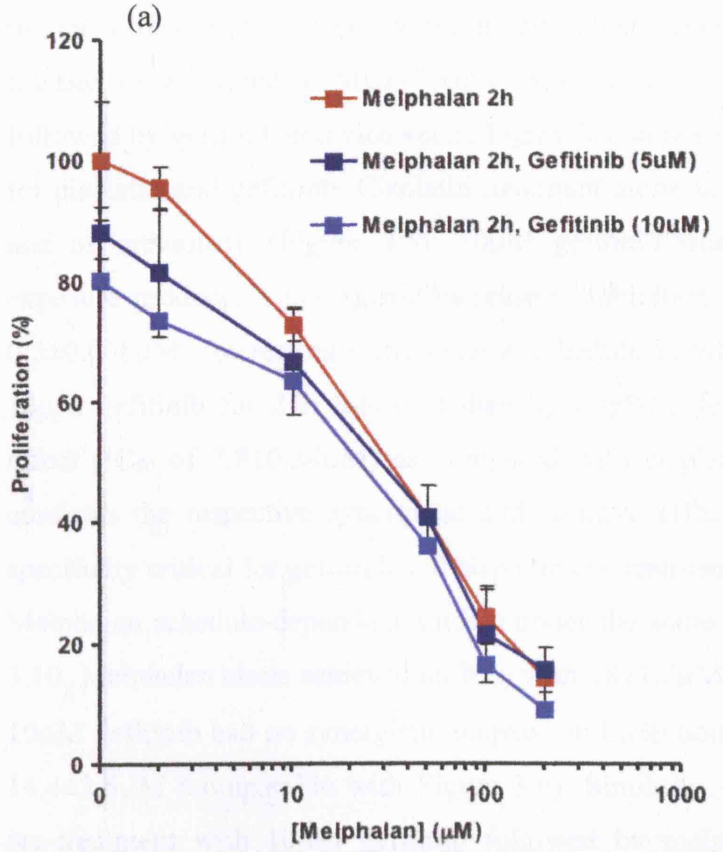

	IC_{50} (μM)
Melphalan 2h:	30.5±3.3
Melphalan 2h & Gefitinib (5μM):	28±2.7
Melphalan 2h & Gefitinib (10μM):	21.9±1.0

(b)

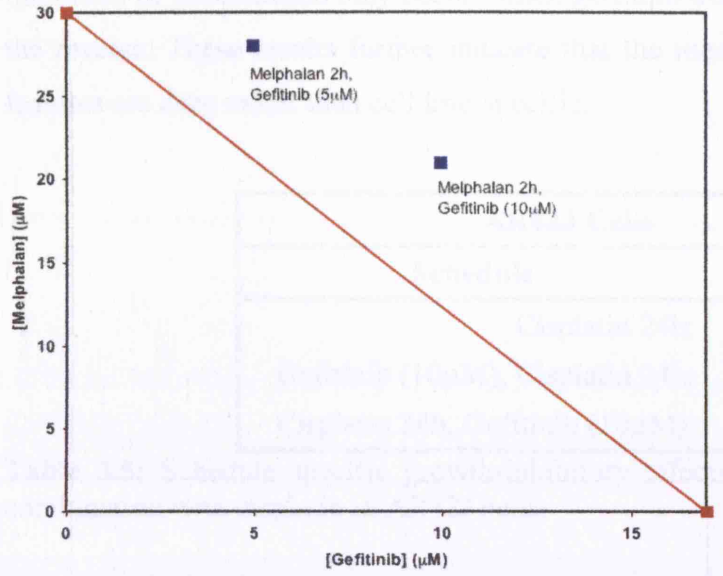

Figure 3.8: *Dual-Agent in vitro growth inhibition and isobologram analysis for melphalan 2h exposure alone and followed by gefitinib on MCF-7 cells.*

(a) Growth inhibition SRB assay: Following 2h exposure to melphalan alone, cells were incubated in drug free medium or gefitinib for 24h and left till Day 6. Data expressed as a percentage of the control untreated well absorbance and represents the averages of three different experiments, each performed in triplicate; *bars,* SD.

(b) Isobologram analysis: Dose pairs (■) IC_{50} of melphalan and gefitinib together.

Experiments were then carried out to investigate whether the sequence of drug delivery has any effect on the synergy between gefitinib and chemotherapy.

Studies were limited to MCF-7 cells exposed sequentially for 24h to chemotherapy followed by gefitinib and vice versa. Figure 3.9 shows the sequence-specific SRB assay for cisplatin and gefitinib. Cisplatin treatment alone achieved an IC_{50} with 8.9±0.6μM and as previously (Figure 3.5), 10μM gefitinib treatment following cisplatin 24h exposure produces a synergistic increase in inhibition of proliferation with an IC_{50} of 0.5±0.008μM. Interestingly the reverse schedule in which cells were first exposed to 10μM gefitinib for 24h followed then by cisplatin for 24h, produced no synergistic effect (IC_{50} of 7.8±0.34μM) as compared with cisplatin alone. Isobologram analysis confirms the respective synergistic and additive effects and highlights the schedule-specificity critical for gefitinib and cisplatin co-treatment.

Melphalan schedule-dependent studies under the same conditions are shown in Figure 3.10. Melphalan alone achieved an IC_{50} with 18±1.2μM. Again, subsequent exposure to 10μM gefitinib had no synergistic increase in inhibition of proliferation with an IC_{50} of 14.4±2.6μM (comparable with Figure 3.6). Similarly, and as in the case of cisplatin, pre-treatment with 10μM gefitinib followed by melphalan produced no synergistic effect (IC_{50} of 16.2±1.07μM) as compared with melphalan alone. Isobologram analysis confirms additive effects for both schedules.

Sequence-specific studies of cisplatin and gefitinib were also carried out on AR42J cells and are summarised in Table 3.5. As with MCF-7 cells, a synergistic increase in inhibition of proliferation only occurs when gefitinib treatment follows cisplatin and not the reverse. These results further indicate that the mechanisms underlying synergistic features are drug rather than cell line-specific.

AR42J Cells	
Schedule	**IC_{50} (μM)**
Cisplatin 24h:	1.7±0.28
Gefitinib (10μM), Cisplatin 24h:	0.18±0.025
Cisplatin 24h, Gefitinib (10μM):	1.7±0.34

Table 3.5: Schedule specific growth-inhibitory effects of treatment with gefitinib in combination with cisplatin in AR42J cells.

(a)

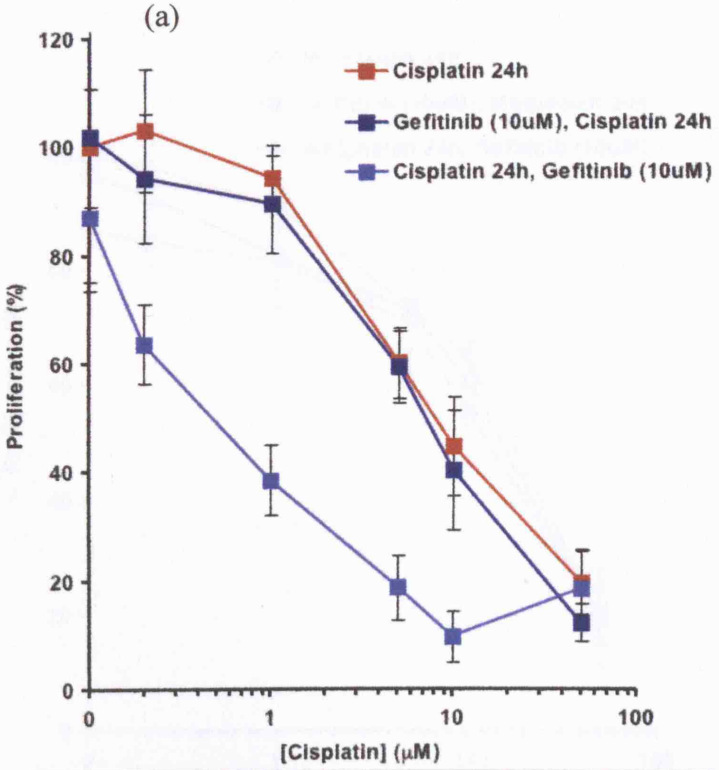

Schedule	IC_{50} (μM)
Cisplatin 24h:	8.9±0.6
Gefitinib (10μM), Cisplatin 24h:	7.8±0.34
Cisplatin 24h, Gefitinib (10μM):	0.5±0.008

(b)

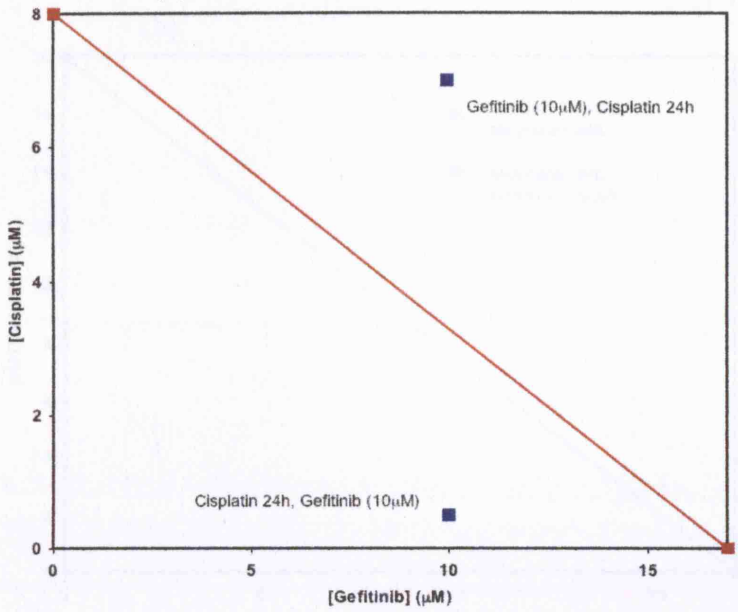

Figure 3.9: *Schedule specific growth-inhibitory effects of treatment with gefitinib in combination with cisplatin on MCF-7 cells.*

(a) Growth inhibition SRB assay: Cells were treated with the indicated schedule. Data expressed as a percentage of the control untreated well absorbance and represents the averages of three different experiments, each performed in triplicate; *bars,* SD.

(b) Isobologram analysis: Dose pairs (■) IC_{50} of cisplatin and gefitinib together.

(a)

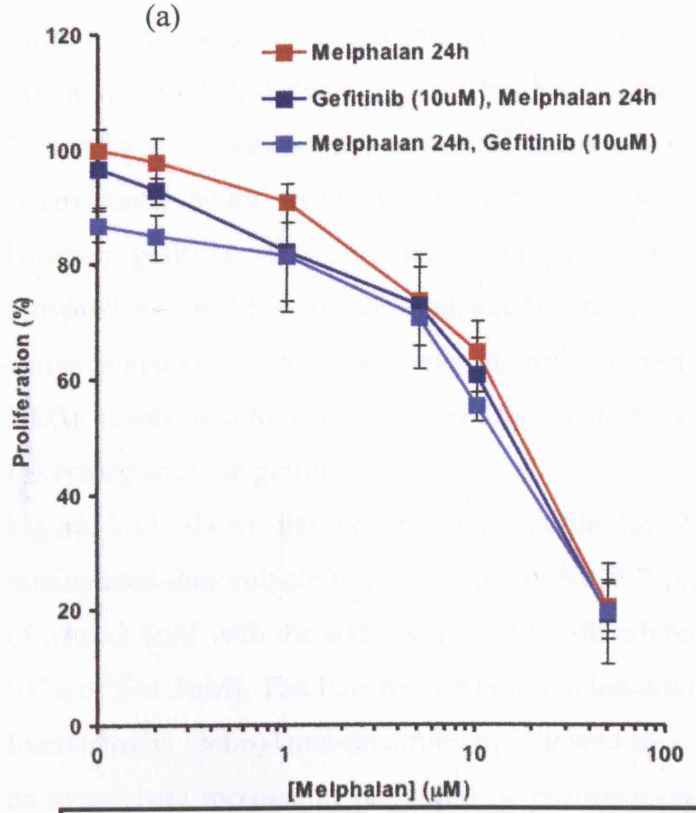

Schedule	IC_{50} (μM)
Melphalan 24h:	18±1.2
Gefitinib (10μM), Melphalan 24h:	16.2±1.07
Melphalan 24h, Gefitinib (10μM):	14.4±2.6

(b)

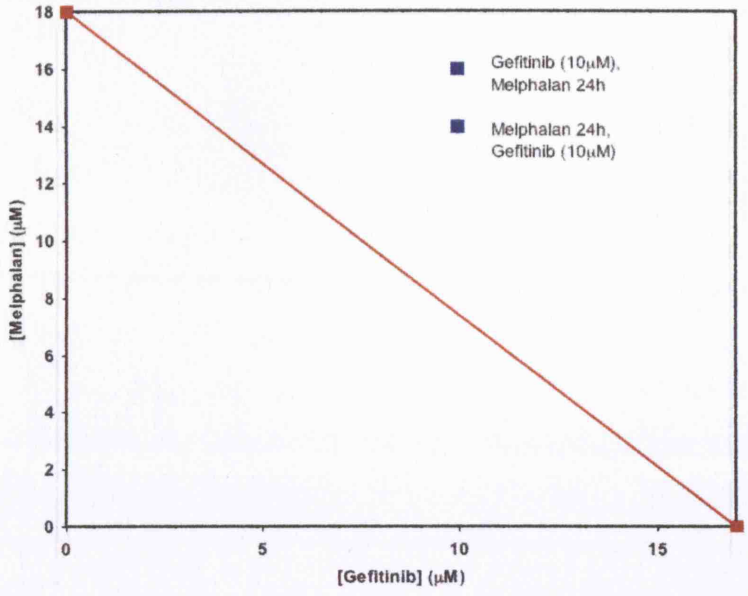

Figure 3.10: *Schedule specific growth-inhibitory effects of treatment with gefitinib in combination with melphalan on MCF-7 cells.*

(a) Growth inhibition SRB assay: Cells were treated with the indicated schedule. Data expressed as a percentage of the control untreated well absorbance and represents the averages of three different experiments, each performed in triplicate; *bars,* SD.

(b) Isobologram analysis: Dose pairs (■) IC_{50} of melphalan and gefitinib together.

3.4 Chemotherapy-Induced DNA Damage Involvement in Synergy with Gefitinib

Since the chemotherapeutic agents used induce DNA damage, it is important to confirm that it is the DNA damage induced by these agents which is necessary for synergism. Doxorubicin induces protein-associated strand breaks by trapping topoisomerase II that is covalently bound to DNA. As already observed, there is a synergistic interaction between gefitinib and doxorubicin (Figure 3.4). Biotinylated-doxorubicin (kindly provided by David Selwood, Wolfson Institute, UCL) is unable to enter the nucleus whilst maintaining the topoisomerase activity seen with doxorubicin (Allart *et al.*, 2003). It was used to assess whether DNA damage induced by doxorubicin is necessary for synergism with gefitinib.

Figure 3.11 shows the proliferation profile for 24h exposure to doxorubicin and biotinylated-doxorubicin with gefitinib on MCF-7 cells. Doxorubicin alone has an IC_{50} of 58.6±3.8nM with the addition of 5μM gefitinib having a synergistic effect as before (IC_{50} of 5±1.5nM). The IC_{50} for the biotinylated-doxorubicin conjugate was 50±6.6nM. Interestingly, biotinylated-doxorubicin followed by exposure to 5μM gefitinib produced no synergistic increase in inhibition of proliferation and had an IC_{50} of 60.7±1.7nM. These results therefore suggest that the DNA damage caused by chemotherapy is important for demonstration of synergy with gefitinib.

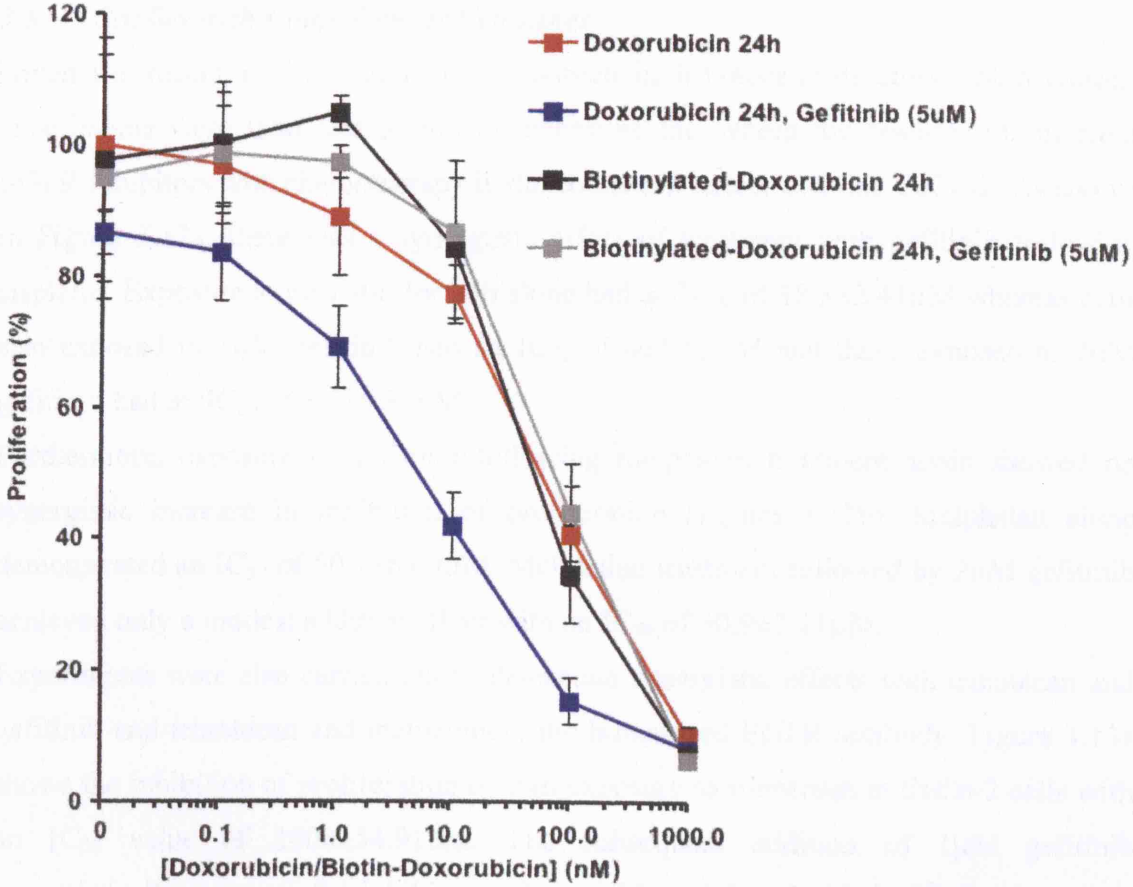

MCF-7 Cells	
Drug	**IC_{50} (nM)**
Doxorubicin 24h	58.6±3.8
Doxorubicin 24h, Gefitinib (5μM)	5±1.5
Biotinylated-Doxorubicin 24h	50±6.6
Biotinylated-Doxorubicin 24h, Gefitinib (5μM)	60.7±1.7

Figure 3.11: *Dual-Agent in vitro growth inhibition for doxorubicin and biotinylated-doxorubicin 24h exposure alone and followed by gefitinib on MCF-7 cells.* Growth inhibition SRB assay: Following 24h exposure to doxorubicin or biotinylated-doxorubicin alone, cells were incubated in drug free medium or gefitinib for 24h and left till Day 6. Data expressed as a percentage of the control untreated well absorbance and represents the averages of three different experiments, each performed in triplicate; *bars,* SD.

3.5 Studies with Colon Cancer Cell Lines

Given the recent positive study of cetuximab in irinotecan-refractory colon cancer, experiments were then carried out to determine the synergistic features of different EGFR inhibitors with chemotherapy in the colorectal cancer cell line CaCo-2. As shown in Figure 3.12a, there was a synergistic effect of treatment with gefitinib following cisplatin. Exposure to cisplatin for 24h alone had an IC_{50} of 18.3±2.41μM whereas cells also exposed to 1μM gefitinib had an IC_{50} of 4±1.03μM and those exposed to 2μM gefitinib had an IC_{50} of 3.5±0.81μM.

Furthermore, exposure to gefitinib following melphalan treatment again showed no synergistic increase in inhibition of proliferation (Figure 3.12b). Melphalan alone demonstrated an IC_{50} of 50.7±6.69μM. Melphalan treatment followed by 2μM gefitinib achieved only a modest additive effect with an IC_{50} of 30.9±7.11μM.

Experiments were also carried out to determine synergistic effects with irinotecan and gefitinib and irinotecan and matuzumab, the humanised EGFR antibody. Figure 3.13a shows the inhibition of proliferation by 24h exposure to irinotecan in CaCo-2 cells with an IC_{50} value of 1000±54.91nM. The subsequent addition of 1μM gefitinib synergistically increases the inhibitory effects with an IC_{50} of 150±13.38nM. A marked synergistic effect with irinotecan is also seen for matuzumab. In Figure 3.13b, irinotecan alone achieves an IC_{50} of 1250±64.22nM. When followed by 5μg/ml matuzumab a synergistic effect is seen with an IC_{50} of 250±14.08nM. Irinotecan 24h treatment followed by 10μg/ml matuzumab produced a 25-fold increase in inhibition of proliferation as compared with irinotecan alone with an IC_{50} of 50±3.57nM.

Synergies were also observed using irinotecan or etoposide in combination with gefitinib on the HCT-116 colorectal cancer cell line and are summarised in Table 3.6 below.

HCT-116 Cells		
Drug 24h	**Gefitinib (μM)**	**IC_{50}**
Etoposide	-	30.3±2.77μM
	5	5±0.62μM
Irinotecan	-	28±3.19nM
	5	2.4±0.59nM
	10	0.05±0.006nM

Table 3.6: IC_{50} values for gefitinib treatment following etoposide or irinotecan 24h exposure on HCT-116 cells.

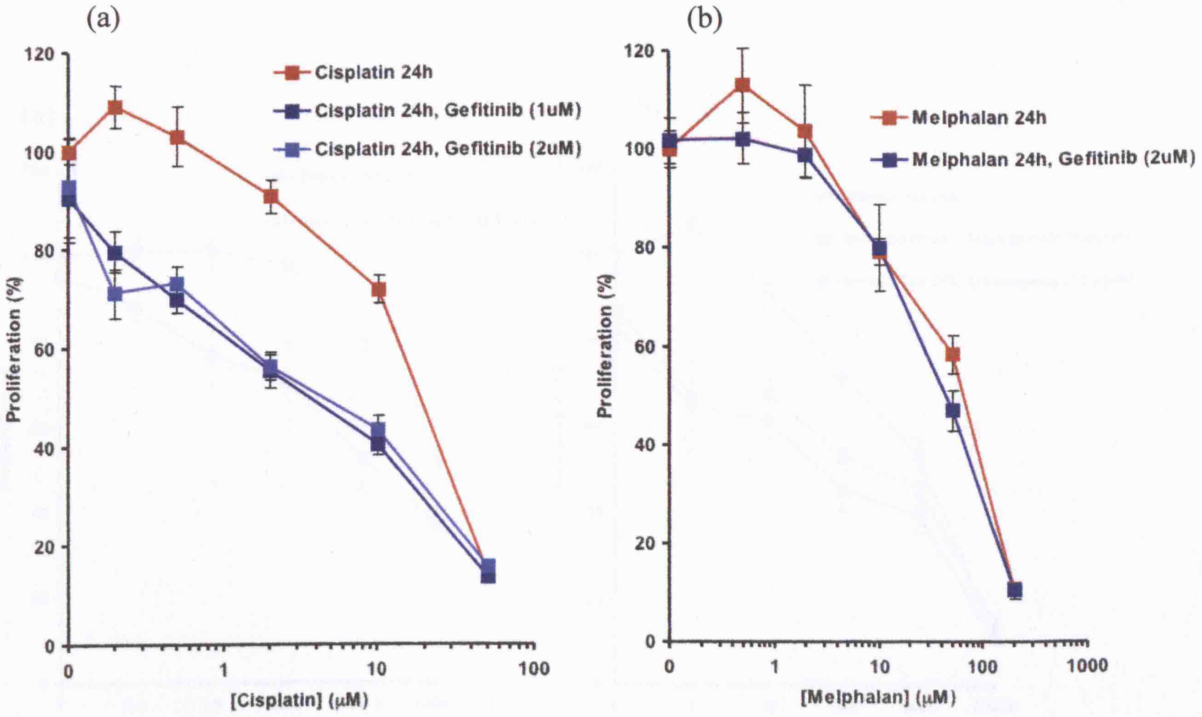

Drug	Gefitinib (μM)	IC_{50} (μM)
Cisplatin 24h	-	18.3±2.41
	1	4±1.03
	2	3.5±0.81
Melphalan 24h	-	50.7±6.69
	2	30.9±7.11

Figure 3.12: *Dual-Agent in vitro growth inhibition for cisplatin and melphalan 24h exposure alone and followed by gefitinib on CaCo-2 cells.* Growth inhibition SRB assay for (a) cisplatin and (b) melphalan: Following 24h exposure to chemotherapy, cells were incubated in drug free medium or gefitinib for 24h and left till Day 6. Data expressed as a percentage of the control untreated well absorbance and represents the averages of three different experiments, each performed in triplicate; *bars,* SD.

(a)

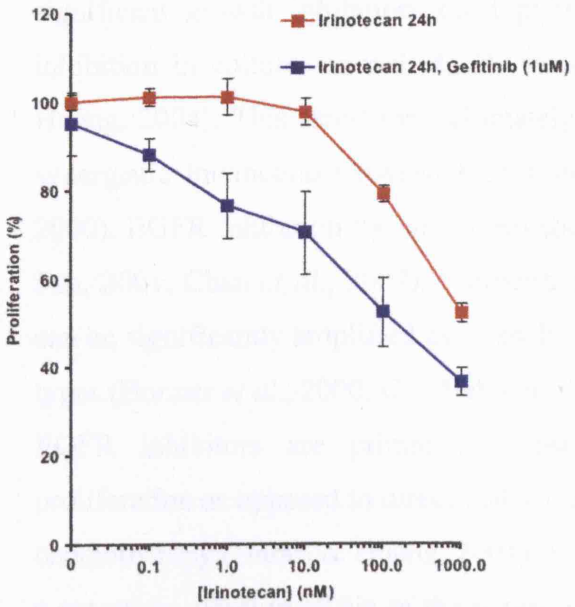

(b)

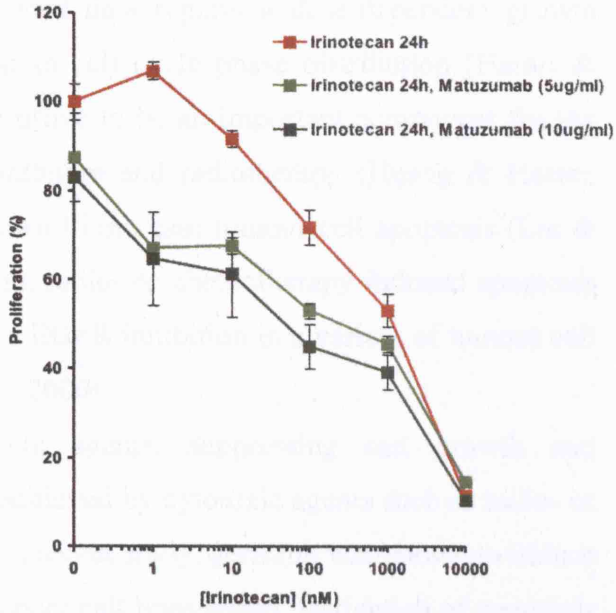

Drug	Gefitinib (μM)	IC_{50} (nM)	Drug	Matuzumab (μg/ml)	IC_{50} (nM)
Irinotecan 24h	-	1000±54.91	Irinotecan 24h	-	1250±64.22
	1	150±13.38		5	250±14.08
				10	50±3.57

Figure 3.13: *Dual-Agent in vitro growth inhibition for irinotecan 24h exposure alone and followed by gefitinib or matuzumab on CaCo-2 cells.* Growth inhibition SRB assay: Following 24h exposure to irinotecan cells were incubated in drug free medium or (a) gefitinib or (b) matuzumab for 24h and left till Day 6. Data expressed as a percentage of the control untreated well absorbance and represents the averages of three different experiments, each performed in triplicate; *bars,* SD.

3.6 Discussion

The ability of anti-EGFR agents to inhibit tumour cell proliferation and modulate cell cycle phase progression is well established (Peng *et al.*, 1996; Zhu *et al.*, 2001; Huang *et al.*, 2002). Although not every tumour cell line and xenograft studied to date confirms significant growth inhibition, most published data reports a dose-dependent growth inhibition in culture, as well as G_1 arrest in cell cycle phase distribution (Harari & Huang, 2004). This arrest may ultimately prove to be an important component for the synergistic interaction between EGFR inhibitors and radiotherapy (Huang & Harari, 2000). EGFR inhibition has also been shown to increase tumour cell apoptosis (Liu & Fan, 2001; Chan *et al.*, 2002). Furthermore, radio- or chemotherapy induced apoptosis can be significantly amplified as a result of EGFR inhibition in a variety of tumour cell types (Bonner *et al.*, 2000; Ciardiello *et al.*, 2000).

EGFR inhibitors are primarily cytostatic agents, suppressing cell growth and proliferation as opposed to direct cell kill achieved by cytotoxic agents such as radio- or chemotherapy (Harari & Huang, 2004). In a recent study, gefitinib was shown to induce a cytostatic effect in all six of the breast cancer cell lines tested. Activation of apoptosis was achieved in only two of them (Campiglio *et al.*, 2004). Furthermore, the study found no correlation between the cytostatic or cytotoxic effects of gefitinib and its ability to downregulate MAPK and AKT activity in the tumour cell lines. They conclude that the antitumor activity of gefitinib is due to a cytostatic effect, involving induction of apoptosis in only a subset of sensitive cells, and that neither MAPK nor AKT is a reliable marker of gefitinib activity (Campiglio *et al.*, 2004).

In this study, gefitinib alone and in combination with chemotherapy was assessed using the Sulphorhodamine B (SRB) proliferation assay. This is a short-term proliferation assay and can be more influenced by the rate, rather than the overall level of cell killing which would be more accurately measured using clonogenic assays (Brown & Wouters, 1999). Nonetheless, the SRB assay is well suited to high-volume, automated drug screening. In addition, there is evidence that it does in fact provide a sensitive measure of drug-induced cytotoxicity and is useful in quantitating clonogenicity (Perez *et al.*, 1993; Griffon *et al.*, 1995; Voigt, 2005). Furthermore, it is by no means clear that proliferation assays are inferior to colony forming assays to assess effects of gefitinib alone or in combination with other drugs. Other studies, both preclinical (Sgambato *et al.*, 2004) and clinical (Chan *et al.*, 2002; Albanell *et al.*, 2002), show a major

component of gefitinib action is through inhibition of proliferation as well as apoptosis. In addition, it has been shown that the presence of cell clusters or multiplets introduces large errors in viability measurements with clonogenic assays. This leads to overestimation of radiosensitivity particularly in the low dose range of radiation. This may occur in experiments involving prolonged exposure to cytostatic drugs such as gefitinib as growth arrest by these drugs is seldom complete (Giocanti *et al.*, 2004).

This chapter investigated the *in vitro* antiproliferative effects of the EGFR TKI inhibitor gefitinib, alone and in combination with chemotherapeutic agents. It examined its effects in a variety of cell lines including the human breast adenocarcinoma MCF-7 cells, a cell line widely used in similar studies. Although many studies have used cell lines with higher EGFR expression, there is no association between EGFR levels and response to EGFR-targeted agents (Ciardiello & Tortora, 2003). In predicting the response to EGFR-targeted agents, it is likely that the levels of activated, phosphorylated EGFR are more important than total EGFR levels. Furthermore, tumour cells may escape the EGFR-targeted growth inhibition by using alternative growth pathways or by constitutive activation of downstream signalling effectors. An example is the human A431 cancer cells xenografts which can acquire resistance to cetuximab by increased tumour-induced angiogenesis due to the constitutive overexpression of VEGF (Viloria-Petit *et al.*, 2001; Tortora *et al.*, 2003).

MCF-7 cells were treated with gefitinib for different durations. A 24h treatment achieved an IC_{50} value of 17±0.8μM and is comparable with similar proliferation studies done with gefitinib on the same cell line (Moasser *et al.*, 2001) and in others (Magné *et al.*, 2002). The MCF-7 cell line has been noted to be relatively resistant to inhibition of proliferation by gefitinib as compared with other breast cancer cell lines (Moasser *et al.*, 2001). A longer exposure for 72h did not significantly increase cell sensitivity in either the MCF-7 or AR42J cell lines. The dose-dependent inhibitory effect of daily gefitinib treatments achieved an IC_{50} with the significantly lower dose of 0.4±0.007μM and is comparable with other similar studies (Ciardiello *et al.*, 2000).

It has become clear that measured serum concentrations of gefitinib significantly underestimate the effective tumour concentrations in both xenografts and clinical studies. A recent important study demonstrates that the effective concentration of gefitinib in breast tumour tissue is around 17μM (McKillop *et al.*, 2005). They report

that the gefitinib tumour concentrations are considerably higher than those reportedly required in some *in vitro* studies to achieve complete inhibition of EGFR autophosphorylation. In addition, recent work in xenografts suggests that pulsatile administration of gefitinib at high concentrations is significantly more effective at chemosensitisation (Solit *et al.*, 2005). Higher doses of gefitinib may lead to the inhibition of other targets in particular HER-2 which is inhibited with an IC_{50} of ~10 times higher than that required to inhibit EGFR (Moasser *et al.*, 2001).
Other studies have investigated the effects of combining different anti-EGFR inhibitors. Cetuximab in combination with gefitinib or erlotinib can augment the potency of EGFR signalling inhibition and suggests potential new clinically exploitable strategies (Huang *et al.*, 2004; Matar *et al.*, 2004).

The basis for synergies between gefitinib and a variety of anticancer agents has not been clearly defined. Inhibition of EGFR has been shown to directly affect the threshold of apoptosis within the cell by mechanisms including caspase activation (Janmaat *et al.*, 2003). It is however unclear whether the synergies demonstrated thus far in relation to anticancer activity are specific to particular agents or apply equally to all classes of anticancer drugs. Here the effects were investigated in relation to four commonly used chemotherapeutic agents, namely etoposide, doxorubicin, cisplatin and melphalan in a number of cell lines including MCF-7 cells. The results confirm synergistic interactions previously noted in other cell lines with etoposide, doxorubicin and cisplatin (Ciardiello *et al.*, 2000). Strikingly however, **no** demonstrable synergy was seen with melphalan. Isobologram analysis confirms these observations and these findings have recently been published (Friedmann *et al.*, 2004). The same effects were also seen in the rat pancreatic AR42J and colorectal CaCo-2 cancer cell lines. The fact that sensitisation occurs with some but not all chemotherapeutic agents persistently in different cell lines indicates that a generalised reduction in apoptotic threshold does not fully account for chemosensitisation.

There is an important need to define the optimal schedule of administration of anticancer drugs with EGFR inhibitors as well as identifying the agents with which these synergies occur. A study of gefitinib in colon cancer cell lines found a synergistic effect on both chemosensitivity and removal of DNA adducts when oxaliplatin was

followed by gefitinib; scheduling of oxaliplatin followed by gefitinib resulted in an additive effect but not for the reverse order (Xu *et al.*, 2003). In contrast, the synergistic effects of gefitinib and capecitabine was observed when gefitinib administration preceded drug exposure. Pre-treatment with gefitinib reduced cell proliferation and consequently resulted in a 40-fold reduction in the enzyme thymidylate synthase, a key target of fluoropyrimidines (Magné *et al.*, 2003). Furthermore, it has been reported that sequential therapy of EGFR inhibition followed by the G_2/M blocking agents paclitaxel and vinblastine, antagonised effects of EGFR inhibitors (Piperdi *et al.*, 2004).
In this study, following an acute exposure to chemotherapy, gefitinib (2h) again produced a synergistic increase in inhibition of proliferation with cisplatin but not with melphalan. Subsequent experiments investigating the order of drug delivery produced interesting results. Again melphalan and gefitinib did not synergise with one another irrespective of their order of delivery but also, no synergy was seen with cisplatin when its treatment was preceded by gefitinib. The fact that synergy occurs even after a short exposure to cisplatin and only when gefitinib follows cisplatin treatment suggests that gefitinib may affect the processing of cisplatin-induced DNA damage.

Unlike doxorubicin, biotinylated-doxorubicin is unable to translocate into the nucleus and induce DNA damage. Its lack of synergy with gefitinib suggests that DNA damage occurring in the nucleus contributes towards the synergy with gefitinib. It should be noted however, that synergistic interactions between gefitinib and non-DNA damaging chemotherapeutic agents such as paclitaxel and 5'-FU have also been reported (Sirtonak *et al.*, 2000; Ciardiello *et al.*, 2000; Magné *et al.*, 2002)

As in MCF-7 and AR42J cells, synergies were also found in the colon cancer cell lines CaCo-2 and HCT-116 for gefitinib with cisplatin and etoposide and not with melphalan. In addition, synergy between gefitinib and the topoisomerase I inhibitor irinotecan, was also seen. Interestingly, the magnitude of synergy was comparable with matuzumab, a humanised alternative to cetuximab.

3.6.1 Conclusions

There are clearly general pathways by which inhibition of EGFR results in reduction in cell proliferation and apoptosis. Inhibition of EGFR by gefitinib may directly sensitise cells to chemotherapy and radiation through downregulation of genes involved in the apoptotic pathway including Bcl-2 and Bax (Magné *et al.*, 2003). This may account for the ability of EGFR inhibitors to synergise the effects of a wide variety of agents including cytotoxic drugs, endocrine therapies and radiation. However the generalised reduction in apoptotic threshold cannot explain sensitisation to specific agents. Apart from the clinical studies of cetuximab and irinotecan in colorectal cancer and the preliminary results in head and neck cancer with radiation, the abundant pre-clinical evidence of combining EGFR inhibitors and chemotherapy has not been borne out in clinical studies. Four large phase III clinical trials in patients with either locally advanced stage III disease or stage IV NSCLC failed to show any benefit for combined treatment with cisplatin, carboplatin, gemcitabine and paclitaxel (Giaccone *et al.*, 2004; Herbst *et al.*, 2004; Herbst *et al.*, 2004; Gatzemeier *et al.*, 2004). The reasons for these mixed results are unknown and an antagonistic effect of combined treatments cannot be excluded (Baselga, 2004). A similar situation to the scenario of the schedule-dependent antagonism observed between tamoxifen and chemotherapy in the adjuvant treatment of breast cancer may well be the reason (Baselga & Arteaga, 2005). As has been discussed in detail in Chapter 1 other explanations exist such as the activation of compensatory signalling pathways as a result of EGFR TKI inhibition. It should be noted however, that a recent study reported that the combination of gemcitabine and erlotinib did improve the survival and progression free survival in advanced pancreatic cancer as compared to gemcitabine alone (Moore *et al.*, 2005). Although this was modest, it does demonstrate that there are at least additive effects for combining chemotherapy with quinazoline-based small molecule inhibitors in the clinic.

The activation of RAD51 by BCR/ABL is essential for enhanced DSB repair and drug resistance. Inhibition of the tyrosine kinase activity of BCR/ABL by imatinib therefore reverses drug resistance by delaying DNA repair (Slupianek *et al.*, 2001; Skorski, 2002) This study demonstrates that gefinitib, a small molecule inhibitor of EGFR tyrosine kinase activity, may synergise the effects of certain DNA-interactive chemotherapeutic agents by modulating the DNA damage and repair processes. Understanding the effects

of EGFR inhibition on DNA repair pathways will allow the design of novel studies with schedules and agents that could provide major therapeutic benefit.

CHAPTER 4

MODULATION OF CHEMOTHERAPY-INDUCED DNA DAMAGE AND REPAIR BY EGFR INHIBITION

4.1 Introduction

In the previous chapter synergistic interactions were seen for gefitinib with etoposide, irinotecan, doxorubicin and cisplatin but not with melphalan. It is possible that gefitinib, a small molecule inhibitor of EGFR tyrosine kinase activity, synergises the effects of specific DNA-interactive chemotherapeutic agents by modulating the DNA damage and repair processes. Therefore, the kinetics of DNA damage and repair following these combined treatments were investigated. The alkaline single-cell gel electrophoresis (comet) assay was used to assess formation and repair of DNA strand breaks and interstrand crosslinks (ICLs) induced by these agents.

Etoposide is a topoisomerase II poison and forms a ternary complex with DNA. This impairs the DNA strand rejoining function of the enzyme resulting in DNA single- and double-strand breaks. Etoposide is known to induce apoptosis in a number of cell lines (Godard *et al.*, 1999; Li & Liu, 2001).

DNA ICLs are among the most toxic forms of DNA damage and have been demonstrated to be critical in the cellular effects of cisplatin (Zwelling *et al.*, 1981) and melphalan (Hansson *et al.*, 1987; Spanswick *et al.*, 2002). In general, ICLs represent only a small fraction of the adducts formed but are considered to be critical lesions responsible for cytotoxicity due to their inhibition of DNA strand separation and, therefore, of DNA replication, transcription, and segregation. Only 5-8% of the adducts formed by cisplatin are ICLs which take a few hours to form depending on the sequence context of the guanines (Wang & Lippard, 2005). Similarly, ICLs induced by nitrogen mustards such as melphalan make up only 5% of the total DNA adducts. In addition, these agents also cause guanine monoadducts, intrastrand crosslinks, DNA-protein crosslinks and also react with RNA.

The comet assay was originally developed as a method to measure DNA strand breaks in a single cell population (Ostling & Johanson, 1984) and has been modified to study ICL formation and repair (Spanswick *et al.*, 1999). It requires only a few cells, and, because analysis can be made at a single-cell level, the method allows for the detection of heterogeneity of response within a cell population. It is also more sensitive than other techniques used to measure ICL including alkaline elution (Spanswick *et al.*, 2002).

4.1.1 Aims

The purposes of the experiments presented in this chapter are to further characterise the mechanisms of interaction between EGFR inhibitors and DNA-damaging chemotherapeutic agents. To this end, the following questions are addressed:

1. Does gefitinib alter the amount of DNA damage induced by chemotherapy?
2. Does gefitinib alter the repair of DNA damage induced by chemotherapy?
3. Are these effects seen with various DNA damaging agents?
4. Does the anti-EGFR antibody matuzumab, produce the same effects?

4.2 Measurement of DNA Damage and Repair

4.2.1 Drug-Induced DNA Strand Break Formation and Repair

The comet assay allows for detection and visualisation of DNA damage within individual cells. As an example, Figure 4.1 shows screen images of individual MCF-7 cells following a short exposure to etoposide. Cells treated with etoposide at 100μM for 1h produce DNA strand breaks causing the DNA to migrate further on an agarose gel than undamaged DNA. This forms a tail moment which is a function of the amount of DNA in the tail and the length of the tail (measured in μmeters). Within 30 minutes after etoposide treatment, the strand breaks start to be repaired as measured by a shortened tail moment (bottom left-hand panel). After 4h, almost complete repair is achieved with no detectable tail moment (bottom right-hand panel). For analysis, the average tail moment of 50 individual cells is calculated from two independent slides and plotted for each time point.

4.2.2 Drug-Induced DNA Interstrand Crosslink Formation and Repair

Detection and measurement of DNA interstrand crosslinks (ICLs) was achieved using a modification of the comet assay (Hartley *et al.*, 1999). Immediately before analysis, cells were irradiated (12 Gy) to deliver a fixed number of random DNA strand breaks. In the presence of strand breaks, ICLs retard migration thus reducing the tail moment compared to the non-crosslinked irradiated control. An illustration of the decrease in DNA tail moment as a result of ICL achieved by the chemotherapeutic agent cisplatin, is shown in Figure 4.2. Unirradiated and irradiated individual MCF-7 cells are represented in the top left- and right-hand panels, respectively. Immediately following a cisplatin (200μM) 1h treatment no ICLs are detectable with cells producing tail moments comparable with the irradiated control. Formation of ICLs are detectable at 6h as measured by a decreased tail moment (middle right-hand panel). At 12h ICLs are becoming unhooked and the tail moment then increases. Complete unhooking is achieved after 24h.

The tail moment for each image was calculated as the product of the percentage DNA in the comet tail and the distance between the means of the head and tail distributions, based on the definition of Olive *et al.*, 1990 as discussed in Chapter 2.

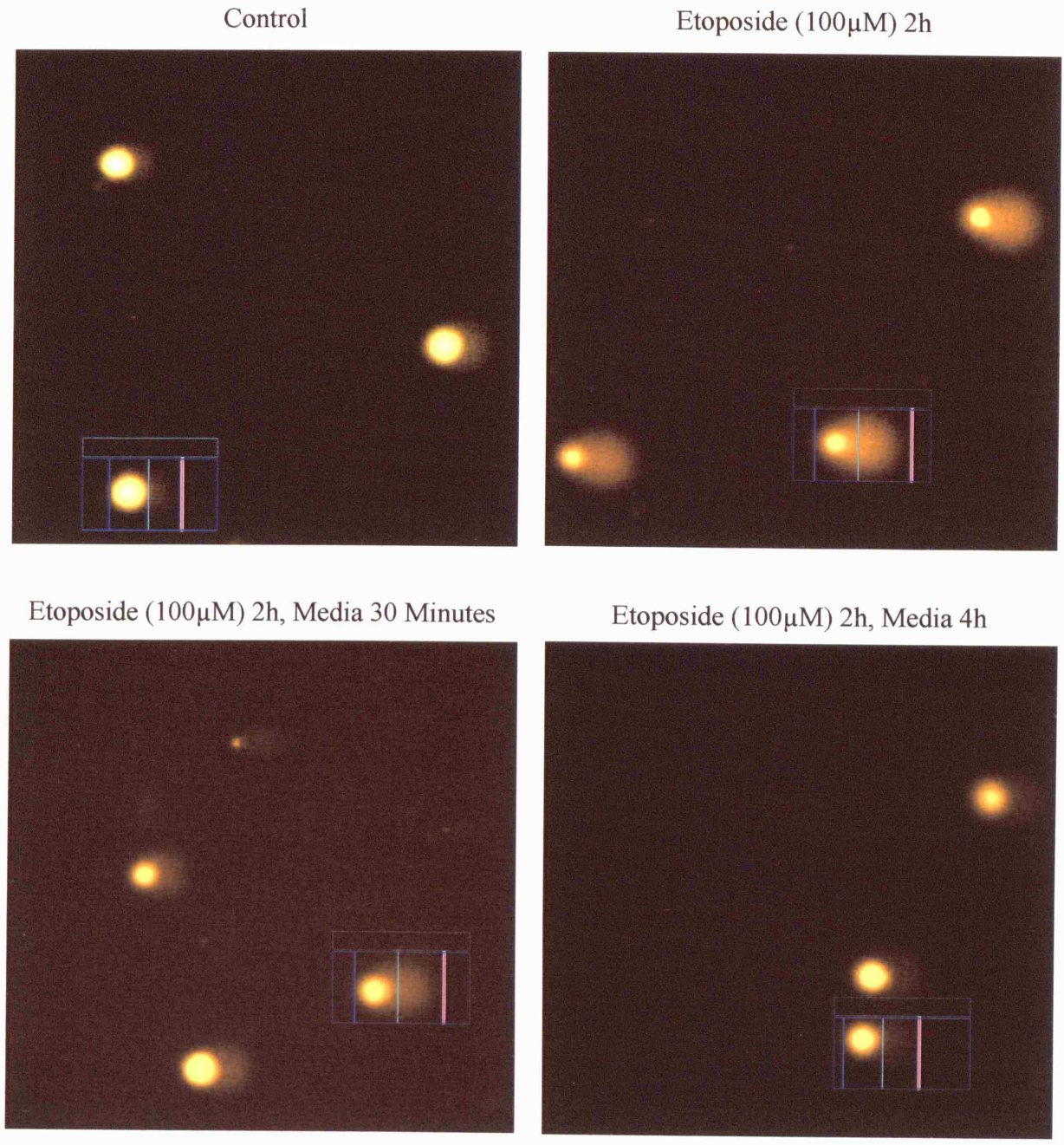

Figure 4.1: *Sample screen display of comet images for etoposide (100μM) 2h and repair after 30 minutes and 1h in MCF-7 cells.* Images were viewed using an inverted fluorescence microscope and analysed using the Komet Analysis Software.

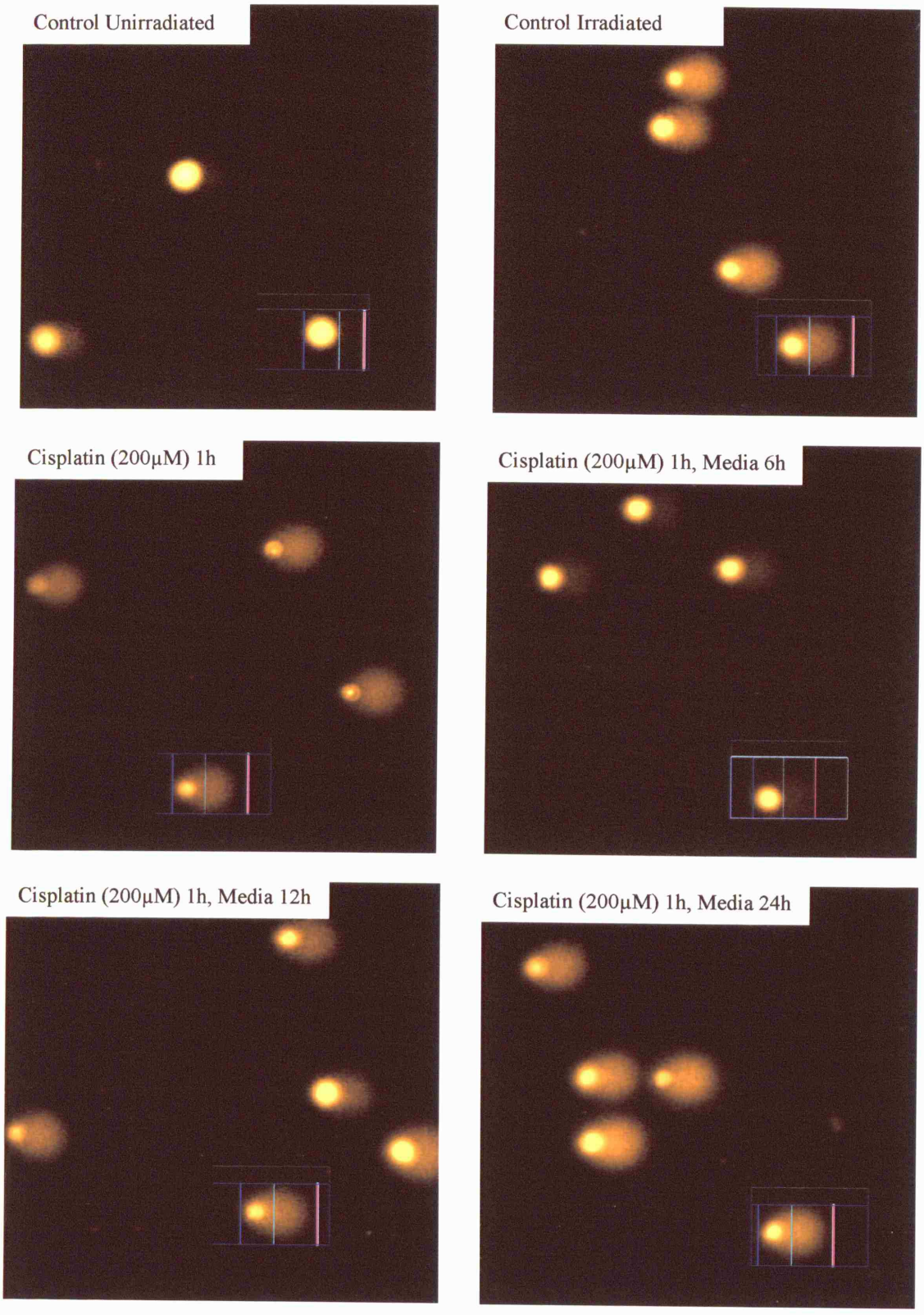

Figure 4.2: *Sample screen display of comet images for unirradiated and irradiated controls and cisplatin treatment in MCF-7 cells.* Cells were treated with cisplatin (200μM) for 1h with crosslink formation occurring after 6h. Images were viewed using an inverted fluorescence microscope and analysed using the Komet Analysis Software.

4.3 Effects of Gefitinib on Etoposide-Induced DNA Strand Breaks and Repair

Prior to investigating whether gefitinib alters the amount of strand breaks or rate of repair induced by etoposide, single-agent gefitinib treatment was assessed in MCF-7 cells and was shown to produce no DNA strand breaks (data not shown). Cells were exposed to gefitinib (10μM) over a 24h period, as this was the optimal dose for a synergistic interaction with etoposide as discussed in Chapter 3.

Quantitation of DNA strand breaks following etoposide treatment has been well characterised (Godard *et al.*, 1999; Boos and Stopper, 2000; Godard *et al.*, 2002). Initial experiments with etoposide confirmed that following exposure of MCF-7 cells to sub-toxic concentrations of drug, maximal strand breakage was detectable after a 2h exposure (data not shown). To determine the etoposide concentration delivering a sufficient tail moment for combination treatments with gefitinib, cells were treated with a range of etoposide concentrations for 2h (Figure 4.3). Etoposide at 100μM produced a tail moment of 12 and is suitable for combination studies since increases or decreases in the amount of strand breaks can easily be monitored.

To examine the kinetics of DNA strand break formation and repair, a 2h exposure to etoposide was followed by a prolonged incubation in the absence or presence of gefitinib. Figure 4.4 shows the formation of strand breaks and subsequent repair for etoposide alone and followed by gefitinib (10μM) in MCF-7 cells. There was no alteration in the quantity of strand breaks at 2h in cells produced with etoposide alone (tail moment of 11.93) and in combination with gefitinib (11.58). After removal of drug, in the absence of gefitinib, strand break repair was detectable within 30 minutes with almost complete repair after 4h. Following combination treatment with both etoposide and gefitinib there was a marked delay in the rate of repair of DNA strand breaks with 69.7% of strand breaks remaining at 1h as compared with only 20.7% for etoposide alone. There was also persistent DNA damage detectable after 24h.

Figure 4.5 shows a similar result in AR42J cells. As for MCF-7 cells, there was no alteration in the quantity of strand breaks at 2h for etoposide alone (11.73) and in combination with gefitinib (11.2). In addition, there was again a marked delay in the rate of repair of DNA strand breaks in the presence of gefitinib with 72.3% of strand breaks remaining at 1h as compared with only 39.4% for etoposide alone, with persistent DNA damage detectable after 24h.

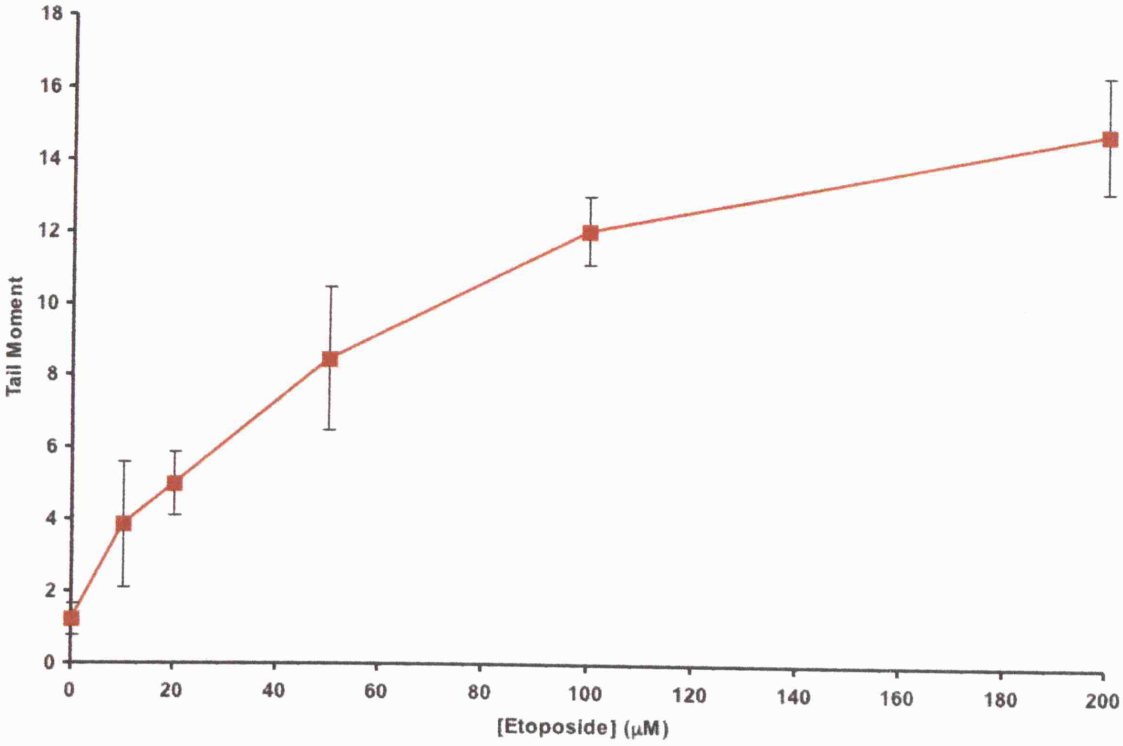

Figure 4.3: *Measurement of etoposide-induced DNA strand breaks in MCF-7 cells.* Cells were treated with indicated concentrations of etoposide for 2h and strand break formation measured as tail moment. Data is a representation of three independent experiments; *bars*, SE.

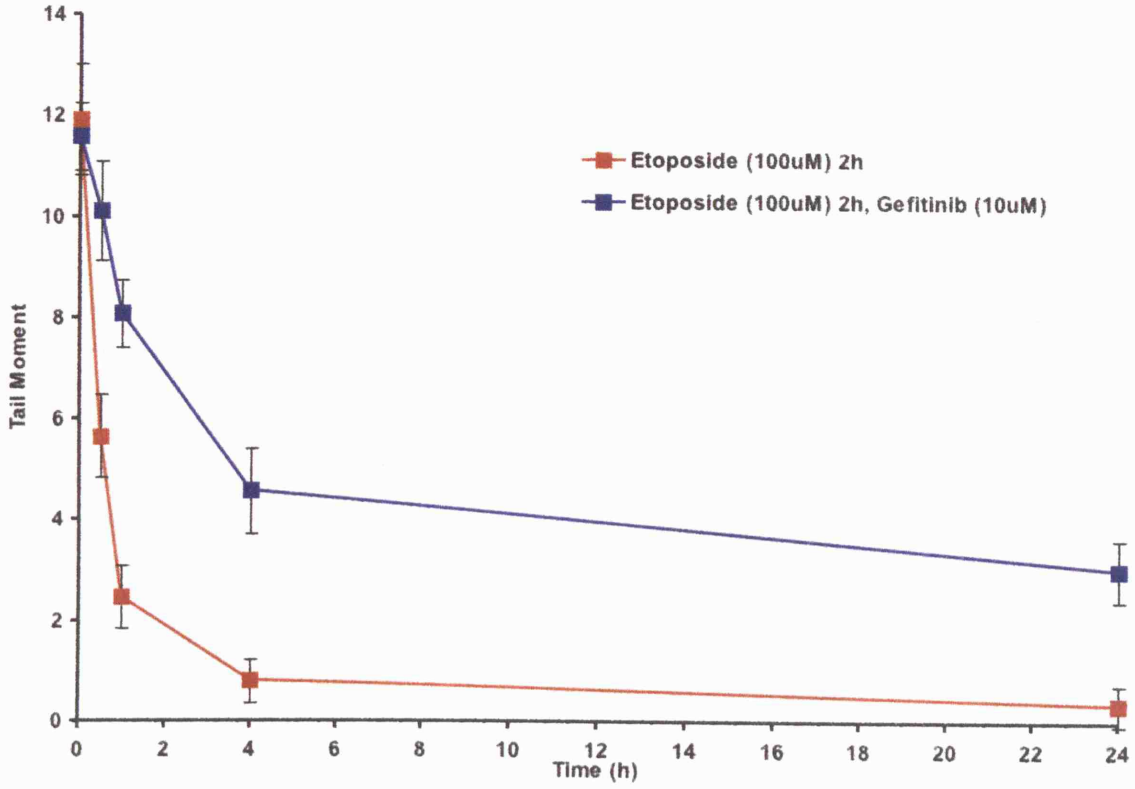

Figure 4.4: *Measurement of etoposide-induced DNA strand breaks and their repair alone or in the presence of gefitinib in MCF-7 cells.* Cells were treated with etoposide (100μM) for 2h and then incubated in fresh media or with gefitinib (10μM) alone where indicated. Strand break formation measured as tail moment, plotted against post-incubation time following removal of etoposide. Data is a representation of three independent experiments; *bars*, SE.

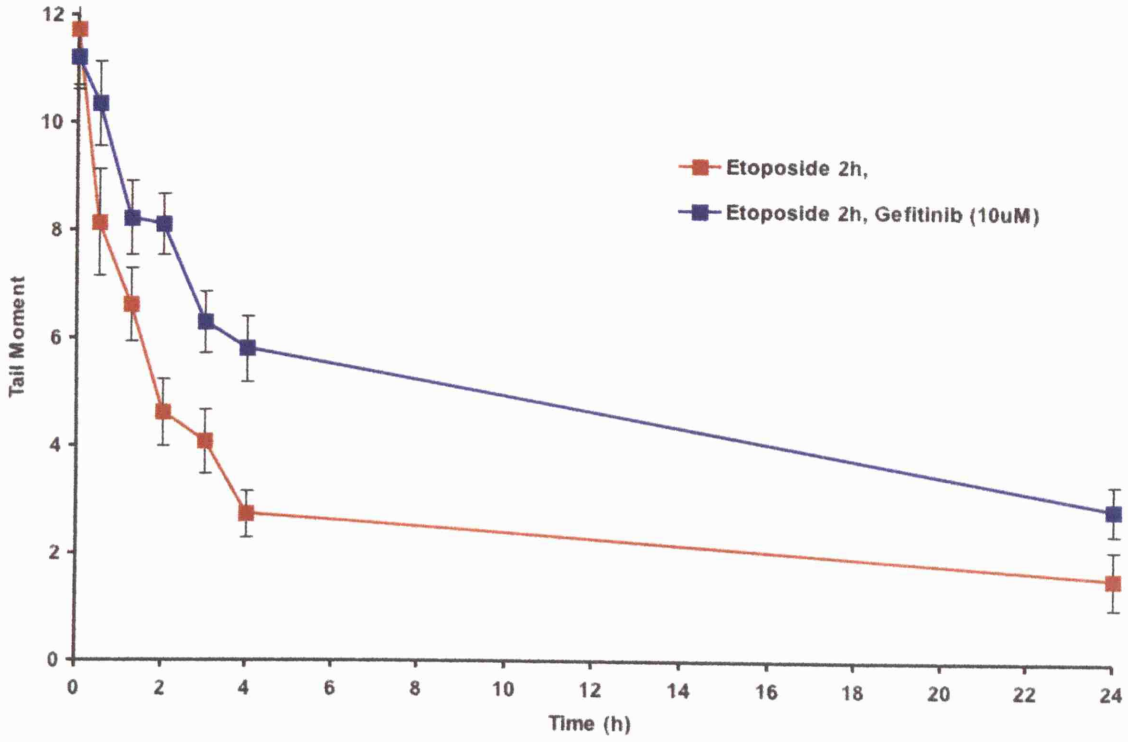

Figure 4.5: *Measurement of etoposide-induced DNA strand breaks and their repair alone or in the presence of gefitinib in AR42J cells.* Cells were treated with etoposide (100μM) for 2h and then incubated in fresh media or with gefitinib (10μM) alone where indicated. Strand break formation measured as tail moment, plotted against post-incubation time following removal of etoposide. Data is a representation of three independent experiments; *bars*, SE.

4.4 Effects of Gefitinib on Drug-Induced DNA ICL Formation and Repair

Single-agent gefitinib treatment was assessed for ICLs in MCF-7 cells. Cells were treated with gefitinib 10μM for varying lengths of time over a 48h period and irradiated (12Gy) prior to analysis. Gefitinib treatment alone did not form any ICLs (Data not shown).

Experiments were performed using MCF-7 cells following incubation with cisplatin and melphalan to measure ICL formation and repair. Figure 4.6a shows the peak of ICLs which are formed after 6h following a 1h exposure to cisplatin in MCF-7 cells. A cisplatin 200μM concentration produces a peak of crosslinking with 66.2% decrease in tail moment as compared with an irradiated control and is a suitable dose for combination studies with gefitinib since increases or decreases in the amount of ICLs can easily be monitored. Figure 4.6b shows a similar study done with melphalan. Peak of crosslinking occurs after 16h following a 1h treatment. A melphalan 200μM concentration produces a peak of crosslinking with 82.9% decrease in tail moment as compared with an irradiated control and is a suitable dose for combination studies with gefitinib.

To investigate whether the addition of gefitinib modulated the formation and repair of cisplatin-induced DNA ICLs, cells were exposed to cisplatin (200μM) for 1h following which the amount of DNA damage and the rate of repair were assessed (Figure 4.7a). For MCF-7 cells incubated with gefitinib and cisplatin, there was no effect on the quantity of ICL produced (62.9% decrease in TM) as compared with cisplatin alone (62.5%) at 6h. However, there was a clear inhibition of cisplatin-induced ICL repair following co-incubation with gefitinib as compared with cisplatin alone. ICLs induced by cisplatin alone were repaired efficiently with almost complete removal by 24h. In contrast, cells treated with the combination of gefitinib and cisplatin showed persistent ICLs at 24h (64.9% decrease in TM) and 48h (35.6%) following removal of drug.

The response of MCF-7 cells to melphalan was also assessed as shown in Figure 4.7b. Melphalan-induced DNA crosslinks peak 16h after a 1h exposure to drug and are repaired after 48h following treatment. In contrast to the results obtained using gefitinib in combination with etoposide and cisplatin, exposure of MCF-7 cells with gefitinib and melphalan (200μM) resulted in no alteration in the kinetics of DNA repair.

Both cisplatin and melphalan produce no detectable strand breaks alone or in the presence of gefitinib and so confirm that strand breaks do not interfere with the measurement of ICL formation and repair (data not shown).

Figure 4.8 shows similar results in AR42J cells. As with MCF-7 cells, there was no alteration on the quantity of ICLs produced by cisplatin and gefitinib (62.5% decrease in TM) as compared with cisplatin alone (53.5%). However, there was again a clear inhibition of cisplatin-induced ICL repair following co-incubation with gefitinib as compared with cisplatin alone. ICLs induced by cisplatin alone were repaired efficiently with almost complete removal by 24h. In contrast, cells treated with the combination of gefitinib and cisplatin showed persistent ICLs at 24h (64.4% decrease in TM) following removal of drug. In addition, exposure of AR42J cells to gefitinib and melphalan (200μM) also resulted in no alteration in the kinetics of DNA repair.

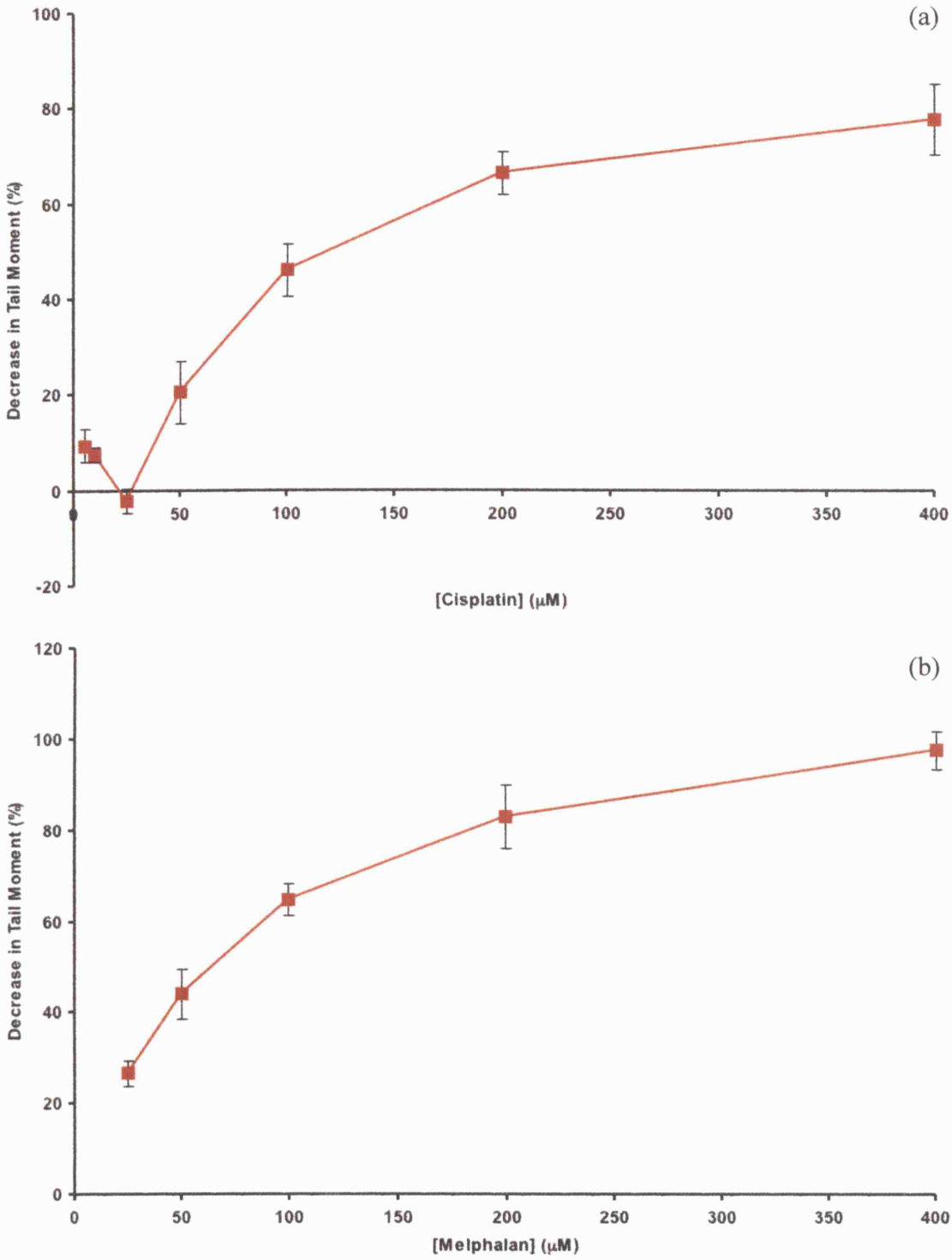

Figure 4.6: *Measurement of cisplatin and melphalan-induced DNA ICL formation in MCF-7 cells.* (a) Cells were treated with indicated concentrations of cisplatin for 1h and then incubated with fresh media for 6h. (b) Cells were treated with indicated concentrations of melphalan for 1h and then incubated with fresh media for 16h. ICL formation measured as percentage decrease in tail moment. Data is a representation of three independent experiments; *bars*, SE.

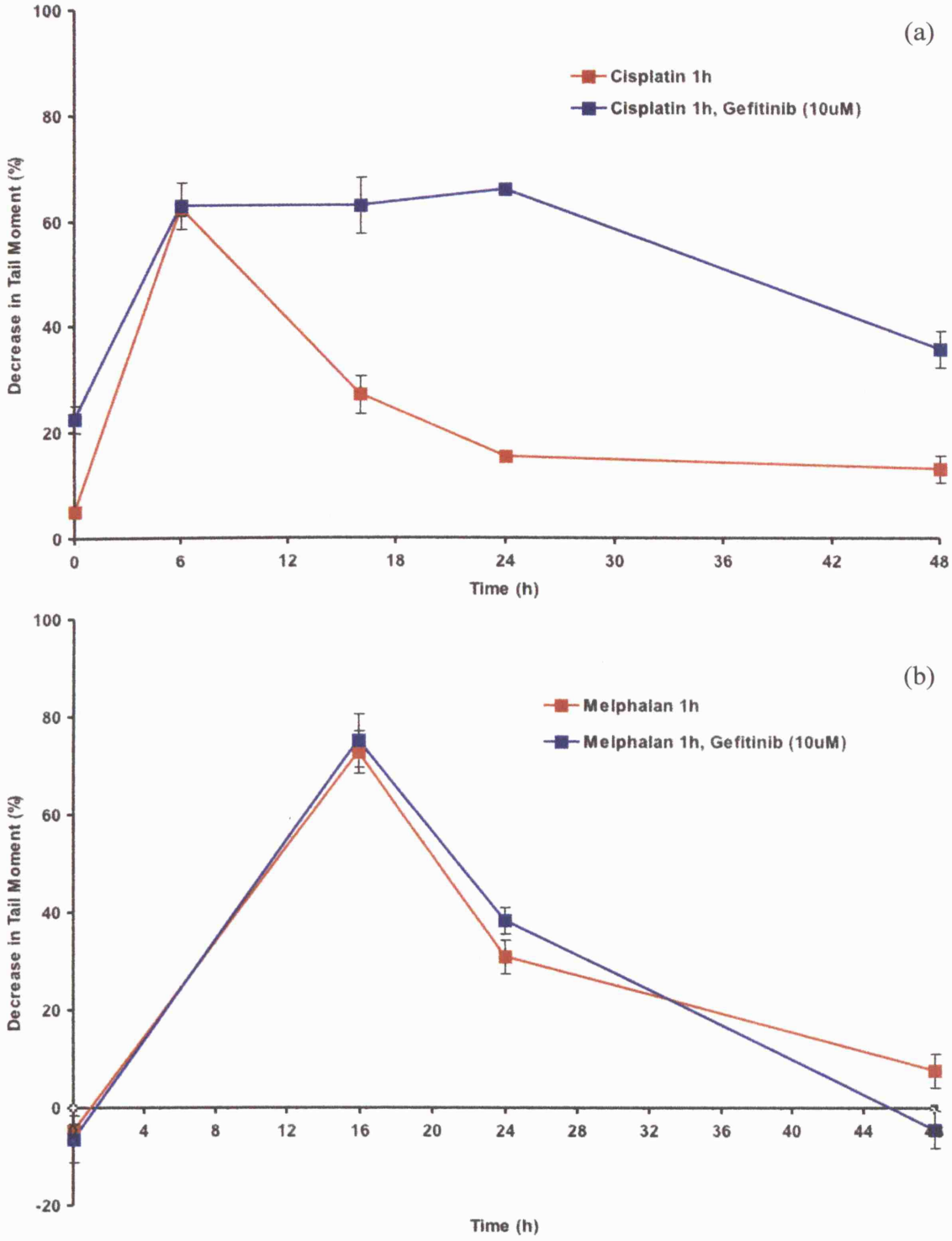

Figure 4.7: *Measurement of cisplatin and melphalan-induced DNA ICL formation and repair alone and in the presence of gefitinib in MCF-7 cells.* Cells were treated with (a) cisplatin (200μM) or (b) melphalan (200μM), for 1h and then incubated in fresh media or with gefitinib (10μM). ICL formation measured as percentage decrease in tail moment, plotted against post-incubation time following removal of drug. Data is a representation of three independent experiments; *bars*, SE.

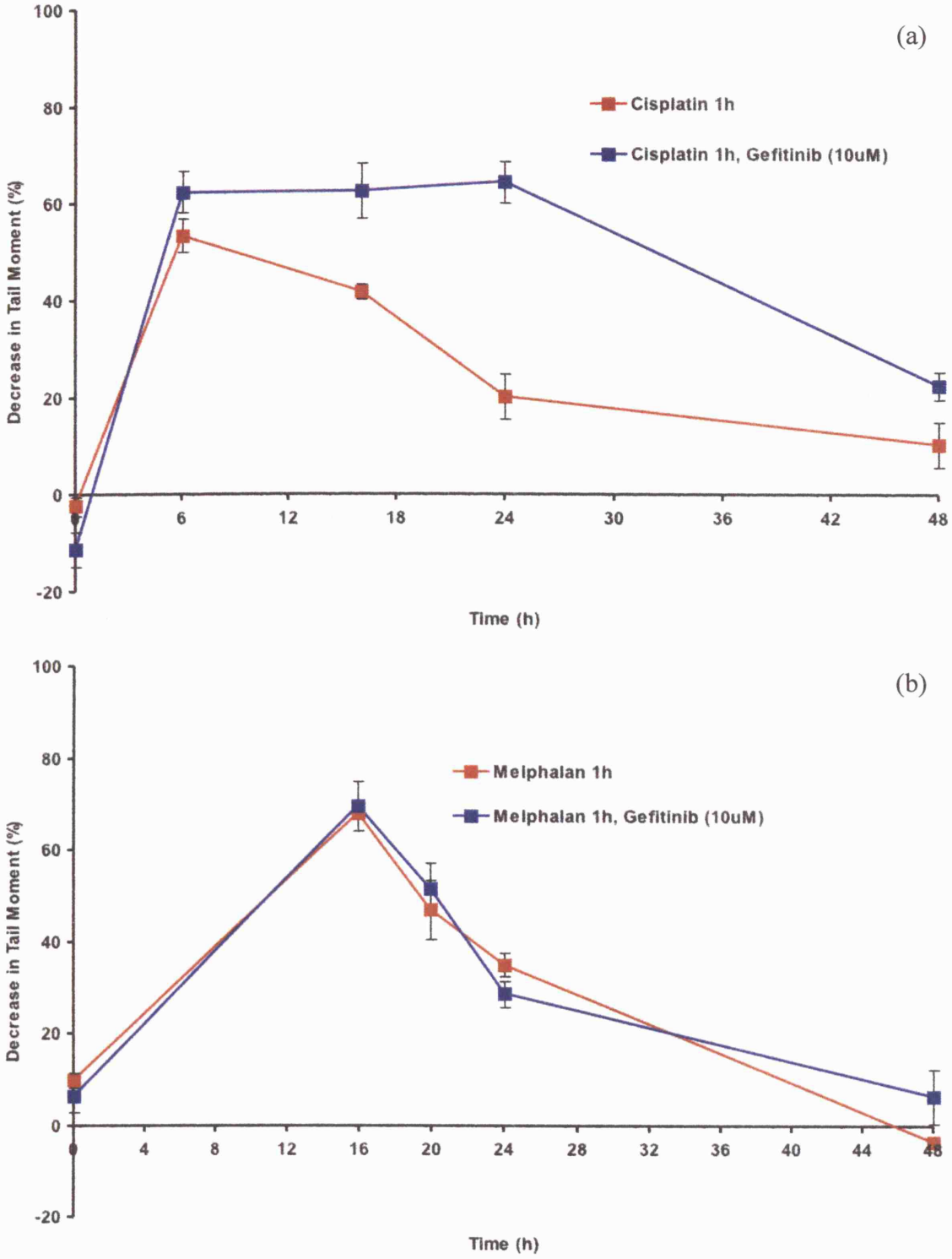

Figure 4.8: *Measurement of cisplatin and melphalan-induced DNA ICL formation and repair alone and in the presence of gefitinib in AR42J cells.* Cells were treated with (a) cisplatin (200μM) or (b) melphalan (200μM), for 1h and then incubated in fresh media or with gefitinib (10μM). ICL formation measured as percentage decrease in tail moment, plotted against post-incubation time following removal of drug. Data is a representation of three independent experiments; *bars*, SE.

4.5 Detection of Apoptosis

The annexin V assay was performed to confirm that the effects on the comet assay in relation to strand breaks were not due to the induction of apoptosis. Figure 4.9 shows the cell scatter plots of annexin V-FITC and PI staining for cisplatin and gefitinib treatments in MCF-7 cells. A 6h treatment with camptothecin (5μM) was included as a positive control which induced 21.42% apoptosis as compared with 7.6% for control untreated cells (Figure 4.9a-b). Cells treated with cisplatin (200μM) for 1h showed no increase in apoptosis (7.18%). Similarly, cells treated with cisplatin and then left for 6h (peak of ICL) had a comparable level of apoptosis (7.29%). Only a very marginal increase is seen after 24h and 48h with apoptosis levels of 11.89% and 10.27% respectively (Figure 4.9c-f). The addition of gefitinib (10μM) had no effect on the level of apoptosis at peak of ICL formation at 6h (6.75% apoptosis) and after 24h (8.76%) (Figure 4.9g-h). Therefore the DNA strand breaks observed in the previous experiments are not due to apoptosis. Experiments were also carried out with etoposide and melphalan which showed similar results (data not shown).

Over a longer period apoptosis will eventually occur as expected as is shown in Figure 4.9i-j. Cells left for 72h following cisplatin (200μM) treatment for 1h had an increased amount of apoptosis (13.26%) as compared with control untreated cells. Importantly, the subsequent addition of gefitinib (10μM) further increased the amount of apoptosis to 17.69% indicating its effect in altering apoptosis pathways in addition to increased inhibition of proliferation discussed in Chapter 3.

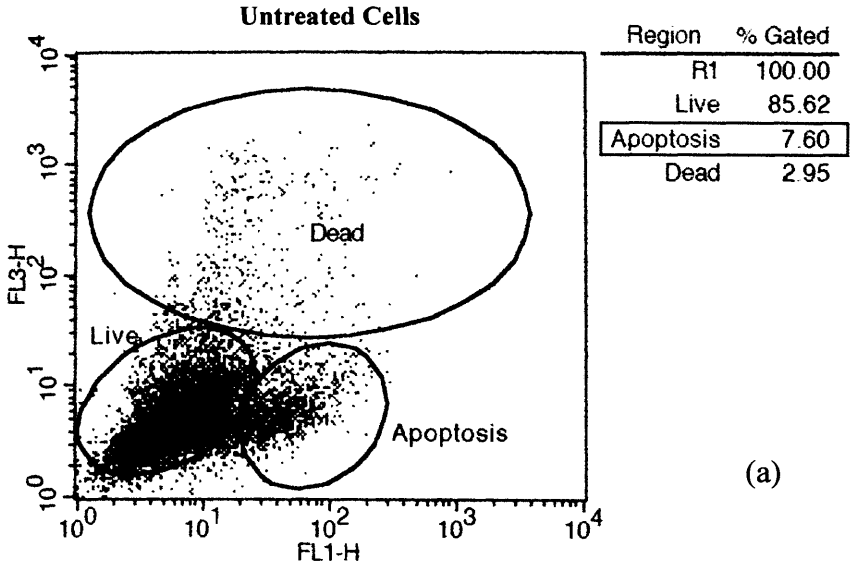
Untreated Cells
Region % Gated
R1 100.00
Live 85.62
Apoptosis 7.60
Dead 2.95
Dead
Live
Apoptosis
FL3-H
FL1-H
10^0 10^1 10^2 10^3 10^4

(a)

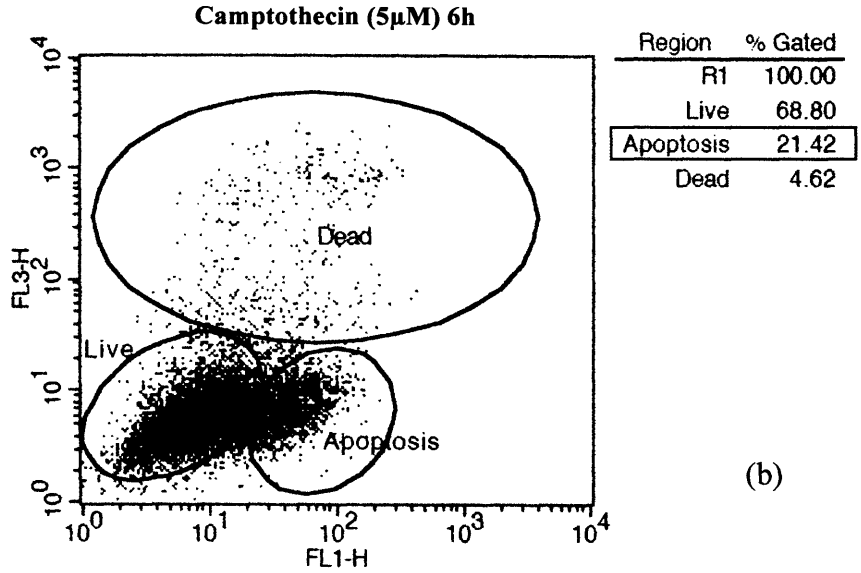
Camptothecin (5μM) 6h
Region % Gated
R1 100.00
Live 68.80
Apoptosis 21.42
Dead 4.62
Dead
Live
Apoptosis
FL3-H
FL1-H
10^0 10^1 10^2 10^3 10^4

(b)

Cisplatin (200μM) 1h

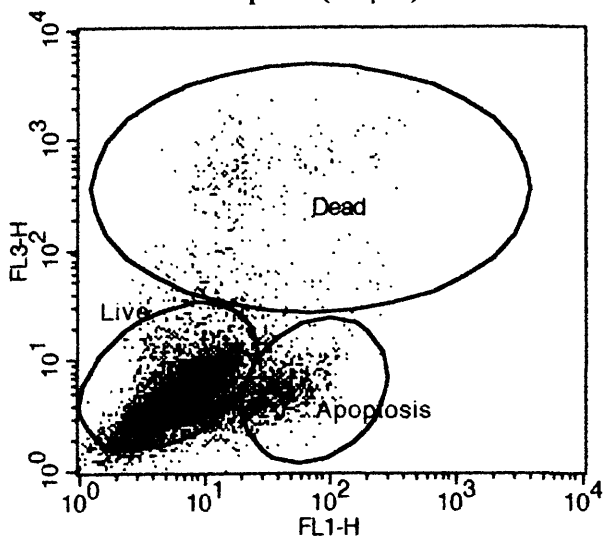

Region	% Gated
R1	100.00
Live	85.67
Apoptosis	7.18
Dead	3.09

(c)

Cisplatin (200μM) 1h, Then Media 6h

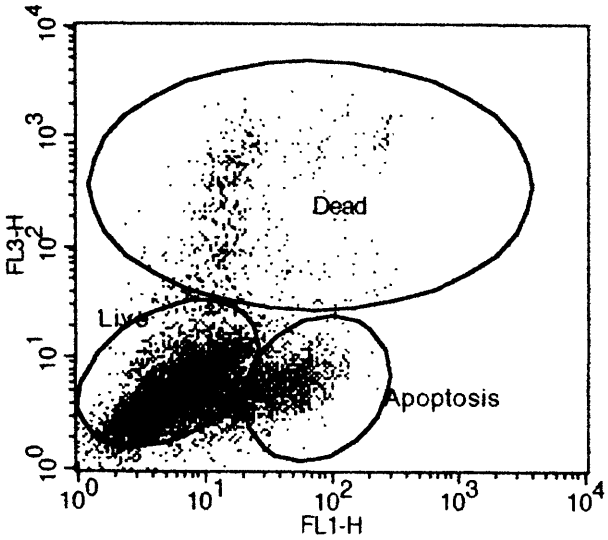

Region	% Gated
R1	100.00
Live	85.69
Apoptosis	7.29
Dead	3.59

(d)

Cisplatin (200μM) 1h, Then Media 24h

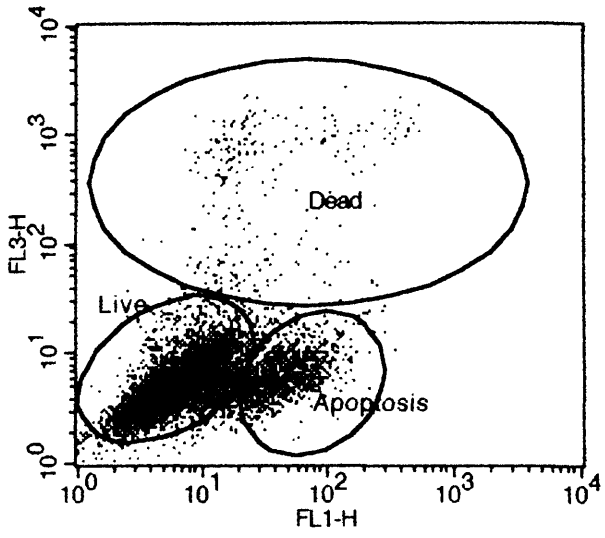

Region	% Gated
R1	100.00
Live	81.88
Apoptosis	11.89
Dead	3.22

(e)

Cisplatin (200μM) 1h, Then Media 48h

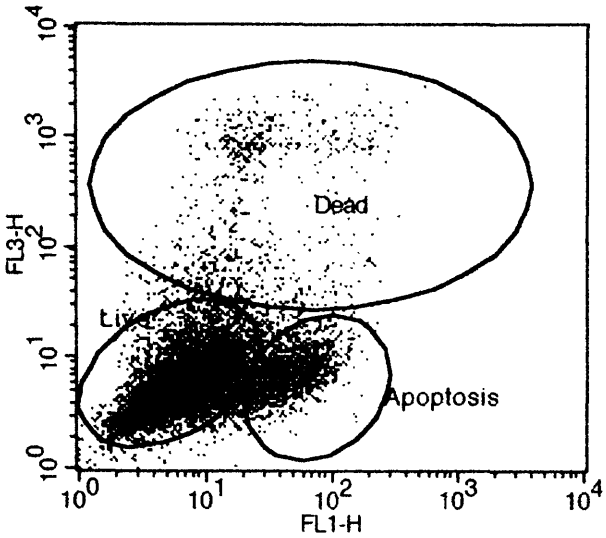

Region	% Gated
R1	100.00
Live	82.18
Apoptosis	10.27
Dead	4.89

(f)

Cisplatin (200μM) 1h, Then Gefitinib (10μM) 6h

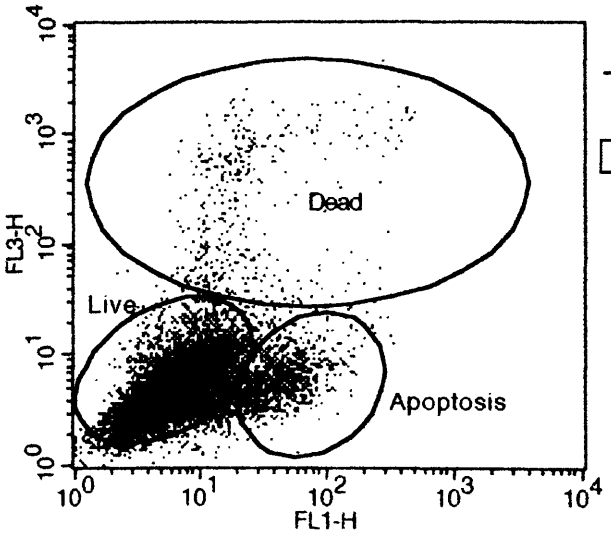

Region	% Gated
R1	100.00
Live	87.14
Apoptosis	6.75
Dead	2.97

(g)

Cisplatin (200μM) 1h, Then Gefitinib (10μM) 24h

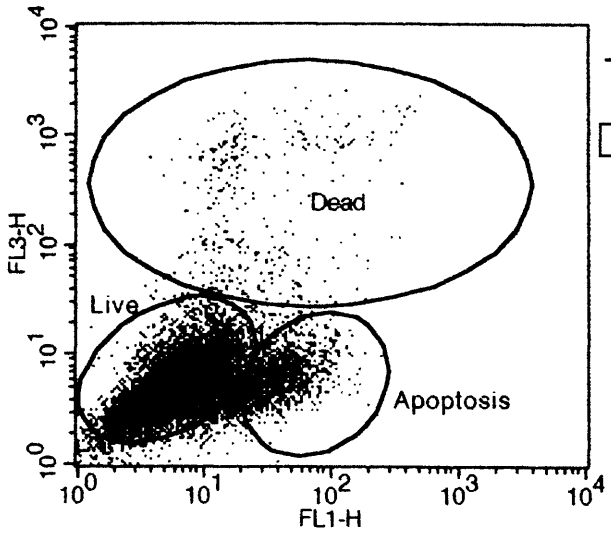

Region	% Gated
R1	100.00
Live	85.14
Apoptosis	8.76
Dead	2.46

(h)

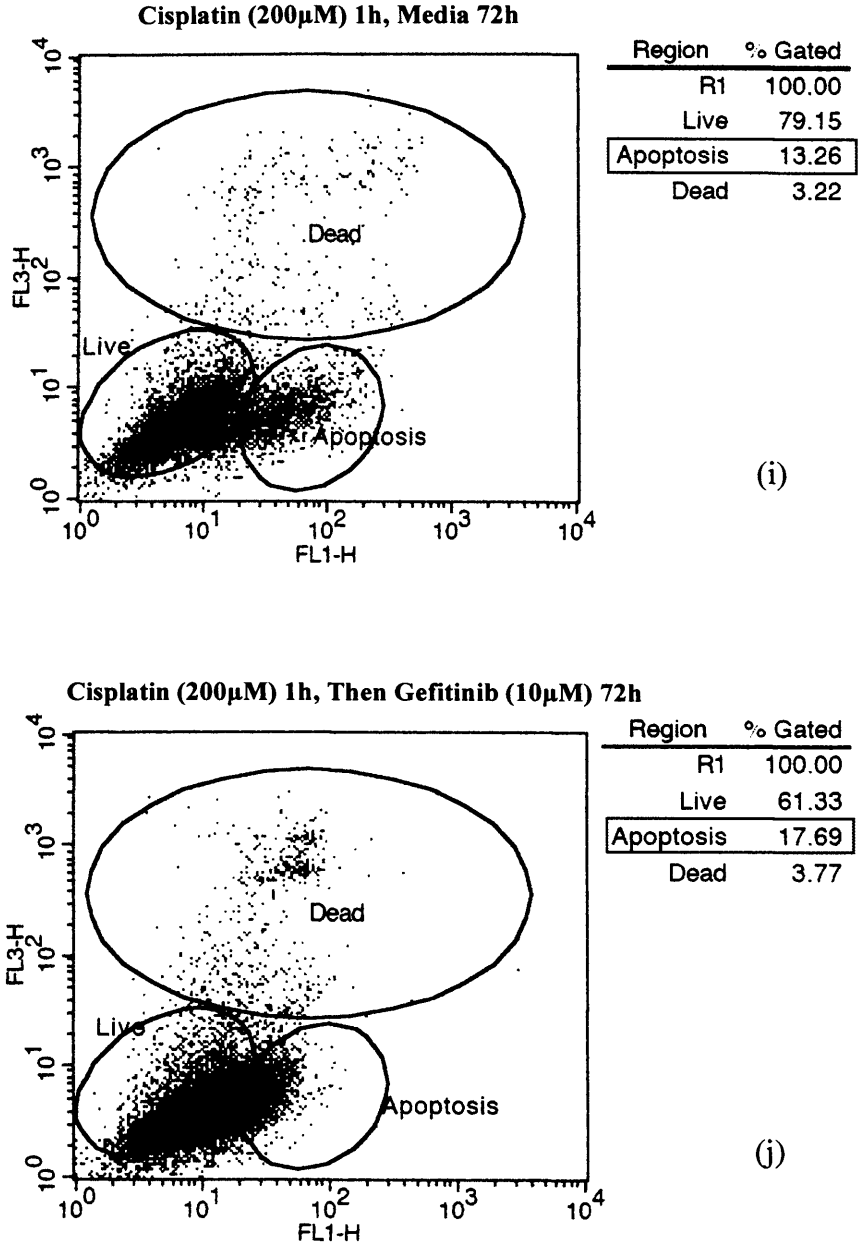

Figure 4.9: *Detection of apoptosis for cisplatin alone and in the presence of gefitinib in MCF-7 cells.* Cells were treated with cisplatin (200μM) for 1h and then incubated with gefitinib (10μM) alone. Camptothecin (5μM) included as a positive control. Apoptosis measured using the Annexin V-FITC assay staining for phosphatidylserine (PS) and propidium iodide (PI). Data is a representation of three independent experiments.

4.6 Studies in Colon Cancer

Experiments were then carried out to determine the synergistic features of different EGFR inhibitors with chemotherapy in the colorectal cancer cell line HCT-116. Figure 4.10a shows the formation of strand breaks and subsequent repair for etoposide (200μM) alone and followed by gefitinib (10μM). Results were similar to those found in MCF-7 and AR42J cells. Again, there was no alteration in the quantity of strand breaks in cells produced by etoposide alone (tail moment of 13.3) and in combination with gefitinib (13.7). After removal of drug, strand break repair was detectable within 30 minutes with almost complete repair after 4h. Following combination treatment with both etoposide and gefitinib there was a marked delay in the rate of repair of DNA strand breaks with 50.5% of strand breaks remaining at 1h as compared with only 21.2% for etoposide alone. There was also persistent DNA damage detectable after 24h. Studies with etoposide and matuzumab were also carried out and showed results similar to those found with gefitinib. Again there was no increase in the quantity of strand breaks but there was a marked delay in the rate of repair (Figure 4.10b).

Similar results were also found for experiments done in the colorectal cancer cell line CaCo-2 and are summarised in Table 4.1.

CaCo-2 Cells	
Treatment	**Strand Break Repair at 1h (%)**
Etoposide (100μM)	79.1
Etoposide (100μM), Gefitinib (10μM)	50.2
Etoposide (100μM), Matuzumab (10μg/ml)	47.9

Table 4.1: Strand break repair for etoposide in combination with gefitinib or matuzumab in CaCo-2 cells.

Quantitation of DNA strand breaks following irinotecan treatment has been well characterised (Godard *et al.*, 1999). Figure 4.11a shows the formation of strand breaks and subsequent repair for irinotecan (5μM) 2h alone and followed by gefitinib (10μM) in HCT-116 cells. As with etoposide, there was no alteration in the quantity of strand breaks in cells produced with irinotecan alone and in combination with gefitinib. Following combination treatment with gefitinib there was a marked delay in the rate of repair of DNA strand breaks with 68.9% of strand breaks remaining at 1h as compared

with only 37.6% for irinotecan alone. There was also persistent DNA damage detectable after 24h. Interestingly, the effects of combining irinotecan with matuzumab were not as marked (Figure 4.11b). Although there was still no increase in the quantity of strand breaks, the amount persisting after 1h was only slightly higher for irinotecan followed by matuzumab (41.7%) as compared with irinotecan alone (33.5%).

Experiments were also carried out to investigate the effects of gefitinib on cisplatin and melphalan-induced DNA ICL formation and rate of repair in HCT-116 cells. Table 4.2 summarises these results. Again, gefitinib treatment inhibited repair of cisplatin-induced ICLs but not those induced by melphalan.

HCT-116 Cells	
Treatment	**ICL Repair at 24h (%)**
Cisplatin (200μM)	51.1
Cisplatin (200μM), Gefitinib (10μM)	21.5
Melphalan (200μM)	61.9
Melphalan (200μM), Gefitinib (10μM)	52.5

Table 4.2: ICL repair for cisplatin and melphalan in combination with gefitinib in HCT-116 cells.

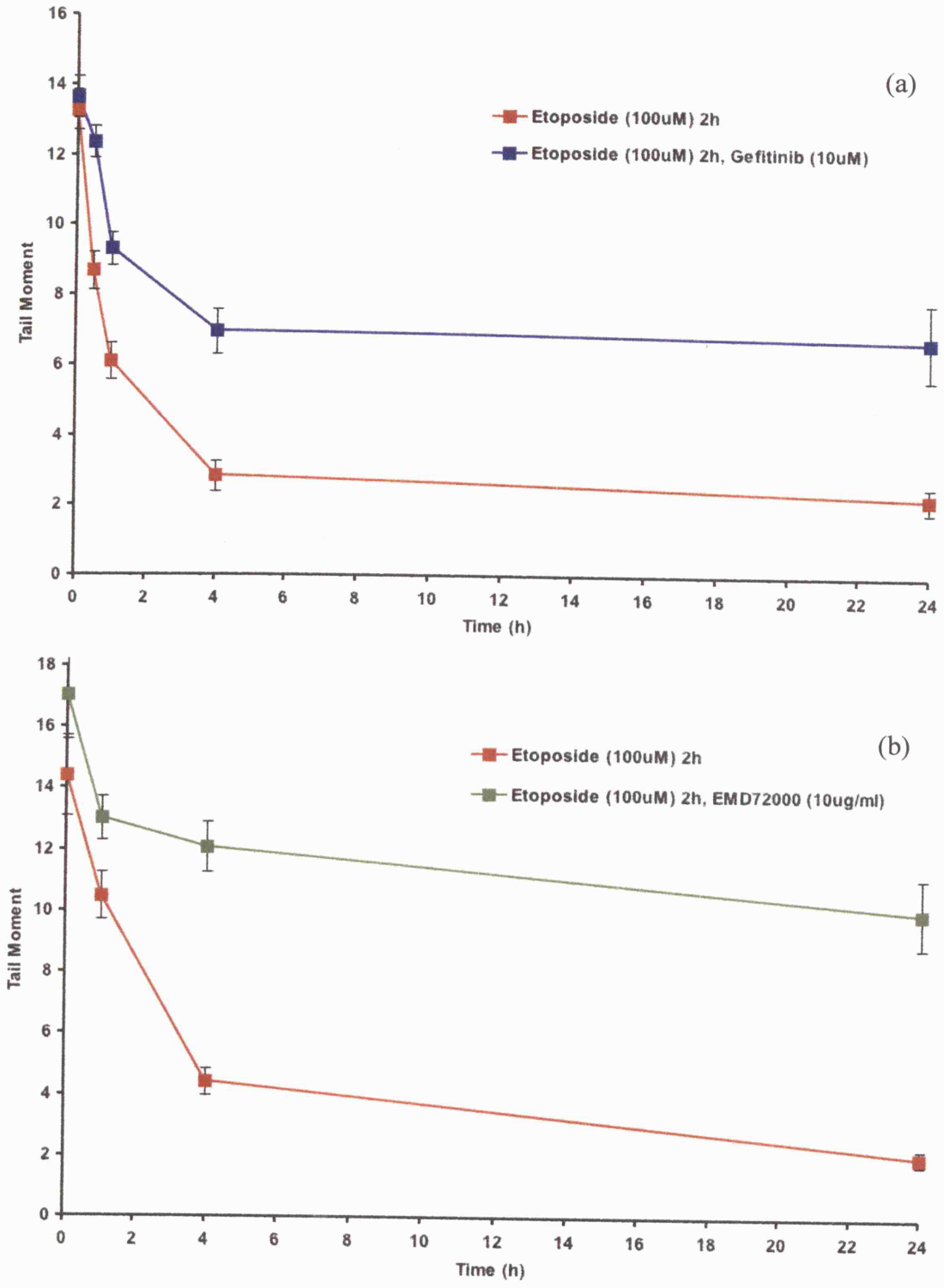

Figure 4.10: *Measurement of etoposide-induced DNA strand breaks and their repair alone or in the presence of gefitinib or matuzumab in HCT-116 cells.* Cells were treated with etoposide (100μM) for 2h and then incubated in fresh media or with (a) gefitinib (10μM) or (b) matuzumab (10μg/ml) alone. Strand break formation measured as tail moment, plotted against post-incubation time following removal of etoposide. Data is a representation of three independent experiments; *bars*, SE.

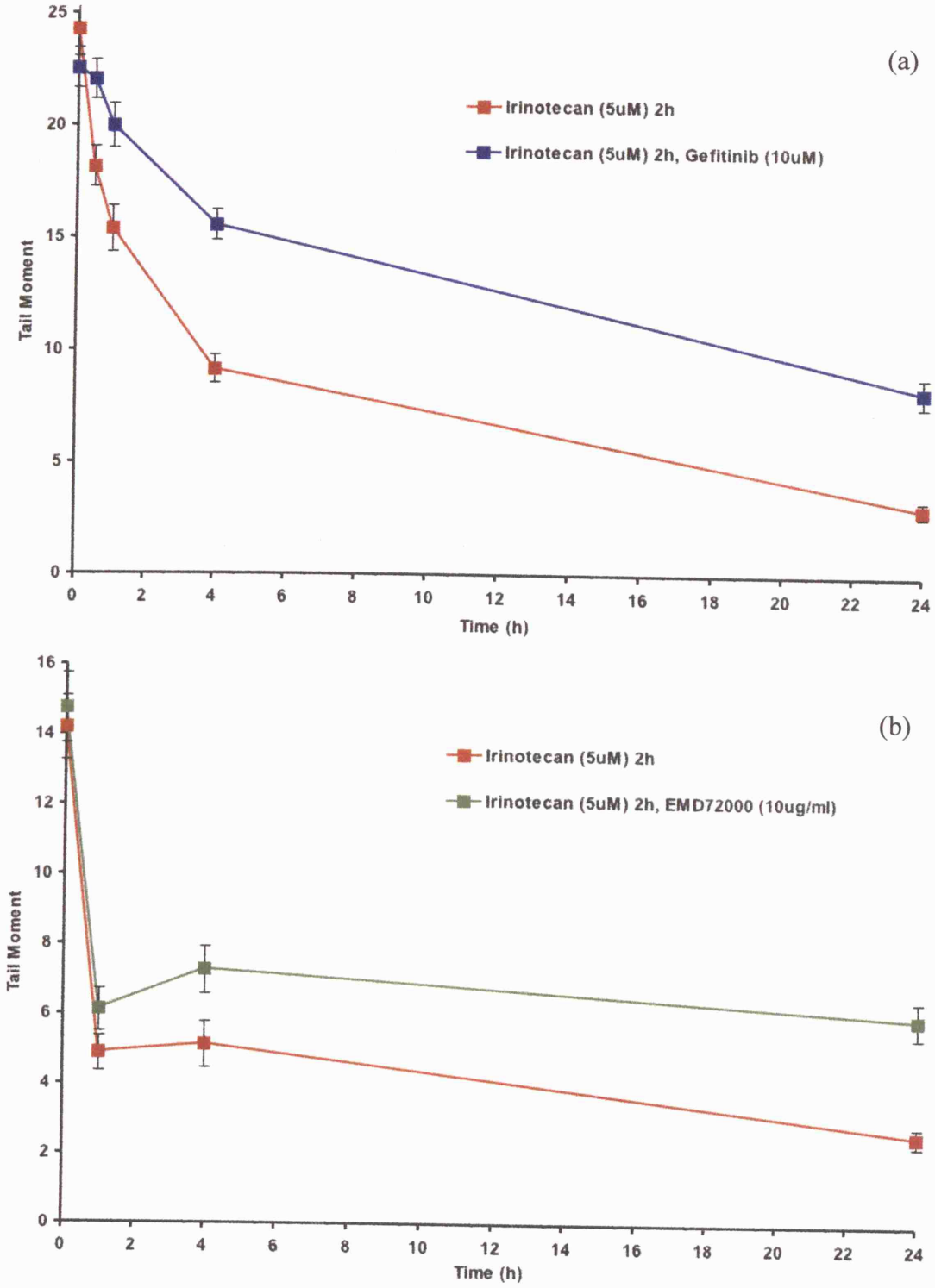

Figure 4.11: *Measurement of irinotecan-induced DNA strand breaks and their repair alone or in the presence of gefitinib or matuzumab in HCT-116 cells.* Cells were treated with irinotecan (5μM) for 2h and then incubated in fresh media or with (a) gefitinib (10μM) or (b) matuzumab (10μg/ml) alone. Strand break formation measured as tail moment, plotted against post-incubation time following removal of irinotecan. Data is a representation of three independent experiments; *bars*, SE.

4.7 Discussion

This chapter investigated the effects of EGFR inhibition on the modulation of DNA damage in the breast cancer cell line MCF-7, the rat pancreatic cell line AR42J and the colon cancer cell lines HCT-116 and CaCo-2. The nature of the DNA damage induced by the agents used is well understood and the comet assay is a validated methodology for quantitating DNA damage and repair following exposure to these drugs (Hartley, *et al.*, 1999; Spanswick *et al.*, 1999).

When gefitinib was added to cells following a short exposure to etoposide, there was no increase in the level of DNA damage as compared with etoposide treatment alone. There was, however, increased delay in repair of the stand breaks in all cell lines tested. Given that gefitinib treatment alone did not produce any strand breaks, this data suggests that gefitinib inhibition of EGFR results in alterations in the downstream processing of DNA damage leading to a delay in the rate of strand break repair. Studies in CHO cells and in yeast have shown that DNA damage induced by etoposide leads to the involvement of multiple single- and double-strand break repair pathways (Caldecott *et al.*, 1990; Nitiss & Wang, 1996). Further investigation is required to determine which of these pathways are altered by gefitinib treatment and the molecular mechanisms by which they are achieved.

The level of cisplatin-induced ICLs formed in MCF-7 cells were not altered when co-treated with gefitinib. However, whilst ICLs induced by cisplatin alone are repaired after 12h, a striking inhibition of DNA repair was seen in the presence of gefitinib, with ICLs still persisting after 24h. Given that similar results were found in the other cell lines tested and that gefitinib alone produced no ICLs, this data suggests that co-treatment with gefitinib alters the downstream processing of cisplatin-induced DNA ICLs leading to a delay in the rate of their repair. In contrast, there was no modulation in the kinetics of DNA repair following treatment with melphalan in any of the cell lines. Studies on colon cancer cell lines also showed that gefitinib delayed the repair of cisplatin-induced ICLs and had no effect on melphalan. It is therefore clear that the processing of ICLs formed by different DNA damaging chemotherapeutic agents are differently altered by inhibition of EGFR with gefitinib. Other studies done in squamous cancer cell lines reported a marked inhibition of repair of radiation-induced DNA damage when added in combination with gefitinib (Shintani *et al.*, 2003). In another study in a human head and neck cancer cell line it was shown that the co-treatment of

gefitinib modulated the repair of cisplatin-5FU-induced DNA damage (Magné *et al.*, 2003). It should be noted however that in both studies the expression of selected repair proteins was being measured by immunoblotting rather than the specific formation of strand breaks or ICLs. In addition, a study done in HT-29 and LoVo colon cancer cell lines reported a marked inhibition of repair of oxaliplatin-induced DNA damage when added in combination with gefitinib (Xu *et al.*, 2003). This was demonstrated using mass spectrometry techniques to measure cellular platinum accumulation and Pt-DNA adducts rather than specific crosslink formation. Interestingly, a recent study showed that gefitinib did not hinder the rejoining of radiation-induced DNA double-strand breaks in a variety of cell lines (Giocanti *et al.*, 2004). However, this was assessed using alkaline elution analysis which is not a single cell assay, requires a large number of cells and radio-labelling and is at least 10-fold less sensitive. By contrast, the comet assay measures DNA strand breaks in a single cell population, requires only a few cells, is more sensitive and can be used at pharmacologically relevant doses (Hartley, *et al.*, 1999; Spanswick *et al.*, 1999).

An intriguing aspect of ICL repair is that several repair pathways are involved to remove or bypass an ICL. As discussed in Chapter 1, the type and frequency of DNA lesions due to cisplatin differ from those produced by melphalan. In contrast to the repair of ICLs produced by melphalan (Clingen *et al.*, 2005), repair of cisplatin ICLs does not involve the formation of DNA double-strand breaks and the repair pathways they require (De Silva *et al.*, 2002). De Silva *et al.*, (2002), used pulsed field gel electrophoresis (PFGE) for analysis of DSBs and showed that XRCC2 and XRCC3 cells are defective in the unhooking step of cisplatin ICL repair suggesting that homologous recombination might be initiated prior to excision of cisplatin-induced crosslinking. Clingen *et al.*, (2005), showed that in addition to XRCC2 and XRCC3, repair of melphalan-induced ICLs are dependent on the XPF-ERCC1 heterodimer component of the nucleotide excision repair pathway as measured by PFGE. It is clear therefore that the mechanisms for the differences in inhibition of repair of melphalan and cisplatin-induced ICLs warrant further investigation.

The formation of strand breaks for all chemotherapy agents alone or in the presence of gefitinib during the time course of these experiments cannot be accounted for by induction of apoptosis. However the comet assay can also be used to detect apoptosis. The apoptotic process causes DNA fragmentation causing most of the DNA to migrate

to the tail which appears "detached" from the head (Spanswick *et al.*, 2002). In accordance with the annexin V data, the number of apoptotic cells in the cell populations analysed by the comet assay was small and did not interfere with the analysis of strand breaks or ICLs.

Furthermore, the use of the anti-EGFR antibody matuzumab had a similar effect to gefitinib on the modulation of etoposide-induced strand breaks. As with gefitinib, matuzumab did not alter the level of DNA strand breaks but did induce a delay in repair. These results suggest that the pathways responsible for the processing of specific forms of DNA damage are equally altered by different anti-EGFR therapies with different modes of action. Similar studies in colorectal, breast and human squamous cell carcinomas showed that the addition of cetuximab affected the rate of DNA repair following radiotherapy (Bandyopadhyay *et al.*, 1998; Huang & Harari, 2000).

Gefitinib treatment also delayed the repair of irinotecan-induced strand breaks despite only a modest delay achieved with matuzumab. This data further demonstrates the differences in anti-EGFR inhibitory effects and their specificity in modulating the repair of DNA damage induced by different chemotherapeutic agents.

4.7.1 Conclusions

These experiments demonstrate that gefitinib inhibition of EGFR does not alter the level of DNA damage induced by conventional DNA-damaging chemotherapy. However, a striking inhibition of DNA repair is achieved by gefitinib of both DNA strand breaks produced by etoposide or irinotecan, and ICLs produced by cisplatin. No delay of melphalan-induced ICLs was detected. These findings build on the synergy studies discussed in Chapter 3 such that those agents showing a synergistic inhibition of proliferation with gefitinib also show a delay in repair of DNA damage in its presence. It is reasonable therefore to conclude that alterations in DNA repair mechanisms induced by gefitinib are responsible, at least in part, for the synergistic effects achieved with some chemotherapeutic agents (Friedmann *et al.*, 2004).

Further understanding of the mechanisms of interaction between EGFR inhibition and chemotherapy will be important in devising novel schedules and combinations for testing in the clinic.

CHAPTER 5

INTERACTION OF THE EPIDERMAL GROWTH FACTOR RECEPTOR AND DNA-DEPENDENT PROTEIN KINASE FOLLOWING GEFITINIB TREATMENT

5.1 Introduction

The results shown in the previous chapters indicate that the mechanisms of synergy between gefitinib and specific chemotherapeutic agents may be partly due to gefitinib-induced modulations of DNA repair. Thus, molecular blockade of EGFR signalling may influence the capacity of tumour cells to repair DNA lesions effectively after cytotoxic damage.

Cisplatin adducts are recognised by a number of cellular proteins, including the DNA damage-recognition factors XPC, hHR23b, MSH2, MSH6 and the high-mobility group protein HMG1 (Wang & Lippard, 2005). The adducts are subject to repair by several pathways, including nucleotide excision repair, mismatch repair and homologous recombination. Other repair factors include the DNA-dependent protein kinase (DNA-PK) complex. This is comprised of the Ku70/80 heterodimer and the catalytic subunit, DNA-PK_{CS} and participates in non-homologous end joining (NHEJ) and V(D)J recombination (Khanna & Jackson, 2001). DNA-PK is a member of the PI3-kinase-related family and is proposed to have a role in cell signalling after DNA damage. It has been shown that the Ku70/80 heterodimer can bind to DNA ends at double-strand breaks and to DNA fragments with cisplatin-DNA adducts (Turchi *et al.*, 1999). DNA-PK_{CS} is auto-phosphorylated following exposure to radiation (Ding *et al.*, 2003; Lou *et al.*, 2004). This modifies its binding with Ku and has been implicated in the phosphorylation of a wide range of DNA damage/checkpoint proteins (Block *et al.*, 2004). MDC1 which is generally associated with the regulation of both intra S-phase and G_2/M phase checkpoints, directly binds to DNA-PK via repeat regions and augments these early auto-phosphorylation events (Lou *et al.*, 2004). DNA-PK has also been implicated in the phosphorylation of a number of other substrates including c-ABL, p53, replication factor A and H2AX but as yet there have been no links to function (Collis *et al.*, 2005). Furthermore, DNA-PK activity has also been shown to be regulated by a number of proteins. One such example is the oncogenic tyrosine kinase c-ABL which phosphorylates DNA-PK thus modulating DNA-PK/Ku/DNA interactions (Kharbanda *et al.*, 1997).

Cisplatin has been shown to induce diverse cellular responses including the activation of the JNK and p38 MAPK cascades as well as members of the ERK subfamily of MAPKs (Benhar *et al.*, 2001). It has been shown that cisplatin-induced ERK activation is significantly elevated in transformed cells, such as NIH3T3 cells that overexpress

EGFR (Benhar *et al.*, 2001). These findings led to further investigations confirming that cisplatin induces activation of EGFR and that by preventing cisplatin-induced activation, drug resistance can be reduced and clinical efficacy improved (Benhar *et al.*, 2002).

It has been demonstrated that cetuximab triggers a specific physical interaction between EGFR and DNA-PK_{CS} or its regulatory heterodimeric complex Ku70/80 in a variety of cell types both *in vitro* and *in vivo* (Bandyopadhyay *et al.*, 1999). Furthermore, it was shown that the cetuximab-induced EGFR/DNA-PK_{CS} association is accompanied by a redistribution of DNA-PK_{CS} from the nucleus to the cytosol (Bandyopadhyay *et al.*, 1999; Huang & Harari, 2000).

5.1.1 Aims

These observations suggest a possible role of EGFR signalling in the maintenance of the nuclear levels of DNA-PK, and interference in EGFR signalling may possibly result in the impairment of DNA repair activity in the nuclei in cetuximab-treated cells. The experiments in this chapter address whether similar effects are achieved with gefitinib with the aim of further characterising the mechanisms of interaction between EGFR tyrosine kinase inhibitors and DNA-damaging chemotherapeutic agents. To this end, the following questions are addressed:

1. Does cisplatin activate EGFR and is this modulated by gefitinib?
2. Does gefitinib modulate DNA-PK expression?
3. Does gefitinib induce EGFR/DNA-PK_{CS} association in different cell lines?
4. Does gefitinib alter subcellular distribution of DNA-PK and EGFR?

RESULTS

5.2 Basal Protein Expressions in Cell Lines Used

Figure 5.1 shows the basal expressions of certain proteins in the human breast cancer cell lines MCF-7 and MDA-453, and the rat pancreatic cell line AR42J. MDA-453 cells have been shown by others to express low levels of EGFR and are resistant to gefitinib (Moasser *et al.*, 2001; Moulder *et al.*, 2001; Campiglio *et al.*, 2004). In contrast, whilst EGFR levels in AR42J cells are similar to MCF-7 cells, the level of phosphorylated-EGFR is significantly higher and is consistent with previous findings (Ishiyama *et al.*, 1998; Piiper *et al.*, 2003). Whilst the level of DNA-PK in all cell lines remains consistent, the basal levels of AKT, p-AKT and p-MAPK in MDA-453 cells are considerably lower than in MCF-7 and AR42J cells.

5.3 Effects of Gefitinib and Cisplatin on Apoptotic Proteins

Cisplatin and gefitinib treatment alone or in combination had no effect on the level of the pro-apoptotic protein Bax, in MCF-7 cells (Figure 5.2). As shown in Figure 5.2, gefitinib (10μM) for 24h induces a 68% inhibition of AKT phosphorylation compared with untreated cells as measured by densitometric analysis. AKT inactivation leads to inhibition of cell proliferation and propagation of pro-apoptotic pathways. A cisplatin (20μM) 24h treatment alone did not induce marked changes in AKT phosphorylation (19%). In contrast, cisplatin treatment in combination with gefitinib inhibited AKT phosphorylation by 51%.

A change in mitochondrial permeability initiates apoptosis and is regulated by the Bax/Bcl-2 ratio which is under the control of p53. Bcl-2 stabilises the mitochondrial membrane thereby preventing release of cytochrome C and subsequent caspase activation. As shown in Figure 5.2, gefitinib alone caused a downregulation of Bcl-2 which persists when added in combination with cisplatin. Cells exposed to cisplatin downregulated expression of the anti-apoptotic protein Bcl_{XL}, by 59% as compared with untreated cells. Interestingly, co-treatment with gefitinib achieved an even greater downregulation (67%) despite gefitinib treatment alone having no effect.

No effect on the level of topoisomerase IIα was detected following gefitinib and cisplatin treatments.

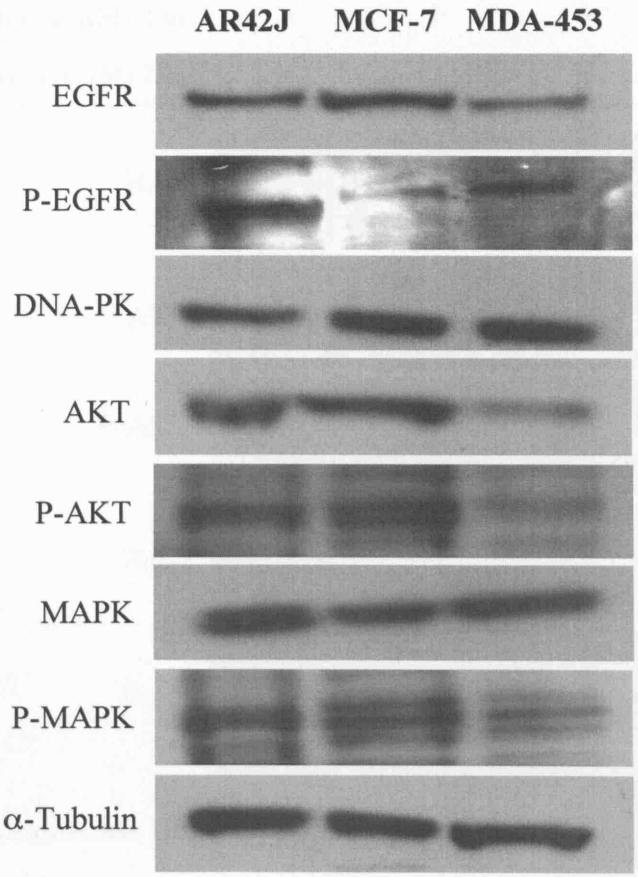

Figure 5.1: *Basal expression of various proteins in the AR42J, MCF-7 and MDA-543 cell lines.* Untreated cells were lysed and immunoblotted with different antibodies as described in figure; α-Tubulin serves as a loading control.

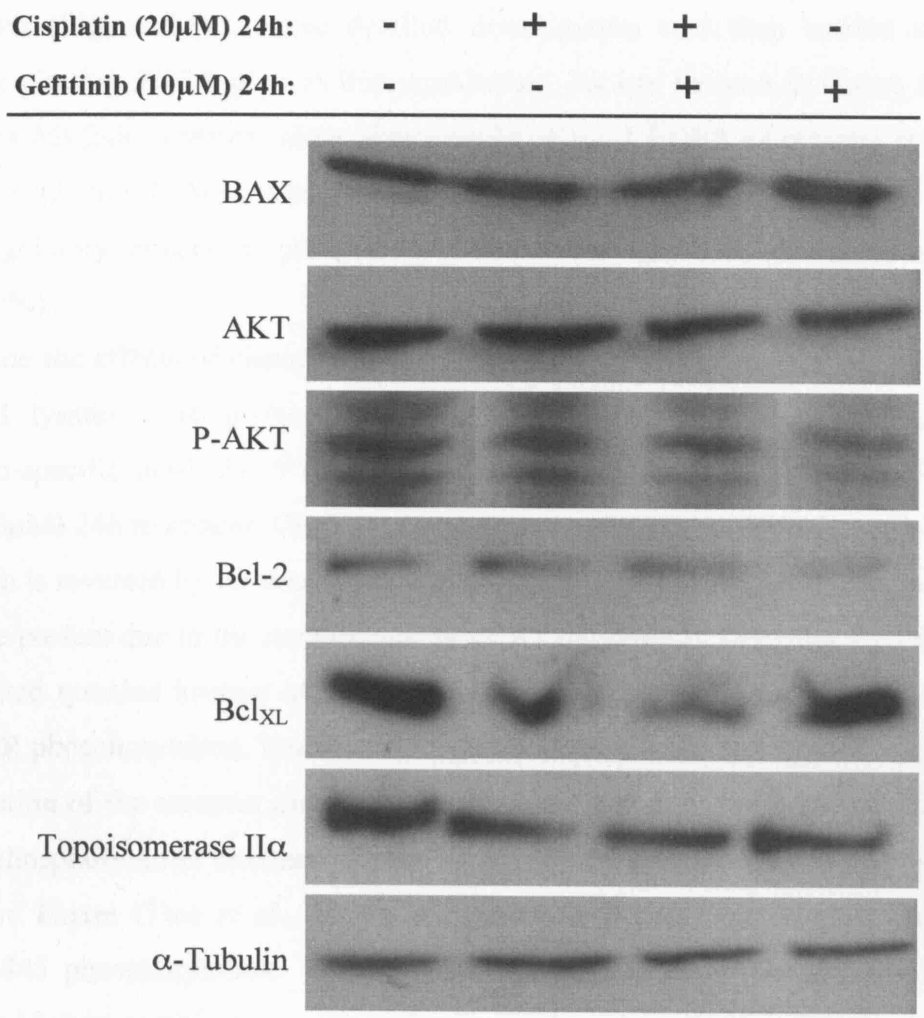

Figure 5.2: *Altered expressions of pro- and anti-apoptotic proteins following cisplatin and gefitinib treatment in MCF-7 cells.* Cells were treated with indicated concentrations of cisplatin and gefitinib for 24h. Lysates were immunoblotted with different antibodies as described in figure; α-Tubulin serves as a loading control.

5.4 Modulation of EGFR by Gefitinib and Chemotherapy

The effects of cisplatin and gefitinib on EGFR expression were assessed in MCF-7 cells and are shown in Figure 5.3. Total cell lysates were immunoblotted with anti-EGFR antibody which detected no significant alterations for treatments with cisplatin, gefitinib or with both (Figure 5.3a). More detailed investigation was then carried out by immunoprecipitating EGFR prior to immunoblotting. As can be seen in Figure 5.3b, a gefitinib (10μM) 24h treatment alone downregulated basal EGFR expression by 94%. In contrast, cisplatin (20μM) treatment for 24h increased expression by 12%. However, the downregulatory effects of gefitinib persisted when added in combination with cisplatin (92%).

To investigate the effects of cisplatin and gefitinib on EGFR tyrosine phosphorylation, MCF-7 cell lysates were probed for phosphorylated-EGFR (P-EGFR) using the tyrosine-non-specific antibody, PY20. Figure 5.4a shows a decrease in P-EGFR for gefitinib (10μM) 24h treatment. Cisplatin (20μM) 24h treatment resulted in increased P-EGFR which is reversed by co-treatment with gefitinib. It should be noted that multiple isoforms are present due to the non-specificity of PY20 which is detecting a number of phosphorylated tyrosine kinases of similar size. To confirm the ability of cisplatin to induce EGFR phosphorylation, lysates were immunoblotted with anti-Tyr-845 antibody. Phosphorylation of the receptor may occur on tyrosine 845 which is positioned outside of the autophosphorylation domain (Benhar *et al.*, 2002) and has been shown to be a target for src kinase (Tice *et al.*, 1999). As shown in Figure 5.4b, cisplatin induces EGFR Tyr-845 phosphorylation. This is downregulated to below basal levels when cisplatin is added in combination with gefitinib. Further investigation was then carried out by immunoprecipitating with anti-EGFR antibody prior to immunoblotting for Tyr-845 phosphorylation (Figure 5.5a). Here, cisplatin induced a 91% increase in Tyr-845 phosphorylation as compared to untreated cells. In contrast, gefitinib treatment alone inhibited Tyr-845 phosphorylation by 87%. A 76% decrease in Tyr-845 phosphorylation was detected following co-treatment of gefitinib with cisplatin. Similar results have been found in other cell lines (Benhar *et al.*, 2002).

The effects of melphalan on EGFR phosphorylation were also investigated in MCF-7 cells and are shown in Figure 5.5b. At an equitoxic concentration to cisplatin, melphalan also induced EGFR phosphorylation with an 86% increase as compared with untreated cells. Interestingly, the addition of gefitinib had only a marginal effect on P-EGFR

upregulation induced by melphalan. Here, increased EGFR phosphorylation still persisted at 22% above basal levels.

Dose- and time-dependent gefitinib inhibition of EGFR Tyr-845 phosphorylation was assessed and is shown in Figure 5.6. Following a 24h exposure, EGFR Tyr-845 phosphorylation was inhibited by 11% with 2μM gefitinib, by 52% with 5μM gefitinib and by 79% with 10μM gefitinib (Figure 5.6a). Gefitinib at 10μM inhibited EGFR Tyr-845 phosphorylation by 84% after 12h and by 88% after 24h (Figure 5.6b).

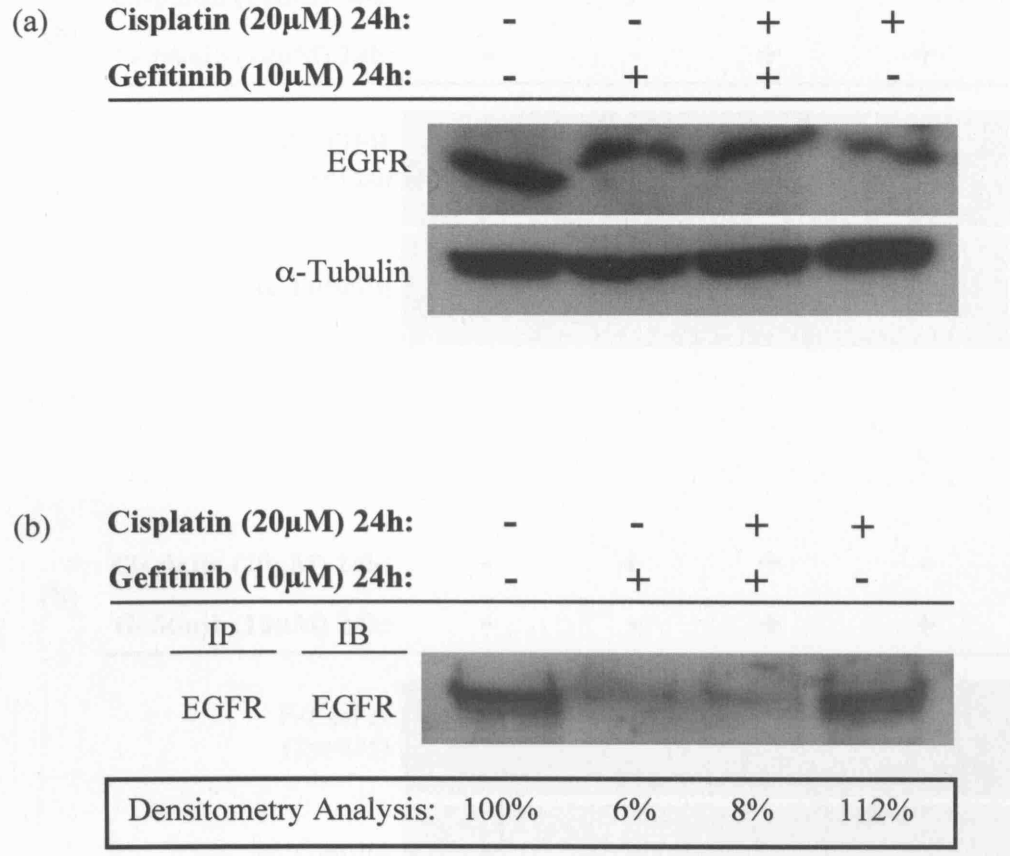

Figure 5.3: *Effects of cisplatin and gefitinib on expression of basal EGFR levels in MCF-7 cells.* Cells were treated with indicated concentrations of cisplatin and gefitinib for 24h. (a) Lysates immunoblotted with anti-EGFR antibody; α-Tubulin serves as a loading control. (b) Lysates immunoprecipitated (IP) with anti-EGFR and then immunoblotted (IB) with anti-EGFR antibody.

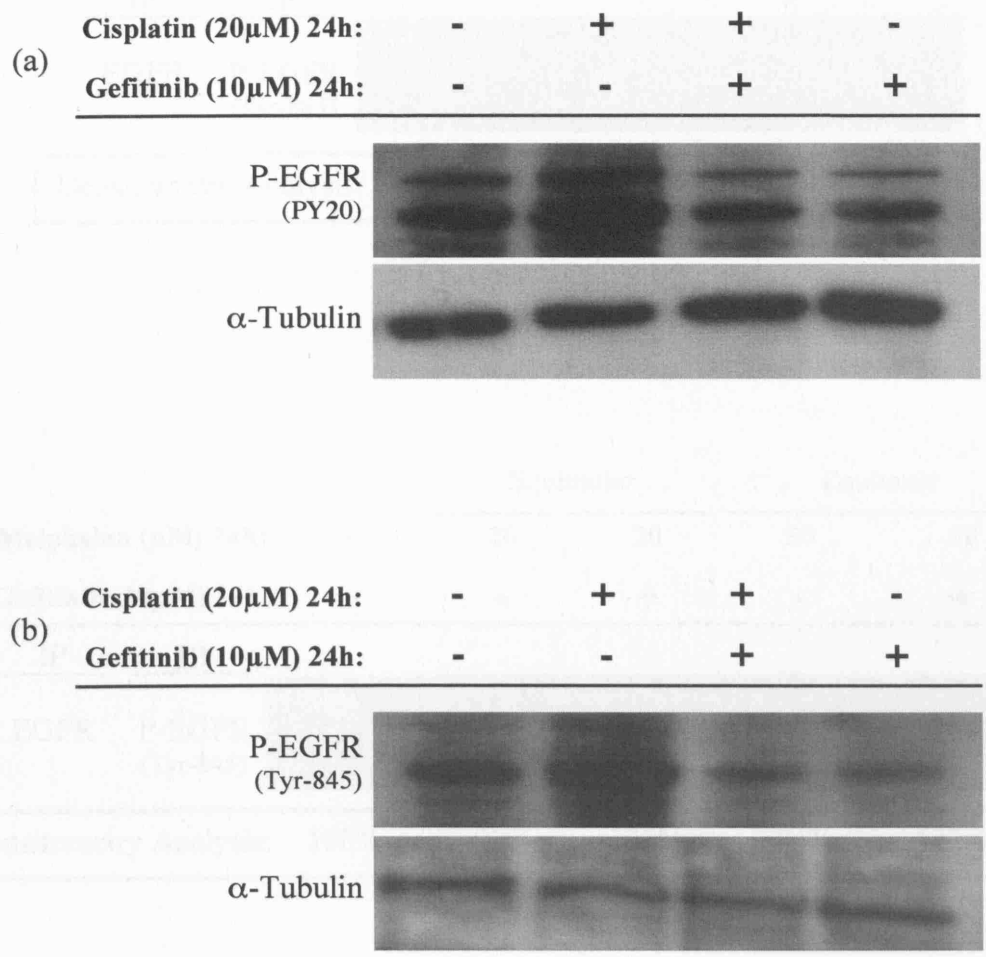

Figure 5.4: *Effects of cisplatin and gefitinib on EGFR tyrosine phosphorylation in MCF-7 cells*. Cells were treated with indicated concentrations of cisplatin and gefitinib for 24h. Lysates were immunoblotted with (a) anti-phospho-tyrosine antibody (PY20) or (b) anti-Tyr-845 EGFR specific antibody; α-Tubulin serves as a loading control.

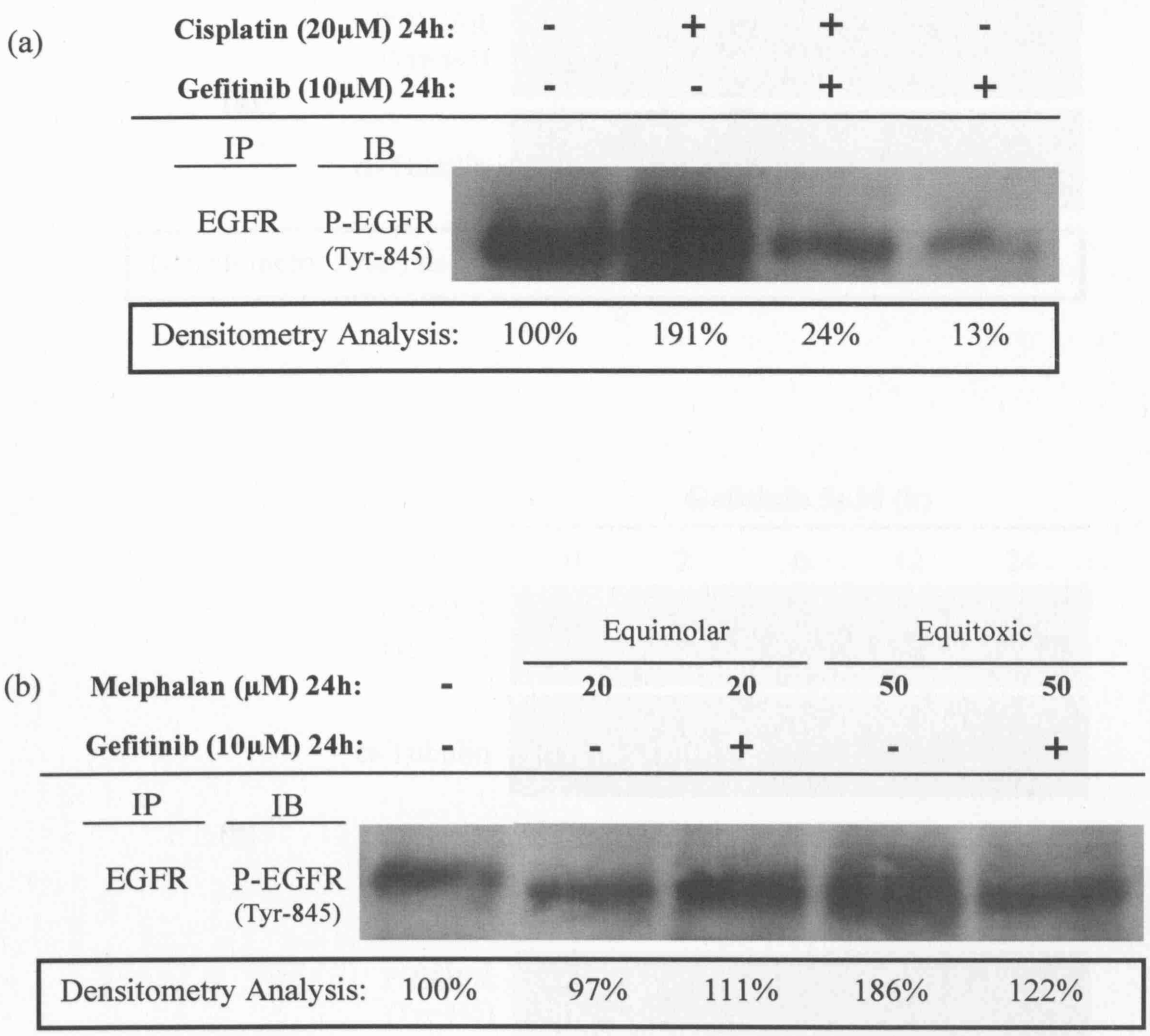

Figure 5.5: *Effects of cisplatin, melphalan and gefitinib on EGFR tyrosine phosphorylation in MCF-7 cells.* Cells were treated with indicated concentrations of (a) cisplatin or (b) melphalan with or without gefitinib for 24h. Lysates were immunoprecipitated (IP) with anti-EGFR antibody and then immunoblotted (IB) with anti-Tyr-845 EGFR specific antibody.

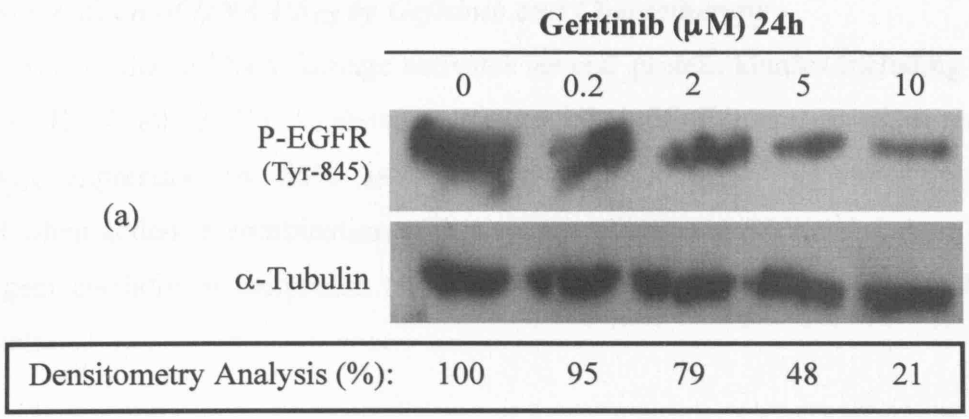

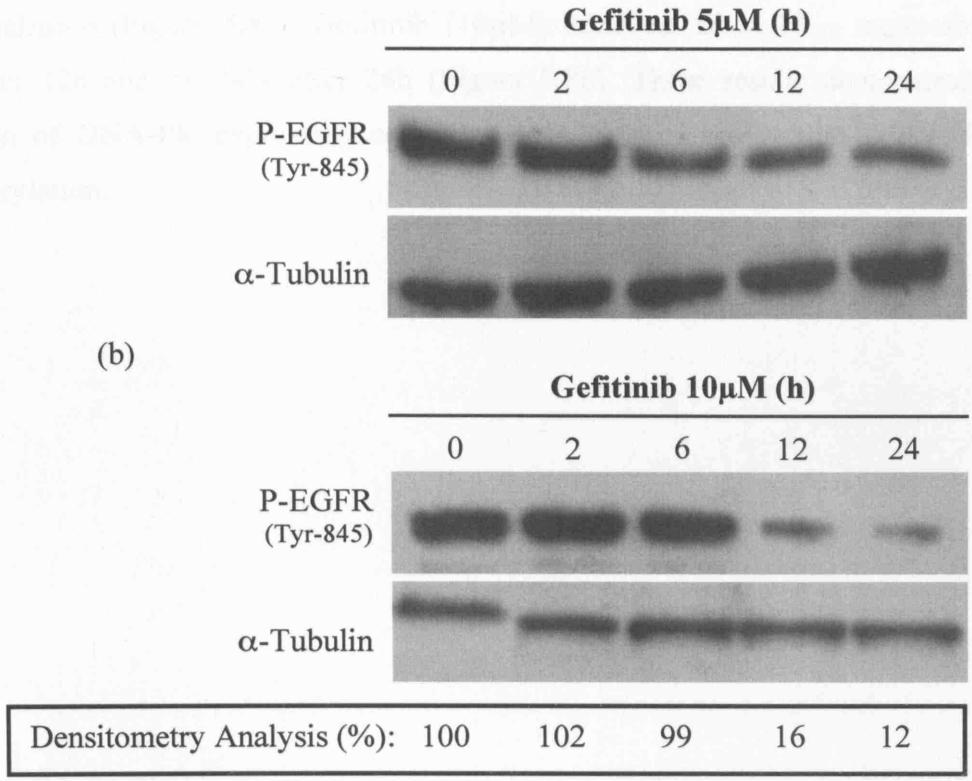

Figure 5.6: *Gefitinib dose- and time-dependent inhibition of EGFR tyrosine phosphorylation in MCF-7 cells.* (a) Cells were treated with indicated concentrations of gefitinib for 24h and lysates immunoblotted with anti-Tyr-845 EGFR specific antibody. (b) Cells were treated with gefitinib (5μM or 10μM) for indicated lengths of time and lysates immunoblotted with anti-Tyr-845 EGFR specific antibody. α-Tubulin serves as a loading control.

5.5 Modulation of DNA-PK$_{CS}$ by Gefitinib and Chemotherapy

Chemotherapy-induced DNA damage activates several protein kinases including ATM and DNA-PK (Shiloh, 2001). As shown in Figure 5.7, gefitinib treatment alone reduced DNA-PK$_{CS}$ expression by 85% as compared with control. This downregulation persisted when added in combination with cisplatin (86%) and with melphalan (82%). Single-agent cisplatin or melphalan treatment alone did not significantly alter DNA-PK$_{CS}$ levels.

Dose- and time-dependent gefitinib inhibition DNA-PK$_{CS}$ was assessed and is shown in Figure 5.8. Following exposure to gefitinib for 24h, DNA-PK$_{CS}$ expression was inhibited by 8% with 2μM gefitinib, by 78% with 5μM gefitinib and by 92% with 10μM gefitinib (Figure 5.8a). Gefitinib (10μM) inhibited DNA-PK$_{CS}$ expression by 89% after 12h and by 94% after 24h (Figure 5.8b). These results demonstrate that inhibition of DNA-PK expression occurs at doses of gefitinib which inhibit EGFR phosphorylation.

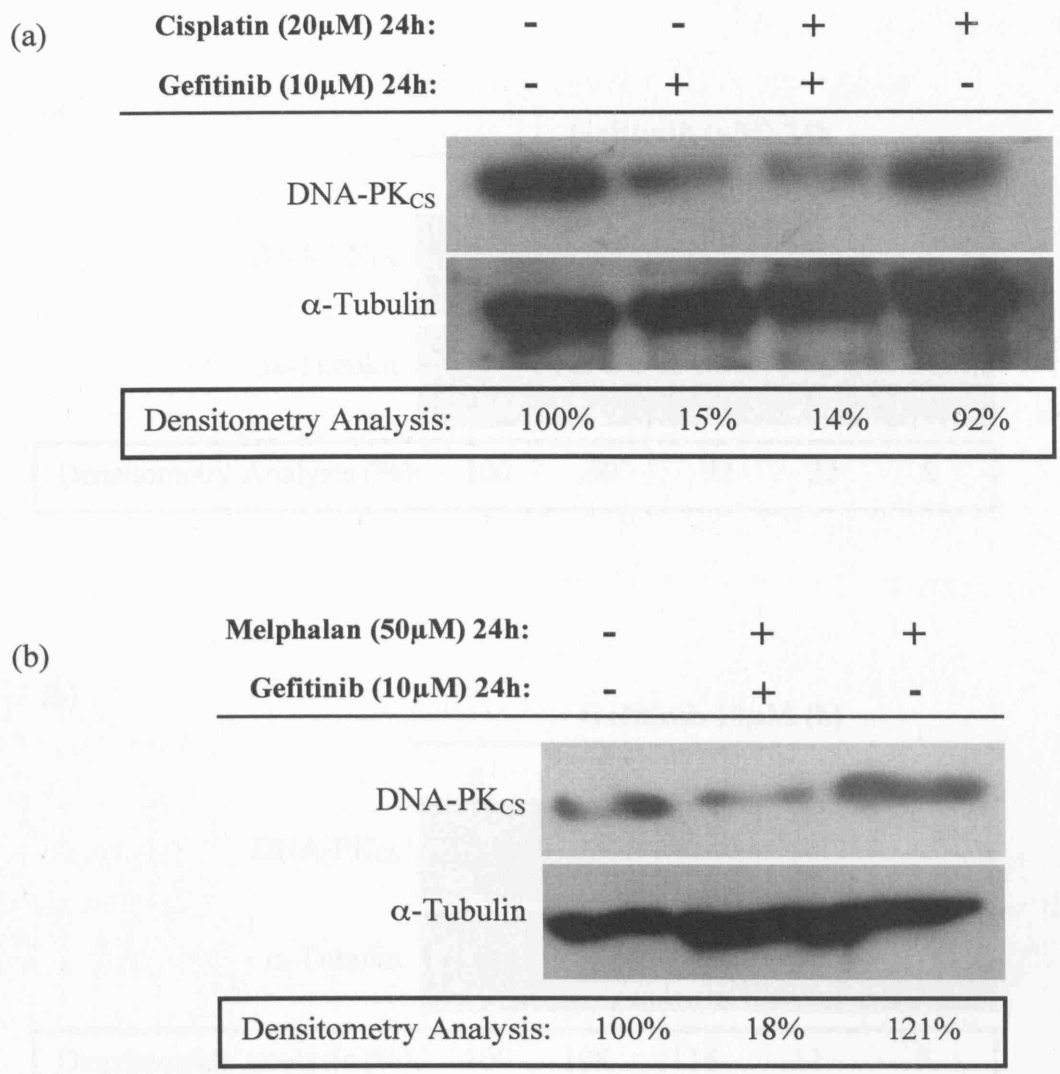

Figure 5.7: *Effects of cisplatin, melphalan and gefitinib on DNA-PK$_{CS}$ expression in MCF-7 cells.* Cells were treated with indicated concentrations of gefitinib and (a) cisplatin or (b) melphalan for 24h. Lysates were immunoblotted with anti-DNA-PK$_{CS}$ antibody; α-Tubulin serves as a loading control.

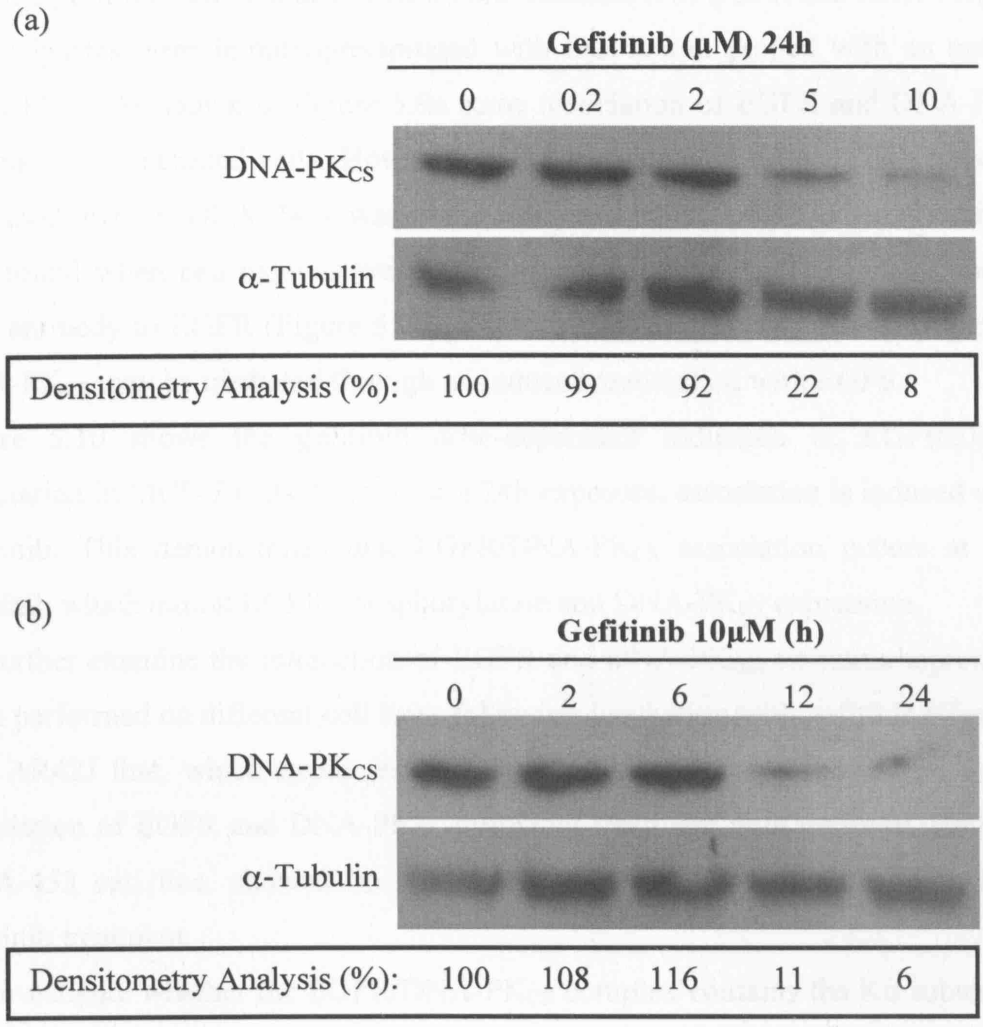

Figure 5.8: *Gefitinib dose- and time-dependent inhibition of DNA-PK$_{CS}$ expression in MCF-7 cells.* (a) Cells were treated with indicated concentrations of gefitinib for 24h and lysates immunoblotted with anti-DNA-PK$_{CS}$ antibody. (b) Cells were treated with gefitinib (10μM) for indicated lengths of time and lysates immunoblotted with anti-DNA-PK$_{CS}$ antibody. α-Tubulin serves as a loading control.

5.6 Gefitinib-Induced Association of EGFR and DNA-PK$_{CS}$

A previous report suggested an association of EGFR and DNA-PK$_{CS}$ in cells treated with the anti-EGFR antibody, cetuximab (Bandyopadhyay *et al.*, 1998). To investigate whether gefitinib had similar effects on the association of EGFR and DNA-PK$_{CS}$, MCF-7 cell lysates were immunoprecipitated with EGFR and probed with an antibody to DNA-PK$_{CS}$. As shown in Figure 5.9a some association of EGFR and DNA-PK$_{CS}$ was detectable in untreated cells. However, following gefitinib (10μM) 24h treatment, an increased level of DNA-PK$_{CS}$ was found to be associated with EGFR. A similar result was found when cell extracts were immunoprecipitated with DNA-PK$_{CS}$ and probed with antibody to EGFR (Figure 5.9b). These results suggest that effects of gefitinib on DNA-PK$_{CS}$ may be mediated through an induced association with EGFR.

Figure 5.10 shows the gefitinib dose-dependent induction of EGFR/DNA-PK$_{CS}$ association in MCF-7 cells. Following a 24h exposure, association is induced with 5μM gefitinib. This demonstrates that EGFR/DNA-PK$_{CS}$ association occurs at doses of gefitinib which inhibit EGFR phosphorylation and DNA-PK$_{CS}$ expression.

To further examine the interaction of EGFR and DNA-PK$_{CS}$, co-immunoprecipitations were performed on different cell lines following incubation with gefitinib (Figure 5.11). The AR42J line, which expresses high levels of EGFR, also showed an increase in association of EGFR and DNA-PK$_{CS}$ following treatment with gefitinib. However, the MDA-453 cell line, showed no alteration in EGFR/DNA-PK association following gefitinib treatment.

To investigate whether the EGFR/DNA-PK$_{CS}$ complex contains the Ku subunits which are required for activation of DNA repair, the blots of lysates immunoprecipitated with EGFR were stripped and reprobed with antibody to Ku70. This indicated that the Ku70 complex is also associated with EGFR after treatment with gefitinib in MCF-7 and AR42J cells (Figure 5.12a). Given the ability for EGFR and HER-2 to heterodimerise, lysates immunoprecipitated with EGFR revealed that HER-2 protein was detectable by immunoblotting as expected. However, following immunoprecipitation with DNA-PK$_{CS}$, HER-2 was not detectable by immunoblotting (Figure 5.12b). This indicates that that the association between EGFR and DNA-PK$_{CS}$ does not additionally involve an interaction with HER-2.

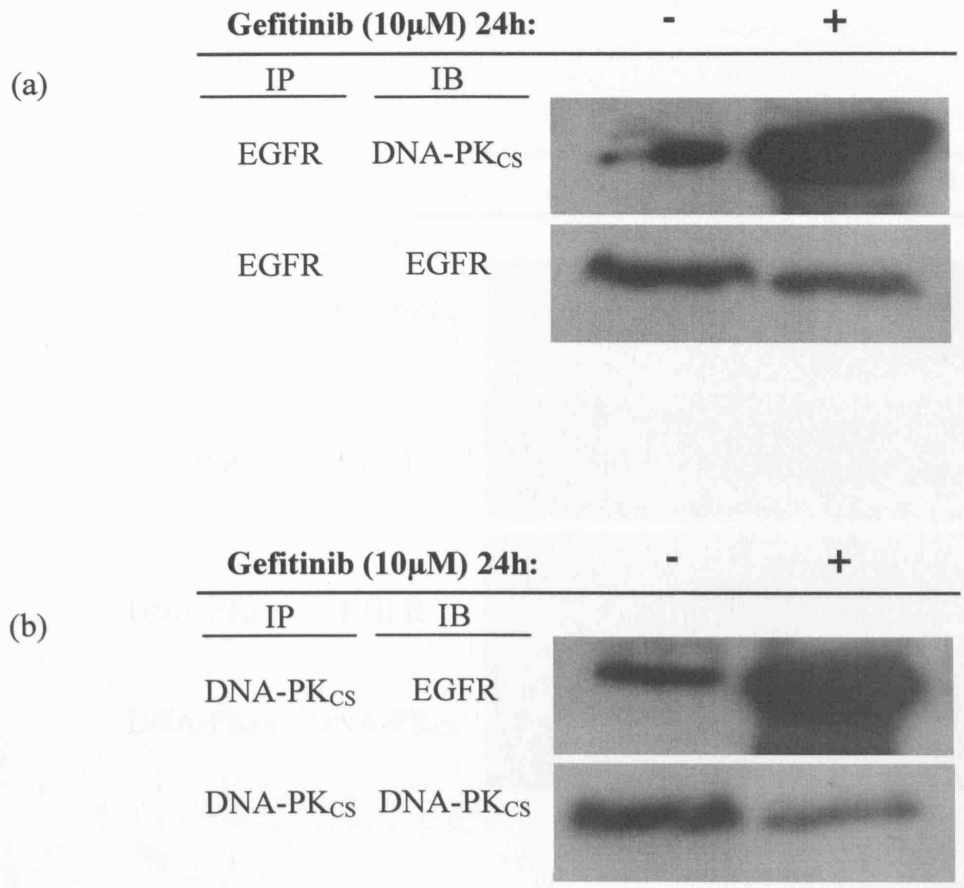

Figure 5.9: *Gefitinib-induced EGFR/DNA-PK$_{CS}$ association in MCF-7 cells*. Cells were treated with gefitinib (10μM) for 24h. Lysates were immunoprecipitated (IP) with (a) anti-EGFR antibody or (b) anti-DNA-PK$_{CS}$ antibody and then immunoblotted (IB) as described in figure.

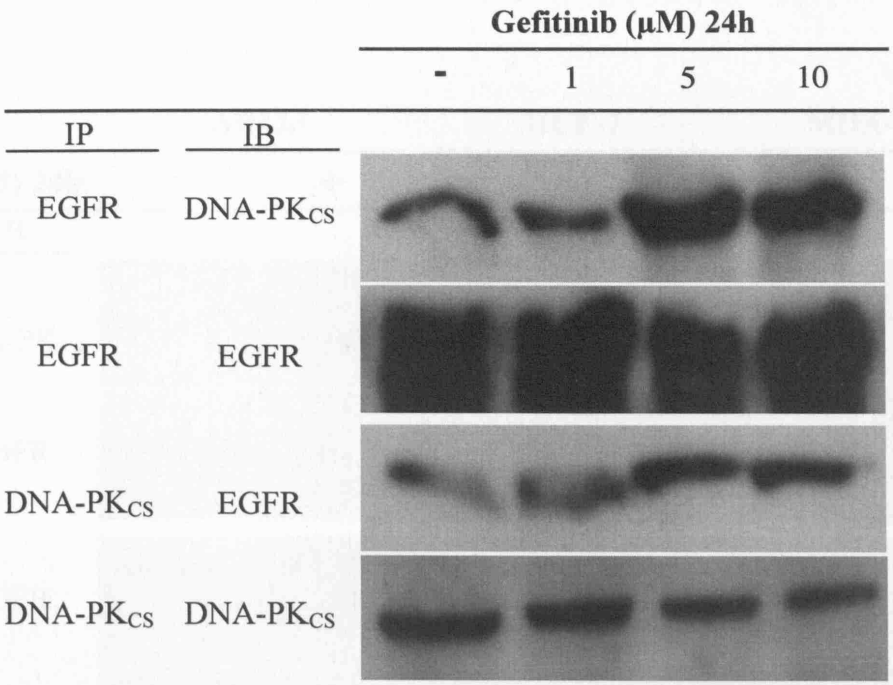

Figure 5.10: *Gefitinib dose-dependent induction of EGFR/DNA-PK$_{CS}$ association in MCF-7 cells*. Cells were treated with indicated concentrations of gefitinib for 24h. Lysates were immunoprecipitated (IP) with anti-EGFR or anti-DNA-PK$_{CS}$ antibody and then immunoblotted (IB) as described in figure.

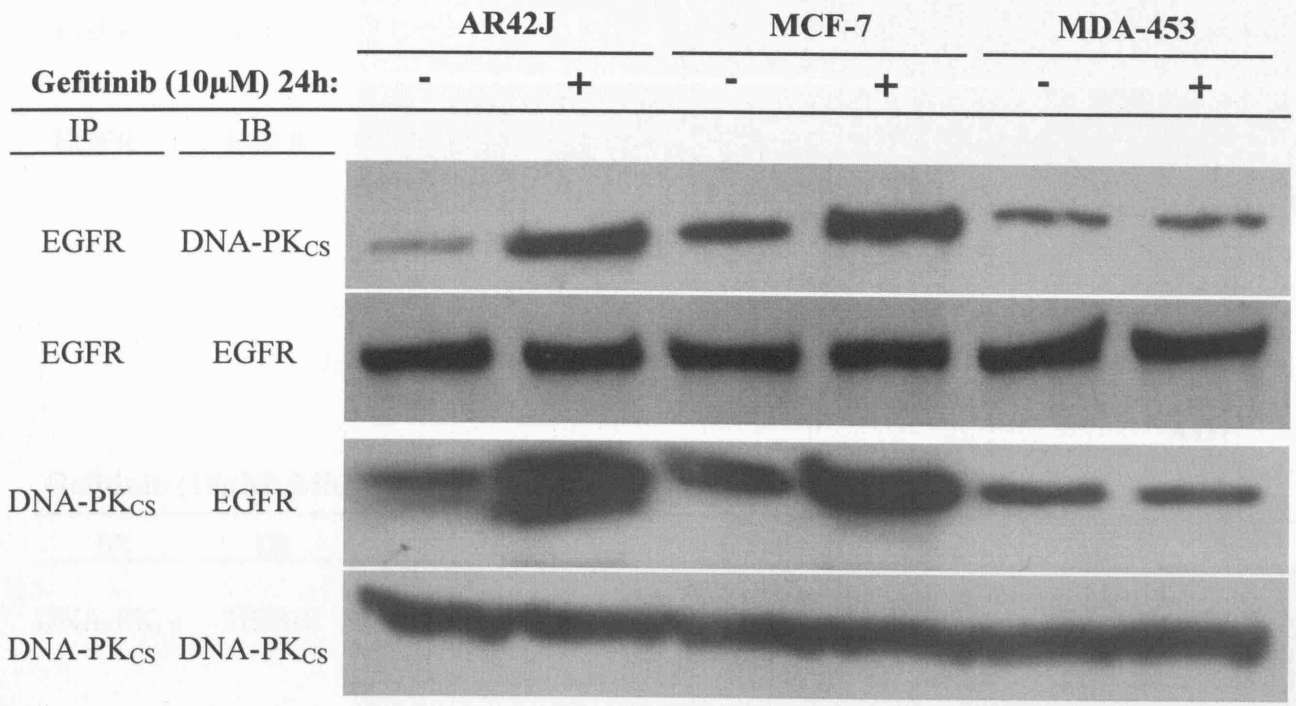

Figure 5.11: *Cell line specific gefitinib-induced EGFR/DNA-PK$_{CS}$ associations.* Cells were treated with gefitinib (10μM) for 24h. Lysates were immunoprecipitated (IP) with anti-EGFR or anti-DNA-PK$_{CS}$ antibody and then immunoblotted (IB) as described in figure.

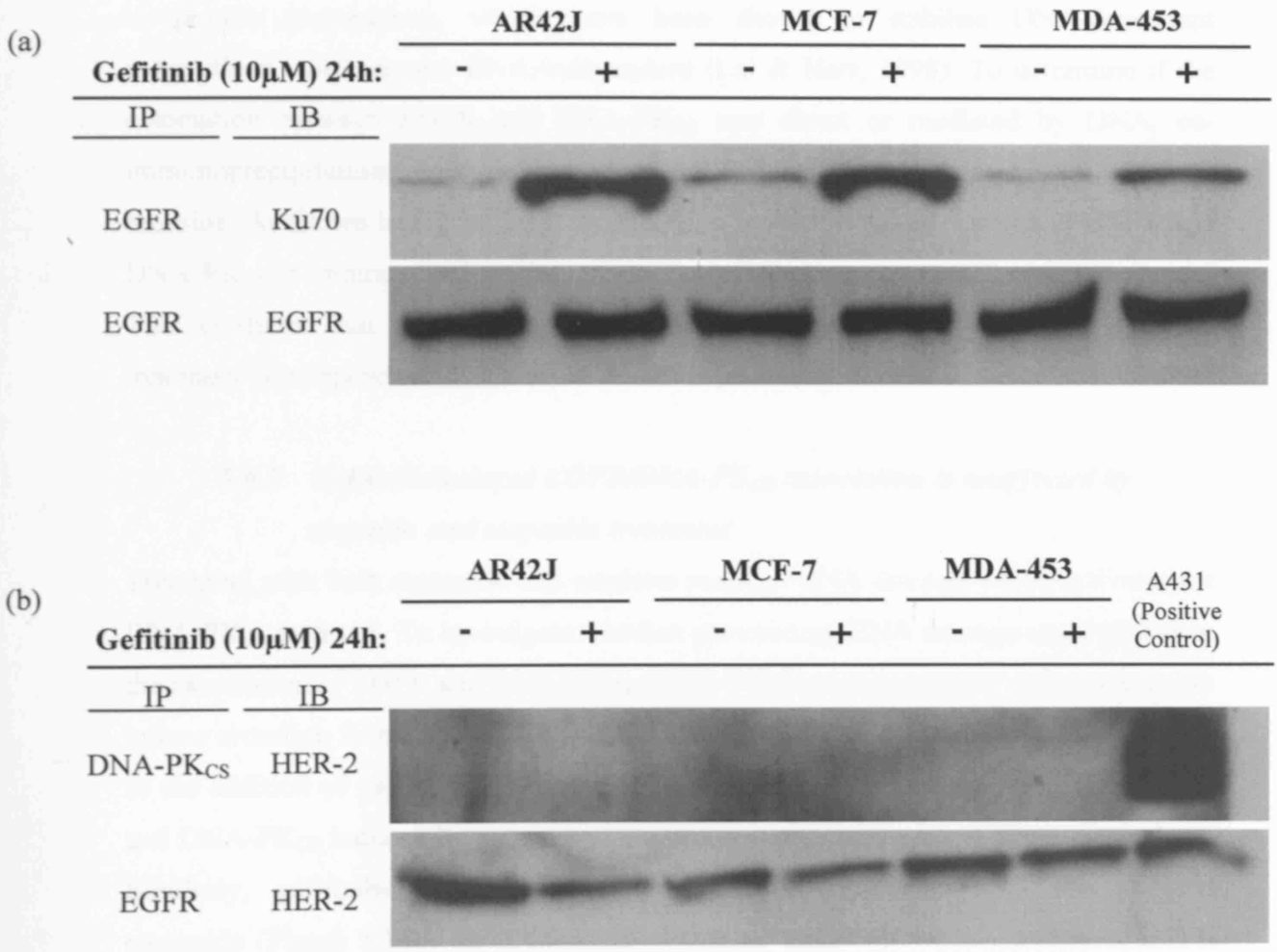

Figure 5.12: *Gefitinib-induced EGFR/Ku70 and DNA-PK$_{CS}$/HER-2 associations.* Cells were treated with gefitinib (10μM) for 24h. Lysates were immunoprecipitated (IP) with anti-EGFR or anti-DNA-PK$_{CS}$ antibody and then immunoblotted (IB) as described in figure.

5.6.1 Gefitinib-induced EGFR/DNA-PK$_{CS}$ association is DNA independent

The main functions of DNA-PK$_{CS}$ involve association with nuclear DNA. It was therefore possible that the immunoprecipitation results were due to contaminating DNA in protein preparations, which have been shown to stabilise DNA-dependent associations which appear DNA-independent (Lai & Herr, 1998). To determine if the association between EGFR and DNA-PK$_{CS}$ was direct or mediated by DNA, co-immunoprecipitations were performed on MCF-7 cell lysates treated with ethidium bromide. As shown in Figure 5.13, no alteration is seen in the association of EGFR and DNA-PK$_{CS}$ in immunoprecipitation experiments following ethidium bromide treatment. This confirms that the association of DNA-PK$_{CS}$ and EGFR following gefitinib treatment is independent of DNA.

5.6.2 Gefitinib-induced EGFR/DNA-PK$_{CS}$ association is unaffected by cisplatin and etoposide treatment

Treatment with both etoposide and cisplatin result in DNA damage which activates the DNA-PK$_{CS}$ pathway. To investigate whether pre-existing DNA damage could influence the association of EGFR and DNA-PK$_{CS}$, MCF-7 cells were incubated with cisplatin (to induce crosslink formation) and etoposide (to induce DNA double-strand breaks) prior to the addition of gefitinib. As shown in Figure 5.14a, increased association of EGFR and DNA-PK$_{CS}$ induced by gefitinib alone was not affected by the addition of cisplatin. Similarly, gefitinib-induced association remained unchanged with the addition etoposide (Figure 5.14b). In addition, there was no effect on the association of EGFR and DNA-PK$_{CS}$ following treatment with these agents alone.

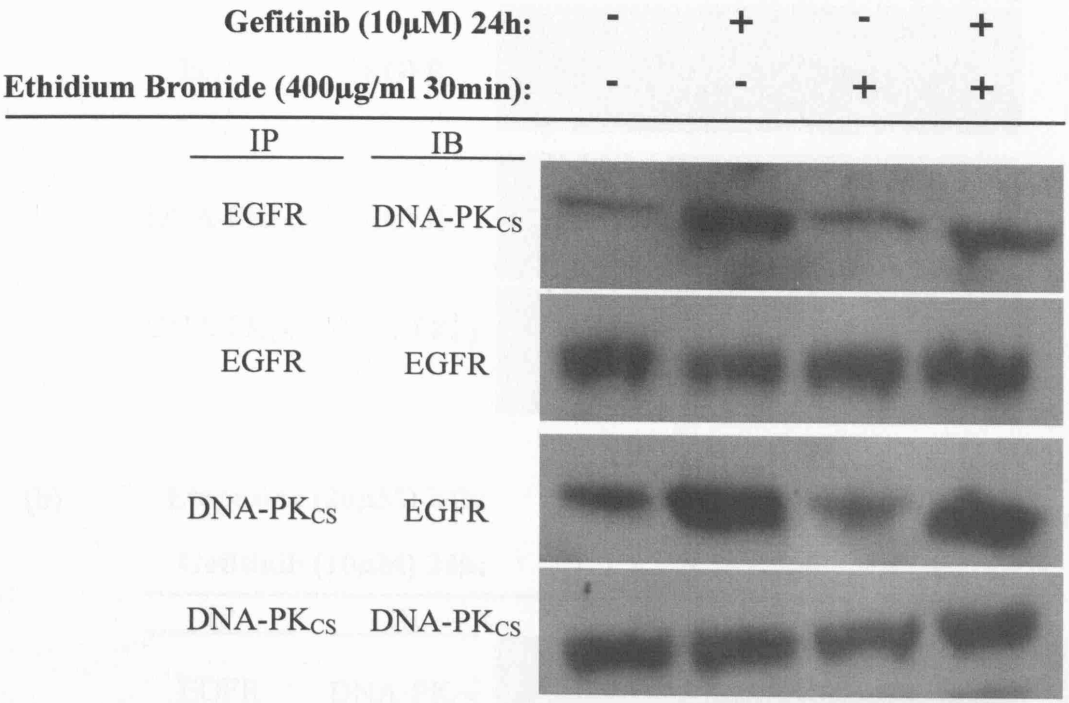

Figure 5.13: *Gefitinib-induced DNA-independent association of EGFR with DNA-PK in MCF-7 cells.* Cells were treated with gefitinib (10μM) for 24h and ethidium bromide (400μg/ml) for 30min. Lysates were immunoprecipitated (IP) with anti-EGFR or anti-DNA-PK$_{CS}$ antibody and then immunoblotted (IB) as described in figure.

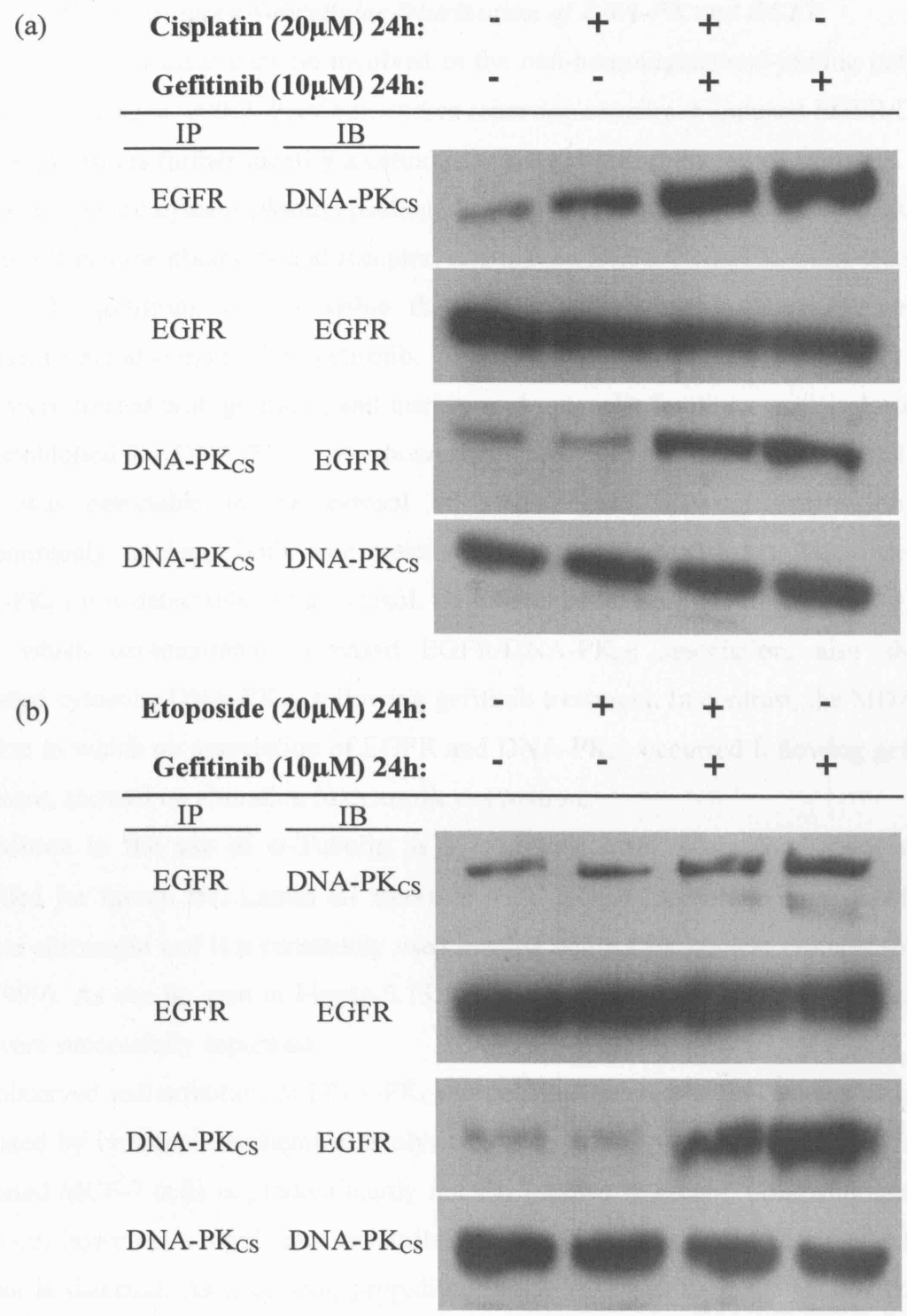

Figure 5.14: *Gefitinib-induced EGFR/DNA-PK$_{CS}$ association persists following chemotherapy treatment in MCF-7 cells.* Cells were treated with (a) cisplatin (20μM) or (b) etoposide (20μM) for 24h followed by gefitinib for 24h. Lysates were immunoprecipitated (IP) with anti-EGFR or anti-DNA-PK$_{CS}$ antibody and then immunoblotted (IB) as described in figure.

5.7 Gefitinib-Induced Subcellular Distribution of DNA-PK and EGFR

DNA-PK_{CS} is a nuclear enzyme involved in the non-homologous end-joining pathway (Khanna & Jackson, 2001). Previous studies reporting cetuximab-induced EGFR/DNA-PK_{CS} associations further identify a cetuximab-induced redistribution of DNA-PK from the nucleus to the cytosol (Bandyopadhyay *et al.*, 1998; Huang & Harari, 2000). Given that EGFR is a membrane-bound receptor, and that an EGFR/DNA-PK_{CS} association is induced by gefitinib, it is possible that similar alterations in DNA-PK cellular localisation are also induced by gefitinib.

Cells were treated with gefitinib, and nuclear and cytosolic fractions were isolated and immunoblotted for DNA-PK_{CS}. As shown in Figure 5.15, basal expression of DNA-PK_{CS} was detectable in the cytosol of MCF-7 cells although expression was predominantly nuclear. Following treatment with gefitinib (10μM) 24h, increased DNA-PK_{CS} was detectable in the cytosol. Cellular extracts from gefitinib-treated AR42J cells, which demonstrated increased EGFR/DNA-PK_{CS} association, also showed increased cytosolic DNA-PK_{CS} following gefitinib treatment. In contrast, the MDA-453 cell line in which no association of EGFR and DNA-PK_{CS} occurred following gefitinib treatment, showed no alteration in cytosolic expression.

In addition to the use of α-Tubulin as a loading control, blots were stripped and reprobed for Lamin B1. Lamin B1 interacts with nuclear membrane components and nuclear chromatin and is a commonly used loading control for nuclear proteins (Neri *et al.*, 1999). As can be seen in Figure 5.15, nuclear and cytosolic fractions for each cell line were successfully separated.

The observed redistribution of DNA-PK_{CS} in gefitinib-treated MCF-7 cells was further validated by immunohistochemical analysis (Figure 5.16). As expected, DNA-PK_{CS} in untreated MCF-7 cells is predominantly nuclear (shown in green). Following gefitinib treatment however, a significant redistribution of DNA-PK_{CS} from the nucleus to the cytosol is detected. As a control, propidium iodide (PI) was used for nuclear counter staining and is shown in blue.

Additionally, although EGFR is a membrane-associated glycoprotein, there are reports that EGFR is detectable in the nucleus and binds to DNA acting as a transcription factor (Lin *et al.*, 2001; Lo *et al.*, 2005a; Lo *et al.*, 2005b; Dittmann *et al.*, 2005a). Figure 5.17 shows the levels of EGFR expression in the nuclear and cytosolic fractions of MCF-7 cells following gefitinib treatment. As expected gefitinib causes a downregulation in

cytosolic EGFR as compared with control. Interestingly, whilst untreated cells show EGFR present in the nucleus, a decrease in nuclear EGFR is detected in cells exposed to gefitinib. Further experiments were performed using different time-points and doses of gefitinib treatments (Figure 5.18) in MCF-7 cells. Following treatment with gefitinib, there was decreased nuclear and increased cytosolic DNA-PK_{CS} detectable at 6 hours following gefitinib (10μM) treatment (Figure 5.18a). An effect on cellular distribution of DNA-PK_{CS} was found following treatment with gefitinib (5μM) (Figure 5.18b).

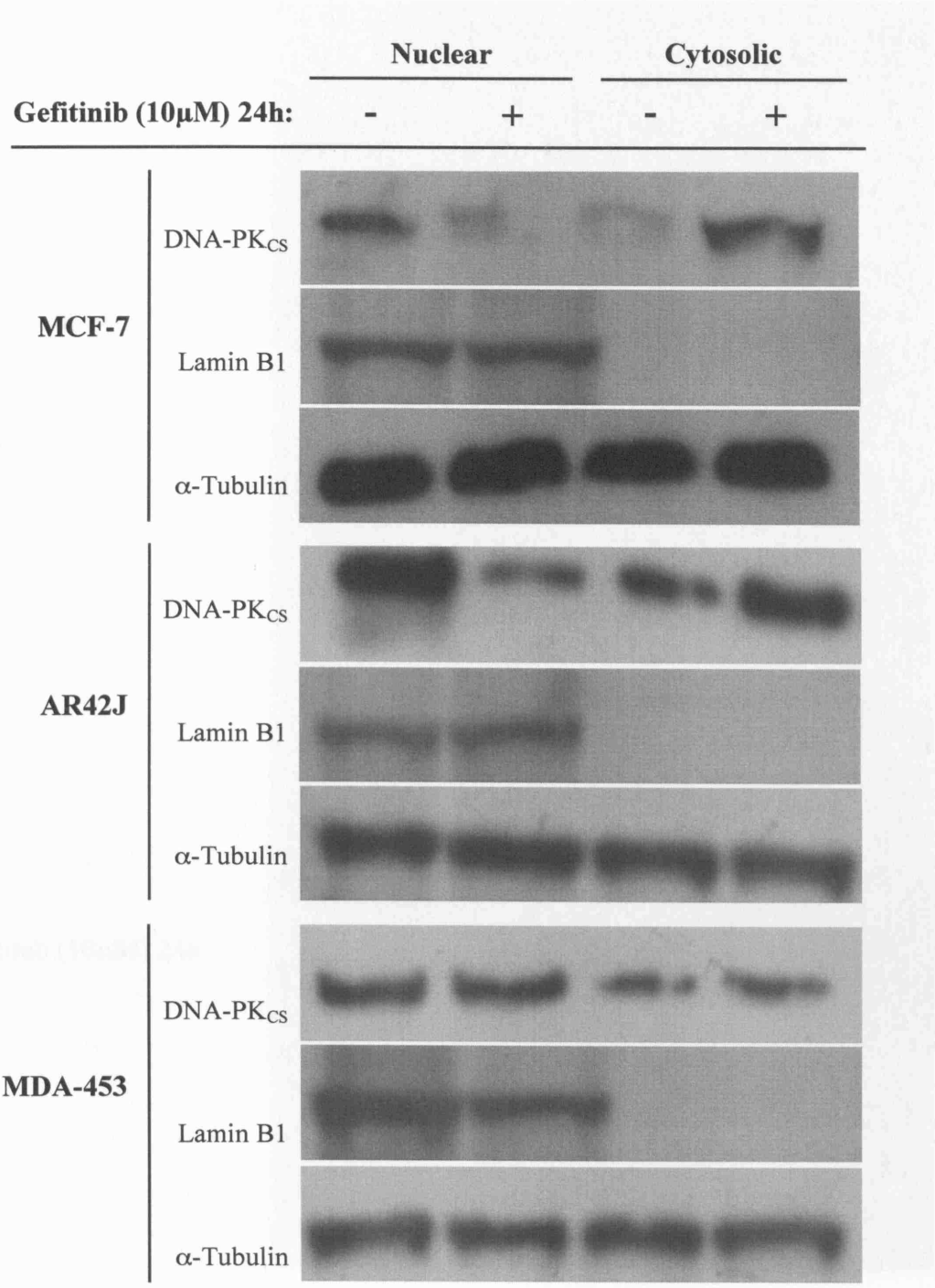

Figure 5.15: *Gefitinib-induced subcellular redistribution of DNA-PK in MCF-7 and AR42J cell lines.* Cells were treated with gefitinib (10μM) for 24h, lysed and separated into nuclear and cytosolic extracts using the Clontech TransFactor Extraction Kit. Lysates were immunoblotted with anti-DNA-PK$_{CS}$ antibody; Lamin B1 and α-Tubulin serve as loading controls.

Control

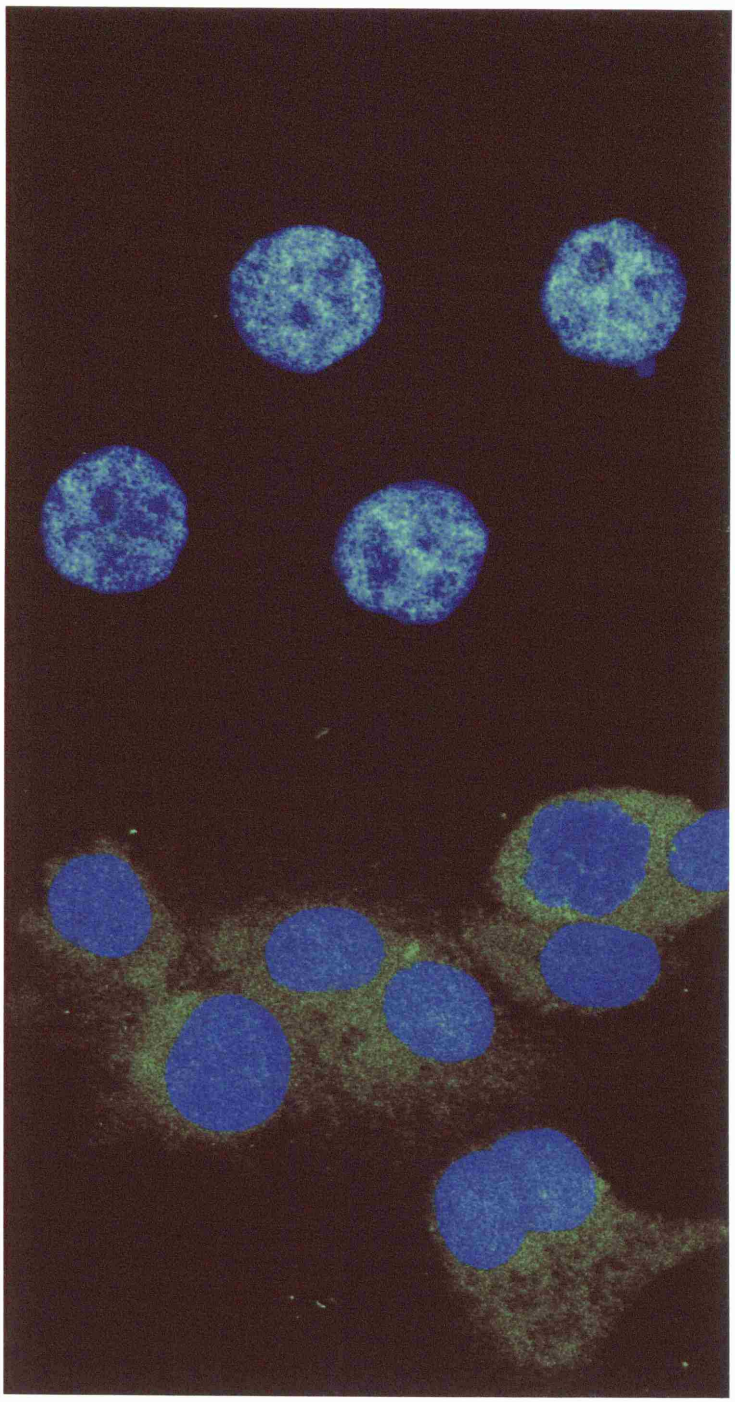

Gefitinib (10μM) 24h

Figure 5.16: *Immunohistochemical analysis of Gefitinib-induced subcellular redistribution of DNA-PK in MCF-7 cells.* Cells were treated with gefitinib (10μM) for 24h, fixed with acetone and methanol and permeablised. Cells were then probed for DNA-PK_{CS} using an anti-DNA-PK_{CS} antibody. Propidium iodide (PI) was used for nuclear counter staining. For detection appropriate fluorescently labelled secondary antibodies were used (PI: Blue; DNA-PK_{CS}: Green) images were obtained using confocal microscopy.

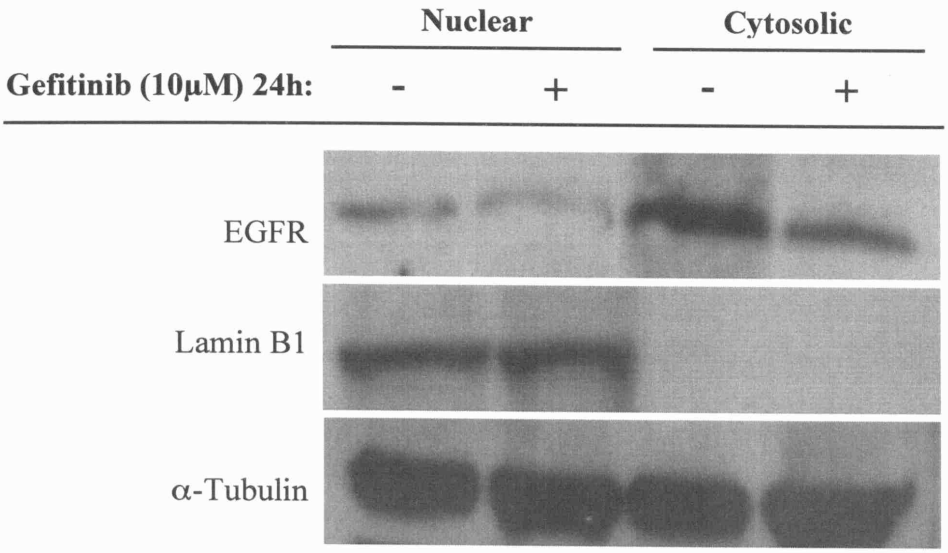

Figure 5.17: *Gefitinib-induced subcellular redistribution of EGFR in MCF-7 cells.* Cells were treated with gefitinib (10μM) for 24h, lysed and separated into nuclear and cytosolic extracts using the Clontech TransFactor Extraction Kit. Lysates were immunoblotted with anti-EGFR antibody; Lamin B1 and α-Tubulin serve as loading controls.

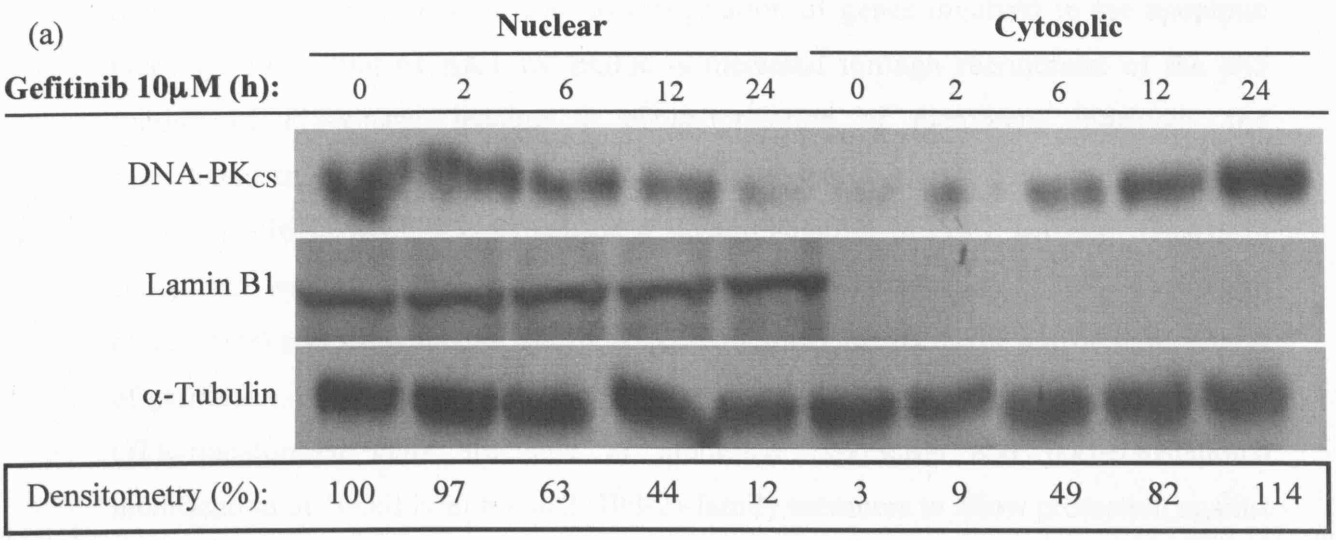

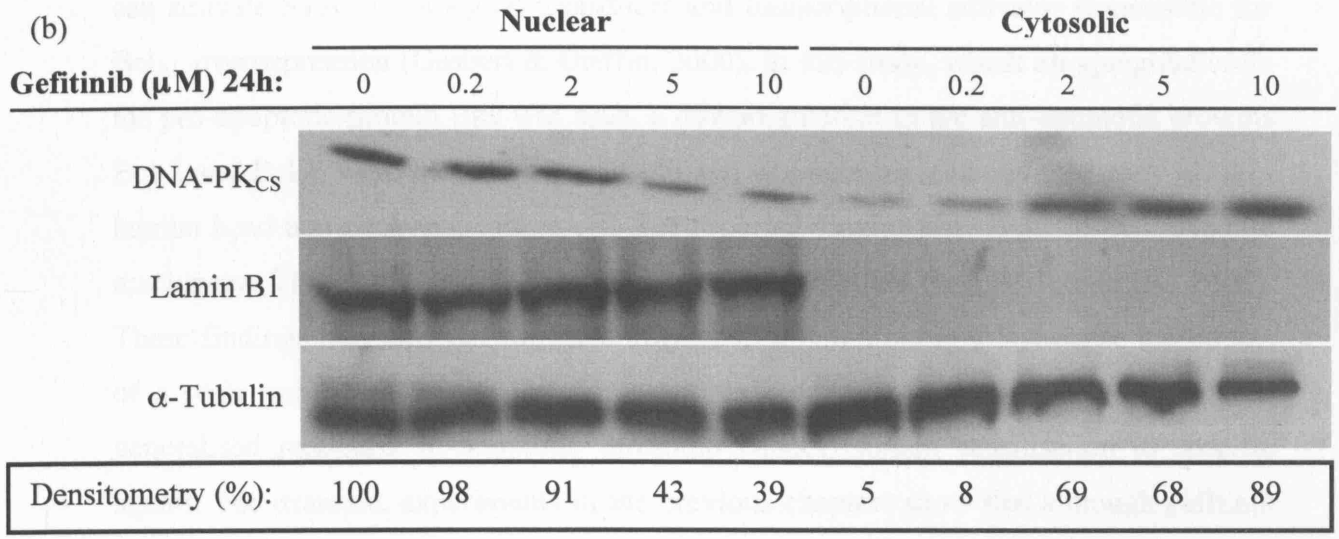

Figure 5.18: *Time- and dose-dependent gefitinib-induced subcellular redistribution of DNA-PK in MCF-7 cells.* (a) Cells were treated with gefitinib (10μM) for indicated lengths of time, lysed and separated into nuclear and cytosolic extracts using the Clontech TransFactor Extraction Kit. (b) Cells were treated with indicated concentrations of gefitinib for 24h, lysed and separated into nuclear and cytosolic extracts as before. Lysates were immunoblotted with anti-DNA-PK$_{CS}$ antibody; Lamin B1 and α-Tubulin serve as loading controls.

5.8 Discussion

Inhibition of EGFR by gefitinib sensitises cells to chemotherapy and radiation through reduction in cell proliferation and downregulation of genes involved in the apoptotic pathway. Activation of AKT by EGFR is mediated through recruitment of the p85 subunit of PI3-kinase, leading to phosphorylation of membrane inositides and recruitment and phosphorylation of AKT. Gefitinib treatment alone and in combination with cisplatin in MCF-7 cells caused a downregulation in AKT activity. This is in accordance with other similar studies (She *et al.*, 2003; Janmaat *et al.*, 2003; Campiglio *et al.*, 2004) and suggests that the PI3K/AKT pathway mediates the anti-tumour effects of gefitinib.

OTK-transformed cells are able to modulate expression and post-translational modification of B-cell lymphoma 2 (Bcl-2)-family members to allow protection against apoptosis. They can stimulate anti-apoptotic proteins such as Bcl_{XL} and Bcl-2 and inhibit the pro-apoptotic protein Bad and Bax (Skorski, 2002). BCR-ABL for example can activate STAT5 – a signal transducer and transcriptional activator responsible for Bcl_{XL} overexpression (Gesbert & Griffin, 2000). In this study, whilst no upregulation in the pro-apoptotic protein Bax was seen, a downregulation in the anti-apoptotic proteins Bcl-2 and Bcl_{XL} were induced by gefitinib and cisplatin respectively. A study using a human head and neck can cancer cell line reported similar alterations in the apoptotic machinery. This study also showed gefitinib to upregulate Bax (Magné *et al.*, 2003). These findings may account for the ability of EGFR inhibitors to synergise the effects of a wide variety of agents including cytotoxic drugs and irradiation. However the generalised reduction in apoptotic threshold cannot explain sensitisation to specific agents. For example, experiments in the previous chapters show that although gefitinib had a synergistic effect with etoposide, doxorubicin and cisplatin there was no effect with melphalan. The fact that sensitisation occurs with some but not all chemotherapeutic agents indicates that a generalised reduction in apoptotic threshold does not fully account for chemosensitisation.

Whilst cisplatin treatment had no effect on basal EGFR expression, it did induce EGFR tyrosine phosphorylation which is reversed when added in combination with gefitinib. Tyrosine 845 is positioned outside of the autophosphorylation domain and has been shown to be a target for Src kinase (Tice *et al.*, 1999). Cisplatin-induced upregulation of Tyr-845 specifically, suggests that Src mediates cisplatin-induced EGFR activation. It is

thought that phosphorylation of Tyr-845 stabilises the activation loop of EGFR, maintains the enzyme in the active state and provides a binding surface for protein substrates (Tice *et al.*, 1999). Furthermore, Src-dependent EGFR activation may also involve formation of multi-protein complexes and plays a major role in coupling various extracellular and intracellular signals to EGFR activation and to its downstream signalling pathways (Benhar *et al.*, 2002). EGFR activation was also triggered by melphalan with only a slight reversal by the addition of gefitinib. Nonetheless, this finding illustrates that EGFR activation is not unique to cisplatin and given that Benhar *et al.*, (2002), show similar effects for doxorubicin and camptothecin but not for vinblastine and paclitaxel, it supports the notion that a DNA damage signal activates a signalling pathway that culminates in EGFR activation. In addition, a recent study showed that cisplatin induced ERK and caspase-3 activation is EGFR and c-Src dependent (Arany *et al.*, 2004). It has also been reported that EGFR expression correlates with cisplatin resistance. Overexpression of the *EGFR* gene significantly enhances drug resistance, suggesting that EGFR may be one of the contributing factors that affect drug resistance of cancer cells (Park *et al.*, 2005).

In a previous study (Magné *et al.*, 2003) gefitinib was shown to reduce DNA-PK expression and was suggested as one of the explanatory phenomenon for the synergistic interaction between gefitinib and cisplatin, given that DNA repair is one of the biochemical modulators of cisplatin sensitivity (Perez, 1998; Jenson & Glazer, 2004). The effect of gefitinib-induced DNA-PK_{CS} downregulation persisting with cisplatin co-treatment was also found with melphalan. Therefore this cannot account for the lack of synergy found with gefitinib and melphalan. In another study, it has also been demonstrated that EGFR and DNA-PK activity are mutually regulated by each other (Um *et al.*, 2004). They show that treatment with the EGFR inhibitor PKI166, suppressed etoposide-induced activation of DNA-PK in metastatic melanoma cells.

In this chapter there is evidence that inhibition of EGFR by gefitinib induced a DNA-independent EGFR/DNA-PK_{CS} association in MCF-7 and AR42J cells but not in MDA-453 cells which express low EGFR levels. It will clearly be important to define the molecular basis of the interaction between EGFR and DNA-PK_{CS} and to investigate the reasons for the differences between cell lines. No association between DNA-PK_{CS} and HER-2 was detected indicating that the EGFR-DNA-PK_{CS} association does not additionally involve an interaction with HER-2.

DNA-PK$_{CS}$ has been reported to associate with another tyrosine kinase in response to DNA damage (Kumar *et al.*, 1998). Ionising radiation and certain other DNA-damaging agents activate the Src-like protein-tyrosine kinase Lyn, whereas DNA-PK requires double-stranded breaks for activation. Lyn associates constitutively with DNA-PK$_{CS}$ via an SH3 domain of Lyn interacting directly with DNA-PK$_{CS}$ near a leucine zipper homology domain. This inhibits DNA-PK$_{CS}$ activity and its ability to form a complex with Ku/DNA (Kumar *et al.*, 1998).

The major functions of DNA-PK$_{CS}$ have been localised to the nucleus (Peterson *et al.*, 1995). A study on radiation response following treatment of squamous cancer cells to the anti-EGFR antibody cetuximab, demonstrated inhibition of DNA repair and a redistribution of DNA-PK$_{CS}$ from nucleus to cytosol. It should be noted that the effect of cetuximab treatment alone was not included (Huang & Harari, 2000). Given that the majority of EGFR is extra-nuclear, and that an EGFR/DNA-PK$_{CS}$ association is also induced by gefitinib, it is possible that similar alterations in DNA-PK cellular localisation are also induced. Indeed, a study of squamous cancer cell lines suggested that there was altered distribution of DNA-PK$_{CS}$ following radiation and gefitinib treatment (Shintani *et al.*, 2003). As in the study with cetuximab, the effects of gefitinib treatment alone were not included and, unusually, DNA-PK$_{CS}$ was not detectable in the nucleus in untreated cells.

The experiments done in this study suggest that there is a strong effect of gefitinib treatment on DNA-PK$_{CS}$ cellular localisation and this is likely to be a factor in the inhibition of cellular DNA-PK activity. Coupled with this is a reduction in DNA-PK$_{CS}$ expression following gefitinib treatment in MCF-7 cells. The results from the MDA-453 cells differed from MCF-7 and AR42J cells in that increased association of EGFR and DNA-PK$_{CS}$ and increased cytosolic DNA-PK$_{CS}$ did not occur following gefitinib treatment.

The functional significance of cytosolic DNA-PK$_{CS}$ remains unclear. Importantly, recent studies have identified DNA-PK as a kinase activating AKT (Feng *et al.*, 2004; Dragoi *et al.*, 2005). DNA-PK$_{CS}$ was shown to be co-localised with AKT at the plasma membrane, and phosphorylated AKT on Ser-473 resulting in a ~10-fold enhancement of activity. Furthermore, DNA-PK$_{CS}$ association with AKT triggers transient nuclear translocation of AKT. These findings provide important evidence that DNA-PK$_{CS}$ can be functionally active within the cytosol and indicate the importance of DNA-PK not

only in the response to DNA repair but also in modulation of the PI3-kinase pathway. It is plausible to suggest that interactions of EGFR and DNA-PK_{CS} may have major significance in determining cellular response to EGFR inhibition.

There has been a considerable focus on the possibility that the plasma membrane contains lipid 'rafts,' microdomains enriched in detergent-insoluble cholesterol and sphingolipid complexes. It has been suggested that such rafts could play important roles in many cellular processes including signal transduction, membrane trafficking, cytoskeletal organisation, and pathogen entry (Munro, 2003). Interestingly, there is evidence for the cytosolic localisation of DNA-PK in lipid rafts (Lucero *et al.*, 2003). This is not a characteristic of all DNA repair proteins and differential protein phosphorylation patterns dependent on DNA-PK_{CS} are induced by ionising radiation. This localisation in lipid rafts may be critical in the initiation and organisation of intracellular signalling cascades. EGFR has also been demonstrated to be sequestered in cholesterol-bound lipid rafts (Chen *et al.*, 2002; Westover *et al.*, 2003). This association results in negative regulation in the form of altered tyrosine phosphorylation and kinase activity. It would be interesting to investigate whether gefitinib treatment results in the localisation of DNA-PK_{CS} to lipid rafts.

Nitric oxide synthase (NOS) activity has been detected in many human tumours (Jenkins *et al.*, 1994; Zhao *et al.*, 1998) and has been shown to significantly increase expression of DNA-PK_{CS} thus protecting cells from the toxic effects of NO and DNA-damaging agents such as cisplatin (Xu *et al.*, 2000). In addition and as shown with MCF-7 cells here, EGFR exists in the nucleus of highly proliferative cells. In the nucleus, EGFR has been shown to function as a transcription factor (Lin *et al.*, 2001). Expression of nuclear EGFR was shown to correlate positively with increased levels of cyclin D1 and Ki67, both of which are indicators of cell proliferation (Lo *et al.*, 2005a). EGFR itself lacks a DNA binding domain and therefore may require a DNA binding transcription cofactor. Interestingly, it has recently been reported that EGFR physically interacts with signal transducers and activators of transcription 3 (STAT3) in the nucleus, leading to transcriptional activation of inducible NOS (iNOS) (Lo *et al.*, 2005b). Furthermore, both ionising radiation and cisplatin trigger increased EGFR translocation into the nucleus (Dittmann *et al.*, 2005a). During this process, the Ku70/80 subunits and the phosphatase PP1 are transported into to the nucleus resulting in increased DNA-PK activity and subsequent DNA repair (Dittmann *et al.*, 2005a).

Inhibition of EGFR with cetuximab was shown to block EGFR import and radiation-induced activation of DNA-PK and immobilise an EGFR/DNA-PK complex in the cytoplasm (Dittmann *et al.*, 2005b). In this study, MCF-7 cells exposed to gefitinib also caused a decrease in nuclear EGFR levels. This data suggests a novel function of EGFR during DNA repair processes. Surprisingly, studies have shown insufficient suppression of STAT3 by gefitinib (Albanell *et al.*, 2001; Lo *et al.*, 2005b). This is probably due to the fact that STAT3 is constitutively activated in many human cancers and can take place in both EGFR-dependent and -independent fashions (Siuranpong *et al.*, 2003). In breast cancer, Src and Jaks contribute to the EGFR-independent activation of STAT3 (Garcia *et al.*, 2003). It is therefore possible that the combining of anti-EGFR and anti-Jak/STAT3 agents would result in a better therapeutic effect.

5.8.1 Conclusions

This chapter shows that interactions between EGFR and the DNA-PK pathway contribute towards cellular sensitisation to cisplatin following gefitinib treatment. This is demonstrated by the cellular redistributions of EGFR and DNA-PK following gefitinib treatment and by the co-localisation of EGFR and DNA-PK induced by gefitinib. These observations suggest a possible role of EGFR signalling in maintenance of the nuclear levels of DNA-PK_{CS}, and interference in EGFR signalling may possibly result in the impairment of DNA repair in the nuclei in gefitinib treated cells.

CHAPTER 6

MODULATION OF THE DNA-DEPENDENT PROTEIN KINASE PATHWAY BY GEFITINIB

6.1 Introduction

The results of the experiments in the previous chapter demonstrate that interactions between EGFR and the DNA-PK pathway contribute towards cellular sensitisation to conventional chemotherapy following gefitinib treatment.

Phosphatidylinositol 3'-Kinases are activated by a wide range of cell surface receptors to generate the lipid second messengers phosphatidylinositol 3,4-bisphosphate (PIP2) and phosphatidylinositol 3,4,5-trisphosphate (PIP3). These lipids regulate a diverse array of physiological processes including glucose homeostasis, cell growth, differentiation, and motility (Katso *et al.*, 2001). These distinct functions are carried out by a family of eight related PI3-Kinases in vertebrates possessing unique substrate specificities, localisation, and modes of regulation (Katso *et al.*, 2001). These include the Class IA PI3-Kinases (p110α, p110β, p110δ) which are activated by receptor tyrosine kinases such as EGFR and the class IB PI3-Kinase (p110γ), which is activated by heterotrimeric G-proteins (Stein, 2001). Despite these known differences in upstream activation, the physiological roles of individual PI3-Kinase isoforms remain largely unassigned, and determining the unique functions of members of this family is a major focus of ongoing investigation (Knight *et al.*, 2004).

As has been discussed in Chapter 1, DNA-PK_{CS} is a 'PI3-Kinase-like protein kinase' or PIKK. The mammalian members of this family, at present, include five additional protein kinases namely, ATM, ATR, ATX/SMG-1, mTOR/FRAP and TRRAP (Vanhaesebroeck *et al.*, 2001). These protein kinases when activated by various stresses phosphorylate key proteins in the corresponding response pathways. Four mammalian PIKKs are known to be involved in the DNA-damage response: DNA-PK, ATM, ATR and ATX (Shiloh, 2003). Whereas ATM and DNA-PK respond primarily to DSBs, ATR and ATX respond to both ultraviolet (UV) light damage (possibly UV-light-induced replication arrest) and DSBs, and ATR also responds to stalled replication forks (Khanna & Jackson, 2001; Shiloh, 2003). Furthermore, it has been shown that DNA-PK plays a vital role in cellular responses to radiation-induced damage (Marples *et al.*, 2002; Dittmann *et al.*, 2005a) and components of the DNA-PK complex are upregulated in cancer cells (Wilson *et al.*, 2000; Zhao *et al.*, 2000; Shintani *et al.*, 2003). These findings highlight the potential of the DNA-PK pathway as an attractive molecular target.

6.1.1 Inhibition of PI3-Kinase Related Kinases

Wortmannin and LY294002 are the two most widely used cell-permeable, low molecular weight, non-selective inhibitors of PI3-Kinase related kinases (Figure 6.1). Both compounds inhibit ATP binding within the catalytic site of DNA-PK_{CS} through different modes of action (Rosenzweig *et al.*, 1997; Sarkaria *et al.*, 1998; Izzard *et al.*, 1999; Vanhaesebroeck *et al.*, 2001).

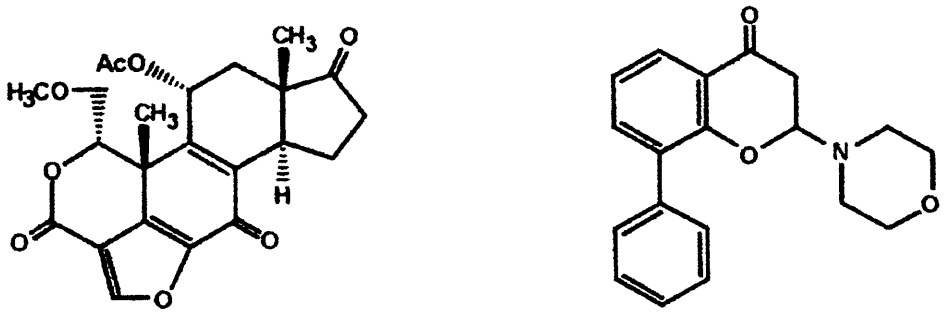

Wortmannin LY294002

Figure 6.1: Chemical structures of the PI3K inhibitors wortmannin and LY294002.

Wortmannin is a non-competitive, general inhibitor of PI3-Kinases with an IC_{50} in the nanomolar range for DNA-PK_{CS} inhibition (Sarkaria *et al.*, 1998; Izzard *et al.*, 1999; Stein, 2001). It inhibits DNA-PK through an irreversible alkylation of lysine 802, which is positioned in the active site and is critical for the phosphate transfer reaction (Collis *et al.*, 2005). Wortmannin does however possess undesirable properties, such as a relatively short half-life, an insolubility in aqueous solutions and *in vivo* toxicity (Vanhaesebroeck *et al.*, 2001).

LY294002 is a flavonoid-based synthetic compound that is structurally unrelated to wortmannin. It too is a non-competitive inhibitor of PI3-Kinases, with an IC_{50} in the low micromolar range for DNA-PK_{CS} (Izzard *et al.*, 1999; Stein, 2001). LY294002 is able to inhibit PI3K-mediated Ras signalling (Liang *et al.*, 2003) and so has been assessed for anti-tumour effects *in vivo* (Edwards *et al.*, 2002; Gupta *et al.*, 2003). These studies investigated the effects of LY294002 alone and in combination with radiation. Although these *in vivo* studies demonstrated the potential of LY294002 to sensitise cells to radiation, its relative instability, quick metabolic clearance and *in vivo* toxicity make its clinical evaluation in humans unfeasible (Collis *et al.*, 2005). However, the basic chemical structure of LY294002 has offered a lead compound upon which more potent

novel inhibitors can be developed that possess more desirable properties to aid their future assessment (Knight *et al.*, 2004).

The purposes of the experiments presented in this chapter are to further characterise the effects of gefitinib-induced inhibition of EGFR on the DNA-dependent protein kinase pathway and its contribution towards cellular sensitisation to conventional chemotherapy. To this end, the following questions are addressed:

6.1.2 Aims

1. Does gefitinib treatment inhibit DNA-PK functional activity?
2. Does inhibition of the PI3-Kinase pathway with LY294002 or wortmannin mimic the effects of gefitinib on chemosensitivity?
3. Does inhibition of DNA-PK_{CS} by RNA interference mimic the effects of gefitinib on chemosensitivity?

6.2 *Inhibition of DNA-PK Functional Activity by Gefitinib*

To investigate whether gefitinib treatment directly affects the functional activity of DNA-PK, the SignaTECT® DNA-Dependent Protein Kinase Assay System was used on cellular extracts (see Chapter 2 for details). It utilises the unique SAM^{2TM} Biotin Capture Membrane and overcomes the problem of non-specific substrate binding by using a biotinylated DNA-PK p53-derived peptide substrate. A preliminary experiment was done on MCF-7 cells exposed to gefitinib for 24h (Figure 6.2). Cells exposed to gefitinib at 10μM showed a 35.5±2.1% decrease in DNA-PK functional activity. This increased to 41.3±4.6% for gefitinib at 20μM. As an example, Figure 6.2a illustrates a visual representation for samples of an individual experiment spotted onto squares of SAM^{2TM} Membrane and exposed to film for 24h. For accurate determination of specific activity, SAM^{2TM} Membrane squares were analysed by scintillation counting.

The dose- and time-dependent inhibition of DNA-PK activity by gefitinib on MCF-7 cells was assessed and is shown in Figure 6.3. Gefitinib 0.2μM treatment had no effect on DNA-PK activity over a 48h period. However, cells exposed to gefitinib at 2μM inhibited DNA-PK activity by 18.3±2.4% after 24h. Gefitinib treatment at 10μM, the optimal dose for a good synergistic interaction with chemotherapeutic agents, inhibited activity by 9.1±0.8% after 12h which increased to 32.2±5.1% after 24h and to 43.2±4.6% after 48h. Cells exposed to gefitinib at 20μM, inhibited DNA-PK activity by 41.7±0.2% after 24h and to 53±1.0% after 48h. Thus, concentrations of gefitinib which synergistically inhibit cell proliferation also significantly inhibit DNA-PK activity.

To determine if the inhibitory effects of gefitinib on DNA-PK activity could be found with other cell lines, extracts from the rat pancreatic AR42J cancer cell line were analysed. This demonstrated comparable results with a 46.5±1.1% decrease in activity following a gefitinib (10μM) 24h treatment (Figure 6.4a). In contrast, the effects of gefitinib treatment on the human breast MDA-453 cell line showed only a minimal reduction in DNA-PK activity (~20%) (Figure 6.4b).

Figure 6.5 shows the effects on DNA-PK activity as a result of EGFR inhibition by matuzumab, in MCF-7 cells. Cells exposed to matuzumab (10μg/ml) showed inhibition of DNA-PK activity after 48h (25.8%±0.1). Matuzumab at 20μg/ml inhibited DNA-PK functional activity by 32.5±2.3% after 24h and by 34.2±3.9% after 48h.

(a)

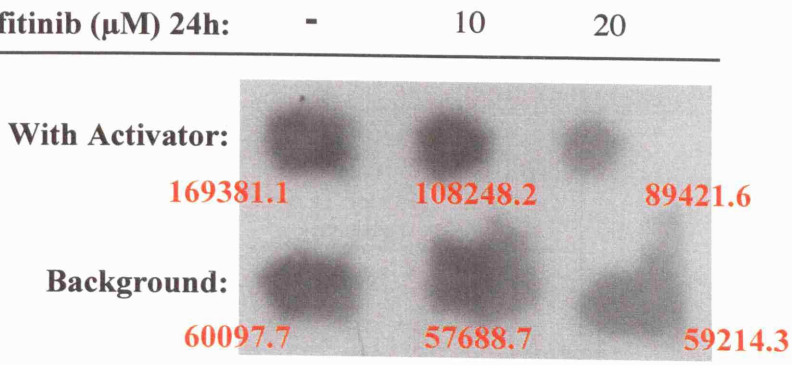

(b)

Gefitinib (μM) 24h	μg of Protein in Reaction	Cpm (Reaction with activator)	Cpm (Background)	Specific Activity (cpm/pmol)	DNA-PK Enzyme Activity (pmol ATP/min/μg protein)	% of Control
-	65.25	164564.5	56448.4	493.69	12.59	100
10	69.25	106377.6	58411.3	319.13	8.13	64.6
20	68	97487.5	59874.7	292.46	7.09	56.3

(c)

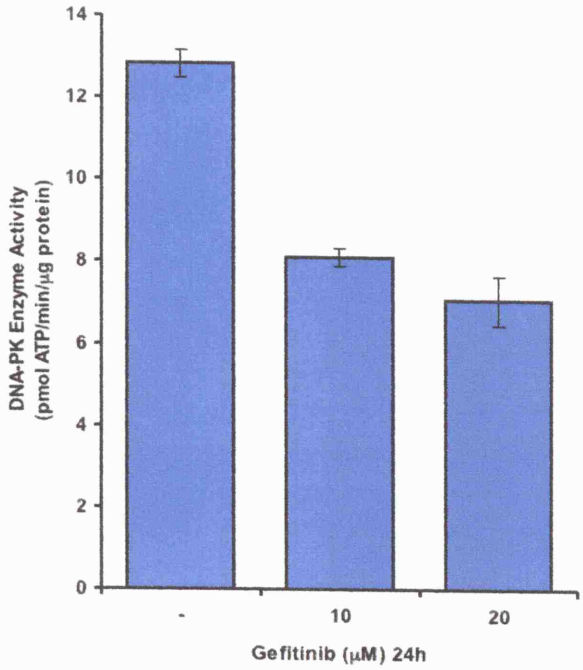

Figure 6.2: *Gefitinib-induced inhibition of DNA-PK functional activity in MCF-7 cells.* Cells were treated with gefitinib (10 or 20μM) for 24h and lysed. DNA-PK activity was measured using the Promega SignaTECT® DNA-PK assay system. (a) A visual, non-mathematical representative of [γ-^{32}P]ATP-incorporated active DNA-PK for a single experiment. (b) and (c) Determination of specific enzymatic activity of DNA-PK. Data is an average of three independent experiments; error bars, SD.

MCF-7 Cells		
Gefitinib Treatment	**DNA-PK Enzyme Activity (pmol ATP/min/µg protein)**	**% of Control**
-	12.27	100
(0.2µM) 6h	11.98	97.6
(0.2µM) 12h	11.14	90.8
(0.2µM) 24h	12.48	101.7
(0.2µM) 48h	11.89	96.9
(2µM) 6h	11.97	97.6
(2µM) 12h	11.61	94.6
(2µM) 24h	10.02	81.7
(2µM) 48h	10.10	82.3

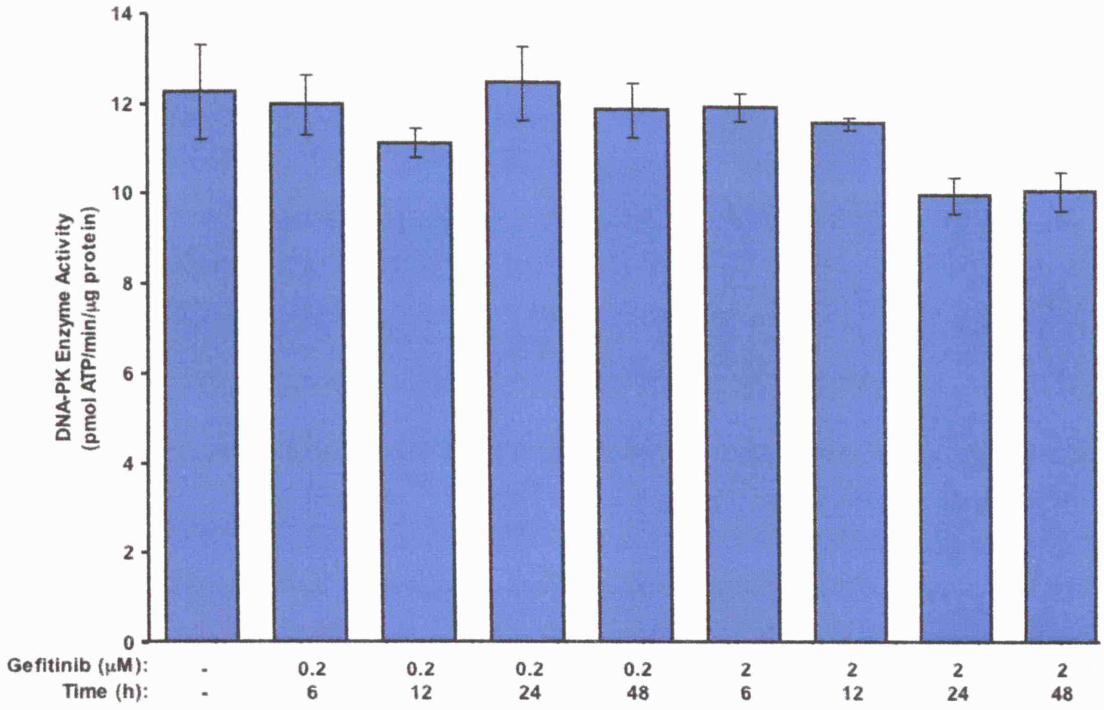

MCF-7 Cells		
Gefitinib Treatment	**DNA-PK Enzyme Activity (pmol ATP/min/µg protein)**	**% of Control**
-	12.52	100
(10µM) 6h	11.45	91.5
(10µM) 12h	11.38	90.9
(10µM) 24h	8.49	67.8
(10µM) 48h	7.11	56.8
(20µM) 6h	11.8	94.2
(20µM) 12h	9.78	78.1
(20µM) 24h	7.3	58.3
(20µM) 48h	5.89	47

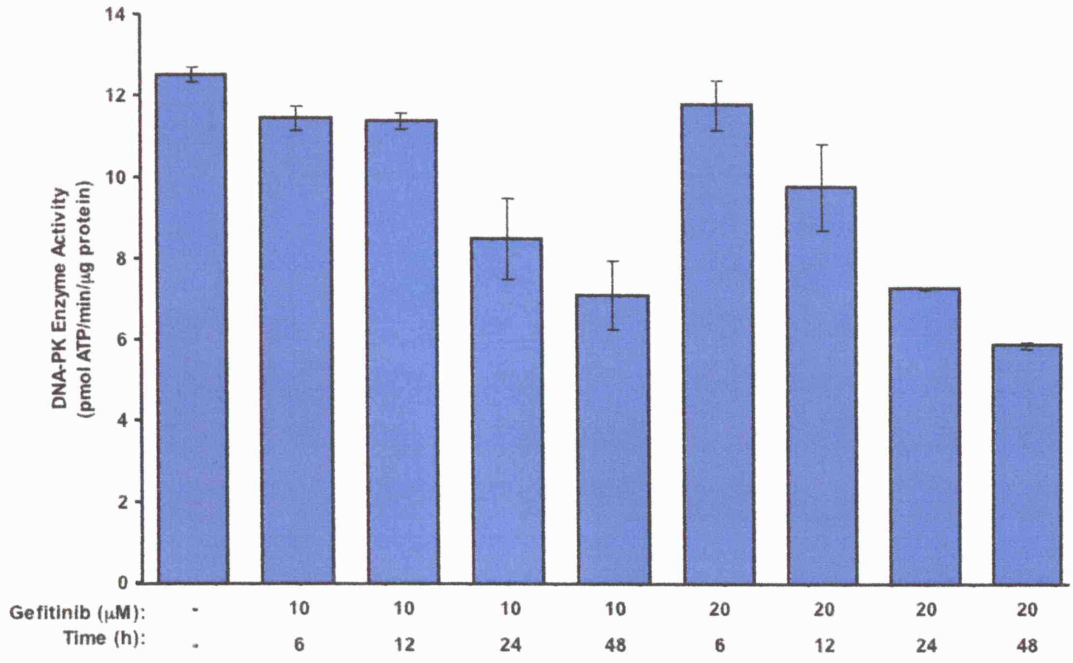

Figure 6.3: *Dose- and time-dependent gefitinib-induced inhibition of DNA-PK functional activity in MCF-7 cells.* Cells were treated with indicated concentrations of gefitinib and for indicated lengths of time. DNA-PK activity was measured using the Promega SignaTECT® DNA-PK assay system and the DNA-PK specific enzymatic activity determined. Data is an average of three independent experiments; error bars, SD.

(a)

AR42J Cells		
Gefitinib Treatment	**DNA-PK Enzyme Activity (pmol ATP/min/µg protein)**	**% of Control**
-	12.96	100
(5µM) 6h	11.89	91.7
(5µM) 12h	11.91	91.9
(5µM) 24h	10.05	77.5
(5µM) 48h	6.82	52.6
(10µM) 6h	11.58	89.4
(10µM) 12h	10.61	81.9
(10µM) 24h	6.94	53.5
(10µM) 48h	6.71	51.8
(20µM) 6h	11.56	89.2
(20µM) 12h	10.08	77.8
(20µM) 24h	5.93	45.8
(20µM) 48h	5.35	41.3

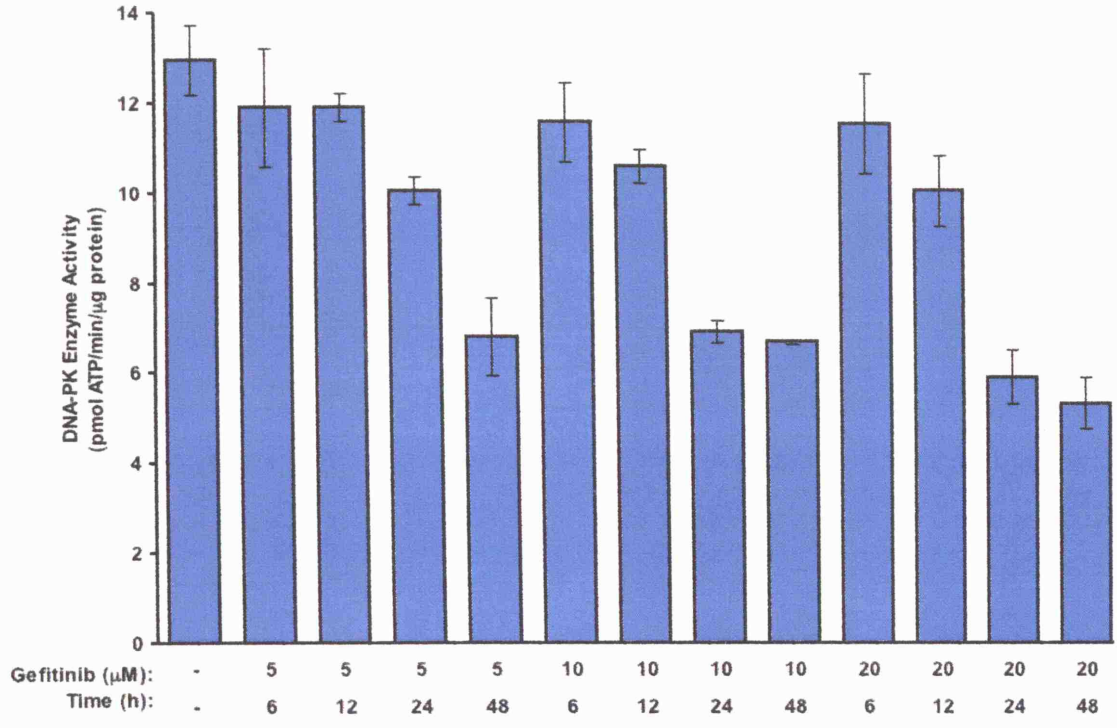

(b)

MDA-453 Cells		
Gefitinib Treatment	**DNA-PK Enzyme Activity (pmol ATP/min/µg protein)**	**% of Control**
-	12.56	100
(10µM) 6h	12.64	100.6
(10µM) 12h	11.33	90.2
(10µM) 24h	11.83	94.2
(10µM) 48h	10.04	80
(20µM) 6h	12.17	96.9
(20µM) 12h	11.86	94.4
(20µM) 24h	10.63	84.6
(20µM) 48h	10.51	83.7

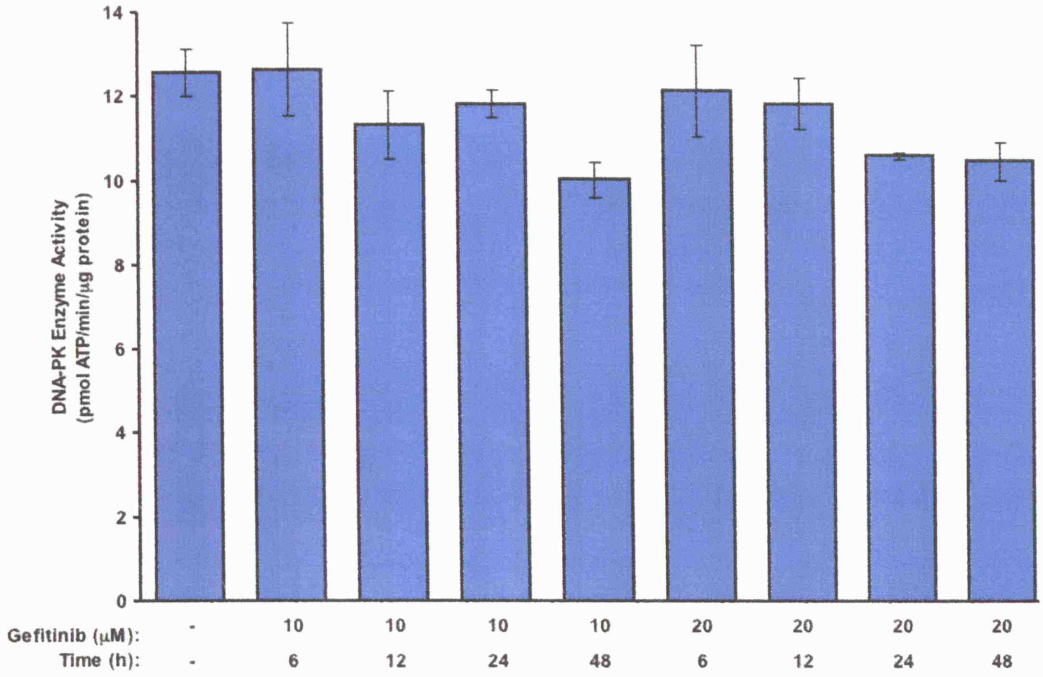

Figure 6.4: *Cell line specific gefitinib-induced inhibition of DNA-PK functional activity.* (a) AR42J and (b) MDA-453 cells were treated with indicated concentrations of gefitinib and for indicated lengths of time. DNA-PK activity was measured using the Promega SignaTECT® DNA-PK assay system and the DNA-PK specific enzymatic activity determined. Data is an average of three independent experiments; error bars, SD.

MCF-7 Cells		
Matuzumab Treatment	**DNA-PK Enzyme Activity (pmol ATP/min/µg protein)**	**% of Control**
-	11.74	100
(10µg/ml) 6h	11.49	97.8
(10µg/ml) 12h	11.05	94.1
(10µg/ml) 24h	9.84	83.8
(10µg/ml) 48h	8.72	74.2
(20µg/ml) 6h	12.39	105.5
(20µg/ml) 12h	11.5	97.6
(20µg/ml) 24h	7.92	67.5
(20µg/ml) 48h	7.72	65.8

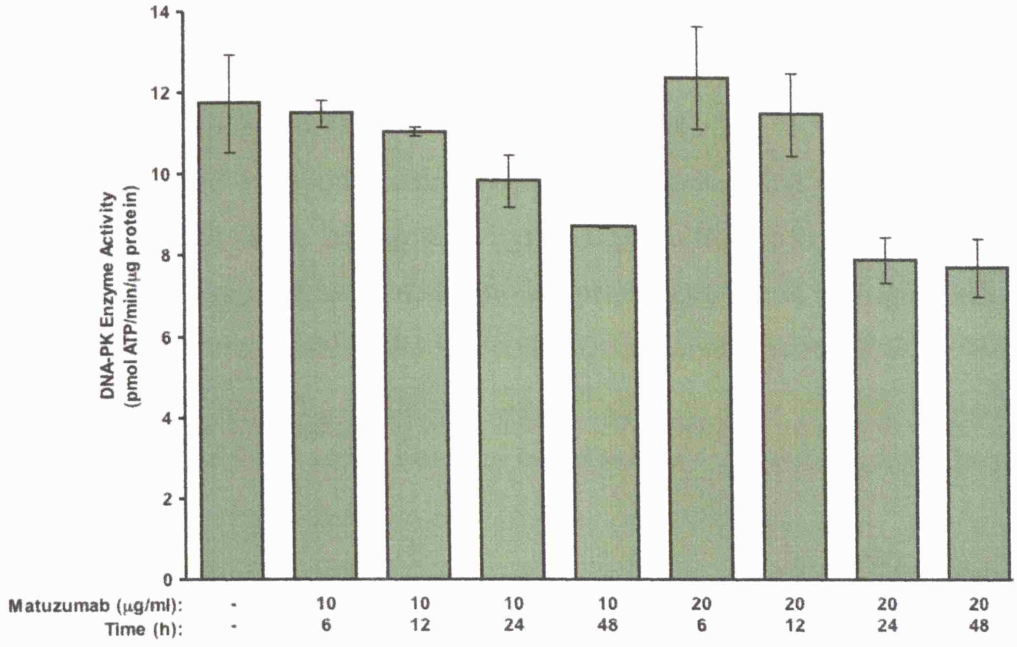

Figure 6.5: *Matuzumab-induced inhibition of DNA-PK functional activity in MCF-7 cells.* Cells were treated with matuzumab (10 or 20µg/ml) for indicated lengths of time and lysed. DNA-PK activity was measured using the Promega SignaTECT® DNA-PK assay system and the DNA-PK specific enzymatic activity determined. Data is an average of three independent experiments; error bars, SD.

6.3 *Inhibition of the Phosphoinositide 3'-Kinase Pathway and Chemosensitivity in MCF-7 Cells*

The PI3-kinase pathway has been implicated in the repair of cisplatin and etoposide-induced DNA lesions (Boulton *et al.*, 2000; Xu *et al.*, 2000). To investigate whether the inhibition of repair found with gefitinib could be mediated through this pathway, MCF-7 cells were exposed to the PI3-kinase inhibitor LY294002. Synergy was demonstrated in an SRB assay on MCF-7 cells treated with cisplatin in combination with LY294002 (Figure 6.6a). The IC_{50} for cells treated with cisplatin and LY294002 was 0.25±0.04μM, comparable to the combination of cisplatin and gefitinib (0.21±0.003μM). Experiments in which cells were exposed to the combination of gefitinib, LY294002 and cisplatin did not result in additional inhibition of cellular proliferation with an IC_{50} of 0.20±0.05μM. Interestingly, as with gefitinib, there was no demonstrable synergy for the combination of LY294002 and melphalan (Figure 6.6b).

To determine if inhibition of the PI3-kinase pathway resulted in effects on DNA repair, comet assays were performed on cells following exposure to cisplatin and LY294002. A delay in repair of the cisplatin-induced ICLs was found with kinetics comparable to that found on exposure to gefitinib and cisplatin. The addition of gefitinib to the combination of cisplatin and LY294002 did not further alter the extent of DNA ICL formation or the time course for DNA repair (Figure 6.7a). These results suggest that the inhibition of repair of cisplatin-induced DNA lesions by gefitinib and LY294002 may occur through the same pathway. As previously found with gefitinib, exposure of cells to melphalan and LY294002 resulted in no alteration of the DNA ICL repair profile as compared with melphalan alone (Figure 6.7b). Therefore the inhibitory effect of LY294002 on DNA repair does not occur with all DNA-interactive chemotherapeutic agents.

Previous experiments demonstrated an interaction between DNA-PK_{CS} and EGFR which was modulated by gefitinib and could contribute to sensitisation by gefitinib of cisplatin treatment. To investigate further the effects of inhibiting the DNA-PK pathway on chemosensitisation to cisplatin as compared with gefitinib treatment, the DNA-PK inhibitor wortmannin was used. MCF-7 cells were treated with cisplatin in combination with gefitinib, wortmannin or both agents (Figure 6.8). The dose of wortmannin used (100nM) has been shown to be inhibitory to PI3-kinase related kinases (Sarkaria *et al.*, 1998). The IC_{50} for cells treated with both cisplatin and wortmannin was 3±0.8μM,

whereas cells exposed to cisplatin and gefitinib achieved an IC_{50} of 0.23±0.07. By comparison, experiments in which cells were exposed to the combination of gefitinib, wortmannin and cisplatin did not result in additional inhibition of cellular proliferation with an IC_{50} of 0.20±0.05μM. These results further suggest that the effects of gefitinib on inhibition of DNA repair may be modulated through the DNA-PK pathway.

As has been discussed, repair of cisplatin-induced ICLs is inhibited following exposure to the PI3-kinase inhibitor LY294002 mimicked the results with gefitinib. The comet assay was used to measure the production and rate of repair of ICLs following cisplatin, in combination with wortmannin and/or gefitinib treatment in MCF-7 cells. Figure 6.9 shows the delay in ICL repair in cells treated with cisplatin in combination with wortmannin at both 100nM and 1μM. By 16h ~50% of ICLs were repaired in cells treated with cisplatin alone, as compared with ~28% in cells treated with a combination of cisplatin and wortmannin at both concentrations (28.12% at 100nM and 28.03% at 1μM). Cells treated with cisplatin and gefitinib showed ~10% repair at 16h suggesting that the DNA-PK pathway does not fully contribute to the observed synergy.

To confirm that wortmannin treatment directly affects the functional activity of DNA-PK in MCF-7 cells, the SignaTECT® DNA-Dependent Protein Kinase Assay System was used on MCF-7 cellular extracts. Cells exposed to wortmannin at 100nM showed a 22.8±3.3% decrease in DNA-PK functional activity after 24h and a 42.3±1.8% decrease after 48h. Whilst cells exposed to a higher dose of wortmannin (1μM) showed a greater decrease in DNA-PK activity after 24h (44.8±3.8%), the effect seen after 48h was more comparable with a 46.1±0.4% decrease in DNA-PK activity (Figure 6.10). It should also be noted that the decrease in activity achieved by wortmannin is comparable with the effect of gefitinib (10μM) treatment which inhibited DNA-PK activity by 32.3±5.1% after 24h and by 43.2±4.6% after 48h (Figure 6.3).

(a)

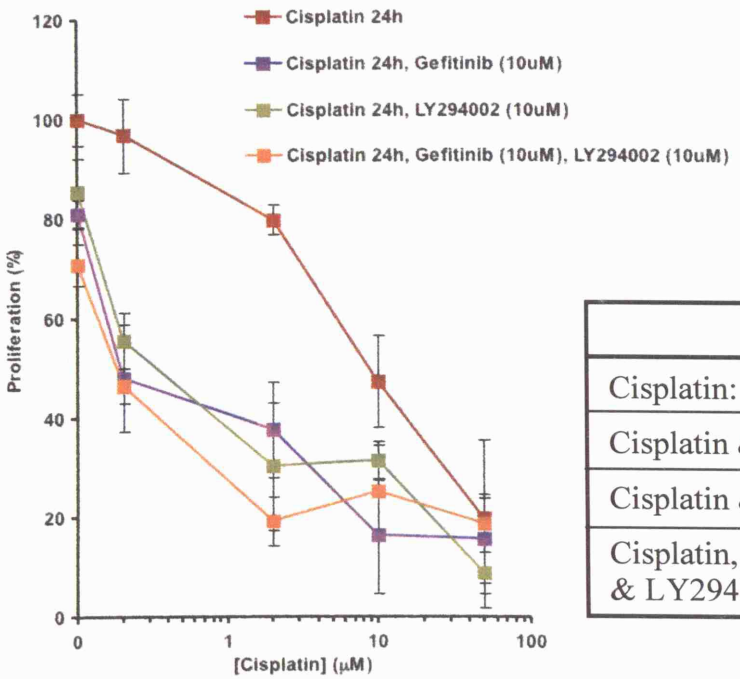

	IC_{50} (μM)
Cisplatin:	9±0.41
Cisplatin & Gefitinib:	0.21±0.003
Cisplatin & LY294002:	0.25±0.04
Cisplatin, Gefitinib & LY294002:	0.20±0.05

(b)

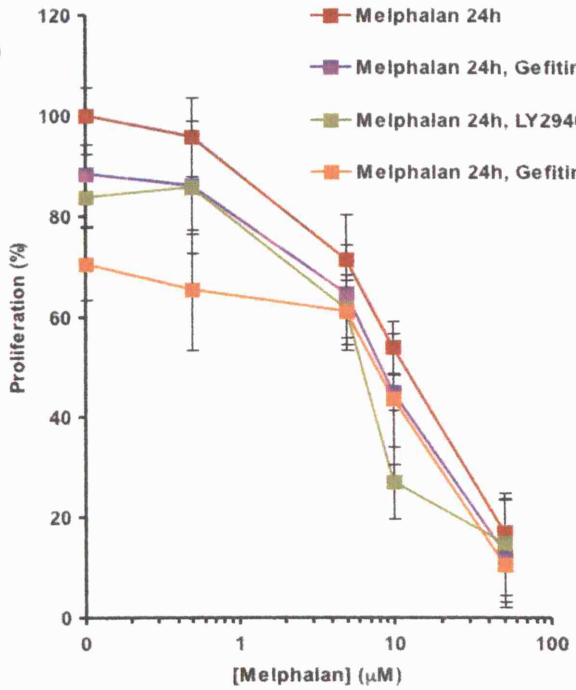

	IC_{50} (μM)
Melphalan:	13±1.7
Melphalan & Gefitinib:	9.4±1.88
Melphalan & LY294002:	8.3±0.97
Melphalan, Gefitinib & LY294002:	6±0.66

Figure 6.6: *Growth inhibition of MCF-7 cells by cisplatin and melphalan alone and followed by gefitinib and/or LY294002.* Growth inhibition SRB assay for (a) cisplatin and (b) melphalan. Following 24h exposure to chemotherapy, cells were incubated in drug free medium or gefitinib (10μM) and/or LY294002 (10μM) for 24h and left till Day 6. Data expressed as a percentage of the control untreated well absorbance and represents the averages of three different experiments, each performed in triplicate; *bars,* SD.

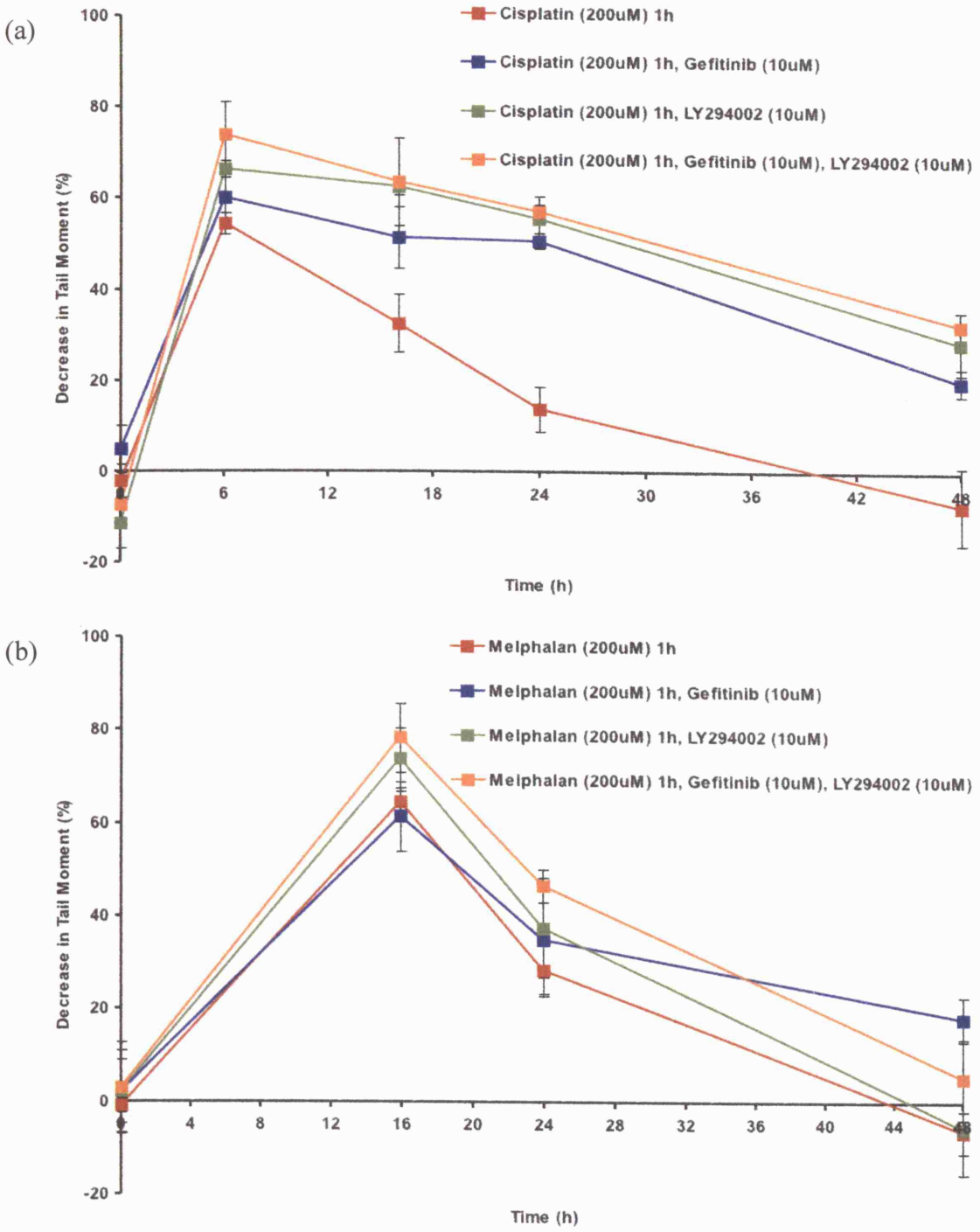

Figure 6.7: *Measurement of cisplatin and melphalan-induced DNA ICL formation and repair alone and in the presence of gefitinib and/or LY294002 in MCF-7 cells.* Cells were treated with (a) cisplatin (200μM) or (b) melphalan (200μM), for 1h and then incubated in fresh media or with gefitinib (10μM) and/or LY294002 (10μM). ICL formation is measured as percentage decrease in tail moment. Data is a representation of three independent experiments; *bars*, SE.

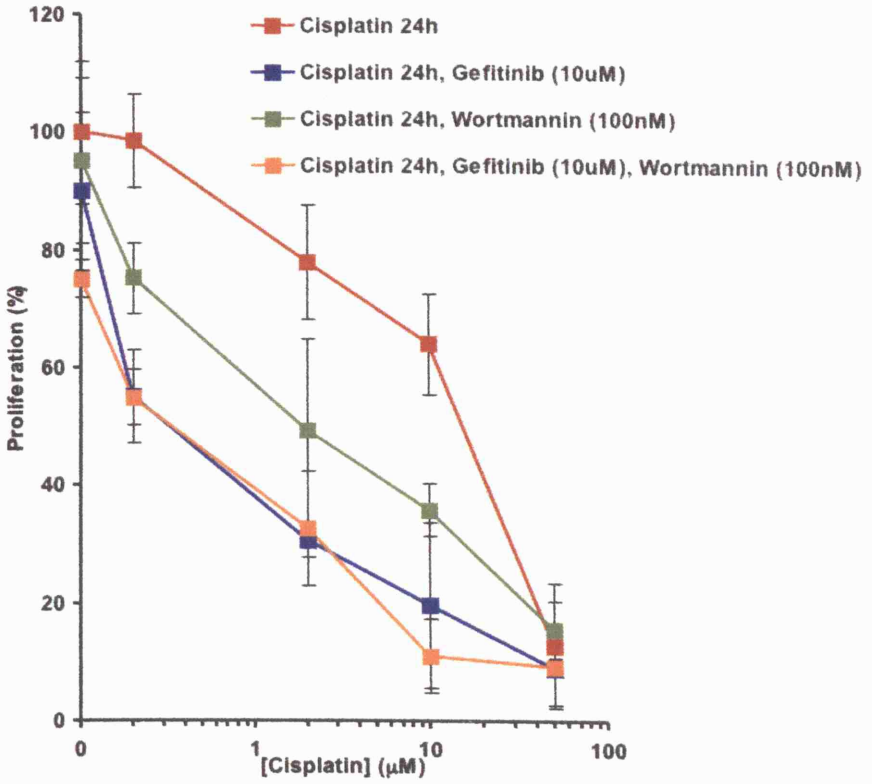

	IC_{50} (μM)
Cisplatin:	11±2.8
Cisplatin & Gefitinib:	0.23±0.07
Cisplatin & Wortmannin:	3±0.8
Cisplatin, Gefitinib & Wortmannin:	0.2±0.05

Figure 6.8: *Growth inhibition of MCF-7 cells by cisplatin alone and followed by gefitinib and/or wortmannin.* Growth inhibition SRB assay: Following 24h exposure to cisplatin alone, cells were incubated in drug free medium or gefitinib (10μM) and/or wortmannin (100nM) for 24h and left till Day 6. Data expressed as a percentage of the control untreated well absorbance and represents the averages of three different experiments, each performed in triplicate; *bars,* SD.

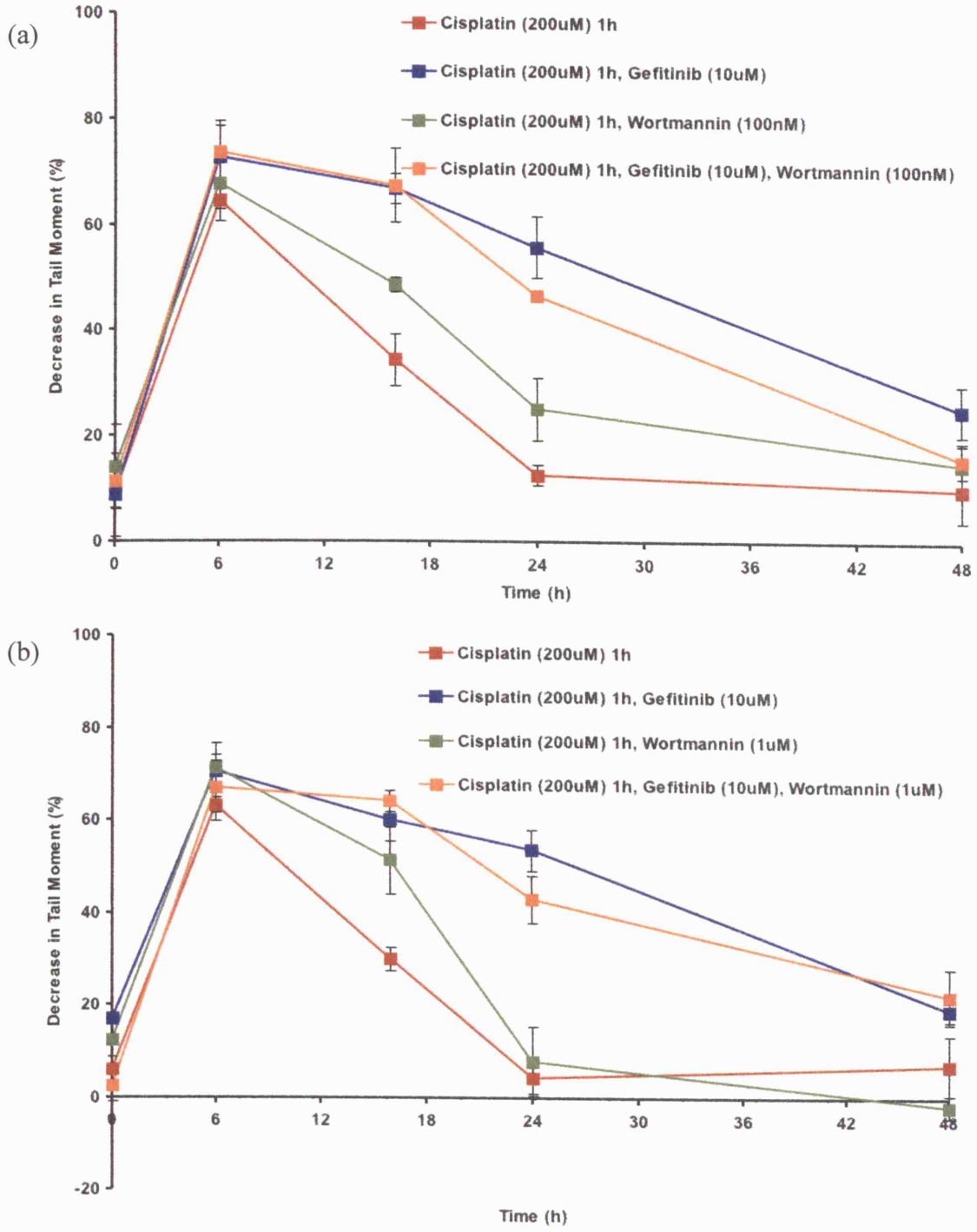

Figure 6.9: *Measurement of cisplatin-induced DNA ICL formation and repair alone and in the presence of gefitinib and/or wortmannin in MCF-7 cells.* Cells were treated with cisplatin (200μM) for 1h and then incubated in fresh media or with gefitinib (10μM) and/or (a) wortmannin (100nM) or (b) wortmannin (10μM). ICL formation is measured as percentage decrease in tail moment. Data is a representation of three independent experiments; *bars*, SE.

MCF-7 Cells		
Wortmannin Treatment	DNA-PK Enzyme Activity (pmol ATP/min/µg protein)	% of Control
-	11.56	100
(100nM) 24h	8.93	77.2
(100nM) 48h	6.67	57.7
(1µM) 24h	6.38	55.2
(1µM) 48h	6.24	53.9

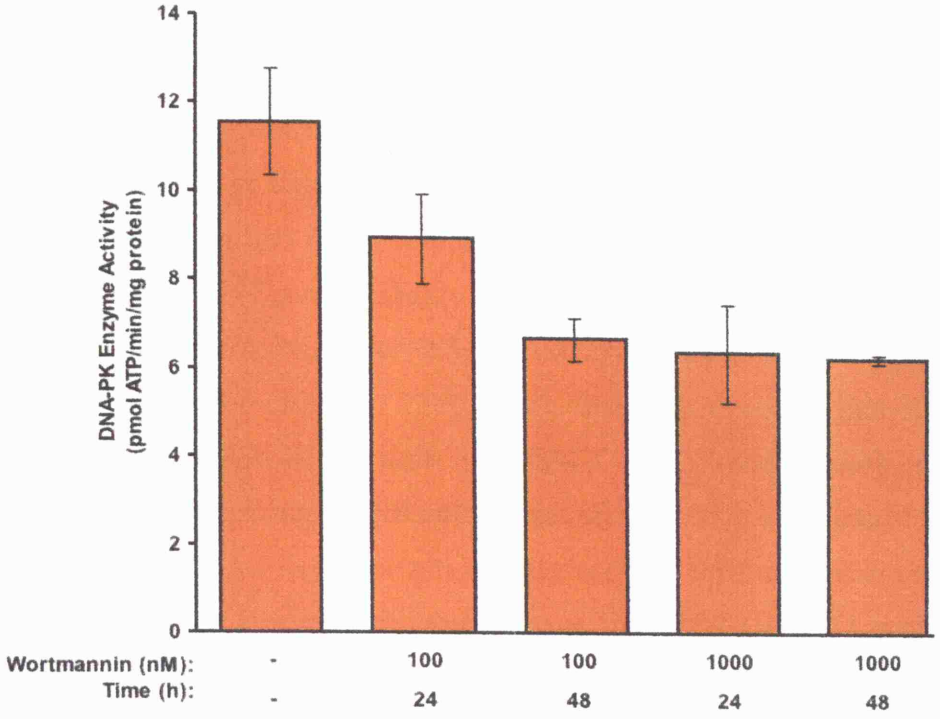

Figure 6.10: *Dose- and time-dependent wortmannin-induced inhibition of DNA-PK functional activity in MCF-7 cells.* Cells were treated with wortmannin (100nM or 1µM) and for indicated lengths of time. DNA-PK activity was measured using the Promega SignaTECT® DNA-PK assay system and the DNA-PK specific enzymatic activity determined. Data is an average of three independent experiments; error bars, SD.

6.4 Inhibition of DNA-PK$_{CS}$ by RNA Interference

Although LY294002 and wortmannin have inhibitory effects on the DNA-PK pathway, they have limited specificity and also have inhibitory effects on other members of the PI3-kinase family (Knight *et al.*, 2004). To examine more precisely the interaction between inhibition of DNA-PK and treatment with gefitinib, plasmid-directed RNA interference was used to reduce expression of DNA-PK$_{CS}$. Five different gene-specific pSuper plasmid constructs expressing siRNA directed against DNA-PK$_{CS}$ were generated and included a scrambled control. As shown in Figure 6.11, none of the constructs transfected into MCF-7 cells altered DNA-PK$_{CS}$ expression over a 24h or 36h period. At 48h, MCF-7 cells transfected with the pSUPER-CFP-117 plasmid reduced DNA-PK$_{CS}$ expression by 74% as measured by densitometry. Figure 6.12 shows the time-dependent transient reduction of DNA-PK$_{CS}$ which occurs 40h following transfection and persists for approximately 18 hours as measured by immunoblotting. No effects were seen with a pSuper plasmid expressing a scrambled siRNA (pSUPER-CFP-Scrambled). All experiments were therefore carried out within this time frame.

To investigate the effects of reduction in DNA-PK$_{CS}$ levels on sensitisation to cisplatin, an SRB assay was performed on MCF-7 cells transfected with pSUPER-CFP-117 or pSUPER-CFP-Scrambled (Figure 6.13a). The IC_{50} for cells treated with cisplatin and pSUPER-CFP-117 to DNA-PK$_{CS}$ was 2.5±0.1μM, comparable to the combination of cisplatin and wortmannin (100nM) (3±0.8μM). Experiments in which cells were exposed to the combination of gefitinib, pSUPER-CFP-117 and cisplatin resulted in additional inhibition of cellular proliferation with an IC_{50} of 0.18±0.04μM indicating that the inhibition of DNA-PK$_{CS}$ does not entirely account for the cellular sensitisation by gefitinib to cisplatin. However as noted above, pSUPER-CFP-117 achieves only partial inhibition of DNA-PK$_{CS}$ expression (~50%). Figure 6.13b, confirms reduction in DNA-PK$_{CS}$ expression by immunoblotting during the time-course of this experiment. Inhibition of repair of ICLs was shown in cells transfected with pSUPER-CFP-117 to DNA-PK$_{CS}$ and treated with cisplatin (Figure 6.14a). There was a reduction of 22% in cells transfected with pSUPER-CFP-117 to DNA-PK$_{CS}$ at 16h compared with no effect seen following transfection of pSUPER-CFP-Scrambled. Addition of gefitinib with pSUPER-CFP-117 to DNA-PK$_{CS}$ and cisplatin did not result in inhibition of repair greater than that seen with gefitinib and cisplatin. Figure 6.14b confirms reduction in DNA-PK$_{CS}$ expression.

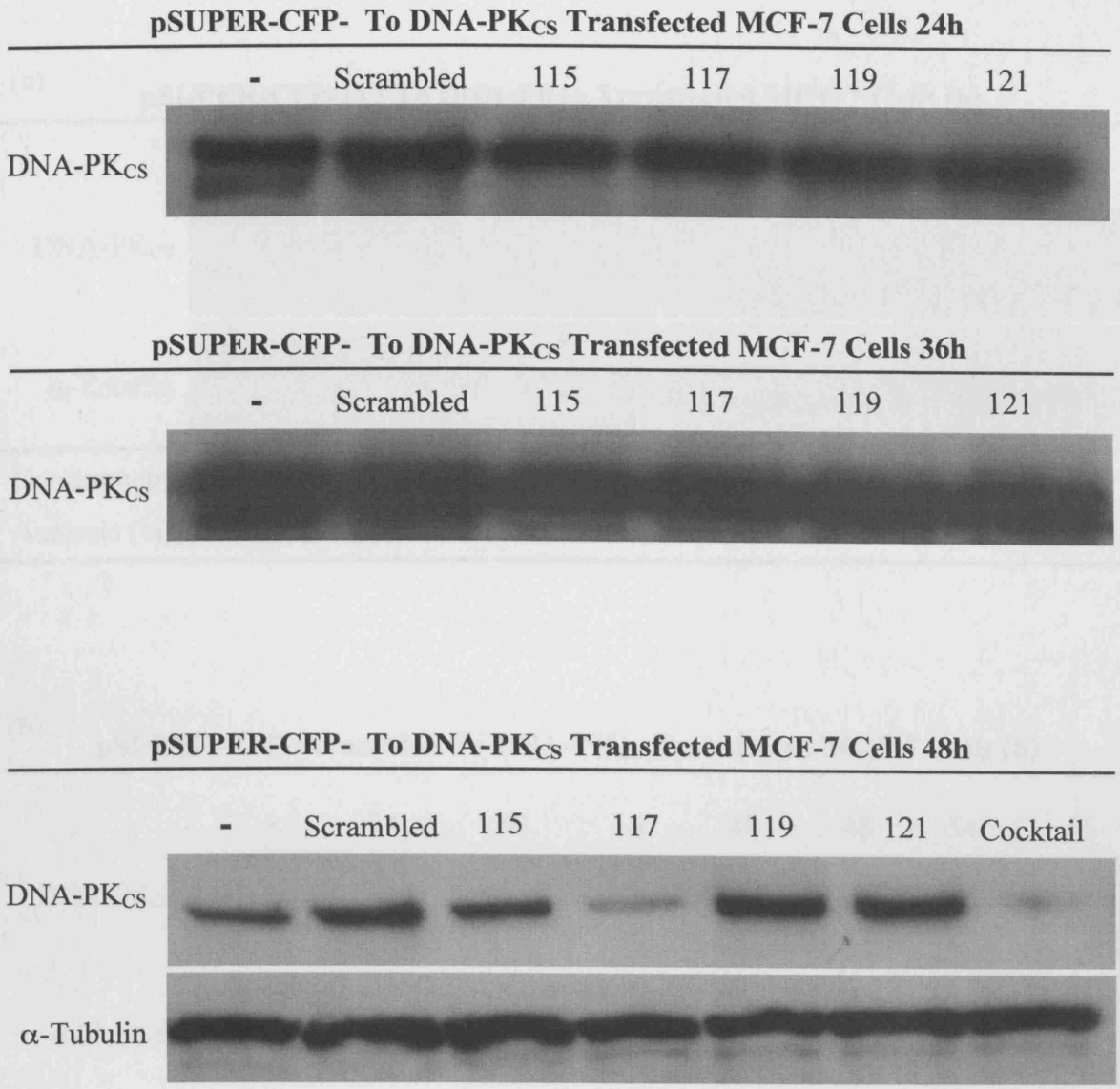

Figure 6.11: *DNA-PK$_{CS}$ expressions following transient transfection with different pSuper plasmids expressing DNA-PK$_{CS}$ -specific RNAi in MCF-7 cells.* Cells were transfected for indicated lengths of time with different RNAi and lysates immunoblotted with anti-DNA-PK$_{CS}$ antibody. α-Tubulin serves as a loading control.

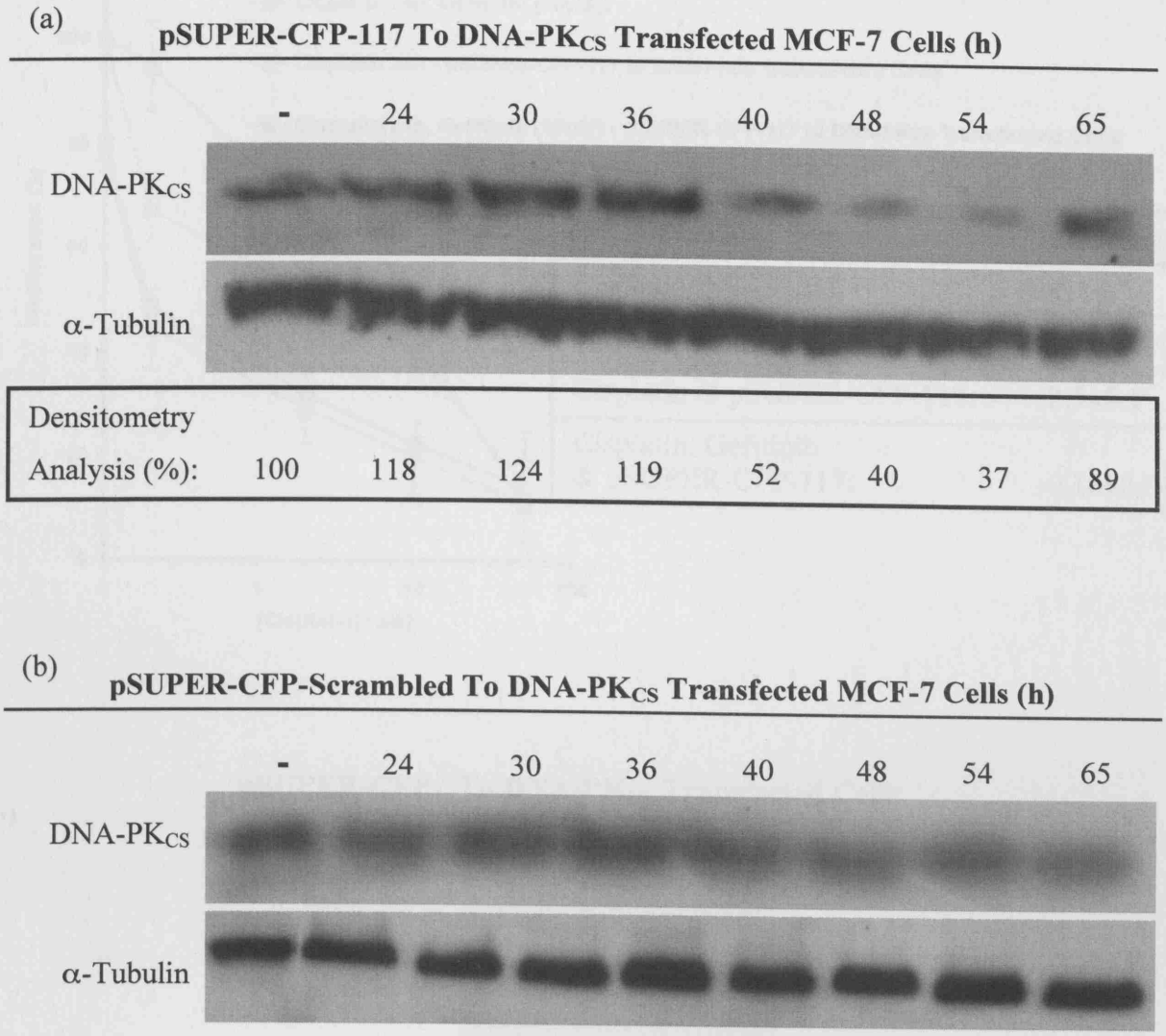

Figure 6.12: *Time-dependent reduction of DNA-PK$_{CS}$ expression following transient transfection with pSuper plasmids expressing DNA-PK$_{CS}$ -specific RNAi in MCF-7 cells.* Cells were transfected with (a) pSUPER-CFP-117 or (b) pSUPER-CFP-Scrambled RNAi for indicated lengths of time and lysates immunoblotted with anti-DNA-PK$_{CS}$ antibody. α-Tubulin serves as a loading control.

(a)

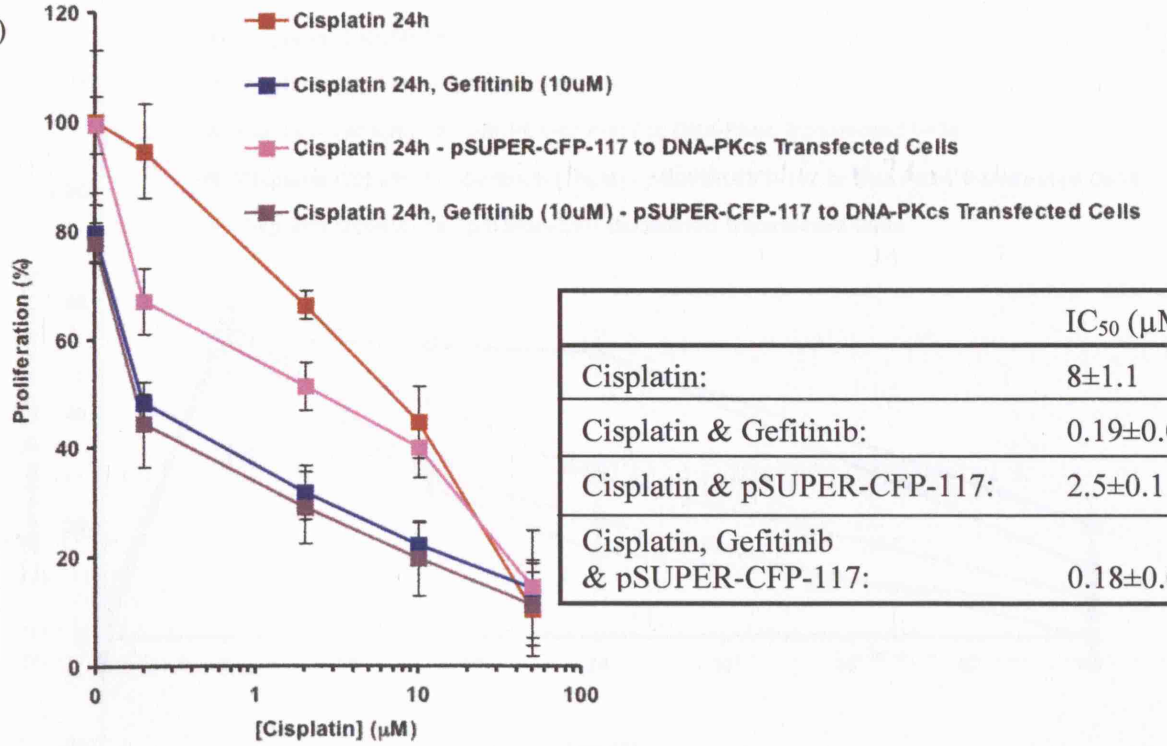

	IC_{50} (μM)
Cisplatin:	8±1.1
Cisplatin & Gefitinib:	0.19±0.07
Cisplatin & pSUPER-CFP-117:	2.5±0.1
Cisplatin, Gefitinib & pSUPER-CFP-117:	0.18±0.04

(b)

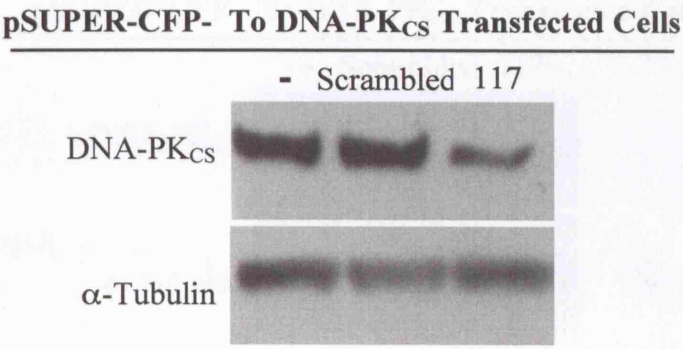

Figure 6.13: *Growth inhibition of MCF-7 cells by cisplatin alone and followed by gefitinib and/or pSUPER-CFP-117 RNAi.* (a) Cells were left in fresh medium or transfected with pSUPER-CFP-117 RNAi directed against DNA-PK_{CS} for 36h prior to a cisplatin 24h exposure. Following this, cells were then incubated in drug free medium or gefitinib (10μM) for 24h and left till Day 6. Data expressed as a percentage of the control untreated well absorbance and represents the averages of three different experiments, each performed in triplicate; *bars,* SD. (b) Reduction of DNA-PK_{CS} by RNAi at 48h confirmed by immunoblotting.

(a)

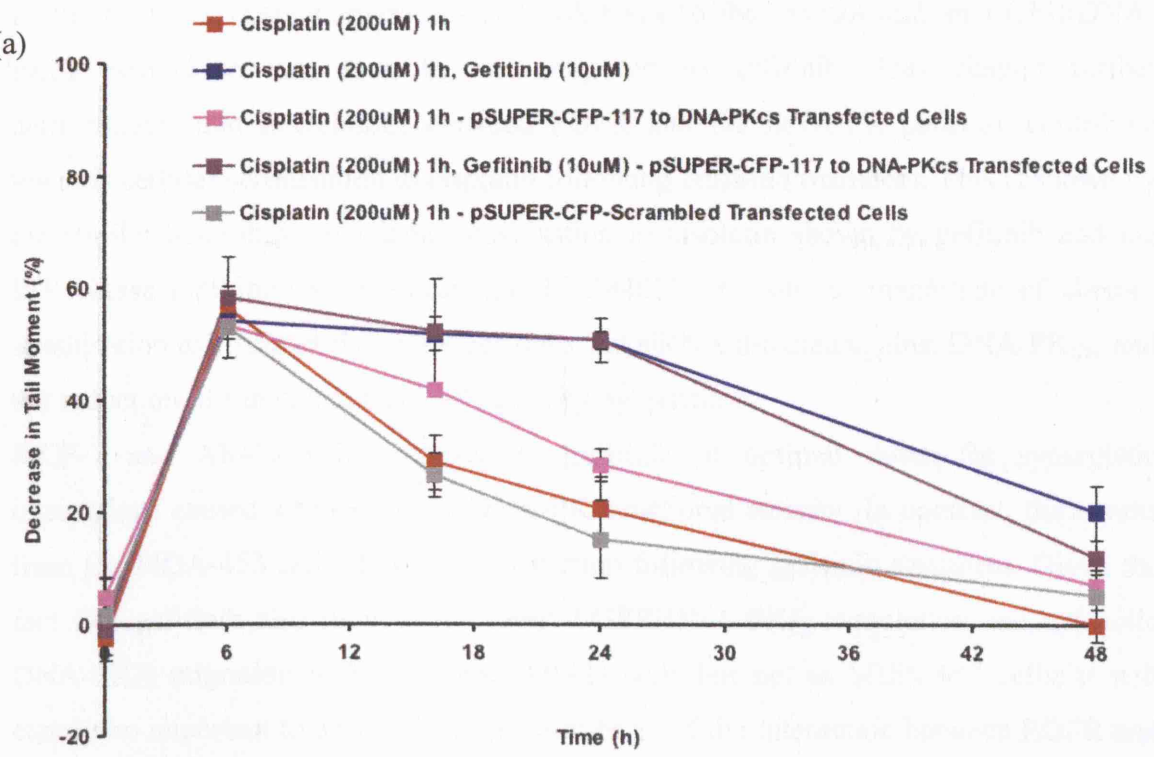

(b)

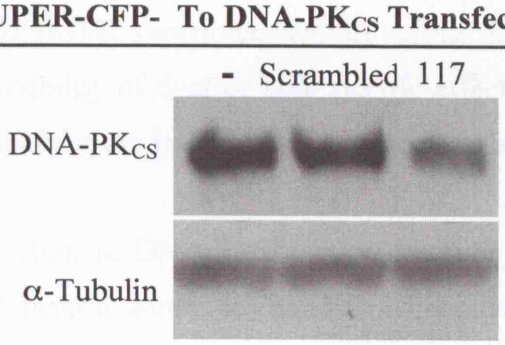

Figure 6.14: *Measurement of cisplatin-induced DNA ICL formation and repair alone and in the presence of gefitinib and/or pSUPER-CFP-117 RNAi in MCF-7 cells.* (a) Cells were left in fresh medium or transfected with pSUPER-CFP-117 RNAi directed against DNA-PK$_{CS}$ for 36h prior to a cisplatin (200μM) for 1h and then incubated in fresh media or with gefitinib (10μM). ICL formation is measured as percentage decrease in tail moment. Data is a representation of three independent experiments; *bars*, SE. (b) Reduction of DNA-PK$_{CS}$ by RNAi at 48h confirmed by immunoblotting.

6.5 Discussion

In the previous chapter migration of DNA-PK_{CS} to the cytosol and an EGFR/DNA-PK_{CS} association was seen in cells exposed to gefitinib. This chapter further demonstrates that interactions between EGFR and the DNA-PK pathway contribute towards cellular sensitisation to cisplatin following gefitinib treatment. This is shown by the similar magnitude of chemo-sensitisation to cisplatin shown by gefitinib and the PI3-Kinase inhibitors wortmannin and LY294002, the similar magnitude of chemo-sensitisation to cisplatin shown by gefitinib and siRNA directed against DNA-PK_{CS}, and the reduction of functional DNA-PK activity by gefitinib.

MCF-7 and AR42J cells exposed to gefitinib at optimal doses for synergistic interactions caused a reduction in DNA-PK functional activity. In contrast, the results from the MDA-453 cells showed no reduction following gefitinib treatment. Given the fact that gefitinib also induces increased EGFR/DNA-PK_{CS} association and cytosolic DNA-PK_{CS} migration in MCF-7 and AR42J cells but not in MDA-453 cells, it will clearly be important to define the molecular basis of the interaction between EGFR and DNA-PK_{CS} and to investigate the reasons for the differences between cell lines. In a recent study in metastatic melanoma cell lines, it was shown that the EGFR inhibitor PKI166 also inhibited DNA-PK functional activity using the same assay (Um *et al.*, 2004). However, the possibility of dual or non-specific effects of PKI166 could not be excluded as this agent inhibits the intracellular tyrosine kinase domains of both EGFR and of HER-2.

Cetuximab-induced reduction in DNA-PK functional activity in the nucleus was also shown using a DNA-PK peptide substrate (Bandyopadhyay *et al.*, 1998). Similarly, the results in this chapter demonstrate a comparable reduction in DNA-PK functional activity with the humanised cetuximab antibody, matuzumab. Furthermore, the study recently showing that both ionising radiation and cisplatin triggers increased EGFR translocation into the nucleus to act as a transcription factor in human bronchial carcinoma cells (see Chapter 5), also showed that radiation strongly increased DNA-PK functional activity which was nearly completely abolished by adding cetuximab to cells prior to irradiation (Dittmann *et al.*, 2005a).

To investigate these findings further the DNA-PK pathway was studied in more detail. Synergy of the effects of cisplatin on cell proliferation was found when MCF-7 cells were exposed to LY294002 and wortmannin, which block PIKK family members. This

was associated with inhibition of repair to a similar extent as that found with gefitinib. In addition, and as with gefitinib, cells exposed to melphalan in combination with LY294002 showed no synergistic effects on cytotoxicity or effects on DNA repair.

The significance of DNA-PK in repair of drug-induced DNA damage has been shown for cells lacking NHEJ activity, which are hypersensitive to etoposide (Adachi *et al.*, 2003). Furthermore, an inhibitory effect of wortmannin on etoposide-induced DNA damage has also been demonstrated (Boulton *et al.*, 2000). Sarkaria *et al.*, (1998), showed that wortmannin inhibits PIKK family members *in vitro* with an IC_{50} for DNA-PK inhibition of 16nM. Interestingly, others have reported the IC_{50} for inhibition of DNA-PK *in vitro* to be >100nM (Izzard *et al.*, 1999; Christodoulopoulos *et al.*, 1998; Knight *et al.*, 2004). In light of the fact that in this study, cells exposed to wortmannin at both 100nM and 1μM delayed repair of cisplatin-induced ICLs to the same extent and in a similar fashion to that of gefitinib, and given the fact that both concentrations similarly inhibit DNA-PK_{CS} functional activity, it is clear that treatment with wortmannin at 100nM is indeed inhibiting DNA-PK activity specifically thus contributing to the delay in repair observed.

The role of NHEJ in repair of DNA crosslinks produced by cisplatin is unclear, but cellular sensitisation to cisplatin has been found with other inhibitors of DNA-PK. For example, vanillin inhibited DNA-PK activity via an interaction with specific lysine residues in the active site and was shown to be specific to NHEJ and selective for DNA-PK_{CS} over ATM and ATR (Durrant & Karran, 2003). A study in B-cell chronic lymphocytic leukaemia showed that treatment with wortmannin synergistically sensitised cells to the effects of chlorambucil which showed a significant correlation with a decrease in DNA-PK activity (Christodoulopoulos *et al.*, 1998). In contrast, a study in human malignant glioma cell lines showed that LY294002 synergistically interacted with the antimicrotubule agents vincristine and paclitaxel, but showed only an additive increase in cytotoxicity and apoptosis with etoposide and cisplatin (Shingu *et al.*, 2003).

The basic chemical structure of LY294002 has however offered a lead compound upon which more potent novel inhibitors can be developed that posses more desirable properties to aid their future assessment (Knight *et al.*, 2004). One such inhibitor, OK-1035, has been shown to selectively inhibit DNA-PK *in vitro*; however, with an IC_{50} of 100μM it is unlikely to be useful for *in vivo* studies (Stockley *et al.*, 2001). Another

compound designed to show increased sensitivity for DNA-PK_{CS} is NU7026. This demonstrated the most potent activity with a 70-fold increase in selectivity for DNA-PK_{CS} compared to other PI3-Kinases and 5-fold more selective for DNA-PK_{CS} than for ATM or ATR (Hollick *et al.*, 2003). Furthermore, the chemically synthesised inhibitor SU11752 was shown to competitively inhibit DNA-PK_{CS} by binding to its ATP binding site resulting in less efficient repair of DNA DSBs (Ismail *et al.*, 2003). It would be of interest to investigate whether these more specific DNA-PK_{CS} inhibitors also mimic the effects of gefitinib in combination with cisplatin.

To examine more precisely the interaction between inhibition of DNA-PK and treatment with gefitinib, plasmid-directed RNA interference was used to reduce expression of DNA-PK_{CS}. This caused a ~60-70% reduction in DNA-PK_{CS} protein expression resulting in a similar magnitude of chemo-sensitisation to cisplatin shown by gefitinib. These experiments therefore show that specific reduction of DNA-PK has similar effects as gefitinib.

6.5.1 Conclusions

These studies suggest that there is a significant effect of gefitinib on the DNA-PK_{CS} pathway. It is plausible to suggest that interactions of EGFR and DNA-PK_{CS} may have major significance in determining cellular response to EGFR inhibition.

CHAPTER 7

MODULATION OF CHEMOTHERAPY BY GEFITINIB IN CELLS EXPRESSING SPECIFIC EGFR MUTATIONS

7.1 Introduction

Approximately 10% of NSCLC patients respond to treatment with tyrosine kinase inhibitors such as gefitinib or erlotinib (Fukuoka *et al.*, 2003; Kris *et al.*, 2003; Giaccone *et al.*, 2004). Nearly all gefitinib- or erlotinib-responsive lung cancers have been shown to express somatic mutations within the EGFR kinase domain, whereas no mutations have been seen in non-responsive cases (Lynch *et al.*, 2004; Paez *et al.*, 2004; Shepherd *et al.*, 2005; Tsao *et al.*, 2005). These heterozygous mutations include missense substitutions and small in-frame deletions clustered within the ATP-binding pocket (See Chapter 1). Table 7.1 shows the distribution of 35 different mutations in exons 18 through 21 of the *EGFR* gene.

Exon	Point Mutation	Deletion or Insertion
18	L688P P694L P694S	
19 All exon 19 deletions lack amino acids ELREA except for one (Paez *et al.*, 2004)	L730F P733L G735S V742A E746K T751I S752Y D761N R776C	delE746-A750 delE746-S752V delE746-P753insLS delL747-A750 **delL747-P753insS** delL747-A750insLS del747-T751insS del747-T751insP
20	S784F **T790M** L792P L798F G810S	
21	N826S H835L T8471 H850N V851A I853T **L858R** L861Q A864T E866K G873E	

Table 7.1: Mutations in the *EGFR* gene.

Studies *in vitro* have shown that tumour cell lines expressing these mutant forms of

EGFR are more susceptible to apoptosis following gefitinib as compared with wild-type cells (Tracy *et al.*, 2004; Amann *et al.*, 2005). Furthermore, it has been shown that the apoptotic pathways in NSCLC tumours expressing mutant forms of EGFR differ from those in wild-type cells (Sordella *et al.*, 2004). Cells with mutant EGFR preferentially activate the AKT and signal transducer and activator of transcription (STAT) anti-apoptotic signalling pathway, and EGFR inhibition with gefitinib results in rapid cell death. This could underlie the marked responses to gefitinib in patients with mutant EGFR (Sordella *et al.*, 2004). However, the functional impact of all the EGFR-TK mutations discovered so far, and their clinical significance, is not yet known. Whilst it may be possible to predict which patients are most likely to achieve an objective response with gefitinib, other mechanisms might be involved in determining sensitivity to gefitinib and other EGFR tyrosine kinase inhibitors. At least one patient with gefitinib-responsive NSCLC did not have any of these mutations (Lynch *et al.*, 2004), and in one study exploring treatment with erlotinib, one non-responder had EGFR-TK mutations whereas five patients with stable disease did not (Janne, 2004).

Cells expressing specific EGFR mutations have also been shown to have increased sensitivity to disruption of AKT and STAT-mediated anti-apoptotic signals (as measured using LY294002 and AG490 respectively). In contrast, they demonstrated markedly increased resistance to cell death signals induced by cisplatin and doxorubicin (Sordella *et al.*, 2004).

7.1.1 Aims

Experiments presented in Chapter 4 showed that gefitinib treatment delayed the repair of cisplatin-induced ICLs but had no effect on those induced by melphalan in all cell lines tested. The purposes of the experiments presented in this chapter are to further characterise the mechanisms of interaction between gefitinib and DNA-damaging chemotherapeutic agents in cells expressing mutant forms of EGFR. To this end, the following questions are addressed:

1. Does gefitinib alter the repair of DNA damage induced by chemotherapy in cells expressing the **L858R** and **delL747-P753insS** mutant forms of EGFR?
2. Are these effects seen with all DNA damaging agents?
3. How are these effects comparable with those found in cells expressing wild type EGFR?

7.2 Modulation of EGFR by Gefitinib and Chemotherapy in Cells Expressing Specific EGFR Mutations

The African green monkey kidney Cos-7 cells were transiently transfected with the pUSEamp vector expressing different EGFR constructs. These were: wild type EGFR, the L858R missense substitution and the DelL747-P753insS in-frame deletion (kindly provided by Daphne Bell and Matthew Myerson from the MGH Cancer Centre, Harvard Medical School, Boston, USA). As shown in Figure 7.1, untransfected Cos-7 cells express no EGFR. EGFR expression was seen in transfected cells after 24h and was still detectable after 72h. To assess ligand induced EGFR activation, cells were stimulated with 100ng/μL EGF for 30 min and probed for EGFR Tyr-1068 phosphorylation (Figure 7.2). As expected, no EGFR phosphorylation was seen in untransfected Cos-7 cells. Cells transfected with the wild type, DelL747-P753insS or L858R mutant EGFR sequences expressed comparable levels of P-EGFR immediately which was still detectable 3h following stimulation (Figure 7.2).

To investigate the effects of gefitinib on EGFR tyrosine phosphorylation in cells expressing EGFR mutations, transfected cells were stimulated with 100ng/μL EGF for 30 min and treated with gefitinib as shown in Figures 7.3. Lysates were then probed for phosphorylated-EGFR (P-EGFR) using the tyrosine-non-specific antibody, PY20. In addition, to assess the ability of gefitinib to inhibit activation of specific tyrosine phosphorylation sites, lysates were immunoblotted with the anti-Tyr-845 and anti-Tyr-1068 antibodies. As can be seen in Figure 7.3, inhibition of EGFR phosphorylation was seen with gefitinib at 0.2μM for 3h in wild type EGFR transfected cells. By contrast, the same inhibitory effects were seen in both the DelL747-P753insS and the L858R mutant EGFR transfected cell lines with 0.02μM gefitinib for 3h – a ten-fold increase in sensitivity.

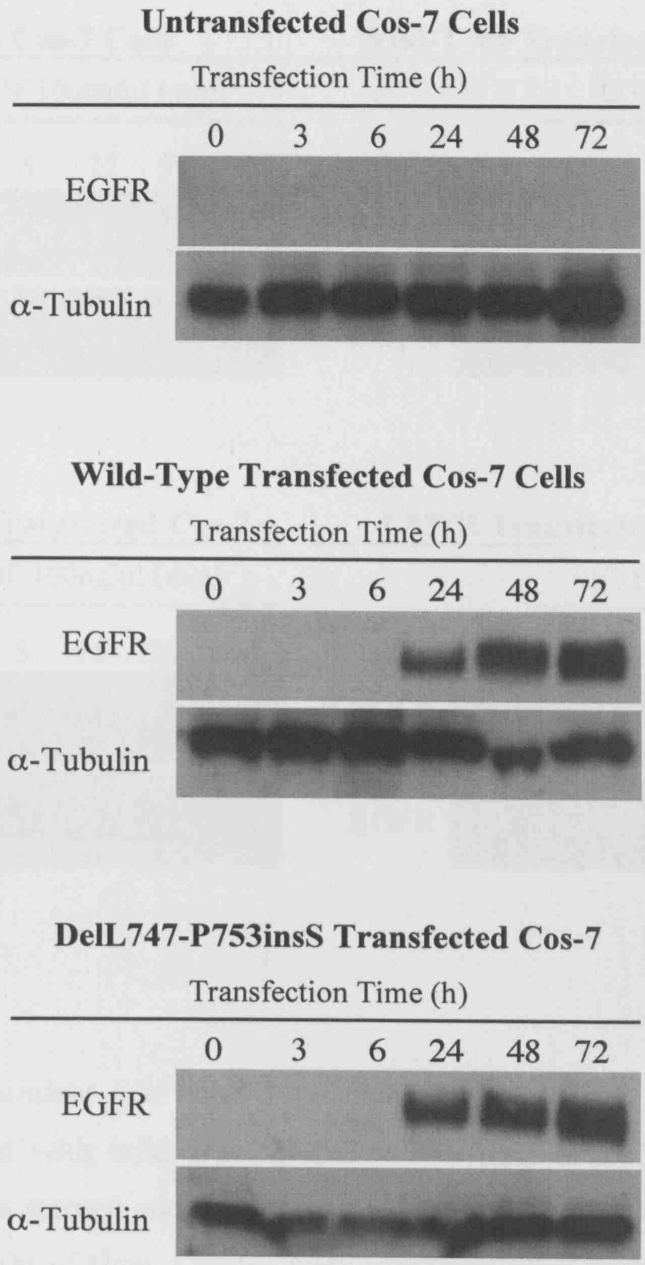

Figure 7.1: *Time-dependent transfection efficiency of mutant EGFR sequences in Cos-7 cells*. Cells were incubated with Genejuice® plasmid complexes containing wild type or DelL747-P753insS EGFR sequences for indicated lengths of time. Lysates were immunoblotted with anti-EGFR antibody; α-Tubulin serves as a loading control.

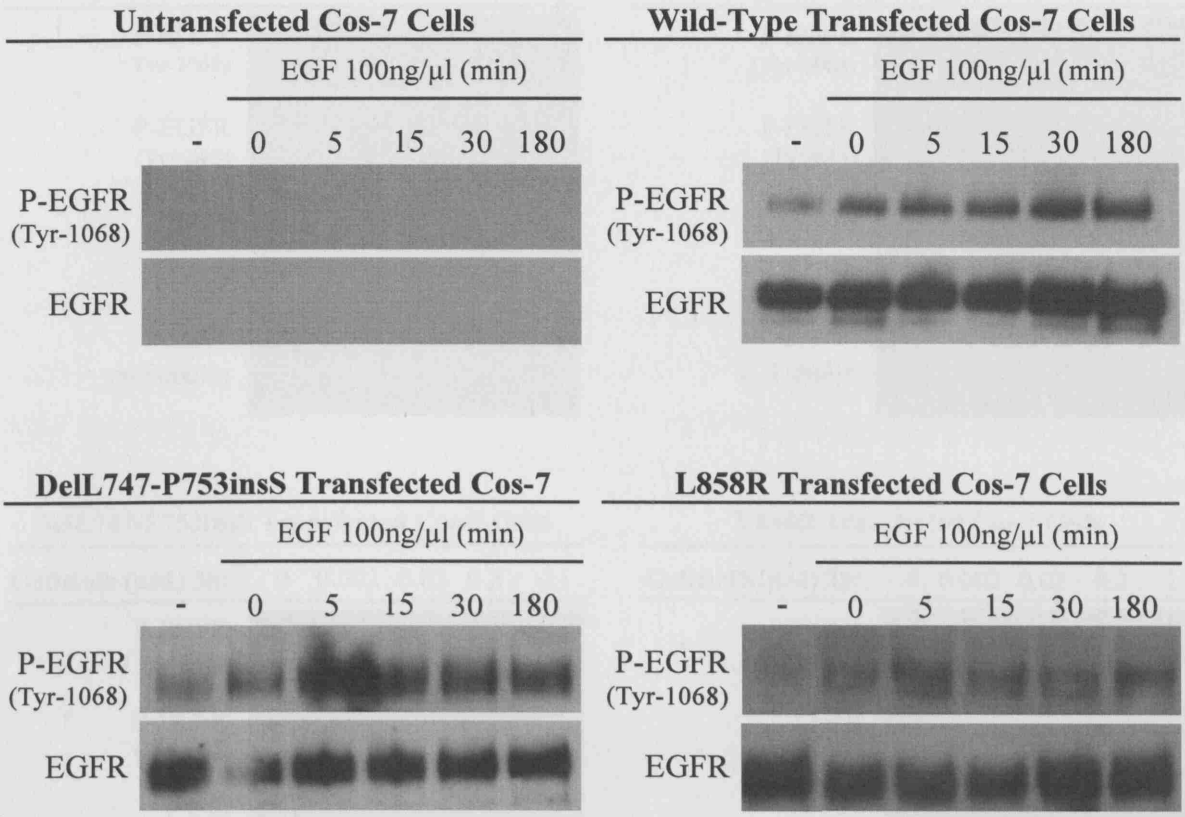

Figure 7.2: *Time-dependent EGF-stimulated activation of EGFR mutant Cos-7 cells.* Cells were transfected with wild type, DelL747-P753insS or L858R EGFR mutant sequences, were serum starved and then stimulated with 100ng/µl EGF for 30 min and left for indicated lengths of time. Lysates were immunoblotted with anti-phospho-Tyr-845 EGFR specific antibody; EGFR serves as a loading control.

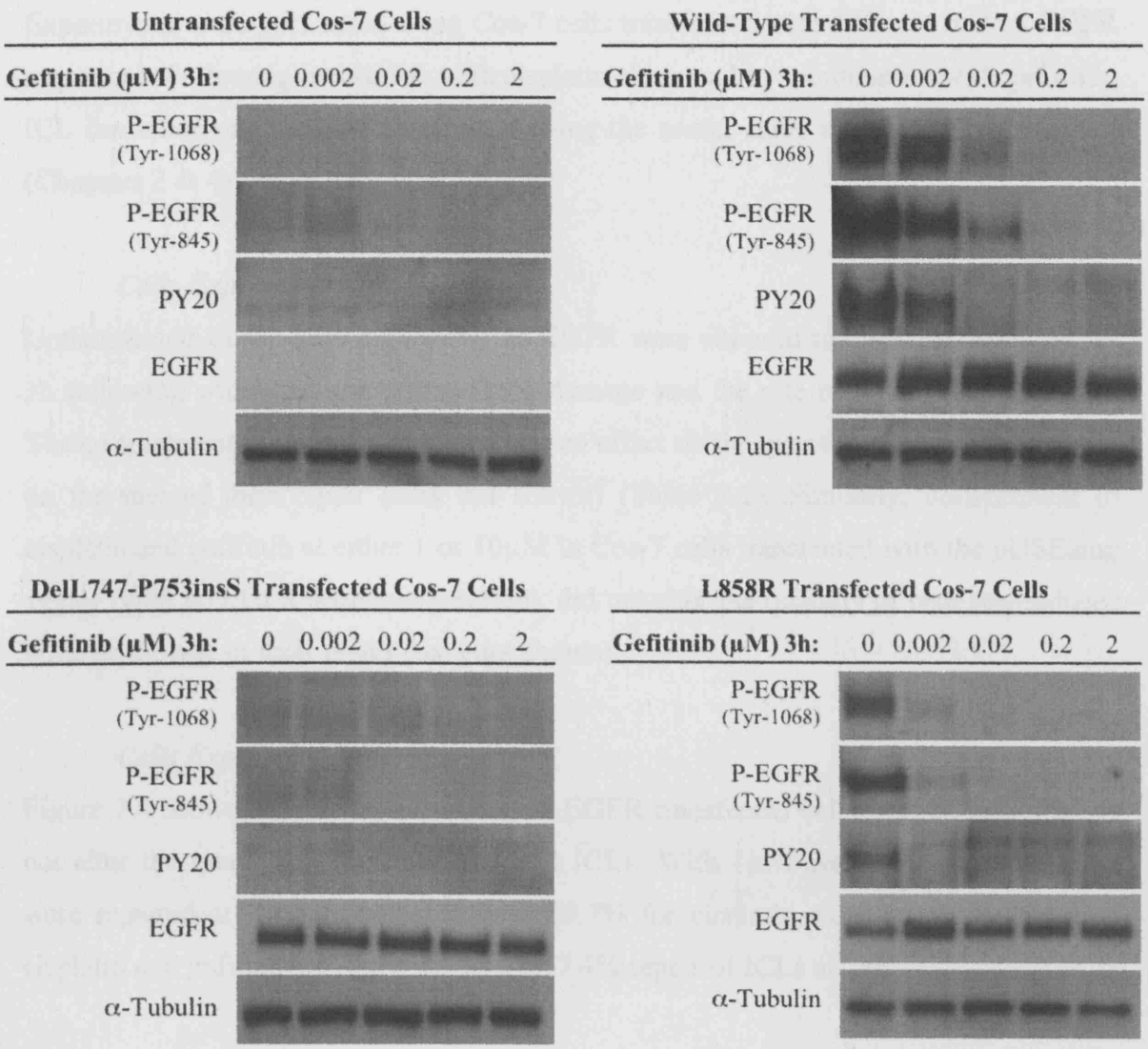

Figure 7.3: *Dose-dependent gefitinib-induced inhibition of EGFR mutant Cos-7 cells.* Cells transfected with wild type, DelL747-P753insS or L858R EGFR mutant sequences were treated with indicated concentrations of gefitinib for 3h followed by stimulation with 100ng/μl EGF for 30 min. Lysates were immunoblotted with indicated antibodies; α-Tubulin serves as a loading control.

7.3 *Effects of Gefitinib on Cisplatin-Induced DNA ICL Formation and Repair in Cells Expressing Specific EGFR Mutations*

Experiments were performed using Cos-7 cells transfected with different mutant EGFR sequences. Following incubation with cisplatin alone and in combination with gefitinib, ICL formation and repair was assessed using the comet assay as previously described (Chapters 2 & 4) (Spanswick *et al.*, 1999).

Cells Expressing No EGFR

Untransfected Cos-7 cells expressing no EGFR were exposed to cisplatin (200μM) for 1h following which the amount of DNA damage and the rate of repair were assessed. The co-treatment of gefitinib at 10μM had no effect on the quantity of ICLs produced or on the rate of their repair (data not shown) (Table 7.2). Similarly, co-treatment of cisplatin and gefitinib at either 1 or 10μM in Cos-7 cells transfected with the pUSEamp vector (with no EGFR sequence inserted), did not alter the quantity of cisplatin-induced ICLs or the rate of their repair (data not shown).

Cells Expressing Wild Type EGFR

Figure 7.4 shows the results for wild type EGFR transfected cells. Again, gefitinib did not alter the quantity of cisplatin-induced ICLs. With 1μM gefitinib, 34.5% of ICLs were repaired at 24h as compared with 59.7% for cisplatin alone. Cells treated with cisplatin and gefitinib at 10μM showed a 17.4% repair of ICLs at 24h.

Cells Expressing EGFR Mutations

As shown in Figure 7.5, co-treatment of cisplatin and gefitinib at 1μM on DelL747-P753insS mutant EGFR transfected cells, did not alter the quantity of cisplatin-induced ICLs or the rate of their repair. By contrast, gefitinib at 10μM delayed repair of cisplatin-induced ICLs with a magnitude comparable to that of wild type EGFR transfected cells. Measurement of cisplatin-induced DNA ICL formation and repair alone and in the presence of gefitinib on L858R mutant EGFR transfected Cos-7 cells is shown in Figure 7.6. Interestingly, co-treatment of gefitinib at 1μM shows an increased delay in repair of cisplatin-induced ICLs with no repair detectable at 24h and only 21.7% removal at 48h. Co-treatment with gefitinib at 10μM delayed repair further with only 12.8% of ICLs repaired at 48h.

Table 7.2 summarises the results from the experiments following incubation with cisplatin alone and in combination with gefitinib on the differently transfected Cos-7 cells.

Cell Line	Treatment	ICL Repair at 24h (%)
Untransfected	Cisplatin	-
	Cisplatin, Gefitinib (10μM)	No Delay
pUSEamp Vector Transfected	Cisplatin	-
	Cisplatin, Gefitinib (10μM)	No Delay
Wild Type EGFR Transfected	Cisplatin	59.7
	Cisplatin, Gefitinib (1μM)	34.5
	Cisplatin, Gefitinib (10μM)	17.4
DelL747-P753insS Mutant EGFR	Cisplatin	44.7
	Cisplatin, Gefitinib (1μM)	No Delay
	Cisplatin, Gefitinib (10μM)	14.9
L858R Mutant EGFR	Cisplatin	63.5
	Cisplatin, Gefitinib (1μM)	0
	Cisplatin, Gefitinib (10μM)	2.4

Table 7.2: ICL repair for cisplatin in combination with gefitinib in the differently transfected Cos-7 cells.

These results therefore confirm that gefitinib-induced inhibition of DNA repair is dependent on EGFR.

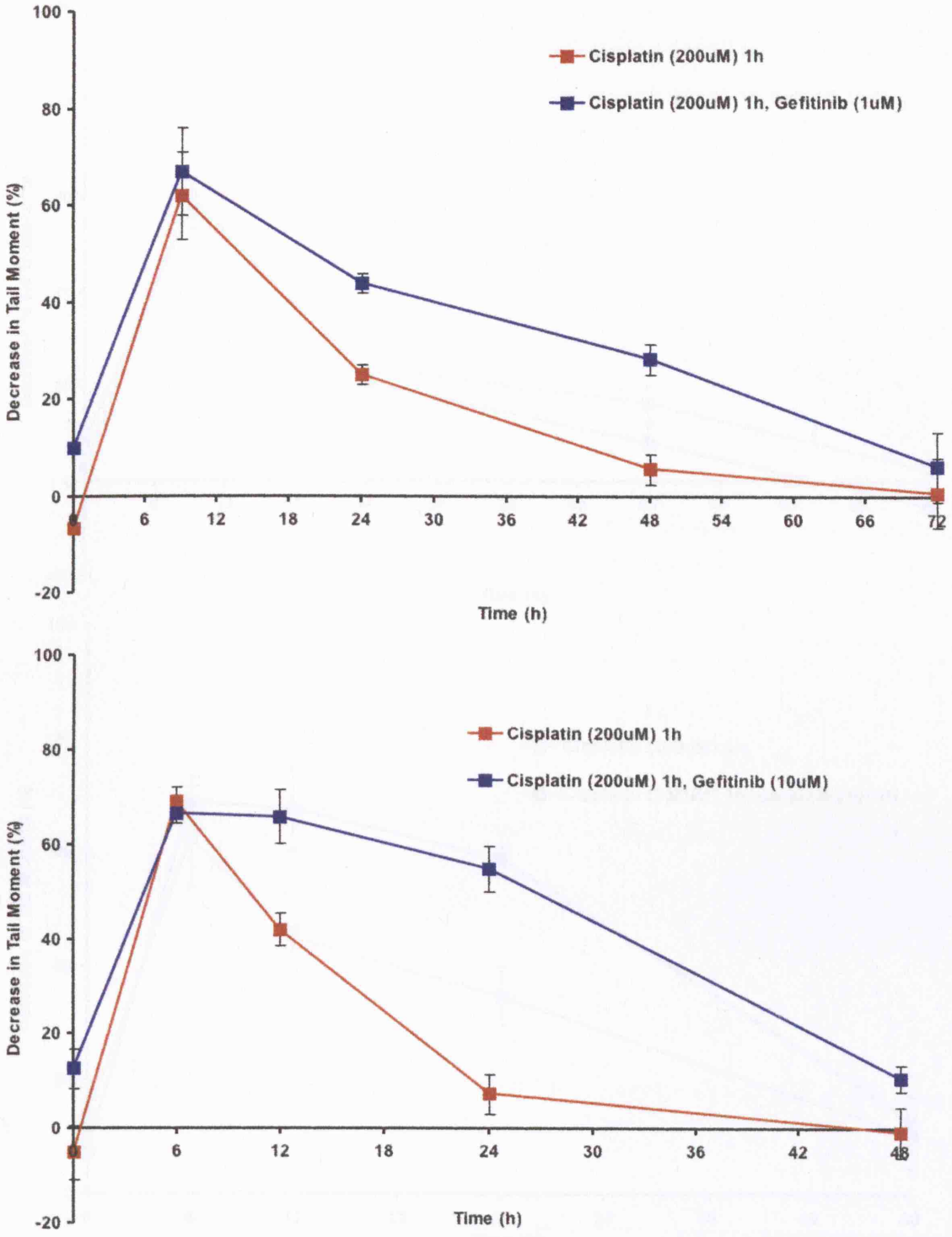

Figure 7.4: *Measurement of cisplatin-induced DNA ICL formation and repair alone and in the presence of gefitinib on Wild Type EGFR transfected Cos-7 cells.* Cells were transfected with wild type EGFR and stimulated with 100ng/μl EGF followed by cisplatin (200μM) for 1h and then incubated in fresh media or with gefitinib (1 or 10μM). ICL formation is measured as percentage decrease in tail moment. Data is a representation of three independent experiments; *bars*, SE.

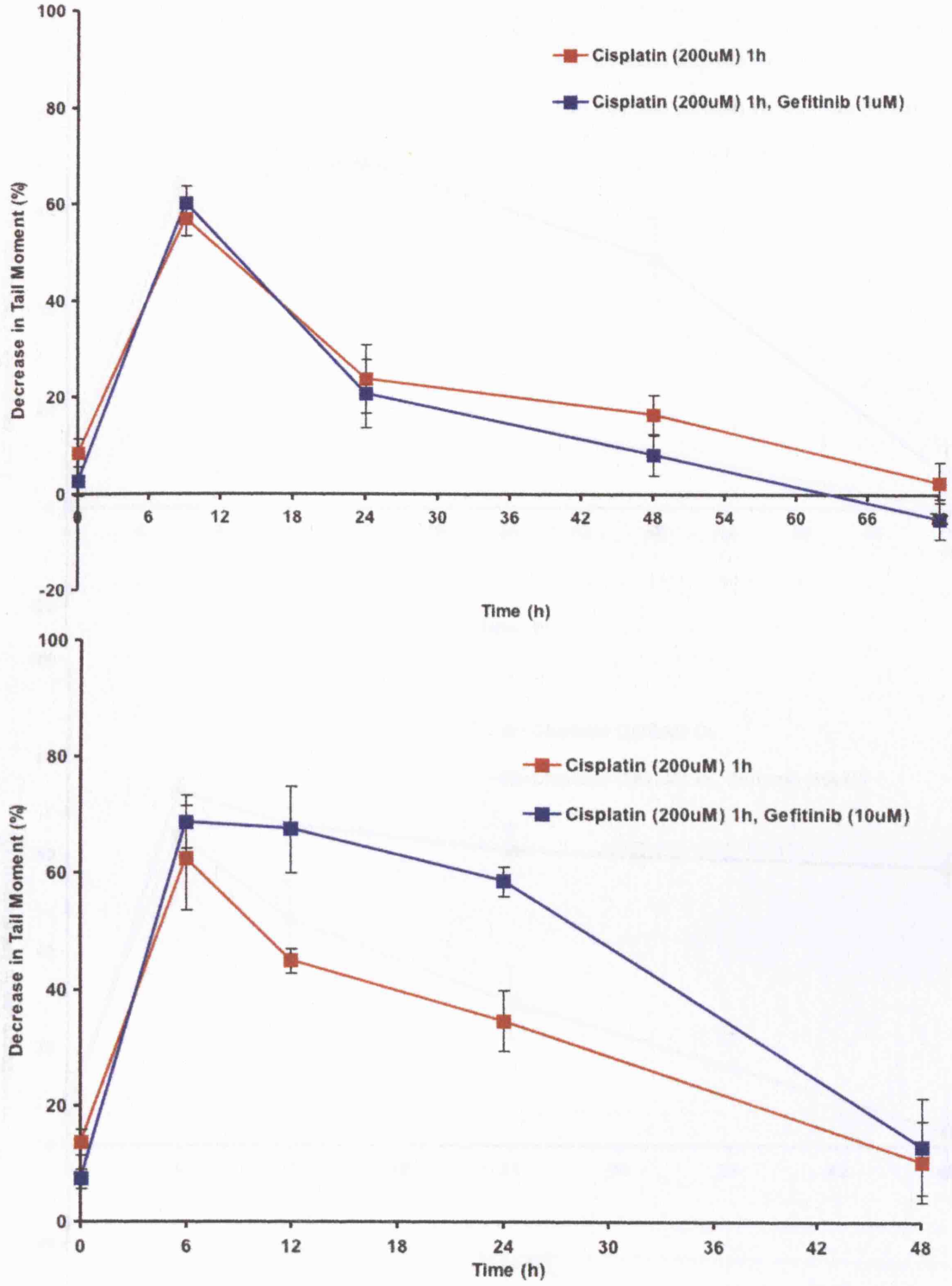

Figure 7.5: *Measurement of cisplatin-induced DNA ICL formation and repair alone and in the presence of gefitinib on DelL747-P753insS mutant EGFR transfected Cos-7 cells.* Cells were transfected with DelL747-P753insS mutant EGFR and stimulated with 100ng/µl EGF followed by cisplatin (200µM) for 1h and then incubated in fresh media or with gefitinib (1 or 10µM). ICL formation is measured as percentage decrease in tail moment. Data is a representation of three independent experiments; *bars*, SE.

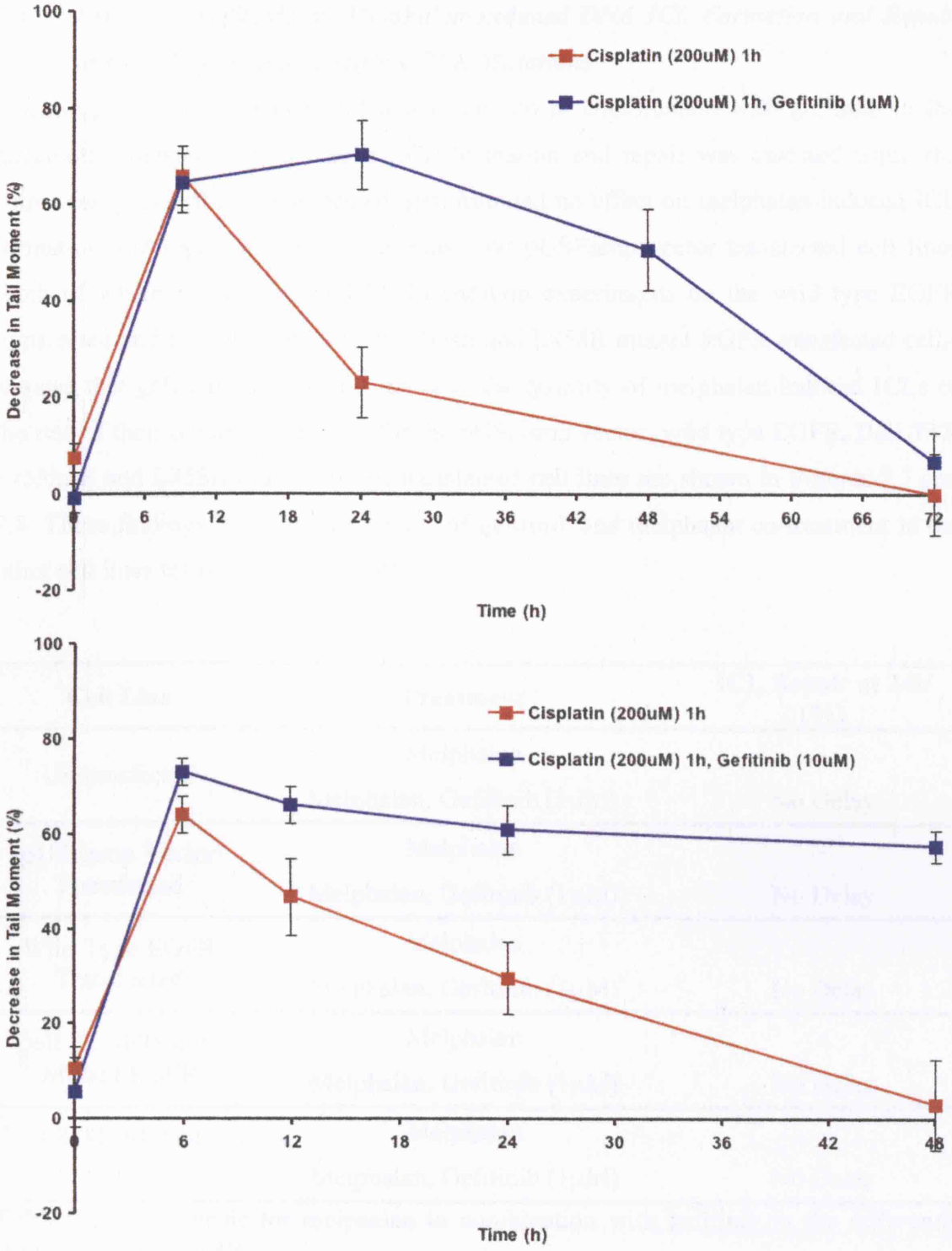

Figure 7.6: *Measurement of cisplatin-induced DNA ICL formation and repair alone and in the presence of gefitinib on L858R mutant EGFR transfected Cos-7 cells.* Cells were transfected with L858R mutant EGFR and stimulated with 100ng/μl EGF followed by cisplatin (200μM) for 1h and then incubated in fresh media or with gefitinib (1 or 10μM). ICL formation is measured as percentage decrease in tail moment. Data is a representation of three independent experiments; *bars*, SE.

7.4 *Effects of Gefitinib on Melphalan-Induced DNA ICL Formation and Repair in Cells Expressing Specific EGFR Mutations*

Following incubation with melphalan alone and in combination with gefitinib in the differently transfected Cos-7 cells, ICL formation and repair was assessed using the comet assay as before. As expected, gefitinib had no effect on melphalan-induced ICL formation and repair in the untransfected and pUSEamp vector transfected cell lines (both of which express no EGFR). In addition experiments on the wild type EGFR transfected and both the DelL747-P753insS and L858R mutant EGFR transfected cells, showed that gefitinib at 1μM did not alter the quantity of melphalan-induced ICLs or the rate of their repair. The results for the pUSEamp vector, wild type EGFR, DelL747-P753insS and L858R mutant EGFR transfected cell lines are shown in Figures 7.7 and 7.8. These findings reinforce the results of gefitinib and melphalan co-treatment in the other cell lines tested (see Chapter 4).

Cell Line	Treatment	ICL Repair at 24h (%)
Untransfected	Melphalan	-
	Melphalan, Gefitinib (1μM)	No Delay
pUSEamp Vector Transfected	Melphalan	-
	Melphalan, Gefitinib (1μM)	No Delay
Wild Type EGFR Transfected	Melphalan	-
	Melphalan, Gefitinib (1μM)	No Delay
DelL747-P753insS Mutant EGFR	Melphalan	-
	Melphalan, Gefitinib (1μM)	No Delay
L858R Mutant EGFR	Melphalan	-
	Melphalan, Gefitinib (1μM)	No Delay

Table 7.3: ICL repair for melphalan in combination with gefitinib in the differently transfected Cos-7 cells.

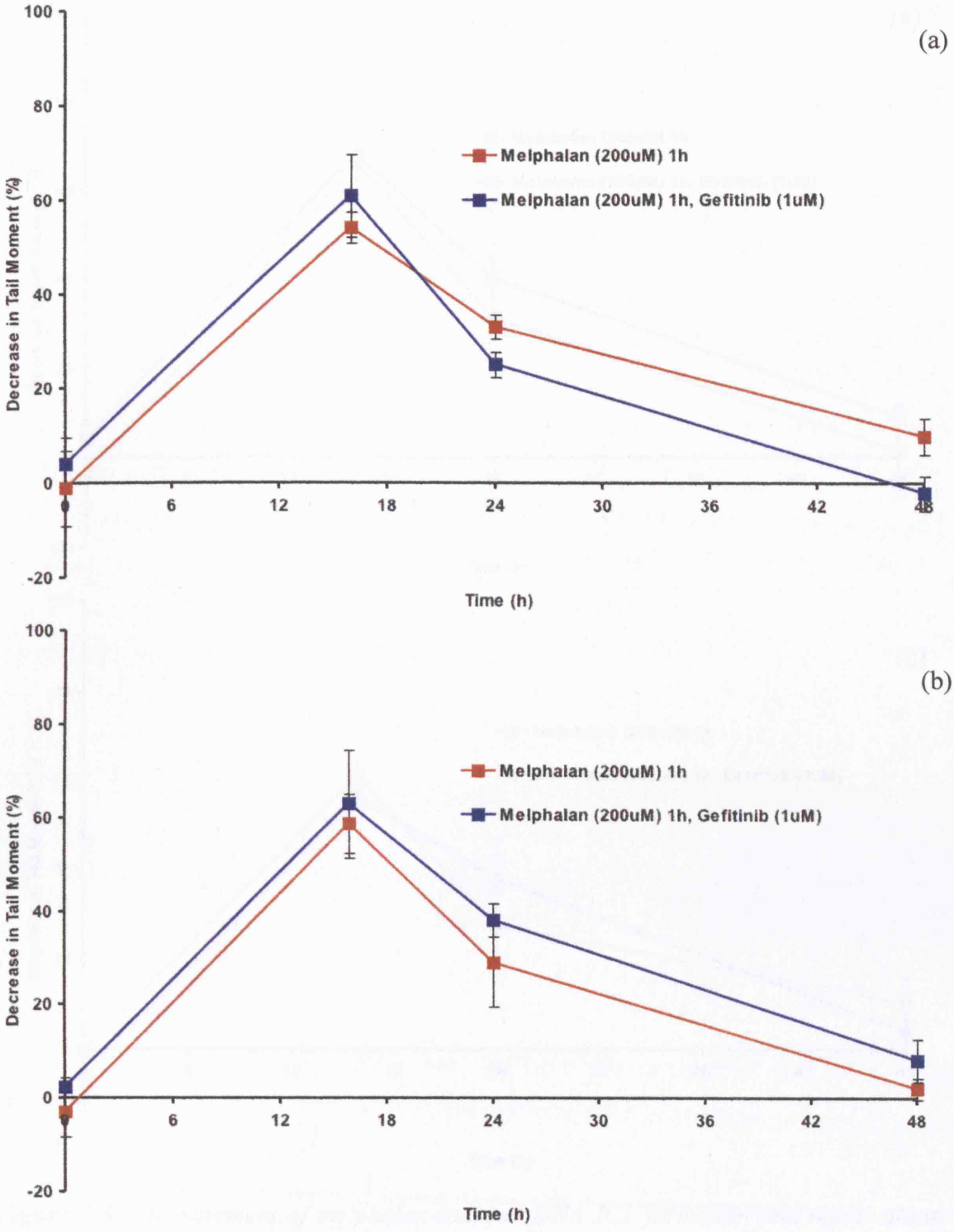

Figure 7.7: *Measurement of melphalan-induced DNA ICL formation and repair alone and in the presence of gefitinib on pUSEamp vector or Wild Type EGFR transfected Cos-7 cells.* Cells were transfected with (a) vector or (b) wild type EGFR and stimulated with 100ng/μl EGF followed by melphalan (200μM) for 1h and then incubated in fresh media or with gefitinib (1μM). ICL formation is measured as percentage decrease in tail moment. Data is a representation of three independent experiments; *bars*, SE.

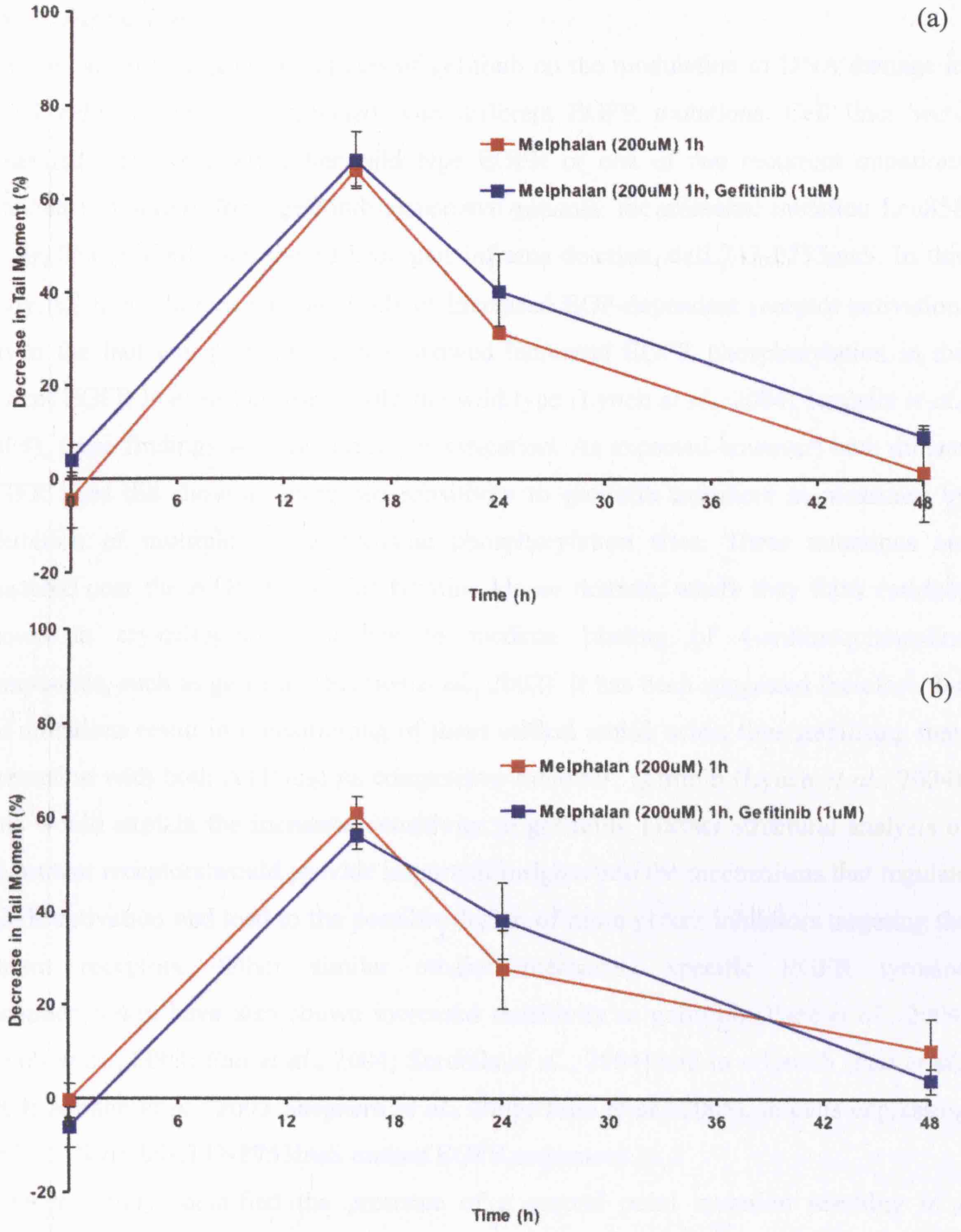

Figure 7.8: *Measurement of melphalan-induced DNA ICL formation and repair alone and in the presence of gefitinib on DelL747-P753insS or L858R EGFR mutations transfected Cos-7 cells.* Cells were transfected with (a) DelL747-P753insS or (b) L858R and stimulated with 100ng/μl EGF followed by melphalan (200μM) for 1h and then incubated in fresh media or with gefitinib (1μM). ICL formation is measured as percentage decrease in tail moment. Data is a representation of three independent experiments; *bars*, SE.

7.5 Discussion

This chapter investigated the effects of gefitinib on the modulation of DNA damage in Cos-7 cells transiently transfected with different EGFR mutations. Cell lines were generated that expressed either wild type EGFR or one of two recurrent mutations detected in tumours from gefitinib-responsive patients: the missense mutation Leu858 → Arg858 (L858R) and the 18 base pair inframe deletion, delL747-P753insS. In this study, all lines showed similar levels of increased EGF-dependent receptor activation. Given the fact that previous studies showed increased EGFR phosphorylation in the mutant EGFR lines as compared with the wild type (Lynch *et al.*, 2004; Sordella *et al.*, 2004), these findings warrant further investigation. As expected however, both mutant EGFR lines did show an increased sensitivity to gefitinib treatment as measured by inhibition of multiple EGFR tyrosine phosphorylation sites. These mutations are clustered near the ATP cleft of the tyrosine kinase domain, where they flank residues shown in crystallographic studies to mediate binding of 4-anilinoquinazoline compounds, such as gefitinib (Stamos *et al.*, 2002). It has been suggested therefore that the mutations result in repositioning of these critical amino acids, thus stabilising their interaction with both ATP and its competitive inhibitor, gefitinib (Lynch *et al.*, 2004). This would explain the increased sensitivity to gefitinib. Further structural analysis of the mutant receptors would provide important insights into the mechanisms that regulate EGFR activation and lead to the possible design of more potent inhibitors targeting the mutant receptors. Other similar studies measuring specific EGFR tyrosine phosphorylation have also shown increased sensitivity to gefitinib (Paez *et al.*, 2004; Lynch *et al.*, 2004; Pao *et al.*, 2004; Sordella *et al.*, 2004) and to erlotinib (Pao *et al.*, 2004; Amann *et al.*, 2005 Shepherd *et al.*, 2005; Tsao *et al.*, 2005), in cells expressing the L858R or delL747-P753insS mutant EGFR sequences.

A recent study identified the presence of a second point mutation resulting in a threonine-to-methionine amino acid change at position 790 of EGFR (See Table 7.1). Patients with advanced NSCLC expressing this mutant *EGFR* gene had a relapse after two years of complete remission during treatment with gefitinib (Kobayashi *et al.*, 2005). Structural modelling and biochemical studies showed that this second mutation led to gefitinib resistance. This was due to steric hindrance as a result of the bulkier methionine side chain in the ATP-kinase-binding pocket (Kobayashi *et al.*, 2005). The identification of a second mutation in the *EGFR* gene rendering resistancy to gefitinib

treatment suggests that the tumour cells remain dependent on an active EGFR pathway for their proliferation. Interestingly, another recent study has identified a family with multiple cases of NSCLC associated with germline transmission of the T790M mutation. They report that four of the six tumours analysed showed a secondary somatic activating *EGFR* mutation, arising in *cis* with the germline EGFR mutation T790M (Bell *et al.*, 2005). These observations implicate altered EGFR signalling in genetic susceptibility to lung cancer.

In chronic myeloid leukaemia and gastrointestinal stromal tumours, the two main mechanisms of resistance to imatinib (Gleevec) are point mutations or amplification of the *BCR-ABL* gene (Gorre *et al.*, 2001; Azam *et al.*, 2003). Knowledge of these mechanisms has led to the development of second-line BCR-ABL inhibitors (Shah *et al.*, 2004). Interestingly, one of the most common imatinib resistance mutations in BCR-ABL replaces threonine at position 315 (the amino acid structurally corresponding to T790 of EGFR) with isoleucine in the ABL tyrosine kinase domain, leading to a structural change very similar to that observed with EGFR T790M (Gorre *et al.*, 2001; Kobayashi *et al.*, 2005). Such studies may guide the selection of second-generation EGFR-inhibitor therapy.

As discussed in Chapter 4, co-treatment with gefitinib delayed the repair of cisplatin-induced ICLs but had no effect on repair of ICLs induced by melphalan in all cell lines tested. Experiments in this chapter show that gefitinib had no effect on the amount of cisplatin-induced ICL formation or the rate of its repair in cells expressing no EGFR. Interestingly, in cells transfected with wild type EGFR, whilst ICLs induced by cisplatin alone were repaired after 24h, a striking inhibition of DNA repair was seen in the presence of 10μM gefitinib, with ICLs still persisting after 24h. Given that similar results were found in the other cell lines tested (Chapter 4), this data reinforces the suggestion that co-treatment with gefitinib alters the downstream processing of cisplatin-induced DNA ICLs leading to a delay in the rate of their repair. Importantly therefore, the experiments in this chapter suggest it is unlikely that the effects on DNA repair of 10μM gefitinib treatment are due to inhibition of pathways other than EGFR. This is reinforced by a recent study which investigated the kinase specificity for 20 clinical kinase inhibitors including gefitinib and erlotinib (Fabian *et al.*, 2005). The

study confirms the high level of specificity for EGFR these agents have over the other 119 protein kinases. Kinase specificity dendrograms are shown in Figure 7.9.

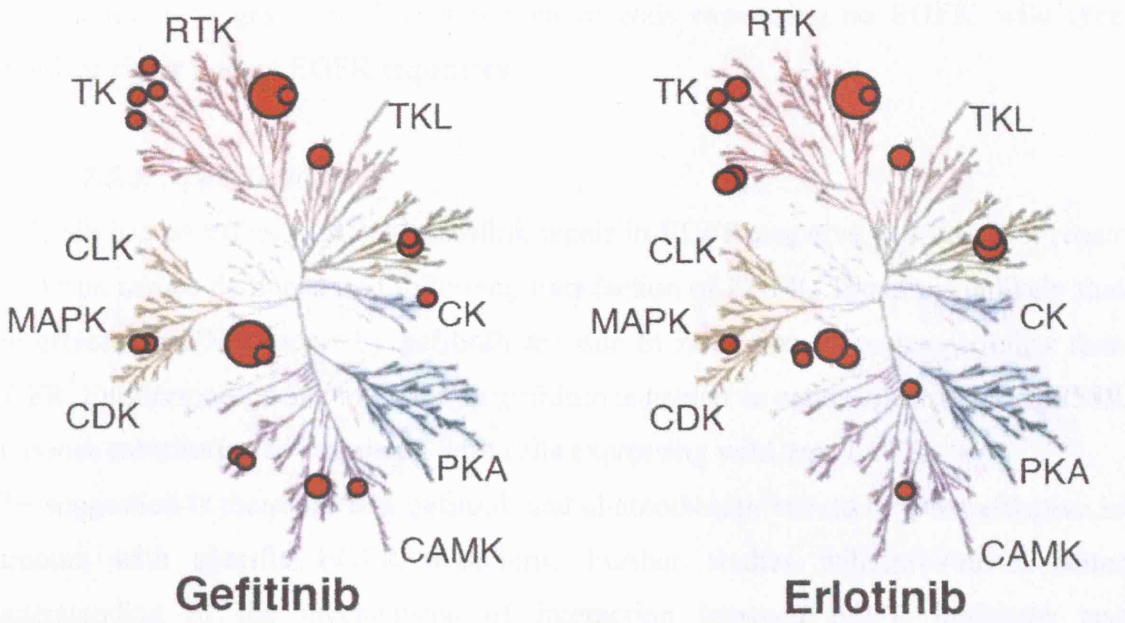

Figure 7.9: Kinase specificity dendrograms for gefitinib and erlotinib.
Source: M.A. Fabian et al., Nature Biotechnology, 2005.

Furthermore, Fabian *et al.*, (2005), show that the mutations in the EGFR tyrosine kinase domain which confer sensitivity to gefitinib do not fundamentally affect the intrinsic interaction between the ATP site of EGFR and small molecule EGFR inhibitors.

Experiments on the delL747-P753insS mutants showed that although gefitinib (10μM) delayed repair of cisplatin ICLs, the effect was comparable with that seen in wild type EGFR transfected cells. Given that the delL747-P753insS mutant has increased sensitivity to gefitinib, the reasons as to why this does not lead to an in increased delay in cisplatin-induced ICL repair as compared to the wild type line warrants further investigation. Experiments on the L858R mutant line showed that gefitinib at 1μM, which has little effect on cells expressing wild type EGFR, induced a marked increase in delay of cisplatin-induced damage with peak of ICLs still persisting after 48h as compared with complete repair seen at 24h for cisplatin alone. It is important to investigate further the altered cellular response in cells expressing the L858R missense substitution which lead to increased delay in repair of cisplatin-induced ICLs as a result of co-treatment with gefitinib.

Furthermore, and as was seen with MCF-7 and AR42J cells (Chapter 4), there was again no modulation in the kinetics of DNA repair following treatment with melphalan in combination with gefitinib. This was seen in cells expressing no EGFR, wild type EGFR or either mutant EGFR sequences.

7.5.1 Conclusions

Gefitinib has no effect on DNA crosslink repair in EGFR-negative cell lines but repair inhibition can be demonstrated following transfection of EGFR. Thus, it is unlikely that the effects on DNA repair by gefitinib are due to inhibition of pathways other than EGFR. Furthermore, delay in repair by gefitinib is greater in cells expressing the L858R missense substitution as compared with cells expressing wild type EGFR.

The suggestion is therefore that gefitinib and chemotherapy would be most effective in tumours with specific EGFR mutations. Further studies will provide a better understanding of the mechanisms of interaction between EGFR inhibitors and chemotherapy in these cells and will ultimately be important in devising novel schedules and combinations for testing in the clinic.

CHAPTER 8

CONCLUSIONS AND FUTURE WORK

EGFR is commonly expressed in human tumours and provides an important target for therapy. Several classes of agents including small molecule inhibitors and antibodies are currently under clinical development. These agents have shown interaction with chemotherapeutic agents *in vitro* and *in vivo*. However, the mechanisms of these interactions are not clearly understood. The purpose of this study was to investigate mechanisms for this modulation.

Chapter 3 focused on the synergistic effects of the EGFR inhibitor gefitinib (Iressa^{TM}, ZD1839) in combination with a variety of chemotherapeutic agents in several cancer cell lines and was analysed pharmacologically. Synergy was found with the topoisomerase II poison, etoposide; the topoisomerase II intercalating agent, doxorubicin and the DNA crosslinking platinum based compound, cisplatin. Interestingly no synergy was found with the DNA crosslinking alkylating agent, melphalan, in any of the cell lines tested. Using the alkaline single-cell gel electrophoresis (comet) assay, the kinetics of DNA damage and repair following treatment with these chemotherapeutic drugs combined with gefitinib were investigated. These results are presented in **Chapters 4** and demonstrated a delay in repair of DNA strand breaks and inter-strand cross-links (ICLs) by gefitinib following treatment with etoposide and cisplatin respectively. In addition (**Chapter 7**), gefitinib had no effect on the processing of cisplatin-induced DNA damage in cells expressing no EGFR. Once transformed with wild type EGFR, gefitinib delayed the repair of cisplatin-induced lesions. This confirms that repair is mediated through the EGFR pathway and that this is modulated by co-treatment with gefitinib. Furthermore, cells expressing specific EGFR tyrosine kinase mutations have an increased sensitivity to gefitinib coupled with an increased delay in repair of cisplatin-induced DNA damage as compared with wild type EGFR. In contrast, no alteration in melphalan-induced ICL formation and repair was seen following co-treatment with gefitinib in any of the cell lines tested.

Chapter 5 focused on the modulation of the DNA repair protein DNA-PK, by gefitinib and was quantitated using a variety of techniques including immunoprecipitations, immunoblotting, cellular fraction extractions and confocal microscopy. These experiments suggested that gefitinib treatment induces a cellular re-distribution of DNA-PK from the nucleus to the cytosol, a physical interaction between EGFR and the DNA-PK complex, and a fall in DNA-PK functional activity. Furthermore, in **Chapter 6**, the effects of inhibiting DNA-PK activity with LY294002, wortmannin and siRNA to

its catalytic subunit (DNA-PK_{CS}) were investigated in the same cancer cell lines and compared with the effects of gefitinib. These direct interferences with the DNA-PK pathway mimicked the effects of EGFR inhibition by gefitinib.

These experiments leave many further questions unanswered. Some of the key issues are briefly outlined below.

8.1 Synergistic Interactions Between Gefitinib and Chemotherapeutic Agents

It is important to investigate whether gefitinib has the same synergistic properties with all chemotherapeutic agents of the same class. As with cisplatin, it would be interesting to see if synergy occurs with other platinum-based compounds such as oxaliplatin or carboplatin, and as with melphalan, not with nitrogen mustard. As discussed in Chapter 1, novel chemical approaches have been made in recent years to address the cellular, molecular and genetic basis of cancer in the hope of designing effective therapies (Neidle & Thurston, 2005). They exploit the structure and reactivity of small molecules and macromolecules and the chemical interactions associated with them. Molecules in development include those that selectively target a unique DNA sequence which inhibit transcription. An example of this is SJG-136, a pyrrolobenzodiazepine (PBD) dimer novel minor-groove ICL agent (Gregson *et al.*, 2001; Hartley *et al.*, 2004). It would be of interest to investigate whether there is any increased synergistic interactions between these potentially more potent DNA crosslinking agents and gefitinib.

If synergy with gefitinib does discriminate between different classes of agents, understanding the differences in their modes of action (i.e. types of DNA damage and the repair pathways they require) would provide a better understanding of the molecular mechanisms of interaction leading to novel schedules and combinations for testing in the clinic.

As discussed in Chapter 3, the synergy with gefitinib is dependent on the administering schedule. Indeed, synergy with cisplatin is only seen when gefitinib treatment is preceded by cisplatin suggesting that gefitinib modulates the processing of cisplatin-induced DNA damage. In addition to further studies on scheduling with DNA damaging agents, it would be important to address whether synergy between gefitinib and non-DNA damaging agents also exists and whether this too is dependent on the administering schedule. As discussed in Chapter 3, it has been reported that sequential therapy of EGFR inhibition followed by the G_2/M blocking agents paclitaxel and

vinblastine, antagonised effects of EGFR inhibitors (Piperdi *et al.*, 2004). Furthermore, synergistic interactions between gefitinib and non-DNA damaging chemotherapeutic agents such as paclitaxel and 5'-FU have also been reported but schedule-dependent experiments were not included (Sirtonak *et al.*, 2000; Ciardiello *et al.*, 2000; Magné *et al.*, 2002).

In contrast to the preclinical data, and as discussed in Chapters 1 and 3, four large phase III clinical trials in patients with either locally advanced stage III disease or stage IV NSCLC failed to show any benefit for combined treatment with cisplatin, carboplatin, gemcitabine and paclitaxel (Giaccone *et al.*, 2004; Herbst *et al.*, 2004; Gatzemeier *et al.*, 2004). The reasons for these mixed results are unknown and an antagonistic effect of combined treatments cannot be excluded (Baselga, 2004). A similar situation to the scenario of the schedule-dependent antagonism observed between tamoxifen and chemotherapy in the adjuvant treatment of breast cancer may well be the reason (Baselga & Arteaga, 2005). It should be noted however, that a recent study reported that the combination of gemcitabine and erlotinib did improve the survival and progression free survival in advanced pancreatic cancer as compared to gemcitabine alone (Moore *et al.*, 2005). Although this was modest, it does demonstrate that there are at least additive effects for combining chemotherapy with quinazoline-based small molecule inhibitors in the clinic.

Gefitinib co-treatment on cells expressing the L858R missense EGFR tyrosine kinase mutation showed an increased delay in repair of cisplatin-induced ICLs as compared with cells expressing wild type EGFR (Chapters 4 & 7). It would be interesting to investigate whether there is also an increased synergistic interaction and therefore increased sensitivity to specific chemotherapeutic agents. No delay in melphalan-induced ICLs was detected in any of the mutant EGFR cell lines. Nonetheless, it is important to determine whether gefitinib increases sensitivity to melphalan in these cell lines with regard to inhibition of proliferation.

8.2 Effects of Gefitinib on Chemotherapy-Induced DNA Damage and Repair

The comet assay was originally developed as a method to measure DNA strand breaks in a single cell population (Ostling & Johanson, 1984) and has been modified to study ICL formation and repair (Spanswick *et al.*, 1999). An intriguing aspect of ICL repair is that several repair pathways are activated to remove or bypass an ICL. As discussed in

Chapter 1, the type and frequency of DNA lesions due to cisplatin differ from those produced by melphalan. In contrast to the repair of ICLs produced by melphalan (Clingen *et al.*, 2005), repair of cisplatin ICLs does not involve the formation of DNA double-strand breaks and the repair pathways they require (De Silva *et al.*, 2002). The increased cytotoxic effects of ICLs induced by cisplatin and melphalan can be associated with defects in the XPF-ERCC1 heterodimer component of the NER pathway and in XRCC2 and XRCC3 (Rad51 paralogues) involved in the HR pathway (De Silva *et al.*, 2002; Clingen *et al.*, 2005). It would be interesting to investigate what the effects of gefitinib co-treatment are on repair of cisplatin or melphalan-induced ICLs in cells defective in any of these repair pathway components. As discussed in Chapter 4, pulsed field gel electrophoresis (PFGE) can be used for analysis of DSBs. In addition, three PCR-based methods have been described (Grimaldi *et al.*, 2002) that allow covalent drug-DNA adducts, and their repair, to be studied at various levels of resolution from gene regions to the individual nucleotide level in single copy genes. These are: a quantitative PCR (QPCR) method which measures the total damage on both DNA strands in a gene region, usually between 300 and 3,000 base pairs in length, strand-specific QPCR which measures damage in the same region as QPCR but in a strand-specific manner and single-strand ligation PCR which detects adduct formation at the level of single nucleotides, on individual strands, in a single copy gene in mammalian cells (Grimaldi *et al.*, 2002). These types of further experiments on the specific forms of DNA damage as a result of co-treatment of cisplatin or melphalan with gefitinib may provide a better understanding of the mechanisms for the differences in inhibition of repair.

The further experiments on DNA damage and repair outlined above may provide an insight into the mechanism for increased sensitivity in cell lines with specific EGFR mutations.

8.3 EGFR and DNA-PK Physical Interactions

To evaluate the stoichiometry of gefitinib-induced interactions between DNA-PK and EGFR, deletion constructs expressing either protein can be generated and, following gefitinib treatment, co-immunoprecipitations done as before (Chapter 5). The use of GST-bound fusion proteins would be a useful tool for determining the specific regions of each protein involved in their interaction. Identifying these regions could have

potential pharmacological and commercial implications for the designing of specific novel inhibitors such as peptide mimetics as well as perhaps biological relevance in the role of EGFR and DNA-PK in DNA repair following chemotherapy and/or gefitinib treatment.

Furthermore, it would be important to determine the effects of gefitinib on EGFR/DNA-PK association in cells expressing specific mutations.

8.4 EGFR and DNA-PK Subcellular Distribution

As discussed in Chapter 5, there is evidence for the cytosolic localisation of DNA-PK and EGFR to lipid rafts which results in altered tyrosine phosphorylation and kinase activity (Lucero *et al.*, 2003; Chen *et al.*, 2002; Westover *et al.*, 2003). With the use of cholesterol and cholesterol oxidase assays (Westover *et al.*, 2003), it would be interesting to investigate whether gefitinib treatment results in the co-localisation of EGFR and DNA-PK_{CS} to lipid rafts.

8.5 EGFR as a Transcription Factor

In the nucleus, EGFR has been shown to physically interact with STAT3 leading to transcriptional activation of iNOS and resulting in increased DNA-PK activity and subsequent DNA repair (Lin *et al.*, 2001; Lo *et al.*, 2005b) Furthermore, it has been shown that both ionising radiation and cisplatin triggers increased EGFR translocation into the nucleus (Dittmann *et al.*, 2005a). Inhibition of EGFR with cetuximab was shown to block EGFR import and radiation-induced activation of DNA-PK and immobilise an EGFR/DNA-PK complex in the cytoplasm (Dittmann *et al.*, 2005b). Results from experiments in Chapter 5 show that cells exposed to gefitinib also showed a decrease in nuclear EGFR levels. Further studies should be carried out to determine whether cisplatin-induced EGFR nuclear translocation is inhibited by co-treatment with gefitinib. Furthermore, similar studies on the mutant EGFR cell lines and other specific EGFR deletion constructs will enable the mapping of the EGFR regions involved in transcriptional activation. It would also be interesting to investigate whether melphalan has any effect of EGFR transcriptional activity and whether or not this too is inhibited by co-treatment with gefitinib.

8.6 Conclusion

In conclusion, these results highlight the important effects EGFR inhibitors have on DNA repair and its associated machinery when added in combination with specific chemotherapeutic agents. It would be interesting to extend the study to include other related receptor tyrosine kinases such as HER-2 and VEGFR. These results will form the design of further clinical schedules combining these classes of agents and point the way to further studies to investigate the molecular mechanisms of these interactions.

REFERENCES

Aboud-Pirak E, Hurwitz E, Pirak ME, Bellot F, Schlessinger J, Sela M. Efficacy of antibodies to epidermal growth factor receptor against KB carcinoma in vitro and in nude mice. J Natl Cancer Inst. 1988; 80: 1605-11.

Adachi N, Suzuki H, Iiizumi S, Koyama H. Hypersensitivity of nonhomologous DNA end-joining mutants to VP-16 and ICRF-193: implications for the repair of topoisomerase II-mediated DNA damage. J Biol Chem. 2003; 278: 35897- 902.

Akita RW, Sliwkowski MX. Preclinical studies with Erlotinib (Tarceva). Semin Oncol. 2003; 30 (3 Suppl 7): 15-24.

Albanell J, Rojo F, Baselga J. Pharmacodynamic studies with the epidermal growth factor receptor tyrosine kinase inhibitor ZD1839. Semin Oncol. 2001; 28 (5 Suppl 16): 56-66.

Albanell J, Rojo F, Averbuch S, Feyereislova A, Mascaro JM, Herbst R, LoRusso P, Rischin D, Sauleda S, Gee J, Nicholson RI, Baselga J. Pharmacodynamic studies of the epidermal growth factor receptor inhibitor ZD1839 in skin from cancer patients: histopathologic and molecular consequences of receptor inhibition. J Clin Oncol. 2002; 20: 110-124.

Allart B, Lehtolainen P, Yla-Herttuala S, Martin JF and Selwood DL. A stable Bis-Allyloxycarbonyl biotin aldehyde derivative for biotinylation via reductive alkylation: Application to the synthesis of a biotinylated doxorubicin derivative. Bioconjugate Chem. 2003; 14: 187-194.

Amann J, Kalyankrishna S, Massion PP, Ohm JE, Girard L, Shigematsu H, Peyton M, Juroske D, Huang Y, Stuart Salmon J, Kim YH, Pollack JR, Yanagisawa K, Gazdar A, Minna JD, Kurie JM, Carbone DP. Aberrant epidermal growth factor receptor signaling and enhanced sensitivity to EGFR inhibitors in lung cancer. Cancer Res. 2005; 65: 226-35.

Arany I, Megyesi JK, Kaneto H, Price PM, Safirstein RL. Cisplatin-induced cell death is EGFR/src/ERK signaling dependent in mouse proximal tubule cells. Am J Physiol Renal Physiol. 2004; 287: F543-9.

Azam M, Latek RR, Daley GQ. Mechanisms of autoinhibition and STI-571/imatinib resistance revealed by mutagenesis of BCR-ABL. Cell. 2003; 112: 831-43.

Bakalkin G, Yakovleva T, Selivanova G, Magnusson KP, Szekely L, Kiseleva E, Klein G, Terenius L, Wiman KG. p53 binds single-stranded DNA ends and catalyzes DNA renaturation and strand transfer. Proc Natl Acad Sci USA. 1994; 4: 91(1): 413-7.

Bancroft CC, Chen Z, Yeh J, Sunwoo JB, Yeh NT, Jackson S, Jackson C, Van Waes C. Effects of pharmacologic antagonists of epidermal growth factor receptor, PI3K and MEK signal kinases on NF-kappaB and AP-1 activation and IL-8 and VEGF expression in human head and neck squamous cell carcinoma lines. Int J Cancer. 2002; 99: 538-48.

Bandyopadhyay D, Mandal M, Adam L, Mendelsohn J, Kumar R. Physical interaction between epidermal growth factor receptor and DNA-dependent protein kinase in mammalian cells. J Biol Chem. 1998; 273: 1568-73.

Barker AJ, Gibson KH, Grundy W, Godfrey AA, Barlow JJ, Healy MP, Woodburn JR, Ashton SE, Curry BJ, Scarlett L, Henthorn L, Richards L. Studies leading to the identification of ZD1839 (IRESSA): an orally active, selective epidermal growth factor receptor tyrosine kinase inhibitor targeted to the treatment of cancer. Bioorg Med Chem Lett. 2001; 11: 1911-4.

Baselga J, Norton L, Masui H, Pandiella A, Coplan K, Miller WH Jr, Mendelsohn J. Antitumor effects of doxorubicin in combination with anti-epidermal growth factor receptor monoclonal antibodies. J Natl Cancer Inst. 1993 Aug; 85: 1327-33.

Baselga J, Rischin D, Ranson M, Calvert H, Raymond E, Kieback DG, Kaye SB, Gianni L, Harris A, Bjork T, Averbuch SD, Feyereislova A, Swaisland H, Rojo F, Albanell J. Phase I safety, pharmacokinetic, and pharmacodynamic trial of ZD1839, a selective oral epidermal growth factor receptor tyrosine kinase inhibitor, in patients with five selected solid tumor types. J Clin Oncol. 2002; 20: 4292-302.

Baselga J, Trigo JM, Bourthis J. Cetuximab (C225) plus cisplatin/carboplatin is active in patients (pts) with recurrent/metastatic squamous cell carcinoma of the head and neck (SCCHN) progressing on a same dose and schedule platinum based agent. Proc Am Soc Clin Oncol. 2002; 21: 226a, (abstr 900).

Baselga J. Combining the anti-EGFR agent gefitinib with chemotherapy in non-small-cell lung cancer: how do we go from INTACT to impact? J Clin Oncol. 2004; 22: 759-61.

Baselga J, Arteaga CL. Critical update and emerging trends in epidermal growth factor receptor targeting in cancer. J Clin Oncol. 2005; 23: 2445-59.

Batra SK, Castelino-Prabhu S, Wikstrand CJ, Zhu X, Humphrey PA, Friedman HS, Bigner DD. Epidermal growth factor ligand-independent, unregulated, cell-transforming potential of a naturally occurring human mutant EGFRvIII gene. Cell Growth Differ. 1995; 6: 1251-9.

Batty DP and Wood RD. Damage recognition in nucleotide excision repair of DNA. Gene. 2000; 241: 193-204.

Bell DW, Gore I, Okimoto RA, Godin-Heymann N, Sordella R, Mulloy R, Sharma SV, Brannigan BW, Mohapatra G, Settleman J, Haber DA. Inherited susceptibility to lung cancer may be associated with the T790M drug resistance mutation in EGFR. Nat Genet. 2005; Ahead of print.

Benhar M, Dalyot I, Engelberg D, Levitzki A. Enhanced ROS production in oncogenically transformed cells potentiates c-Jun N-terminal kinase and p38 mitogen-activated protein kinase activation and sensitization to genotoxic stress. Mol Cell Biol. 2001; 21: 6913-2.

Benhar M, Engelberg D, Levitzki A. Cisplatin-induced activation of the EGF receptor. Oncogene. 2002; 21: 8723-31.

Bernier J, Hall EJ, Giaccia A. Radiation oncology: a century of achievements. Nat Rev Cancer. 2004; 4:737-47.

Bianco C, Bianco R, Tortora G, Damiano V, Guerrieri P, Montemaggi P, Mendelsohn J, De Placido S, Bianco AR, Ciardiello F. Antitumor activity of combined treatment of human cancer cells with ionizing radiation and anti-epidermal growth factor receptor monoclonal antibody C225 plus type I protein kinase A antisense oligonucleotide. Clin Cancer Res. 2000; 6: 4343-50.

Bianco C, Tortora G, Bianco R, Caputo R, Veneziani BM, Caputo R, Damiano V, Troiani T, Fontanini G, Raben D, Pepe S, Bianco AR, Ciardiello F. Enhancement of antitumor activity of ionizing radiation by combined treatment with the selective epidermal growth factor receptor-tyrosine kinase inhibitor ZD1839 (Iressa). Clin Cancer Res. 2002; 8: 3250-8.

Bier H, Hoffmann T, Haas I, van Lierop A. Anti-(epidermal growth factor) receptor monoclonal antibodies for the induction of antibody-dependent cell-mediated cytotoxicity against squamous cell carcinoma lines of the head and neck. Cancer Immunol Immunother. 1998; 46: 167-73.

Blackledge G, Averbuch S. Gefitinib ('Iressa', ZD1839) and new epidermal growth factor receptor inhibitors. Br J Cancer. 2004; 90: 566-72.

Block WD, Yu Y, Merkle D, Gifford JL, Ding Q, Meek K, Lees-Miller SP. Autophosphorylation-dependent remodelling of the DNA-dependent protein kinase catalytic subunit regulates ligation of DNA ends. Nucleic Acids Res. 2004; 32: 4351-7.

Blume-Jensen P and Hunter T. Oncogenic kinase signalling. Nature. 2001; 411: 355-65.

Bogue MA, Jhappan C, Roth DB. Analysis of variable (diversity) joining recombination in DNA-dependent protein kinase (DNA-PK)-deficient mice reveals DNA-PK-independent pathways for both signal and coding joint formation. Proc Natl Acad Sci USA. 1998; 95:15559-64.

Bonner JA, Raisch KP, Trummell HQ, Robert F, Meredith RF, Spencer SA, Buchsbaum DJ, Saleh MN, Stackhouse MA, LoBuglio AF, Peters GE, Carroll WR, Waksal HW. Enhanced apoptosis with combination C225/radiation treatment serves as the impetus for clinical investigation in head and neck cancers. J Clin Oncol. 2000; 18 (21 Suppl): 47S-53S.

Bonner JA, Giralt J, Harari PM, Cohen R, Jones C, Sur RK, et al. Cetuximab prolongs survival in patients with locoregionally advanced squamous cell carinoma of head and neck: a phase III study of high dose radiation therapy with or without cetuximab. Proc Am Soc Clin Oncol. 2004; abstr 5507.

Boos G, Stopper H. Genotoxicity of several clinically used topoisomerase II inhibitors. Toxicol Lett. 2000; 116: 7-16.

Borrell-Pages M, Rojo F, Albanell J, Baselga J, Arribas J. TACE is required for the activation of the EGFR by TGF-alpha in tumors. EMBO J. 2003; 22: 1114-24.

Boskovic, J., Rivera-Calzada, A., Maman, J.D., Chaco´n, P., Willison, K.R., Pearl, L.H., Llorca, O. Visualization of DNA-induced conformational changes in the DNA repair kinase DNA-PKcs. The EMBO Journal.2003; 22, 5875-5882.

Boulton S, Kyle S, Durkacz BW. Mechanisms of enhancement of cytotoxicity in etoposide and ionising radiation-treated cells by the protein kinase inhibitor wortmannin. Eur J Cancer. 2000; 36: 535-41.

Brendel M and Ruhland A. Relationships between functionality and genetic toxicology of selected DNA-damaging agents. Mutation Res. 1984; 133: 51-85.

Brewerton, S.C., Dore, A.S., Drake, A.C.B., Leuther, K.K., Blundell, T.L. Structural analysis of DNA-PKcs: modelling of the repeat units and insights into the detailed molecular architecture. Journal of Structural Biology. 2004; 145: 295–306.

Brown JM, Wouters BG. Apoptosis, p53, and tumor cell sensitivity to anticancer agents. Cancer Res. 1999; 59: 1391-9.

Brummelkamp TR, Bernards R, Agami, R. A system for stable expression for short interfering RNAs in mammalian cells. Science. 2002; 296:550-553.

Burgess AW, Cho HS, Eigenbrot C, Ferguson KM, Garrett TP, Leahy DJ, Lemmon MA, Sliwkowski MX, Ward CW, Yokoyama S. An open-and-shut case? Recent insights into the activation of EGF/ErbB receptors. Mol Cell. 2003; 12: 541-52.

Burton DR, Woof J. Human antibody effector function. Adv Immunol. 1992; 51: 1-84.

Caldecott K, Banks G, Jeggo P. DNA double-strand break repair pathways and cellular tolerance to inhibitors of topoisomerase II. Cancer Res. 1990; 50: 5778-83.

Cambier N, Chopra R, Strasser A, Metcalf D, Elefanty AG. BCR-ABL activates pathways mediating cytokine independence and protection against apoptosis in murine hematopoietic cells in a dose-dependent manner. Oncogene. 1998; 16: 335-48.

Camp ER, Summy J, Bauer TW, Liu W, Gallick GE, Ellis LM. Molecular mechanisms of resistance to therapies targeting the epidermal growth factor receptor. Clin Cancer Res. 2005; 11: 397-405.

Campiglio M, Locatelli A, Olgiati C, Normanno N, Somenzi G, Vigano L, Fumagalli M, Menard S, Gianni L. Inhibition of proliferation and induction of apoptosis in breast cancer cells by the epidermal growth factor receptor (EGFR) tyrosine kinase inhibitor ZD1839 ('Iressa') is independent of EGFR expression level. J Cell Physiol. 2004; 198: 259-68.

Chan DW, Chen BP, Prithivirajsingh S, Kurimasa A, Story MD, Qin J, Chen DJ. Autophosphorylation of the DNA-dependent protein kinase catalytic subunit is required for rejoining of DNA double-strand breaks. Genes Dev. 2002; 16: 2333-8.

Chan KC, Knox WF, Gee JM, Morris J, Nicholson RI, Potten CS, Bundred NJ. Effect of epidermal growth factor receptor tyrosine kinase inhibition on epithelial proliferation in normal and premalignant breast. Cancer Res. 2002; 62: 122-8.

Chen G, Hitomi M. Dissociation of CDK2 from cyclin A in response to the topoisomerase II inhibitor etoposide in v-src-transformed but not normal NIH 3T3 cells. Exp Cell Res. 1999; 249: 327-36.

Chen X, Resh MD. Cholesterol depletion from the plasma membrane triggers ligand-independent activation of the epidermal growth factor receptor. J Biol Chem. 2002; 277: 49631-7.

Cho HS, Mason K, Ramyar KX, Stanley AM, Gabelli SB, Denney DW Jr, Leahy DJ. Structure of the extracellular region of HER2 alone and in complex with the Herceptin Fab. Nature. 2003; 421: 756-60.

Christodoulopoulos G, Muller C, Salles B, Kazmi R, Panasci L. Potentiation of chlorambucil cytotoxicity in B-cell chronic lymphocytic leukemia by inhibition of DNA-PK activity using wortmannin. Cancer Res. 1998; 58: 1789-92.

Chu G. Cellular responses to cisplatin. The roles of DNA-binding proteins and DNA repair. J Biol Chem. 1994; 269: 787-790.

Ciardiello F, Bianco R, Damiano V, De Lorenzo S, Pepe S, De Placido S, Fan Z, Mendelsohn J, Bianco AR, Tortora G. Antitumor activity of sequential treatment with topotecan and anti-epidermal growth factor receptor monoclonal antibody C225. Clin Cancer Res. 1999; 5: 909-16.

Ciardiello F, Caputo R, Bianco R, Damiano V, Pomatico G, De Placido S, Bianco AR, Tortora G. Antitumor effect and potentiation of cytotoxic drugs activity in human cancer cells by ZD1839 (Iressa), an epidermal growth factor receptor-selective tyrosine kinase inhibitor. Clin Cancer Res. 2000; 6: 2053-63.

Ciardiello F, Tortora G. A novel approach in the treatment of cancer: targeting the epidermal growth factor receptor. Clin Cancer Res. 2001; 7: 2958-70.

Ciardiello F, Tortora G. Epidermal growth factor receptor (EGFR) as a target in cancer therapy: understanding the role of receptor expression and other molecular determinants that could influence the response to anti-EGFR drugs. Eur J Cancer. 2003; 39: 1348-54.

Clingen PH, De Silva IU, McHugh PJ, Ghadessy FJ, Tilby MJ, Thurston DE, Hartley JA. The XPF-ERCC1 endonuclease and homologous recombination contribute to the repair of minor groove DNA interstrand crosslinks in mammalian cells produced by the pyrrolo[2,1-c][1,4]benzodiazepine dimer SJG-136. Nucleic Acids Res. 2005; 33: 3283-91.

Collis SJ, Swartz MJ, Nelson WG, DeWeese TL. Enhanced radiation and chemotherapy-mediated cell killing of human cancer cells by small inhibitory RNA silencing of DNA repair factors. Cancer Res. 2003; 63: 1550.

Collis SJ, DeWeese TL, Jeggo PA and Parker AR. The life and death of DNA-PK. Oncogene. 2005; 24: 949-961.

Cortes J, O'Brian S and Kantarjian H. Discontinuation of imatinib therapy after achieving a molecular response. Blood. 2004; 104: 2204-2205.

Cory S and Adams JM. The Bcl2 family: regulators of the cellular life-or-death switch. Nat Rev Cancer. 2002; 2: 647-656.

Critchlow SE, Jackson SP. DNA end-joining: from yeast to man. Trends Biochem Sci. 1998; 23: 394-8.

Cunningham D, Humblet Y, Siena S, Khayat D, Bleiberg H, Santoro A, Bets D, Mueser M, Harstrick A, Verslype C, Chau I, Van Cutsem E. Cetuximab monotherapy and cetuximab plus irinotecan in irinotecan-refractory metastatic colorectal cancer. N Engl J Med. 2004; 351: 337-45.

Daaka Y. G proteins in cancer: the prostate cancer paradigm. Sci STKE. 2004; 2004: re2.

Davies AA, Masson JY, McIlwraith MJ, Stasiak AZ, Stasiak A, Venkitaraman AR, West SC. Role of BRCA2 in control of the RAD51 recombination and DNA repair protein. Mol Cell. 2001; 7: 273-82.

Davis CG, Gallo ML, Corvalan JR. Transgenic mice as a source of fully human antibodies for the treatment of cancer. Cancer Metastasis Rev. 1999; 18: 421-5.

De Silva IU, McHugh PJ, Clingen PH, Hartley JA. Defects in interstrand cross-link uncoupling do not account for the extreme sensitivity of ERCC1 and XPF cells to cisplatin. Nucleic Acids Res. 2002; 30: 3848-56.

DeFazio LG, Stansel RM, Griffith JD, Chu G. Synapsis of DNA ends by DNA-dependent protein kinase. EMBO J. 2002; 21: 3192-200.

Deisseroth AB, Andreeff M, Champlin R. Chronic Leukemias. In: VT DeVita (editor), Cancer: principles and practice of oncology, 1994; 1965-1979, Philadelphia: JB Lippincott Co.

Deutsch E, Dugray A, AbdulKarim B, Marangoni E, Maggiorella L, Vaganay S, M'Kacher R, Rasy SD, Eschwege F, Vainchenker W, Turhan AG, Bourhis J. BCR-ABL down-regulates the DNA repair protein DNA-PKcs. Blood. 2001; 97: 2084-90.

DeVita VT, Hellman S, Rosenberg S. Cancer: Principles and practice of oncology. Lippincott Williams & Wilkins. 2005; Seventh Edition.

Di Gennaro E, Barbarino M, Bruzzese F, De Lorenzo S, Caraglia M, Abbruzzese A, Avallone A, Comella P, Caponigro F, Pepe S, Budillon A. Critical role of both p27KIP1 and p21CIP1/WAF1 in the antiproliferative effect of ZD1839 ('Iressa'), an epidermal growth factor receptor tyrosine kinase inhibitor, in head and neck squamous carcinoma cells. J Cell Physiol. 2003; 195: 139-50.

Ding Q, Reddy YV, Wang W, Woods T, Douglas P, Ramsden DA, Lees-Miller SP, Meek K. Autophosphorylation of the catalytic subunit of the DNA-dependent protein kinase is required for efficient end processing during DNA double-strand break repair. Mol Cell Biol. 2003; 23: 5836-48.

Dittmann K, Mayer C, Fehrenbacher B, Schaller M, Raju U, Milas L, Chen DJ, Kehlbach R, Rodemann HP. Radiation-induced Epidermal Growth Factor Receptor Nuclear Import Is Linked to Activation of DNA-dependent Protein Kinase. J Biol Chem. 2005a; 280: 31182-31189.

Dittmann K, Mayer C, Rodemann HP. Inhibition of radiation-induced EGFR nuclear import by C225 (Cetuximab) suppresses DNA-PK activity. Radiother Oncol. 2005b; 76: 157-161.

Dragoi AM, Fu X, Ivanov S, Zhang P, Sheng L, Wu D, Li GC, Chu WM. DNA-PKcs, but not TLR9, is required for activation of Akt by CpG-DNA. EMBO J. 2005; 24: 779-89.

Dronkert MLG and Kanaar R. Repair of DNA interstrand crosslinks. Mut Res. 2001; 486: 217-247.

Durant S, Karran P. Vanillins - A novel family of DNA-PK inhibitors. Nucleic Acids Res. 2003; 31: 5501-12.

Edwards E, Geng L, Tan J, Onishko H, Donnelly E, Hallahan DE. Phosphatidylinositol 3-kinase/Akt signaling in the response of vascular endothelium to ionizing radiation. Cancer Res. 2002; 62: 4671-7.

Ekstrand AJ, Sugawa N, James CD, Collins VP. Amplified and rearranged epidermal growth factor receptor genes in human glioblastomas reveal deletions of sequences encoding portions of the N- and/or C-terminal tails. Proc Natl Acad Sci USA. 1992; 89: 4309-13.

Espejel S, Martin M, Klatt P, Martin-Caballero J, Flores JM, Blasco MA. Shorter telomeres, accelerated ageing and increased lymphoma in DNA-PKcs-deficient mice. EMBO Rep. 2004; 5: 503-9.

Fabian MA, Biggs WH 3rd, Treiber DK, Atteridge CE, Azimioara MD, Benedetti MG, Carter TA, Ciceri P, Edeen PT, Floyd M, Ford JM, Galvin M, Gerlach JL, Grotzfeld RM, Herrgard S, Insko DE, Insko MA, Lai AG, Lelias JM, Mehta SA, Milanov ZV, Velasco AM, Wodicka LM, Patel HK, Zarrinkar PP, Lockhart DJ. A small molecule-kinase interaction map for clinical kinase inhibitors. Nat Biotechnol. 2005; 23: 329-36.

Fan Z, Shang BY, Lu Y, Chou JL, Mendelsohn J. Reciprocal changes in p27(Kip1) and p21(Cip1) in growth inhibition mediated by blockade or overstimulation of epidermal growth factor receptors. Clin Cancer Res. 1997; 3: 1943-8.

Fedi P, Pierce JH, di Fiore PP, Kraus MH. Efficient coupling with phosphatidylinositol 3-kinase, but not phospholipase C gamma or GTPase-activating protein, distinguishes ErbB-3 signaling from that of other ErbB/EGFR family members. Mol Cell Biol. 1994; 14: 492-500.

Feng J, Park J, Cron P, Hess D, Hemmings BA. Identification of a PKB/Akt hydrophobic motif Ser-473 kinase as DNA-dependent protein kinase. J Biol Chem. 2004; 279: 41189-96.

Ferguson KM. Active and inactive conformations of the epidermal growth factor receptor. Biochem Soc Trans. 2004; 32: 742-5.

Fichtinger-Shepman AM, Van der Veer JL, Den Hartog JH, Lohman PH and Reedijk J. Adducts of the anti-tumour drug cis-diamminedichloroplatinum(II) with DN: formation, identification and quantitaion. Biochemistry. 1985; 24: 707-13.

Franklin MC, Carey KD, Vajdos FF, Leahy DJ, de Vos AM, Sliwkowski MX. Insights into ErbB signaling from the structure of the ErbB2-pertuzumab complex. Cancer Cell. 2004; 5: 317-28.

Friedmann B, Caplin M, Hartley JA, Hochhauser D. Modulation of DNA repair in vitro after treatment with chemotherapeutic agents by the epidermal growth factor receptor inhibitor gefitinib (ZD1839). Clin Cancer Res. 2004; 10: 6476-86.

Fukuoka M, Yano S, Giaccone G, Tamura T, Nakagawa K, Douillard JY, Nishiwaki Y, Vansteenkiste J, Kudoh S, Rischin D, Eek R, Horai T, Noda K, Takata I, Smit E, Averbuch S, Macleod A, Feyereislova A, Dong RP, Baselga J. Multi-institutional randomized phase II trial of gefitinib for previously treated patients with advanced non-small-cell lung cancer (The IDEAL 1 Trial) [corrected] J Clin Oncol. 2003; 21: 2237-46.

Garcia R, Bowman TL, Niu G, Yu H, Minton S, Muro-Cacho CA, Cox CE, Falcone R, Fairclough R, Parsons S, Laudano A, Gazit A, Levitzki A, Kraker A, Jove R. Constitutive activation of Stat3 by the Src and JAK tyrosine kinases participates in growth regulation of human breast carcinoma cells. Oncogene. 2001; 20: 2499-513.

Gardembas M, Rousselot P, Tulliez M, Vigier M, Buzyn A, Rigal-Huguet F, Legros L, Michallet M, Berthou C, Cheron N, Maloisel F, Mahon FX, Facon T, Berthaud P, Guilhot J, Guilhot F; CML French Group. Results of a prospective phase 2 study combining imatinib mesylate and cytarabine for the treatment of Philadelphia-positive patients with chronic myelogenous leukemia in chronic phase. Blood. 2003; 102: 4298-305.

Garrett TP, McKern NM, Lou M, Elleman TC, Adams TE, Lovrecz GO, Zhu HJ, Walker F, Frenkel MJ, Hoyne PA, Jorissen RN, Nice EC, Burgess AW, Ward CW. Crystal structure of a truncated epidermal growth factor receptor extracellular domain bound to transforming growth factor alpha. Cell. 2002; 110: 763-73.

Garrett TP, McKern NM, Lou M, Elleman TC, Adams TE, Lovrecz GO, Kofler M, Jorissen RN, Nice EC, Burgess AW, Ward CW. The crystal structure of a truncated ErbB2 ectodomain reveals an active conformation, poised to interact with other ErbB receptors. Mol Cell. 2003; 11: 495-505.

Gatzemeier U, Pluzanska A, Szczesna A. Results of a phase III trial of erlotinib (OSI-774) combined with cisplatin and gemcitabine (GC) chemotherapy in advanced non-small cell lung cancer (NSCLC). ASCO Meeting Abstracts. 2004; 22: 617 (abstr 7010).

Gesbert F, Griffin JD. Bcr/Abl activates transcription of the Bcl-X gene through STAT5. Blood. 2000; 96: 2269-76.

Giaccone G, Herbst RS, Manegold C, Scagliotti G, Rosell R, Miller V, Natale RB, Schiller JH, Von Pawel J, Pluzanska A, Gatzemeier U, Grous J, Ochs JS, Averbuch SD, Wolf MK, Rennie P, Fandi A, Johnson DH. Gefitinib in combination with gemcitabine and cisplatin in advanced non-small-cell lung cancer: a phase III trial - INTACT 1. J Clin Oncol. 2004; 22: 777-84.

Giocanti N, Hennequin C, Rouillard D, Defrance R, Favaudon V. Additive interaction of gefitinib ('Iressa', ZD1839) and ionising radiation in human tumour cells in vitro. Br J Cancer. 2004; 91: 2026-33.

Godard T, Fessard V, Huet S, Mourot A, Deslandes E, Pottier D, Hyrien O, Sichel F, Gauduchon P, Poul J. Comparative in vitro and in vivo assessment of genotoxic effects of etoposide and chlorothalonil by the comet assay. Mutat Res. 1999; 444: 103-16.

Godard T, Deslandes E, Sichel F, Poul JM, Gauduchon P. Detection of topoisomerase inhibitor-induced DNA strand breaks and apoptosis by the alkaline comet assay. Mutat Res. 2002; 520: 47-56.

Gorre ME, Mohammed M, Ellwood K, Hsu N, Paquette R, Rao PN, Sawyers CL. Clinical resistance to STI-571 cancer therapy caused by BCR-ABL gene mutation or amplification. Science. 2001; 293:876-80.

Gottlieb TM, Jackson SP. The DNA-dependent protein kinase: requirement for DNA ends and association with Ku antigen. Cell. 1993; 72: 131-42.

Gregson SJ, Howard PW, Hartley JA, Brooks NA, Adams LJ, Jenkins TC, Kelland LR, Thurston DE. Design, synthesis, and evaluation of a novel pyrrolobenzodiazepine DNA-interactive agent with highly efficient cross-linking ability and potent cytotoxicity. J Med Chem. 2001; 44:737-48.

Griffon G, Merlin JL, Marchal C. Comparison of sulforhodamine B, tetrazolium and clonogenic assays for in vitro radiosensitivity testing in human ovarian cell lines. Anticancer Drugs. 1995; 6: 115-23.

Grimaldi KA, McGurk CJ, McHugh PJ, Hartley JA. PCR-based methods for detecting DNA damage and its repair at the sub-gene and single nucleotide levels in cells. Mol Biotechnol. 2002; 20:181-96.

Gschwind A, Fischer OM, Ullrich A. The discovery of receptor tyrosine kinases: targets for cancer therapy. Nat Rev Cancer. 2004; 4: 361-70.

Gupta AK, Cerniglia GJ, Mick R, Ahmed MS, Bakanauskas VJ, Muschel RJ, McKenna WG. Radiation sensitization of human cancer cells in vivo by inhibiting the activity of PI3K using LY294002. Int J Radiat Oncol Biol Phys. 2003; 56: 846-53.

Haber J. Partners and pathways repairing a double-strand break. Trends Genet. 2000; 16: 259-264.

Hammarsten O, Chu G. DNA-dependent protein kinase: DNA binding and activation in the absence of Ku. Proc Natl Acad Sci USA. 1998; 95: 525-30.

Hanahan D, and Weinberg RA. The hallmarks of cancer. Cell. 2000; 100, 57-70.

Hansson J, Lewensohn R, Ringborg U, Nilsson B. Formation and removal of DNA cross-links induced by melphalan and nitrogen mustard in relation to drug-induced cytotoxicity in human melanoma cells. Cancer Res. 1987; 47: 2631-7.

Harari PM. Epidermal growth factor receptor inhibition strategies in oncology. Endocr Rel Cancer. 2004; 11: 689-708.

Harari PM, Huang SM. Combining EGFR inhibitors with radiation or chemotherapy: will preclinical studies predict clinical results? Int J Radiat Oncol Biol Phys. 2004; 58: 976-83.

Harlow E, Lane D. Using Antibodies: A Laboratory Manual. 1999; Cold Spring Harbour Press, New York.

Harris R, Esposito D, Sankar A, Maman JD, Hinks JA, Pearl LH, Driscoll PC. The 3D solution structure of the C-terminal region of Ku86 (Ku86CTR). J Mol Biol. 2004; 335: 573-82.

Hartley JA. Alkylating agents. *In* Souhami RL, Tannock I, Hohenberger P, Horiot JC. 2001; (ed.) Oxford Textbook of Oncology, Second Edition ed. Oxford University Press.

Hartley JA, Spanswick VJ, Brooks N, Clingen PH, McHugh PJ, Hochhauser D, Pedley RB, Kelland LR, Alley MC, Schultz R, Hollingshead MG, Schweikart KM, Tomaszewski JE, Sausville EA, Gregson SJ, Howard PW, Thurston DE. SJG-136 (NSC 694501), a novel rationally designed DNA minor groove interstrand cross-linking agent with potent and broad spectrum antitumor activity: part 1: cellular pharmacology, in vitro and initial in vivo antitumor activity. Cancer Res. 2004; 64: 6693-9.

Hartley JM, Spanswick VJ, Gander M, Giacomini G, Whelan J, Souhami RL, Hartley JA. Measurement of DNA cross-linking in patients on ifosfamide therapy using the single cell gel electrophoresis (comet) assay. Clin Cancer Res. 1999; 5:507-12.

Henderson, D. & Hurley, L. H. Molecular struggle for transcriptional control. Nature Med. 1995; 1, 525–527.

Herbst RS, Shin DM. Monoclonal antibodies to target epidermal growth factor receptor-positive tumors: a new paradigm for cancer therapy. Cancer. 2002; 94: 1593-611.

Herbst RS, Maddox AM, Rothenberg ML, Small EJ, Rubin EH, Baselga J, Rojo F, Hong WK, Swaisland H, Averbuch SD, Ochs J, LoRusso PM. Selective oral epidermal growth factor receptor tyrosine kinase inhibitor ZD1839 is generally well-tolerated and has activity in non-small-cell lung cancer and other solid tumors: results of a phase I trial. J Clin Oncol. 2002; 20: 3815-25.

Herbst RS, Fukuoka M, Baselga J. Gefitinib - a novel targeted approach to treating cancer. Nat Rev Cancer. 2004; 4: 956-65.

Herbst RS, Giaccone G, Schiller JH, Natale RB, Miller V, Manegold C, Scagliotti G, Rosell R, Oliff I, Reeves JA, Wolf MK, Krebs AD, Averbuch SD, Ochs JS, Grous J, Fandi A, Johnson DH. Gefitinib in combination with paclitaxel and carboplatin in advanced non-small-cell lung cancer: a phase III trial - INTACT 2. J Clin Oncol. 2004; 22: 785-94.

Herbst RS, Prager D, Hermann R. TRIBUTE-A phase III trial of erlotinib HCl (OSI-774) combined with carboplatin and paclitaxel (CP) chemotherapy in advanced non-small cell lung cancer (NSCLC). Proc Am Soc Clin Oncol. 2004; 23: 7011.

Hoeijmakers JH. Genome maintenance mechanisms for preventing cancer. Nature. 200; 411(6835): 366-74.

Hollick JJ, Golding BT, Hardcastle IR, Martin N, Richardson C, Rigoreau LJ, Smith GC, Griffin RJ. 2,6-disubstituted pyran-4-one and thiopyran-4-one inhibitors of DNA-Dependent protein kinase (DNA-PK). Bioorg Med Chem Lett. 2003; 13: 3083-6.

Hoppe BS, Jensen RB, Kirchgessner CU. Complementation of the radiosensitive M059J cell line. Radiat Res. 2000; 153: 125-30.

Huang SM, Harari PM. Modulation of radiation response after epidermal growth factor receptor blockade in squamous cell carcinomas: inhibition of damage repair, cell cycle kinetics, and tumor angiogenesis. Clin Cancer Res. 2000; 6: 2166-74.

Huang SM, Bock JM, Harari PM. Epidermal growth factor receptor blockade with C225 modulates proliferation, apoptosis, and radiosensitivity in squamous cell carcinomas of the head and neck. Cancer Res. 1999; 59: 1935-40.

Huang SM, Li J, Armstrong EA, Harari PM. Modulation of radiation response and tumor-induced angiogenesis after epidermal growth factor receptor inhibition by ZD1839 (Iressa) Cancer Res. 2002; 62: 4300-6.

Huang S, Armstrong EA, Benavente S, Chinnaiyan P, Harari PM. Dual-agent molecular targeting of the epidermal growth factor receptor (EGFR): combining anti-EGFR antibody with tyrosine kinase inhibitor. Cancer Res. 2004; 64: 5355-62.

Hurley LH. DNA and its associated processes as targets for cancer therapy. Nature Reviews Cancer. 2002; 2, 188-200.

Hynes NE, Lane HA. ERBB receptors and cancer: the complexity of targeted inhibitors. Nat Rev Cancer. 2005; 5: 341-54.

Igney FH and Krammer PH. Death and anti-death: Tumour resistance to apoptosis. Nat Rev Cancer. 2002; 2: 277-288.

Ishiyama N, Kanzaki M, Seno M, Yamada H, Kobayashi I, Kojima I. Studies on the betacellulin receptor in pancreatic AR42J cells. Diabetologia. 1998; 41: 623-8.

Ismail IH, Martensson S, Moshinsky D, Rice A, Tang C, Howlett A, McMahon G, Hammarsten O. SU11752 inhibits the DNA-dependent protein kinase and DNA double-strand break repair resulting in ionizing radiation sensitization. Oncogene. 2004; 23: 873-82.

Iwata KK, Provoncha K and Gibson N. Inhibition of mutant EGFRvIII transformed cells by tyrosine kinase inhibitor OSI774 (Tarceva). Proceedings of the American Society of Clinical Oncology. 2002; 2121a: Abstract 79.

Izzard RA, Jackson SP, Smith GC. Competitive and noncompetitive inhibition of the DNA-dependent protein kinase. Cancer Res. 1999; 59: 2581-6.

Janmaat ML, Kruyt FA, Rodriguez JA, Giaccone G. Response to epidermal growth factor receptor inhibitors in non-small cell lung cancer cells: limited antiproliferative effects and absence of apoptosis associated with persistent activity of extracellular signal-regulated kinase or Akt kinase pathways Clin Cancer Res. 2003; 9: 2316-26.

Janne PA. EGFR mutations predict response to gefitinib – Now what? (Education Program). Mutations in EGFR and response to gefitinib and erlotinib [online]. 2004; http://www.asco.org/ac/1,1003,_12-002511-00_18-0026-00_19-0011694-00_21-008,00.asp.

Jenkins DC, Charles IG, Baylis SA, Lelchuk R, Radomski MW, Moncada S. Human colon cancer cell lines show a diverse pattern of nitric oxide synthase gene expression and nitric oxide generation. Br J Cancer. 1994; 70: 847-9.

Jensen R, Glazer PM Cell-interdependent cisplatin killing by Ku/DNA-dependent protein kinase signaling transduced through gap junctions. Proc Natl Acad Sci USA. 2004; 101: 6134-9.

Jhappan C, Morse HC 3rd, Fleischmann RD, Gottesman MM, Merlino G. DNA-PKcs: a T-cell tumour suppressor encoded at the mouse scid locus. Nat Genet. 1997; 17: 483-6.

Karrann P and Bignami N. DNA damage tolerance, mismatch repair and genome instability. BioEssays. 1994; 16: 833-839.

Katso R, Okkenhaug K, Ahmadi K, White S, Timms J, Waterfield MD. Cellular function of phosphoinositide 3-kinases: implications for development, homeostasis, and cancer. Annu Rev Cell Dev Biol. 2001; 17: 615-75.

Khanna KK and Jackson SP. DNA double-strand breaks: signalling, repair and the cancer connection. Nature Genet. 2001; 27: 247-254.

Kharbanda S, Pandey P, Jin S, Inoue S, Bharti A, Yuan ZM, Weichselbaum R, Weaver D, Kufe D. Functional interaction between DNA-PK and c-Abl in response to DNA damage. Nature. 1997; 386: 732-5.

Kim ES, Khuri FR, Herbst RS. Epidermal growth factor receptor biology (IMC-C225). Curr Opin Oncol. 2001; 13: 506-13.

Kim ES, Mauer AM, Fossella FV. A phase II study of Erbitux (IMC-C225), an epidermal growth factor receptor (EGFR) blocking antibody, in combination with docetaxel in chemotherapy refractory/resistant patients with advanced non-small cell lung cancer (NSCLC). Proc Am Soc Clin Oncol. 2002; 21: 293a, (abstr 1168).

Klein S, McCormick F, Levitzki A. Opinion: Killing time for cancer cells. Nat Rev Cancer. 2005; advanced publication p1-8.

Knight ZA, Chiang GG, Alaimo PJ, Kenski DM, Ho CB, Coan K, Abraham RT, Shokat KM. Isoform-specific phosphoinositide 3-kinase inhibitors from an arylmorpholine scaffold. Bioorg Med Chem. 2004; 12: 4749-59.

Kobayashi S, Boggon TJ, Dayaram T, Janne PA, Kocher O, Meyerson M, Johnson BE, Eck MJ, Tenen DG, Halmos B. EGFR mutation and resistance of non-small-cell lung cancer to gefitinib. N Engl J Med. 2005; 352: 786-92.

Kris MG, Natale RB, Herbst RS, Lynch TJ Jr, Prager D, Belani CP, Schiller JH, Kelly K, Spiridonidis H, Sandler A, Albain KS, Cella D, Wolf MK, Averbuch SD, Ochs JJ, Kay AC. Efficacy of gefitinib, an inhibitor of the epidermal growth factor receptor tyrosine kinase, in symptomatic patients with non-small cell lung cancer: a randomized trial. JAMA. 2003; 290: 2149-58.

Kumar S, Pandey P, Bharti A, Jin S, Weichselbaum R, Weaver D, Kufe D, Kharbanda S. Regulation of DNA-dependent protein kinase by the Lyn tyrosine kinase. J Biol Chem. 1998; 273: 25654-8.

Lai JS, Herr W. Ethidium bromide provides a simple tool for identifying genuine DNA-independent protein associations. Proc. Natl. Acad. Sci. 1992; 89: 6958-6962.

Lane HA, Beuvink I, Motoyama AB, Daly JM, Neve RM, Hynes NE. ErbB2 potentiates breast tumor proliferation through modulation of p27(Kip1)-Cdk2 complex formation: receptor overexpression does not determine growth dependency. Mol Cell Biol. 2000; 20: 3210-23.

Learn CA, Hartzell TL, Wikstrand CJ, Archer GE, Rich JN, Friedman AH, Friedman HS, Bigner DD, Sampson JH. Resistance to tyrosine kinase inhibition by mutant epidermal growth factor receptor variant III contributes to the neoplastic phenotype of glioblastoma multiforme. Clin Cancer Res. 2004; 10: 3216-24.

Lees-Miller SP, Chen YR, Anderson CW. Human cells contain a DNA-activated protein kinase that phosphorylates simian virus 40 T antigen, mouse p53, and the human Ku autoantigen. Mol Cell Biol. 1990; 10: 6472-81.

Lees-Miller SP, Godbout R, Chan DW, Weinfeld M, Day RS 3rd, Barron GM, Allalunis-Turner J. Absence of p350 subunit of DNA-activated protein kinase from a radiosensitive human cell line. Science. 1995; 267:1183-5.

Levitzki A. Protein kinase inhibitors as a therapeutic modality. Acc Chem Res. 2003; 36: 462-469.

Li TK, Liu LF. Tumor cell death induced by topoisomerase-targeting drugs. Annu Rev Pharmacol Toxicol. 2001; 41: 53-77.

Liang K, Jin W, Knuefermann C, Schmidt M, Mills GB, Ang KK, Milas L, Fan Z. Targeting the phosphatidylinositol 3-kinase/Akt pathway for enhancing breast cancer cells to radiotherapy. Mol Cancer Ther. 2003; 2: 353-60.

Lieber MR, Ma Y, Pannicke U, Schwarz K. Mechanism and regulation of human non-homologous DNA end-joining. Nat Rev Mol Cell Biol. 2003; 4: 712-20.

Lin SY, Makino K, Xia W, Matin A, Wen Y, Kwong KY, Bourguignon L, Hung MC. Nuclear localization of EGF receptor and its potential new role as a transcription factor. Nat Cell Biol. 2001; 3: 802-8.

Lindhal T and Wood RD. Quality control of DNA repair. Science. 1999; 286: 1897-1905.

Liu B, Fan Z. The monoclonal antibody 225 activates caspase-8 and induces apoptosis through a tumor necrosis factor receptor family-independent pathway. Oncogene 2001; 20: 3726–3734.

Liu B, Fang M, Schmidt M, Lu Y, Mendelsohn J, Fan Z. Induction of apoptosis and activation of the caspase cascade by anti-EGF receptor monoclonal antibodies in DiFi human colon cancer cells do not involve the c-jun N-terminal kinase activity. Br J Cancer. 2000; 82: 1991-9.

Llorca O and Pearl LH. Electron microscopy studies on DNA recognition by DNA-PK. Micron. 2004; 35: 625-633.

Lo HW, Xia W, Wei Y, Ali-Seyed M, Huang SF, Hung MC. Novel prognostic value of nuclear epidermal growth factor receptor in breast cancer. Cancer Res. 2005a; 65: 338-48.

Lo HW, Hsu SC, Ali-Seyed M, Gunduz M, Xia W, Wei Y, Bartholomeusz G, Shih JY, Hung MC. Nuclear interaction of EGFR and STAT3 in the activation of the iNOS/NO pathway. Cancer Cell. 2005b; 7: 575-89.

Loehrer PJ and Einhorn LH. Drugs five years later. Cisplatin. Ann Intern Med. 1984; 100: 704-713.

Lou Z, Chen BP, Asaithamby A, Minter-Dykhouse K, Chen DJ, Chen J. MDC1 regulates DNA-PK autophosphorylation in response to DNA damage. J Biol Chem. 2004; 279: 46359-62.

Lu Z, Jiang G, Blume-Jensen P, Hunter T. Epidermal growth factor-induced tumor cell invasion and metastasis initiated by dephosphorylation and downregulation of focal adhesion kinase. Mol Cell Biol. 2001; 21: 4016-31.

Lucero H, Gae D, Taccioli GE. Novel localization of the DNA-PK complex in lipid rafts: a putative role in the signal transduction pathway of the ionizing radiation response. J Biol Chem. 2003; 278: 22136-43.

Lynch DH, Yang XD. Therapeutic potential of ABX-EGF: a fully human anti-epidermal growth factor receptor monoclonal antibody for cancer treatment. Semin Oncol. 2002; 29: 47-50.

Lynch TJ, Lilenbaum R, Bonomi P, Ansari R, Govindan R, Janne PA, *et al.* A phase II trial of cetuximab as therapy for recurrent non-small cell lung cancer (NSCLC). Proc Am Soc Clin Oncol 2004; abstr 7084.

Lynch TJ, Bell DW, Sordella R, Gurubhagavatula S, Okimoto RA, Brannigan BW, Harris PL, Haserlat SM, Supko JG, Haluska FG, Louis DN, Christiani DC, Settleman J, Haber DA. Activating mutations in the epidermal growth factor receptor underlying responsiveness of non-small-cell lung cancer to gefitinib. N Engl J Med. 2004; 350: 2129-39.

Magne N, Fischel JL, Dubreuil A, Formento P, Marcie S, Lagrange JL, Milano G. Sequence-dependent effects of ZD1839 ('Iressa') in combination with cytotoxic treatment in human head and neck cancer. Br J Cancer. 2002; 86: 819-27.

Magne N, Fischel JL, Dubreuil A, Formento P, Poupon MF, Laurent-Puig P, Milano G. Influence of epidermal growth factor receptor (EGFR), p53 and intrinsic MAP kinase pathway status of tumour cells on the antiproliferative effect of ZD1839 ("Iressa"). Br J Cancer. 2002; 86: 1518-23.

Magne N, Fischel JL, Dubreuil A, Formento P, Ciccolini J, Formento JL, Tiffon C, Renee N, Marchetti S, Etienne MC, Milano G. ZD1839 (Iressa) modifies the activity of key enzymes linked to fluoropyrimidine activity: rational basis for a new combination therapy with capecitabine. Clin Cancer Res. 2003; 9: 4735-42.

Magne N, Fischel JL, Tiffon C, Formento P, Dubreuil A, Renee N, Formento JL, Francoual M, Ciccolini J, Etienne MC, Milano G. Molecular mechanisms underlying the interaction between ZD1839 ('Iressa') and cisplatin/5-fluorouracil. Br J Cancer. 2003; 8: 585-92.

Marples B, Cann NE, Mitchell CR, Johnston PJ, Joiner MC. Evidence for the involvement of DNA-dependent protein kinase in the phenomena of low dose hyper-radiosensitivity and increased radioresistance. Int J Radiat Biol. 2002; 78: 1139-47.

Martensson, S., Hammarsten, O. DNA-dependent protein kinase catalytic subunit. Journal of Biological Chemistry. 2002; 277: 3020–3029.

Masuda M, Toh S, Koike K, Kuratomi Y, Suzui M, Deguchi A, Komiyama S, Weinstein IB. The roles of JNK1 and Stat3 in the response of head and neck cancer cell lines to combined treatment with all-trans-retinoic acid and 5-fluorouracil. Jpn J Cancer Res. 2002; 93: 329-39.

Masumoto N, Nakano S, Fujishima H, Kohno K, Niho Y. v-src induces cisplatin resistance by increasing the repair of cisplatin-DNA interstrand cross-links in human gallbladder adenocarcinoma cells. Int J Cancer. 1999; 80: 731-7.

Matar P, Rojo F, Cassia R, Moreno-Bueno G, Di Cosimo S, Tabernero J, Guzman M, Rodriguez S, Arribas J, Palacios J, Baselga J. Combined epidermal growth factor receptor targeting with the tyrosine kinase inhibitor gefitinib (ZD1839) and the monoclonal antibody cetuximab (IMC-C225): superiority over single-agent receptor targeting. Clin Cancer Res. 2004; 10: 6487-501.

McHugh PJ, Spanswick VJ, Hartley JA. Repair of DNA interstrand crosslinks: molecular mechanisms and clinical relevance. Lancet Oncol. 2001; 2: 483-90.

McKillop D, Partridge EA, Kemp JV, Spence MP, Kendrew J, Barnett S, Wood PG, Giles PB, Patterson AB, Bichat F, Guilbaud N, Stephens TC. Tumor penetration of gefitinib (Iressa), an epidermal growth factor receptor tyrosine kinase inhibitor. Mol Cancer Ther. 2005; 4: 641-9.

Melisi D, Troiani T, Damiano V, Tortora G, Ciardiello F. Therapeutic integration of signal transduction targeting agents and conventional anti-cancer treatments. Endocr Relat Cancer. 2004; 11: 51-68.

Mendelsohn, J. Blockade of receptors for growth factors: an anticancer therapy. Clin. Cancer Res. 2000; 6: 747-753.

Mendelsohn J, Baselga J. The EGF receptor family as targets for cancer therapy. Oncogene. 2000; 19: 6550-65.

Mendelsohn J. The epidermal growth factor receptor as a target for cancer therapy. Endocr Reat Cancer. 2001; 8: 3-9.

Michel B, Flores MJ, Viguera E, Grompone G, Seigneur M, Bidnenko V. Rescue of arrested replication forks by homologous recombination. Proc Natl Acad Sci USA. 2001; 98: 8181-8.

Mihara M, Erster S, Zaika A, Petrenko O, Chittenden T, Pancoska P, Moll UM. p53 has a direct apoptogenic role at the mitochondria. Mol Cell. 2003; 11(3): 577-90.

Milas L, Mason K, Hunter N, Petersen S, Yamakawa M, Ang K, Mendelsohn J, Fan Z. In vivo enhancement of tumor radioresponse by C225 antiepidermal growth factor receptor antibody. Clin Cancer Res. 2000; 6: 701-8.

Mishima K, Johns TG, Luwor RB, Scott AM, Stockert E, Jungbluth AA, Ji XD, Suvarna P, Voland JR, Old LJ, Huang HJ, Cavenee WK. Growth suppression of intracranial xenografted glioblastomas overexpressing mutant epidermal growth factor receptors by systemic administration of monoclonal antibody (mAb) 806, a novel monoclonal antibody directed to the receptor. Cancer Res. 2001; 61: 5349-54.

Moasser MM, Basso A, Averbuch SD, Rosen N. The tyrosine kinase inhibitor ZD1839 ("Iressa") inhibits HER2-driven signaling and suppresses the growth of HER2-overexpressing tumor cells. Cancer Res. 2001; 61: 7184-8.

Moore MJ, Goldstein D, Hamm J, Kotecha J, Gallinger S, Au HJ, Nomikos D, Ding K, Ptaszynski M, Parulekar W. Erlotinib improves survival when added to gemcitabine in patients with advanced pancreatic cancer. A phase III trial of the National Cancer Institute of Canada Clinical Trials Group [NCIC-CTG]. ASCO Meeting Abstracts. Gastrointestinal Cancers Symposium 2005; (abstract 77).

Moulder SL, Yakes FM, Muthuswamy SK, Bianco R, Simpson JF, Arteaga CL. Epidermal growth factor receptor (HER1) tyrosine kinase inhibitor ZD1839 (Iressa) inhibits HER2/neu (erbB2)-overexpressing breast cancer cells in vitro and in vivo. Cancer Res. 2001; 61: 8887-95.

Moyer JD, Barbacci EG, Iwata KK, Arnold L, Boman B, Cunningham A, DiOrio C, Doty J, Morin MJ, Moyer MP, Neveu M, Pollack VA, Pustilnik LR, Reynolds MM, Sloan D, Theleman A, Miller P. Induction of apoptosis and cell cycle arrest by CP-358,774, an inhibitor of epidermal growth factor receptor tyrosine kinase. Cancer Res. 1997; 57: 4838-48.

Muller C, Salles B. Regulation of DNA-dependent protein kinase activity in leukemic cells. Oncogene. 1997; 15: 2343-8.

Munro S. Lipid rafts: elusive or illusive? Cell. 2003; 115: 377-88.

National Cancer Institute. National Cancer Institute Cancer Therapy Evaluation Program: Common Toxicity Criteria Manual: Common Toxicity Criteria version 2 [online], http://ctep.cancer.gov/forms/CTCManual_v4_10-4-99.pdf> (1999).

Neidle S and Thurston DE. Chemical approaches to the discovery and development of cancer therapies. Nat Cancer Rev. 2005; 5: 285-296.

Neri LM, Raymond Y, Giordano A, Capitani S, Martelli AM. Lamin A is part of the internal nucleoskeleton of human erythroleukemia cells. J Cell Physiol. 1999; 178: 284-95.

Nitiss JL, Wang JC. Mechanisms of cell killing by drugs that trap covalent complexes between DNA topoisomerases and DNA. Mol Pharmacol. 1996; 50: 1095-102.

Niu G, Wright KL, Huang M, Song L, Haura E, Turkson J, Zhang S, Wang T, Sinibaldi D, Coppola D, Heller R, Ellis LM, Karras J, Bromberg J, Pardoll D, Jove R, Yu H. Constitutive Stat3 activity up-regulates VEGF expression and tumor angiogenesis. Oncogene. 2002; 21: 2000-8.

Norbury CJ and Zhivotovsky B. DNA damage-induced apoptosis. Oncogene. 2004; 23: 2797-2808.

Olive PL. The Comet Assay – An overview of techniques. Methods in Molecular Biology. 2002; 203:179-94.

Olive PL, Banath JP, Durand RE. Heterogeneity in radiation-induced DNA damage and repair in tumour and normal cells measured using the "comet" assay. Radiat Res. 1990; 122:86-94.

Ostling O, Johanson KJ. Microelectrophoretic study of radiation-induced DNA damages in individual mammalian cells. Biochem Biophys Res Commun. 1984; 123: 291-8.

Paez JG, Janne PA, Lee JC, Tracy S, Greulich H, Gabriel S, Herman P, Kaye FJ, Lindeman N, Boggon TJ, Naoki K, Sasaki H, Fujii Y, Eck MJ, Sellers WR, Johnson BE, Meyerson M. EGFR mutations in lung cancer: correlation with clinical response to gefitinib therapy. Science. 2004; 304: 1497-500.

Pal SK, Pegram M. Epidermal growth factor receptor and signal transduction: potential targets for anti-cancer therapy. Anticancer Drugs. 2005; 16: 483-94.

Pao W, Miller V, Zakowski M, Doherty J, Politi K, Sarkaria I, Singh B, Heelan R, Rusch V, Fulton L, Mardis E, Kupfer D, Wilson R, Kris M, Varmus H. EGF receptor gene mutations are common in lung cancers from "never smokers" and are associated with sensitivity of tumors to gefitinib and erlotinib. Proc Natl Acad Sci USA. 2004; 101: 13306-11.

Park SJ, Armstrong S, Kim CH, Yu M, Robertson K, Kelley MR, Lee SH. Lack of EGF receptor contributes to drug sensitivity of human germline cells. Br J Cancer. 2005; 92: 334-41.

Pegram MD, Finn RS, Arzoo K, Beryt M, Pietras RJ, Slamon DJ. The effect of HER-2/neu overexpression on chemotherapeutic drug sensitivity in human breast and ovarian cancer cells. Oncogene. 1997; 15: 537-47.

Pegram MD, Konecny GE, O'Callaghan C, Beryt M, Pietras R, Slamon DJ. Rational combinations of trastuzumab with chemotherapeutic drugs used in the treatment of breast cancer. J Natl Cancer Inst. 2004; 96: 739-49.

Peng D, Fan Z, Lu Y, DeBlasio T, Scher H, Mendelsohn J. Anti-epidermal growth factor receptor monoclonal antibody 225 up-regulates p27KIP1 and induces G1 arrest in prostatic cancer cell line DU145. Cancer Res. 1996; 56: 3666-9.

Peng Y, Zhang Q, Nagasawa H, Okayasu R, Liber HL, Bedford JS. Silencing expression of the catalytic subunit of DNA-dependent protein kinase by small interfering RNA sensitizes human cells for radiation-induced chromosome damage, cell killing, and mutation. Cancer Res. 2002; 62: 6400-4.

Perez RP, Godwin AK, Handel LM, Hamilton TC. A comparison of clonogenic, microtetrazolium and sulforhodamine B assays for determination of cisplatin cytotoxicity in human ovarian carcinoma cell lines. Eur J Cancer. 1993; 29: 395-9.

Perez RP. Cellular and molecular determinants of cisplatin resistance. Eur J Cancer. 1998; 34: 1535-42.

Peterson SR, Kurimasa A, Oshimura M, Dynan WS, Bradbury EM, Chen DJ. Loss of the catalytic subunit of the DNA-dependent protein kinase in DNA double-strand-break-repair mutant mammalian cells. Proc Natl Acad Sci USA. 1995; 92: 3171-4.

Petrini JH. The Mre11 complex and ATM: collaborating to navigate S phase. Curr Opin Cell Biol. 2000; 12: 293-296.

Pietras RJ, Fendly BM, Chazin VR, Pegram MD, Howell SB, Slamon DJ. Antibody to HER-2/neu receptor blocks DNA repair after cisplatin in human breast and ovarian cancer cells. Oncogene. 1994; 9: 1829-38.

Piiper A, Elez R, You SJ, Kronenberger B, Loitsch S, Roche S, Zeuzem S. Cholecystokinin stimulates extracellular signal-regulated kinase through activation of the epidermal growth factor receptor, Yes, and protein kinase C. Signal amplification at the level of Raf by activation of protein kinase C epsilon. J Biol Chem. 2003; 278: 7065-72.

Piperdi B, Ling YH, Kroog G, Perez-Soler R. schedule-dependent interaction between epidermal growth factor receptor inhibitors (EGFRI) and G2/M blocking chemotherapeutic agents (G2/MB) on human NSCLC cell lines in vitro. ASCO Meeting Abstracts. 2004; (abstract 7028).

Pizzolato JF, and Saltz LB. The camptothecins. Lancet 2003; 361: 2235-42.

Povirk LF and Shuker DE. DNA damage and mutagenesis induced by nitrogen mustards. Mutation Research. 1994; 318: 205-26.

Prenzel N, Fischer OM, Streit S, Hart S, Ullrich A. The epidermal growth factor receptor family as a central element for cellular signal transduction and diversification. Endocr Relat Cancer. 2001; 8: 11-31.

Prewett MC, Hooper AT, Bassi R, Ellis LM, Waksal HW, Hicklin DJ. Enhanced antitumour activity of anti-epidermal growth factor receptor monoclonal antibody IMC-C225 in combination with irinotecan (CPT-11) against human colorectal tumour xenografts. Clin Cancer Res. 2002; 8: 994-1003.

Prewett MC, Hooper AT, Bassi R, Waksal HW, Hicklin DJ. Enhanced antitumor activity of anti-epidermal growth factor receptor monoclonal antibody ERBITUX (IMC-C225) in combination with irinotecan (CPT-11), 5-FU, and leucovorin against human colorectal carcinoma xenografts. Proc Am Ass Cancer Res 2002; abstr.

Raben D, Helfrich BA, Chan D, et al. ZD1839, a selective epidermal growth factor receptor tyrosine kinase inhibitor, alone and in combination with radiation and chemotherapy as a new therapeutic strategy in non-small cell lung cancer. Semin Oncol 2002; 29 (1 suppl 4): 37–46.

Raderschall E, Stout K, Freier S, Suckow V, Schweiger S, Haaf T. Elevated levels of Rad51 recombination protein in tumor cells. Cancer Res. 2002; 62: 219-25.

Raymond E, Faivre S and Armand JP. Epidermal growth factor recptor tyrosine kinase as a target for anticancer therapy. Drugs Suppl. 2000; 60: 15-23.

Rebuzzini P, Lisa A, Giulotto E, Mondello C. Chromosomal end-to-end fusions in immortalized mouse embryonic fibroblasts deficient in the DNA-dependent protein kinase catalytic subunit. Cancer Lett. 2004; 203: 79-86.

Reed EM, Dabholkar M, Chabner BA. Platinum Analogues, 357-378. *In* Chabiner & Longo (ed.), Cancer Chemotherapy and Biotherapy, Second ed. Lippincott-Raven publishers, Philadelphia.

Reinke V, Lozano G. The p53 targets mdm2 and Fas are not required as mediators of apoptosis in vivo. Oncogene. 1997; 25: 1527-34.

Rosenberg B. Fundamental studies with cisplatin. Cancer. 1985; 55: 2303-2306.

Rosenzweig KE, Youmell MB, Palayoor ST, Price BD. Radiosensitization of human tumor cells by the phosphatidylinositol3-kinase inhibitors wortmannin and LY294002 correlates with inhibition of DNA-dependent protein kinase and prolonged G2-M delay. Clin Cancer Res. 1997; 3: 1149-56.

Rouse J and Jackson SP. Interfaces between the detection, signalling and repair of DNA damage. Science. 2002; 297: 547-551.

Rowinsky EK. The pursuit of optimal outcomes in cancer therapy in a new age of rationally designed target-based anticancer therapy. Drugs Suppl. 2000; 60: 1-14.

Saleh MN, Raisch KP, Stackhouse MA, Grizzle WE, Bonner JA, Mayo MS, Kim HG, Meredith RF, Wheeler RH, Buchsbaum DJ. Combined modality therapy of A431 human epidermoid cancer using anti-EGFr antibody C225 and radiation. Cancer Biother Radiopharm. 1999; 14: 451-63.

Saltz LB, Cox J, Blanke C. Irinotecan plus fluoruracil and leucovorin for metastatic colorectal cancer. Irinotecan study group. N Eng J Med 2000; 343:905-914.

Saltz L, Rubin M, Hochster H. Cetuximab (IMC-C225) plus irinotecan (CPT-11) is active in CPT-11-refractory colorectal cancer (CRC) that expresses epidermal growth factor receptor (EGFR). Proc Am Soc Clin Oncol. 2001; 20: 3a (abstr 7).

Saltz LB, Meropol NJ, Loehrer PJ Sr, Needle MN, Kopit J, Mayer RJ. Phase II trial of cetuximab in patients with refractory colorectal cancer that expresses the epidermal growth factor receptor. J Clin Oncol. 2004; 22: 1201-8.

Sambrook J., Fritsch E. F., Maniatis T. Molecular Cloning: A Laboratory Manual. Cold Spring Harbour Press, New York, Third Edition. 1989; Vol. 1,2,3.

Sarkaria JN, Tibbetts RS, Busby EC, Kennedy AP, Hill DE, Abraham RT. Inhibition of phosphoinositide 3-kinase related kinases by the radiosensitizing agent wortmannin. Cancer Res. 1998; 58: 4375-82.

Sawyers CL. Signal transduction pathways involved in BCR-ABL transformation. Baillieres Clin Haematol. 1997; 10: 223-31.

Schlessinger J. Common and distinct elements in cellular signalling via EGF and FGF receptors. Scince. 2004; 306: 1506-1507.

Sgambato A, Camerini A, Faraglia B, Ardito R, Bianchino G, Spada D, Boninsegna A, Valentini V, Cittadini A. Targeted inhibition of the epidermal growth factor receptor-tyrosine kinase by ZD1839 ('Iressa') induces cell-cycle arrest and inhibits proliferation in prostate cancer cells. J Cell Physiol. 2004; 201: 97-105.

Shah NP, Tran C, Lee FY, Chen P, Norris D, Sawyers CL. Overriding imatinib resistance with a novel ABL kinase inhibitor. Science. 2004; 305: 399-401.

She QB, Solit D, Basso A, Moasser MM. Resistance to gefitinib in PTEN-null HER-overexpressing tumor cells can be overcome through restoration of PTEN function or pharmacologic modulation of constitutive phosphatidylinositol 3'-kinase/Akt pathway signaling. Clin Cancer Res. 2003; 9: 4340-6.

Shepherd FA, Rodrigues Pereira J, Ciuleanu T, Tan EH, Hirsh V, Thongprasert S, Campos D, Maoleekoonpiroj S, Smylie M, Martins R, van Kooten M, Dediu M, Findlay B, Tu D, Johnston D, Bezjak A, Clark G, Santabarbara P, Seymour L; National Cancer Institute of Canada Clinical Trials Group. Erlotinib in previously treated non-small-cell lung cancer. N Engl J Med. 2005; 353: 123-32.

Shiloh Y. ATM and ATR: Networking cellular responses to DNA Damage. Curr Opin Genet Dev. 2001; 11: 71-77.

Shiloh Y. ATM and related protein kinases: safeguarding genome integrity. Nat Rev Cancer. 2003; Vol 3: 155-168.

Shingu T, Yamada K, Hara N, Moritake K, Osago H, Terashima M, Uemura T, Yamasaki T, Tsuchiya M. Synergistic augmentation of antimicrotubule agent-induced cytotoxicity by a phosphoinositide 3-kinase inhibitor in human malignant glioma cells. Cancer Res. 2003; 63: 4044-7.

Shintani S, Li C, Mihara M, Terakado N, Yano J, Nakashiro K, Hamakawa H. Enhancement of tumor radioresponse by combined treatment with gefitinib (Iressa, ZD1839), an epidermal growth factor receptor tyrosine kinase inhibitor, is accompanied by inhibition of DNA damage repair and cell growth in oral cancer. Int J Cancer. 2003; 107: 1030-7.

Shou J, Massarweh S, Osborne CK, Wakeling AE, Ali S, Weiss H, Schiff R. Mechanisms of tamoxifen resistance: increased estrogen receptor-HER2/neu cross-talk in ER/HER2-positive breast cancer. J Natl Cancer Inst. 2004; 96: 926-35.

Sirotnak FM, Zakowski MF, Miller VA, Scher HI, Kris MG. Efficacy of cytotoxic agents against human tumor xenografts is markedly enhanced by coadministration of ZD1839 (Iressa), an inhibitor of EGFR tyrosine kinase. Clin Cancer Res. 2000; 6: 4885-92.

Skehan P, Storeng R, Scudiero D, Monks A, McMahon J, Vistica D, Warren JT, Bokesch H, Kenney S, and Boyd MR. New colorimetric cytotoxicity assay for anticancer-drug screening. J Natl. Cancer Inst. 1990; 82:1107-1112.

Skorski T. BCR/ABL regulates response to DNA damage: the role in resistance to genotoxic treatment and in genomic instability. Oncogene. 2002; 21: 8591-604.

Skorski T. Oncogenic tyrosine kinases and the DNA-damage response. Nat Rev Can. 2002; 2: 1-10.

Sliwkowski MX, Lofgren JA, Lewis GD, Hotaling TE, Fendly BM, Fox JA. Nonclinical studies addressing the mechanism of action of trastuzumab (Herceptin). Semin Oncol. 1999; 26 (4 Suppl 12): 60-70.

Slupianek A, Schmutte C, Tombline G, Nieborowska-Skorska M, Hoser G, Nowicki MO, Pierce AJ, Fishel R, Skorski T. BCR/ABL regulates mammalian RecA homologs, resulting in drug resistance. Mol Cell. 2001; 8: 795-806.

Slupianek A, Hoser G, Majsterek I, Bronisz A, Malecki M, Blasiak J, Fishel R, Skorski T. Fusion tyrosine kinases induce drug resistance by stimulation of homology-dependent recombination repair, prolongation of G(2)/M phase, and protection from apoptosis. Mol Cell Biol. 2002; 22: 4189-201.

Smith GC, Jackson SP. The DNA-dependent protein kinase. Genes Dev. 1999; 13: 916-34.

Solit DB, She Y, Lobo J, Kris MG, Scher HI, Rosen N, Sirotnak FM. Pulsatile administration of the epidermal growth factor receptor inhibitor gefitinib is significantly more effective than continuous dosing for sensitizing tumors to paclitaxel. Clin Cancer Res. 2005; 11: 1983-9.

Solomon B, Hagekyriakou J, Trivett MK, Stacker SA, McArthur GA, Cullinane C. EGFR blockade with ZD1839 ("Iressa") potentiates the antitumor effects of single and multiple fractions of ionizing radiation in human A431 squamous cell carcinoma. Epidermal growth factor receptor. Int J Radiat Oncol Biol Phys. 2003; 55: 713-23.

Sordella R, Bell DW, Haber DA, Settleman J. Gefitinib-sensitizing EGFR mutations in lung cancer activate anti-apoptotic pathways. Science. 2004; 305: 1163-7.

Sorkina T, Huang F, Beguinot L & Sorkin A. Effect of tyrosine kinase inhibitors on clathrin-coated pit recruitment and internalization of epidermal growth factor receptor. Journal of Biological Chemistry. 2002; 277: 27433–27441.

Soule HD, Vazguez J, Long A, Albert S, Brennan M. A human cell line from a pleural effusion derived from a breast carcinoma. J Natl Cancer Inst. 1973; 51: 1409-16.

Spanswick VJ, Hartley JM, Ward TH and Hartley JA. Measurement of drug-induced interstrand crosslinking using single-cell gel electrophoresis (Comet) assay. In Brown,R. and Boger-Brown,U. (eds), Methods in Molecular Medicine 1999, Vol. 28, Cytotoxic Drug Resistance Mechanisms. Humana Press, Totowa, NJ.

Spanswick VJ, Craddock C, Sekhar M, Mahendra P, Shankaranarayana P, Hughes RG, Hochhauser D, Hartley JA. Repair of DNA interstrand crosslinks as a mechanism of clinical resistance to melphalan in multiple myeloma. Blood. 2002; 100: 224-9.

Sridhar SS, Seymour L, Shepherd FA. Inhibitors of epidermal-growth-factor receptors: a review of clinical research with a focus on non-small-cell lung cancer. Lancet Oncol. 2003; 4: 397-406.

Sriuranpong V, Park JI, Amornphimoltham P, Patel V, Nelkin BD, Gutkind JS. Epidermal growth factor receptor-independent constitutive activation of STAT3 in head and neck squamous cell carcinoma is mediated by the autocrine/paracrine stimulation of the interleukin 6/gp130 cytokine system. Cancer Res. 2003; 63: 2948-56.

Stamos J, Sliwkowski MX, Eigenbrot C. Structure of the epidermal growth factor receptor kinase domain alone and in complex with a 4-anilinoquinazoline inhibitor. J Biol Chem. 2002 Nov; 277: 46265-72.

Stein RC. Prospects for phosphoinositide 3-kinase inhibition as a cancer treatment. Endocr Relat Cancer. 2001; 8: 237-48.

Stockley M, Clegg W, Fontana G, Golding BT, Martin N, Rigoreau LJ, Smith GC, Griffin RJ. Synthesis, crystal structure determination, and biological properties of the DNA-dependent protein kinase (DNA-PK) inhibitor 3-cyano-6-hydrazonomethyl-5-(4-pyridyl)pyrid-[1H]-2-one (OK-1035). Bioorg Med Chem Lett. 2001; 11: 2837-41.

Strano S, Rossi M, Fontemaggi G, Munarriz E, Soddu S, Sacchi A, Blandino G. From p63 to p53 across p73. FEBS Lett. 2001; 490: 163-70.

Tallarida RJ. Drug synergism: its detection and applications. J Pharmacol Exp Ther. 2001; 298(3): 865-72.

Taniguchi T, Garcia-Higuera I, Xu B, Andreassen PR, Gregory RC, Kim ST, Lane WS, Kastan MB, D'Andrea AD. Convergence of the fanconi anemia and ataxia telangiectasia signaling pathways. Cell. 2002; 17, 109: 459-72.

Tatosyan AG, Mizenina OA. Kinases of the Src family: structure and functions. Biochemistry (Mosc). 2000; 65: 49-58.

Tew KD, Colvin M and Chabner BA. Alkylating agents. *In* CBA and LDL. 1996; (ed.) Cancer Chemotherapy and Biotherapy, Second ed. Lippincott-Raven publishers, Philadelphia.

Tewey, K. M., Rowe, T. C., Yang, L., Halligan, B. D. & Liu, L. F. Adriamycin-induced DNA damage mediate by mammalian DNA topoisomerase II. Science. 1984; 226, 466–468.

Thatcher N, Chang A, Parikh P, Rodrigues Pereira J, Ciuleanu T, von Pawel J, Thongprasert S, Tan EH, Pemberton K, Archer V, Carroll K. Gefitinib plus best supportive care in previously treated patients with refractory advanced non-small-cell lung cancer: results from a randomised, placebo-controlled, multicentre study (Iressa Survival Evaluation in Lung Cancer). Lancet. 2005; 366: 1527-37.

Tice DA, Biscardi JS, Nickles AL, Parsons SJ. Mechanism of biological synergy between cellular Src and epidermal growth factor receptor. Proc Natl Acad Sci USA. 1999; 96: 1415-20.

Tortora G, Caputo R, Damiano V, Caputo R, Troiani T, Veneziani BM, De Placido S, Bianco AR, Zangemeister-Wittke U, Ciardiello F. Combined targeted inhibition of bcl-2, bcl-XL, epidermal growth factor receptor, and protein kinase A type I causes potent antitumor, apoptotic, and antiangiogenic activity. Clin Cancer Res. 200; 9: 866-71.

Tracy S, Mukohara T, Hansen M, Meyerson M, Johnson BE, Janne PA. Gefitinib induces apoptosis in the EGFRL858R non-small-cell lung cancer cell line H3255. Cancer Res. 2004; 64: 7241-4

Traxler P. Tyrosine kinase inhibitors in cancer treatment (Part II). Expert Opin Ther Pat. 1998; 8: 1599-1625.

Traxler P, Bold G, Buchdunger E, Caravatti G, Furet P, Manley P, O'Reilly T, Wood J, Zimmermann J. Tyrosine kinase inhibitors: from rational design to clinical trials. Med Res Rev. 2001; 21: 499-512.

Trigo J, Hitt R, Koralewski P. Cetuximab monotherapy is active in patients (pts) with platinum-refractory recurrent/metastatic squamous cell carcinoma of the head and neck (SCCHN): Results of a phase II study. Proc Am Soc Clin Oncol 23:487, 2004 (abstr 502).

Trimmer EE and Essigmann JM. Cisplatin. Essay Biochem. 1999; 34: 191-211.

Tsao MS, Sakurada A, Cutz JC, Zhu CQ, Kamel-Reid S, Squire J, Lorimer I, Zhang T, Liu N, Daneshmand M, Marrano P, da Cunha Santos G, Lagarde A, Richardson F, Seymour L, Whitehead M, Ding K, Pater J, Shepherd FA. Erlotinib in lung cancer - molecular and clinical predictors of outcome. N Engl J Med. 2005; 353: 133-44.

Turchi JJ, Henkels KM, Hermanson IL, Patrick SM. Interactions of mammalian proteins with cisplatin-damaged DNA. J Inorg Biochem. 1999; 77: 83-7.

Um JH, Kwon JK, Kang CD, Kim MJ, Ju DS, Bae JH, Kim DW, Chung BS, Kim SH. Relationship between antiapoptotic molecules and metastatic potency and the involvement of DNA-dependent protein kinase in the chemosensitization of metastatic human cancer cells by epidermal growth factor receptor blockade. J Pharmacol Exp Ther. 2004; 311: 1062-70.

VanGent DC, Hoeijmakers JH and Kanaar R. Chromosomal stability and the DNA double-strand break connection. Nature Rev Genet. 2001; 2: 196-206.

Vanhaesebroeck B, Leevers SJ, Ahmadi K, Timms J, Katso K, Driscoll PC, Woscholski R, Parker PJ, and Waterfield MD. Synthesis and function of 3-phosphorylated inositol lipids. Annu. Rev. Biochem. 2001. 70:535–602.

Viloria-Petit A, Crombet T, Jothy S, Hicklin D, Bohlen P, Schlaeppi JM, Rak J, Kerbel RS. Acquired resistance to the antitumor effect of epidermal growth factor receptor-blocking antibodies in vivo: a role for altered tumor angiogenesis. Cancer Res. 2001; 61: 5090-101.

Vogelstein B, and Kinzler KW. The multi-step nature of cancer. Trends Genet. 1993; 9, 138-141.

Voigt W. Sulforhodamine B assay and Chemosensitivity. Methods Mol Med. 2005; 110:39-48.

Wakeling AE, Guy SP, Woodburn JR, Ashton SE, Curry BJ, Barker AJ, Gibson KH. ZD1839 (Iressa): an orally active inhibitor of epidermal growth factor signaling with potential for cancer therapy. Cancer Res. 2002; 62: 5749-54.

Wang D, Lippard SJ. Cellular processing of platinum anticancer drugs. Nat Rev Drug Discov. 2005; 4: 307-20.

Wang JY. Abl tyrosine kinase in signal transduction and cell-cycle regulation. Curr Opin Genet Dev. 1993; 3: 35-43.

Wang JC. DNA topoisomerases. Annu Rev Biochem. 1996; 65: 635-92.

Wang P, Fredlin P, Davis CG & Yang X-D 2002 Therapeutic potential of ABX-EGF, a fully human anti-EGF receptor monoclonal antibody for the treatment of renal cell carcinoma. Proc of the American Society of Clinical Oncology 21 191a Abs: 761.

Warner JK, Wang JC, Hope KJ, Jin L, Dick JE. Concepts of human leukemic development. Oncogene. 2004; 23: 7164-77.

West SC. Molecular views of recombination proteins and their control. Nat Rev Mol Cell Biol. 2003; 4: 1-11.

Westover EJ, Covey DF, Brockman HL, Brown RE, Pike LJ. Cholesterol depletion results in site-specific increases in epidermal growth factor receptor phosphorylation due to membrane level effects. Studies with cholesterol enantiomers. J Biol Chem. 2003; 278: 51125-33.

Wheeler GP. Studies related to the mechanism of action of cytotoxic alkylating agents. Cancer Res. 1962; 22: 651.

Whitehouse CJ, Taylor RM, Thistlethwaite A, Zhang H, Karimi-Busheri F, Lasko DD, Weinfeld M, Caldecott KW. XRCC1 stimulates human polynucleotide kinase activity at damaged DNA termini and accelerates DNA single-strand break repair. Cell. 2001; 12: 104, 107-17.

Wilson CR, Davidson SE, Margison GP, Jackson SP, Hendry JH, West CM. Expression of Ku70 correlates with survival in carcinoma of the cervix. Br J Cancer. 2000; 83: 1702-6.

Wissner A, Overbeek E, Reich MF, Floyd MB, Johnson BD, Mamuya N, Rosfjord EC, Discafani C, Davis R, Shi X, Rabindran SK, Gruber BC, Ye F, Hallett WA, Nilakantan R, Shen R, Wang YF, Greenberger LM, Tsou HR. Synthesis and structure-activity relationships of 6,7-disubstituted 4-anilinoquinoline-3-carbonitriles. The design of an orally active, irreversible inhibitor of the tyrosine kinase activity of the epidermal growth factor receptor (EGFR) and the human epidermal growth factor receptor-2 (HER-2). J Med Chem. 2003; 46: 49-63.

Wolf M, Swaisland H, Averbuch S. Development of the novel biologically targeted anticancer agent gefitinib: determining the optimum dose for clinical efficacy. Clin Cancer Res. 2004; 10: 4607-13.

Xiong HQ, Rosenberg A, LoBuglio A, Schmidt W, Wolff RA, Deutsch J, Needle M, Abbruzzese JL. Cetuximab, a monoclonal antibody targeting the epidermal growth factor receptor, in combination with gemcitabine for advanced pancreatic cancer: a multicenter phase II Trial. J Clin Oncol. 2004; 22: 2610-6.

Xu W, Liu L, Smith GC, Charles G. Nitric oxide upregulates expression of DNA-PKcs to protect cells from DNA-damaging anti-tumour agents. Nat Cell Biol. 2000; 2: 339-45.

Xu B, Kim S & Kastan MB. Involvement of Brca1 in S-phase and G(2)-phase checkpoints after ionizing irradiation. Mol. Cell. Biol. 2001; 21: 3445–3450.

Xu B, O'Donnell AH, Kim ST & Kastan MB. Phosphorylation of serine 1387 in Brca1 is specifically required for the Atm-mediated S-phase checkpoint after ionizing irradiation. Cancer Res. 2002; 62: 4588–4591.

Xu JM, Azzariti A, Severino M, Lu B, Colucci G, Paradiso A. Characterization of sequence-dependent synergy between ZD1839 ("Iressa") and oxaliplatin. Biochem Pharmacol. 2003; 66: 551-63.

Yang XD, Jia XC, Corvalan JR, Wang P, Davis CG. Development of ABX-EGF, a fully human anti-EGF receptor monoclonal antibody, for cancer therapy. Crit Rev Oncol Hematol. 2001; 38: 17-23.

Yarden Y. The EGFR family and its ligands in human cancer: signalling mechanisms and therapeutic opportunities. Eur J Cancer. 2001; 37: S3-S8.

Yarden Y, Sliwkowski MX. Untangling the ErbB signalling network. Nat Rev Mol Cell Biol. 2001; 2: 127-37.

Yu D, Hung MC. Role of erbB2 in breast cancer chemosensitivity. Bioessays. 2000; 22: 673-80.

Yu H, Jove R. The STATs of cancer - new molecular targets come of age. Nat Rev Cancer. 2004; 4: 97-105.

Zhao H, Dugas N, Mathiot C, Delmer A, Dugas B, Sigaux F, Kolb JP. B-cell chronic lymphocytic leukemia cells express a functional inducible nitric oxide synthase displaying anti-apoptotic activity. Blood. 1998; 92: 1031-43.

Zhang QX, Borg A, Fuqua SA. An exon 5 deletion variant of the estrogen receptor frequently coexpressed with wild-type estrogen receptor in human breast cancer. Cancer Res. 1993; 53: 5882-4.

Zhao HJ, Hosoi Y, Yoshida M, Takai Y, Yamada S, Suzuki N, Ono T. DNA-dependent protein kinase activity correlates with Ku70 expression and radiation sensitivity in esophageal cancer cell lines. Clin Cancer Res. 2000; 6: 1073-8.

Zhong, D., Pal, S. K., Wan, C. & Zewail, A. H. Femtosecond dynamics of a drug–protein complex: daunomycin with Aporiboflavin-binding protein. Proc. Natl Acad. Sci USA. 2001; 98, 11873–11878.

Zhou BB and Elledge SJ. The DNA damage response: putting checkpoints in perspective. Nature 2000 408, 433–439.

Zhou BP, Liao Y, Spohn B, Hung MC. HER-2/neu induces p53 ubiquitination via Akt-mediated MDM2 phosphorylation. Nat Cell Biol. 2001; 3: 973-82.

Zhu XF, Liu ZC, Xie BF, Li ZM, Feng GK, Yang D, Zeng YX. EGFR tyrosine kinase inhibitor AG1478 inhibits cell proliferation and arrests cell cycle in nasopharyngeal carcinoma cells. Cancer Lett. 2001; 169: 27-32.

Zwelling LA, Michaels S, Schwartz H, Dobson PP, Kohn KW. DNA cross-linking as an indicator of sensitivity and resistance of mouse L1210 leukaemia to cis-diamminedichloroplatinum(II) and L-phenylalanine mustard. Cancer Res. 1981; 41: 640-9.

Featured Article

Modulation of DNA Repair *In vitro* after Treatment with Chemotherapeutic Agents by the Epidermal Growth Factor Receptor Inhibitor Gefitinib (ZD1839)

Benjamin Friedmann,[1] Martyn Caplin,[2] John A. Hartley,[3] and Daniel Hochhauser[1]

[1]Department of Oncology, Royal Free and University College Medical School, University College London; and [2]Department of Gastroenterology, Royal Free Hospital, London, United Kingdom; [3]Cancer Research United Kingdom Drug-DNA Interactions Research Group,

ABSTRACT

Purpose: **The epidermal growth factor receptor (EGFR) is commonly expressed in human tumors and provides a target for therapy. Gefitinib (Iressa, ZD1839) is a quinazoline derivative that inhibits EGFR tyrosine kinase activity. Gefitinib demonstrated anticancer efficacy *in vivo*, and although experiments *in vitro* have suggested that inhibition of EGFR modulates the activity of chemotherapeutic agents, the mechanism of this interaction is unclear. We investigated mechanisms for this modulation.**

Experimental Design: **The antiproliferative effect of gefitinib alone or combined with cisplatin, melphalan, and etoposide was determined in a human breast (MCF-7) cancer cell line. Using the alkaline single-cell gel electrophoresis (comet) assay, we investigated kinetics of DNA damage and repair after treatment with the chemotherapeutic drugs combined with gefitinib. To investigate whether the phosphatidylinositol 3′-kinase pathway was contributing to repair-inhibition produced by gefitinib, cells were exposed to chemotherapy in combination with the phosphatidylinositol 3′-kinase inhibitor LY294002.**

Results: **A superadditive (synergistic) increase in growth inhibition for combined treatment with gefitinib was found for cisplatin and etoposide, but not with melphalan. There was delayed repair of DNA strand breaks after treatment with etoposide combined with gefitinib, and repair of DNA interstrand cross-links produced by cisplatin is delayed in combination with gefitinib. Inhibition of cell proliferation and DNA repair was identical in cells treated with LY294002. Immunoprecipitation of cell extracts demonstrated that after exposure to gefitinib, there was an association between EGFR and DNA-PK_{CS}.**

Conclusion: **Gefitinib acts through inhibition of repair of cisplatin and etoposide-induced DNA damage; this effect is mimicked by inhibitors of the phosphatidylinositol 3′-kinase suggesting similar mechanisms of action.**

INTRODUCTION

The epidermal growth factor receptor (EGFR) is commonly expressed at high levels in many human cancers including breast, non-small cell lung, and colon (1). EGFR (erbB1) is a member of the family of erbB receptors, the structure of which includes extracellular ligand binding, *trans*-membrane, and intracellular tyrosine kinase domains (2). Activation of the EGFR pathway results in downstream signaling including the lipid kinase phosphatidylinositol 3′-kinase and the serine/threonine kinase pathways (3). This signaling cascade has been implicated in a variety of alterations including proliferation, angiogenesis, and metastasis. EGFR expression increases with tumor progression and is an independent prognostic factor for a variety of malignancies including breast cancer (4).

In view of the importance of the EGFR pathway in human cancer, several approaches to the inhibition of EGFR have been developed with the aim of blocking cancer cell proliferation and promoting apoptosis. These strategies include antibodies blocking the receptor-ligand interaction and small molecules blocking dimerization of the intracellular kinase domain and hence activation of consequent pathways (5, 6).

Gefitinib [Iressa (AstraZeneca, Macclesfield, United Kingdom), ZD1839] is a quinazoline derivative that inhibits EGFR tyrosine kinase activity by competitively inhibiting the ATP-binding domain (7). Gefitinib has demonstrated anticancer efficacy *in vivo* in non-small cell lung cancer (8) and is currently licensed for clinical use. Experiments *in vitro* with several cancer cell types have shown that inhibition of EGFR by antisense mRNA or with gefitinib can increase the cytotoxic effects of several chemotherapeutic agents with differing structure and mode of activity (9, 10); however, the mechanisms underlying these interactions are unclear. Clinical studies have provided additional support for potential interactions between EGFR inhibition and chemotherapy. For example, a recent study with the anti-EGFR antibody cetuximab in irinotecan-refractory colon cancer demonstrated that additional responses to irinotecan could be achieved (11). The mechanism of this resensitization remains unclear, as does the optimal combination of these agents in the treatment of chemotherapy-naïve patients.

To understand the effects of EGFR inhibition on modulat-

Received 3/26/04; revised 6/15/04; accepted 6/22/04.
Grant support: The Times 'Quiet Cancer' Appeal.
The costs of publication of this article were defrayed in part by the payment of page charges. This article must therefore be hereby marked *advertisement* in accordance with 18 U.S.C. Section 1734 solely to indicate this fact.
Requests for reprints: Daniel Hochhauser, Department of Oncology, Royal Free and University College School of Medicine, University College London, Gower Street Campus, 91 Riding House Street, London W1W 7BS, United Kingdom. Phone: 44-20-7679-9326; Fax: 44-20-7436-2956; E-mail: d.hochhauser@ucl.ac.uk.

ing chemotherapeutic drug activity, we investigated the interaction of gefitinib with the widely used drugs cisplatin, etoposide, and melphalan. We investigated the kinetics of DNA damage and repair after treatment with these chemotherapeutic drugs, alone and in combination with gefitinib using the alkaline single-cell gel electrophoresis (comet) assay. There was a significant delay in repair of DNA strand breaks resulting from treatment with etoposide when combined with gefitinib. Additionally, inhibition of repair of cisplatin-induced cross-links was noted with gefitinib. Studies using inhibitors of the phosphatidylinositol 3′-kinase pathway gave similar results in proliferation and repair assays, suggesting involvement of this pathway in the inhibition of repair by these agents.

MATERIALS AND METHODS

Materials. Clinical grade gefitinib was kindly provided by AstraZeneca. Cisplatin, etoposide, and melphalan were purchased from Sigma-Aldrich (Dorset, United Kingdom).

Cell Lines and Culture Conditions. MCF-7 cells (obtained from CR-United Kingdom London Research Institute, London, United Kingdom) were grown in Earle's minimal essential medium (Autogen Bioclear, Wilthshire, United Kingdom) supplemented with 10% fetal calf serum, 1% glutamine, and 0.1% nonessential amino acids and incubated at 37°C in 5% CO_2. For growth inhibition assays, 5×10^3 cells were seeded into 96-well microtiter plates and left for 48 hours. For single-agent studies, drugs were then added at a range of concentrations to triplicate wells and left in contact for 5 days. For combination studies, drugs were either added concomitantly for 5 days or sequentially by adding each drug in turn for 24 hours, followed by 48 hours in drug-free growth medium. Control wells were treated in the same way with aspiration at each 24-hour period. For combination experiments, gefitinib was added at concentrations producing 10 and 20% inhibition of proliferation, to a range of concentrations for the chemotherapeutic agent. Cytotoxicity was assessed using the sulforhodamine B assay (12). At the end of the incubation period, cell numbers were compared in treated *versus* control wells by fixing in ice-cold 10% (w/v) trichloroacetic acid (20 minutes) and staining with 0.4% sulforhodamine B in 1% (v/v) acetic acid (20 minutes). The mean absorbance at 540 nm for each drug concentration was expressed as a percentage of the control untreated well absorbance.

Isobologram Analysis. To assess whether a combination dose of any given chemotherapeutic agent with gefitinib is synergistic or additive, the isobologram method was used as described previously (13). An IC_{50} was selected, and doses of each drug alone that give this effect were plotted as axial points in a Cartesian plot.

The straight line connecting their IC_{50} is the locus of points (dose pairs) that will produce this effect in a simply additive combination. Thus, IC_{50} for two drugs added together lying on the line have an additive effect. Above this line, they are subadditive (antagonistic), and below the line, superadditive (synergistic).

Single-Cell Gel Electrophoresis (Comet) Assay. MCF-7 cells were treated with etoposide and gefitinib for 24 hours at 37°C. The DNA damage in the form of strand breaks was assessed using the single-cell gel electrophoresis (comet) assay as described previously (14). All procedures were carried out on ice and in subdued lighting. All chemicals used were obtained from Sigma Chemical (Poole, United Kingdom) unless otherwise stated. In brief, cells were embedded in 1% agarose on a precoated microscope slide, lysed for 1 hour in lysis buffer [100 mmol/L disodium EDTA, 2.5 mol/L NaCl, and 10 mmol/L Tris-HCl (pH 10.5)] containing 1% Triton X-100 (added immediately before analysis), and washed every 15 minutes in distilled water for 1 hour. Slides were then incubated in alkali buffer [50 mmol/L NaOH and 1 mmol/L disodium EDTA (pH 12.5)] for 45 minutes, followed by electrophoresis in the same buffer for 25 minutes at 18 V (0.6 V/cm), 250 mA. The slides were finally rinsed in neutralizing buffer [0.5 mol/L Tris-HCl (pH 7.5)] and then saline. After drying, the slides were stained with propidium iodide (2.5 μg/mL) for 30 minutes and then rinsed in distilled water. Images were visualized with the use of a Nikon inverted microscope with high-pressure mercury light source (Nikon United Kingdom Limited, Kingston Upon Thames, United Kingdom), 510 to 560 nm excitation filter, and 590 nm barrier filter at ×20 magnification. Images were captured by using an on-line charge-couple device camera and analyzed with Komet Analysis software (Kinetic Imaging, Liverpool, United Kingdom). For each duplicate slide, 25 cells were analyzed. DNA damage was measured by the increase in the tail moment, a function of the amount of DNA in the tail and the length of the tail (14). Detection and measurement of DNA interstrand cross-links was achieved using a modification of the comet assay (15). Immediately before analysis, cells were irradiated (12 Gy) to deliver a fixed number of random DNA strand breaks. The tail moment for each image was calculated by using the Komet Analysis software as the product of the percent DNA in the comet tail and the distance between the means of the head and tail distributions, based on the definition of Olive *et al.* (16). Cross-linking was expressed as the percent decrease in tail moment compared with irradiated controls, calculated by the following formula:

$$\text{Percentage of decrease in tail moment} = [1 - (\text{TMdi} - \text{TMcu}/\text{TMci} - \text{TMcu})] \times 100$$

where TMdi equals tail moment of drug-treated irradiated sample, TMcu equals tail moment of untreated unirradiated control, and TMci equals tail moment of untreated irradiated control.

Immunoprecipitation and Western Blotting. Cells were washed twice in PBS and scraped into lysis buffer [radioimmunoprecipitation assay buffer: 1% deoxycholic acid, 1% Triton X-100, 0.1% SDS, 250 mmol/L NaCl, 50 mmol/L Tris (pH 7.5), 100 μg/mL 4-(2-aminoethyl) benzenesulfonylfluoride, 17 μg/mL aprotinin, 1 μg/mL leupeptin, 1 μg/mL pepstatin, 5 μmol/L fenvalerate, 5 μmol/L potassium bisperoxo(1,10-phenanthroline)-oxovanadate(V) (BpVphen), and 1 μmol/L okadaic acid]. Lysates were refined by centrifugation at 14,000 × *g* for 10 minutes at 4°C, and protein concentrations were determined using a protein assay kit (Bio-Rad, Cambridge, MA).

Two-hundred and fifty μg of protein cell lysates were immunoprecipitated using 2 to 4 μg of antibody (anti-EGFR or anti-DNA-PK_{CS}) overnight at 4°C and then bound to protein G Sepharose. Immune complexes were washed three times in lysis buffer before additional analysis. Cell lysates (15–50 μg) and imunoprecipitates were separated by SDS-

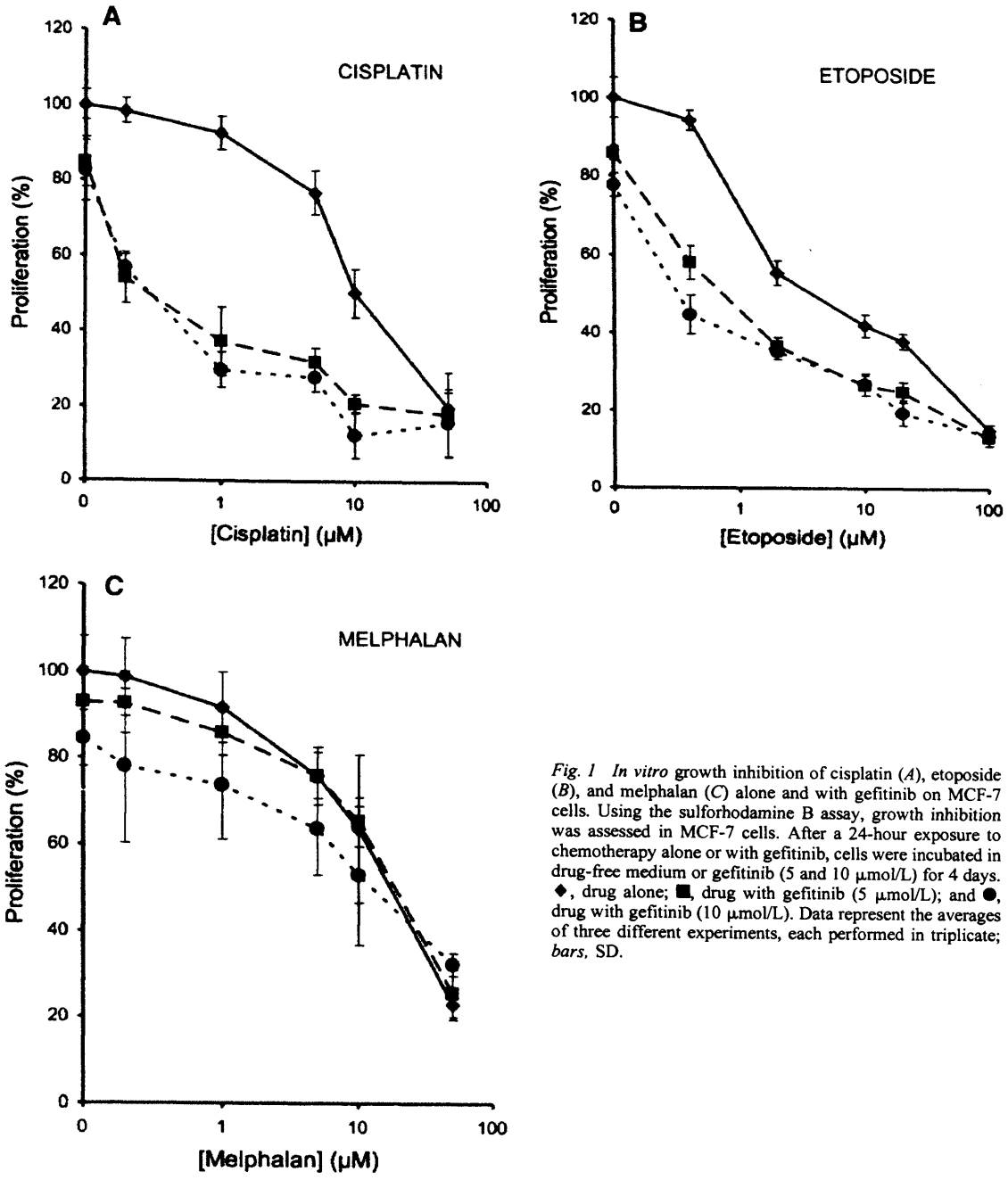

Fig. 1 *In vitro* growth inhibition of cisplatin (*A*), etoposide (*B*), and melphalan (*C*) alone and with gefitinib on MCF-7 cells. Using the sulforhodamine B assay, growth inhibition was assessed in MCF-7 cells. After a 24-hour exposure to chemotherapy alone or with gefitinib, cells were incubated in drug-free medium or gefitinib (5 and 10 μmol/L) for 4 days. ◆, drug alone; ■, drug with gefitinib (5 μmol/L); and ●, drug with gefitinib (10 μmol/L). Data represent the averages of three different experiments, each performed in triplicate; *bars*, SD.

PAGE, electrophoretically transferred to Immobilon P membrane (Millipore), and probed with appropriate primary antibodies (anti-EGFR or anti-DNA-PK_{CS}) and then horseradish peroxidase–conjugated secondary polyclonal antibody. Immunoreactive bands were visualized with the enhanced chemiluminescence system (Amersham Bioclear).

Immunoblotting antibodies were anti-EGFR and horseradish peroxidase–labeled secondary Ab (BD Biosciences), anti-EGFR (phospho-Tyr^{845}; abcam), anti-DNA-PK_{CS}, and anti-tubulin (Sigma).

RESULTS

Gefitinib Treatment Synergizes the Effects of Cisplatin and Etoposide in MCF-7 Cells. There have been several reports on synergistic interactions of several chemotherapeutic

agents and gefitinib (9, 17). We investigated these effects in relation to three commonly used chemotherapeutic agents; cisplatin, etoposide, and melphalan. Treatment of MCF-7 cells with gefitinib alone demonstrated a 50% growth inhibition (IC_{50}) of 17 ± 0.021 μmol/L as measured by a sulforhodamine B proliferation assay (results not shown). This is similar to results obtained in other studies using this cell line (18). The IC_{50} concentration for cisplatin alone was 10 ± 0.9 μmol/L. Cells were treated with cisplatin for 24 hours in combination with gefitinib followed by gefitinib alone. There was a synergistic effect on inhibition of cell proliferation when MCF-7 cells were treated with cisplatin in combination with gefitinib. In contrast to cisplatin alone, incubation of cisplatin and 5 μmol/L gefitinib resulted in an IC_{50} of 0.2 ± 0.003 μmol/L (Fig. 1*A*).

Similar experiments were performed with MCF-7 cells using etoposide, a topoisomerase II poison. Cells exposed to etoposide alone demonstrated an IC_{50} of 3.5 ± 0.08 μmol/L, whereas in the presence of 5 μmol/L gefitinib, the IC_{50} was 0.7 ± 0.005 μmol/L (Fig. 1*B*). In contrast to the results obtained with cisplatin and etoposide, there was no demonstrable synergy with melphalan in combination with gefitinib with an IC_{50} of 19 ± 1.08 μmol/L (Fig. 1*C*). Therefore the effects of gefitinib on cell proliferation in combination with chemotherapy are variable with different chemotherapeutic agents. Analysis of these results by an isobologram methodology (13) confirmed that the combinations of gefitinib with cisplatin and etoposide were synergistic in contrast to the result in combination with melphalan (Fig. 2).

Gefitinib Inhibits Repair of Cisplatin and Etoposide-Induced DNA Damage. In view of the effects of gefitinib on the cytotoxicity of cisplatin and etoposide, but not melphalan, we investigated whether this could be modulated at the level of drug-induced DNA damage. To determine effects on DNA damage and repair, we used the single-cell gel electrophoresis (comet) assay (16). This can be used to quantitate DNA strand breaks and repair after exposure to drug. A modification to measure DNA interstrand cross-links has been developed (14, 15). This involves irradiating the cells immediately before analysis to deliver a fixed level of random DNA strand breaks. In the presence of strand breaks, interstrand cross-links retard migration, thus reducing the tail moment compared with the non-cross-linked irradiated control. To examine the kinetics of DNA repair, a brief exposure to etoposide, cisplatin, and melphalan was followed by prolonged incubation with gefitinib.

Quantitation of DNA strand breaks after etoposide treatment has been well characterized. Initial experiments with etoposide confirmed that after exposure of MCF-7 cells to subtoxic concentrations of drug, maximal strand breakage was detectable after 2 hours of exposure (data not shown). There was no alteration in the quantity of strand breaks in cells produced with etoposide alone and in combination with gefitinib (Fig. 3). After removal of drug, strand-break repair was detectable within 30 minutes with almost complete repair after 4 hours. As shown in Fig. 3, exposure of cells to gefitinib alone produced no DNA strand breaks. After combination treatment with both etoposide and gefitinib, there was a marked delay in the rate of repair of DNA strand breaks with 45% of strand breaks remaining at 1 hour. There was persistent DNA damage detectable after 24 hours, in contrast with the result after exposure to etoposide alone. Both cisplatin and melphalan produce

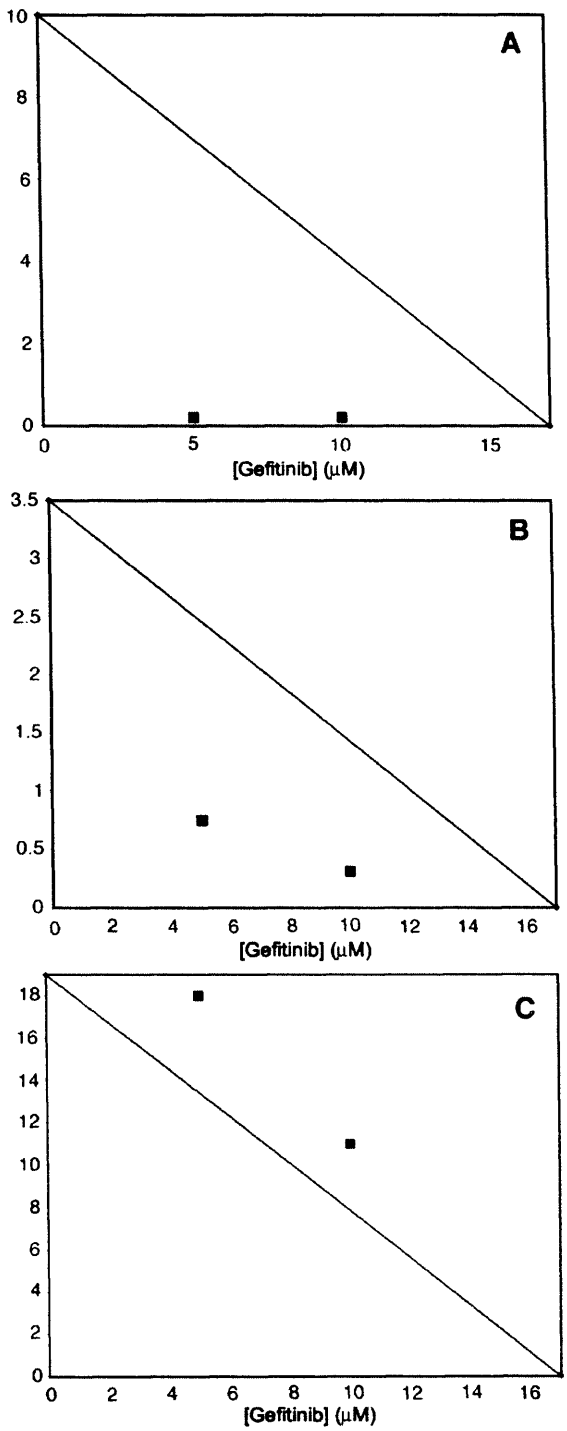

Fig. 2 Isobologram analyses of growth inhibition of cisplatin (*A*), etoposide (*B*), and melphalan (*C*) alone and with gefitinib (5 and 10 μmol/L) on MCF-7 cells. The *straight line* connecting their IC_{50} points (additivity line) is the locus of all dose pairs that, based on these potencies, should give the same effect. A dose pair attaining this effect with lower quantities is superadditive (synergistic), whereas a point appearing close to the line is additive. Dose pairs IC_{50} of drug and gefitinib together.

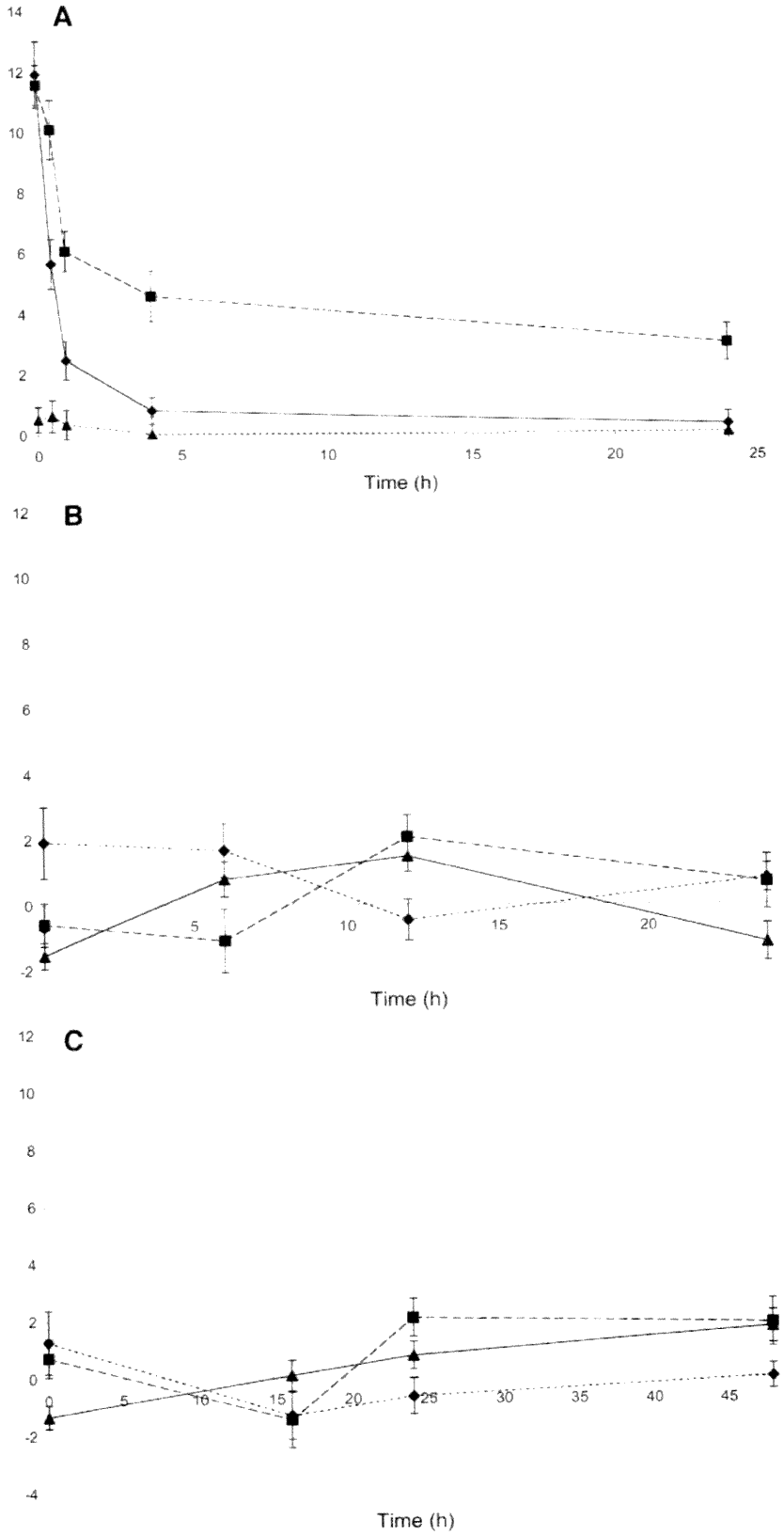

Fig. 3 *A*, measurement of etoposide-induced DNA strand breaks and their repair alone or in the presence of gefitinib in MCF-7 cells. Cells were treated with etoposide (100 μmol/L) and gefitinib (10 μmol/L) for 2 hours and then incubated with gefitinib (10 μmol/L) alone. Strand-break formation measured as tail moment length (micrometers). ♦, etoposide; ■, etoposide with gefitinib (10 μmol/L); and ▲, gefitinib (10 μmol/L). *B*, measurement of cisplatin-induced DNA strand breaks and their repair alone or in the presence of gefitinib in MCF-7 cells. Cells were treated with cisplatin (200 μmol/L) and gefitinib (10 μmol/L) for 1 hour and then incubated with gefitinib (10 μmol/L) alone. Strand-break formation measured as tail moment length (micrometers). ♦, cisplatin; ■, cisplatin with gefitinib (10 μmol/L); ▲, gefitinib (10 μmol/L). *C*, measurement of melphalan-induced DNA strand breaks and their repair alone or in the presence of gefitinib in MCF-7 cells. Cells were treated with melphalan (200 μmol/L) and gefitinib (10 μmol/L) for 1 hour and then incubated with gefitinib (10 μmol/L) alone. Strand-break formation measured as tail moment length (micrometers). ♦, melphalan; ■, melphalan with gefitinib (10 μmol/L); and ▲, gefitinib (10 μmol/L). Data represent the averages of three different experiments; *bars*, SE.

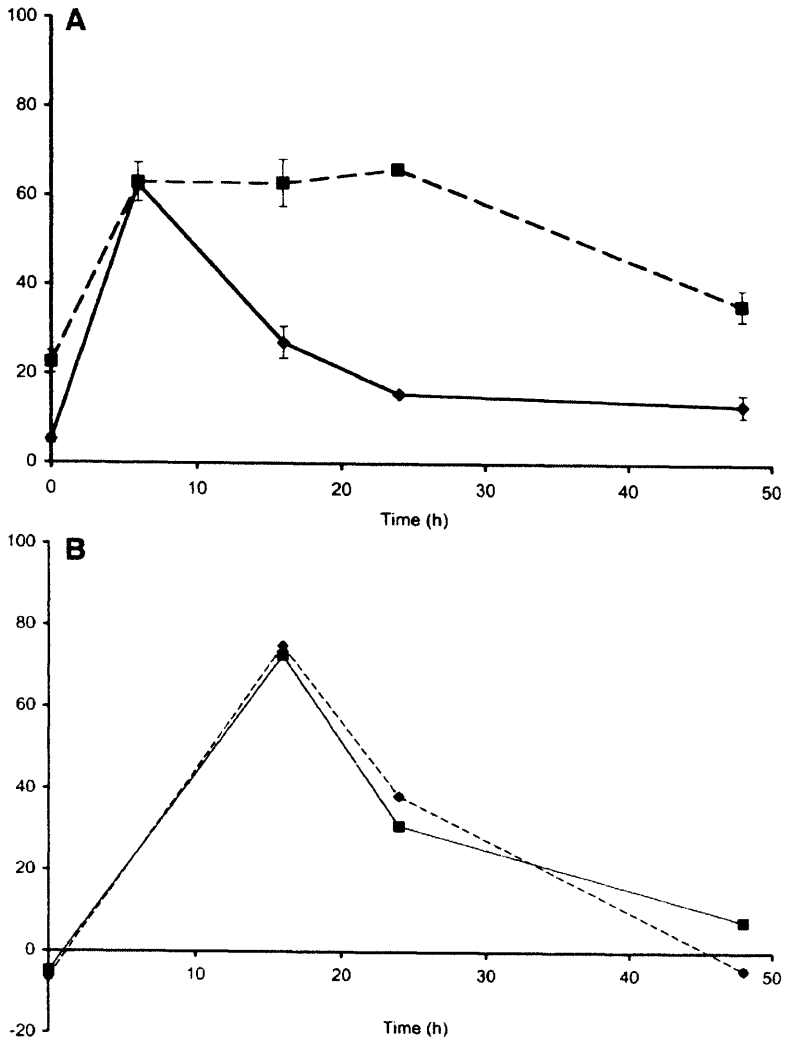

Fig. 4 *A*, measurement of cisplatin-induced DNA interstrand cross-links and repair alone and in the presence of gefitinib in MCF-7 cells. Cells were treated with cisplatin (200 μmol/L) and gefitinib (10 μmol/L) for 1 hour and then incubated with gefitinib (10 μmol/L) alone. Interstrand cross-link formation represented as percent decrease in tail moment. ◆, cisplatin; and ■, cisplatin with gefitinib (10 μmol/L). *B*, measurement of melphalan-induced DNA interstrand cross-links and repair alone or in the presence of gefitinib in MCF-7 cells. Cells were treated with melphalan (100 μmol/L) and gefitinib (10 μmol/L) for 1 hour and then replaced with gefitinib (10 μmol/L) alone. Interstrand cross-link formation represented as percent decrease in tail moment. ◆, melphalan; and ■, melphalan with gefitinib (10 μmol/L). Data represent the averages of three different experiments; *bars*, SE.

no detectable strand breaks alone or in the presence of gefitinib (Fig. 3*B* and *C*).

Additional experiments were performed using MCF-7 cells after incubation with cisplatin. Interstrand cross-links have been demonstrated to be critical in the cellular effects of cisplatin (19). The formation and repair of interstrand cross-links formed after a 1-hour exposure to cisplatin were measured. In MCF-7 cells, interstrand cross-links were repaired efficiently with almost complete removal by 24 hours (Fig. 4*A*). To investigate whether the addition of gefitinib modulated the repair of cisplatin-induced DNA lesions, cells were exposed for 1 hour to cisplatin, after which the amount of DNA damage and the rate of repair were assessed (Fig. 4*A*). For MCF-7 cells incubated with gefitinib and cisplatin, there was no effect on the quantity of interstrand cross-links produced as compared with cisplatin alone. However, there was clear inhibition of cisplatin-induced interstrand cross-link repair after coincubation with gefitinib as compared with cisplatin alone. In contrast, cells treated with the combination of gefitinib and cisplatin showed persistent interstrand cross-links at 48 hours after removal of drug. Gefitinib alone produced no interstrand cross-links (data not shown).

The response of MCF-7 cells to melphalan was also assessed. Previous experiments using the sulforhodamine B assay did not demonstrate a synergistic interaction between gefitinib and melphalan on the inhibition of cell proliferation. Comet assays demonstrated that melphalan-induced DNA cross-links peak 16 hours after a 1-hour exposure to drug and are repaired after 48 hours following treatment. In contrast to the results obtained using gefitinib in combination with etoposide and cisplatin, exposure of MCF-7 cells with gefitinib and melphalan resulted in no alteration in the kinetics of DNA repair (Fig. 4*B*).

To address whether inhibition of DNA damage repair by gefitinib leads to the induction of apoptosis, the annexin V assay was performed. This showed no evidence of apoptosis during the time course of the experiment (data not shown). Therefore the strand breaks are not due to apoptosis.

Inhibition of Phosphatidylinositol 3′-Kinase Pathway and Chemosensitivity in MCF-7 Cells. The phosphatidylinositol 3′-kinase pathway has been implicated in the repair of cisplatin and etoposide-induced DNA lesions (20, 21). To investigate whether the inhibition of repair found with gefitinib could be mediated through this pathway, we exposed MCF-7 cells to the phosphatidylinositol 3′-kinase inhibitor LY294002. Synergy was demonstrated in an sulforhodamine B assay with LY294002 when MCF-7 cells were treated with cisplatin (Fig. 5*A*). The IC_{50} for cells treated with cisplatin and LY294002 was 0.25 ± 0.04 μmol/L, comparable with the combination of cisplatin and gefitinib (0.2 ± 0.003 μmol/L). Experiments in which cells were exposed to the combination of gefitinib, LY294002, and cisplatin did not result in additional inhibition of cellular proliferation with an $IC_{50\ of}$ 0.20 ± 0.05 μmol/L. Interestingly, as with gefitinib, there was no demonstrable synergy for the combination of LY294002 and melphalan (Fig. 5*B*).

To determine the significance of inhibition of the phosphatidylinositol 3′-kinase pathway in the cellular response to cisplatin, we performed comet assays on cells after exposure to cisplatin and LY294002. A delay in repair of the cisplatin-induced interstrand cross-links was found with kinetics comparable with that found on exposure to gefitinib and cisplatin. The addition of gefitinib to the combination of cisplatin and LY294002 did not further alter the extent of DNA interstrand cross-link formation or the time course for DNA repair (Fig. 6*A*). These results suggest that the inhibition of repair of cisplatin-induced DNA lesions by gefitinib and LY294002 may occur through the same pathway. Experiments with cisplatin in combination with the phosphatidylinositol 3′-kinase inhibitor wortmannin showed similar effects to LY294002 on inhibition of cellular proliferation and DNA repair (data not shown).

As previously found with gefitinib, exposure of cells to melphalan and LY294002 resulted in no alteration of the DNA repair profile as compared with melphalan alone as assessed by comet assays (Fig. 6*B*). Therefore the inhibitory effect of LY294002 on DNA repair does not occur with all DNA-interactive chemotherapeutic agents.

Modulation of Epidermal Growth Factor Receptor and DNA-PKcs by Gefitinib. Incubation of cells with cisplatin resulted in increased phosphorylation of EGFR as described previously with other cell lines (Fig. 7*A*; ref. 22). Treatment of cells with gefitinib resulted in a decrease in phosphorylated EGFR. The increase in phosphorylated EGFR after cisplatin treatment was blocked by incubation with gefitinib. Similar results were obtained using the phospho-tyrosine antibody, PY20 (data not shown).

In view of the results above suggesting involvement of the phosphatidylinositol 3′-kinase pathway in response of cells to gefitinib and cisplatin, we performed immunoblotting of MCF-7 cells after exposure to cisplatin and melphalan and assessed protein levels of the catalytic subunit of DNA-PK (DNA-PK_{CS}). After exposure to gefitinib, there was a reduction in DNA-PK_{CS} levels, although neither cisplatin nor melphalan treatment alone had any effect on DNA-PK_{CS} levels. The reduction in DNA-PK_{CS} levels persisted when cells were exposed to combinations of cisplatin and melphalan with gefitinib (Fig. 7*B*).

A previous report suggested association of EGFR and DNA-PK_{CS} in cells treated with the anti-EGFR antibody C225

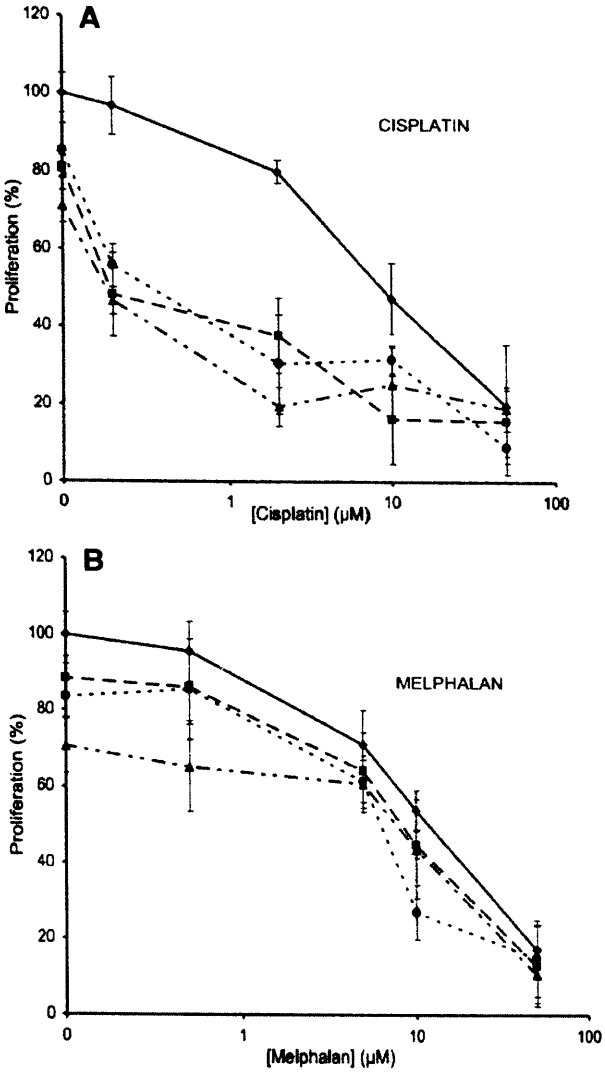

Fig. 5 In vitro growth inhibition of cisplatin (*A*) and melphalan (*B*) alone and with gefitinib and/or LY294002 of MCF-7 cells. Using the SRB assay, growth inhibition was assessed in MCF-7 cells. After a 24-hour exposure to chemotherapy alone or with gefitinib and/or LY294002, cells were incubated in drug-free medium or gefitinib (10 μmol/L) and/or LY294002 (10 μmol/L) for 4 days. ◆, drug alone; ■, drug with gefitinib (10 μmol/L); ●, drug with LY294002 (10 μmol/L); and ▲, drug with gefitinib (10 μmol/L) and LY294002 (10 μmol/L). Data represent the averages of three different experiments, each performed in triplicate; *bars*, SD.

(23). To investigate whether gefitinib had similar effects on the association of EGFR and DNA-PK_{CS}, we performed immunoprecipitations with EGFR and probed with DNA-PK_{CS} on cell lysates after treatment with gefitinib. As shown in Fig. 7*C*, an association of EGFR and DNA-PK_{CS} was detectable in untreated cells. However, after treatment with gefitinib, an increased amount of DNA-PK_{CS} was found to be associated with EGFR. A similar result was found when cell extracts were immunoprecipitated with DNA-PK_{CS} and probed with antibody

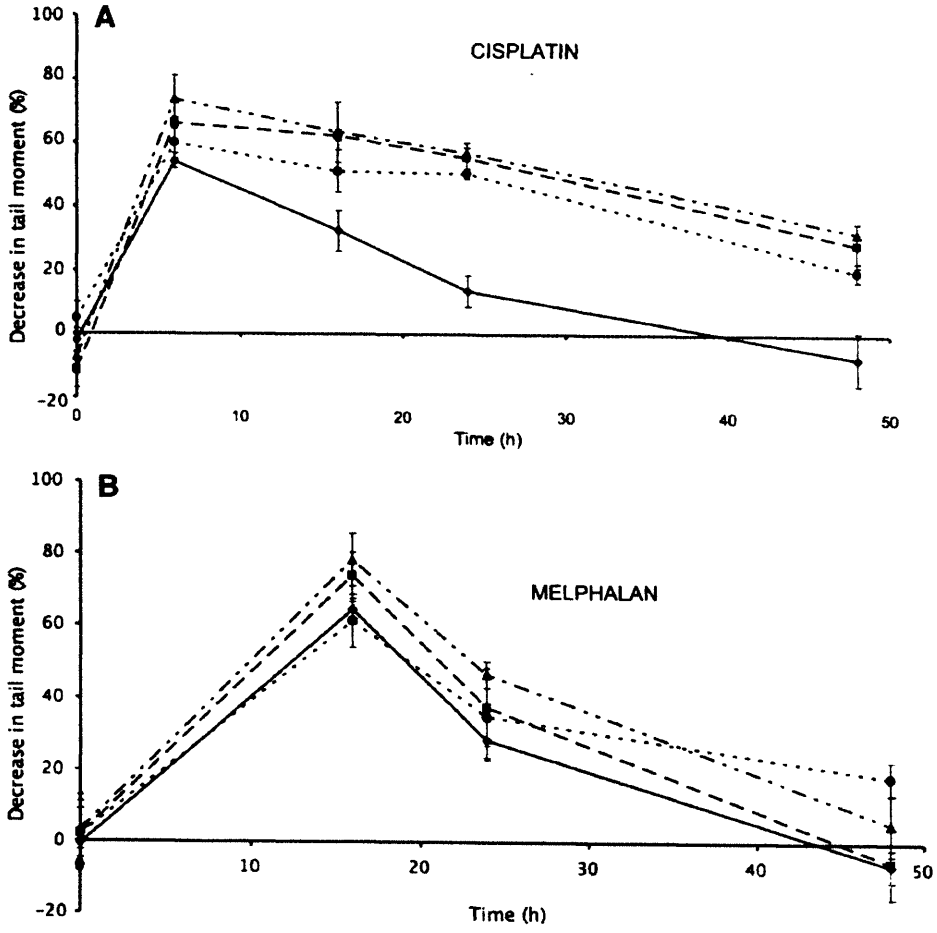

Fig. 6 Measurement of cisplatin (*A*) and melphalan (*B*)-induced DNA interstrand cross-links and repair alone or in the presence of gefitinib and/or LY294002 in MCF-7 cells. Cells were treated with cisplatin (200 μmol/L) or melphalan (100 μmol/L) and gefitinib and/or LY294002 for 1 hour and then incubated with gefitinib and/or LY294002 alone. At various time points after initial exposure, cells were harvested and analyzed using the comet assay. Interstrand cross-link formation is represented as percent decrease in tail moment. ◆, drug alone; ■, drug with LY294002 (10 μmol/L); ●, drug with gefitinib (10 μmol/L); ▲, drug with gefitinib (10 μmol/L) and LY294002 (10 μmol/L). Data represent the averages; *bars*, SE.

to EGFR (Fig. 7*D*). These results suggest that effects of gefitinib on DNA-PK_{CS} may be mediated through induced association with EGFR.

DISCUSSION

This study demonstrates that gefinitib, a small molecule inhibitor of EGFR, may synergize the effects of DNA-interactive chemotherapeutic drugs by modulation of DNA repair. EGFR is commonly expressed in human cancers through a variety of mechanisms including gene amplification and mutation (1). Activation of the EGFR receptor results in modulation of downstream pathways including the *ras/raf*/mitogen-activated protein kinase cascades. The expression of EGFR in tumors may result in increased rate of cellular proliferation, metastasis, and angiogenesis.

Several strategies for the inhibition of EGFR have undergone clinical evaluation and demonstrated *in vitro* and clinical activity in malignancies including colon and non-small cell lung cancers (8, 11). Experimental studies on cell lines and xenografts have shown synergies between gefitinib and a variety of anticancer agents including chemotherapeutic agents and radiation (24). The basis for these synergies has not been clearly defined. Inhibition of EGFR has been shown to directly affect the threshold of apoptosis within the cell by mechanisms including caspase activation (25). However, it is unclear as to whether the synergies demonstrated thus far in relation to anticancer activity are specific to particular agents or apply equally to all classes of anticancer drugs.

This study investigated the effects of EGFR inhibition on the modulation of DNA damage in the breast cancer cell line MCF-7. Studies on cellular proliferation confirmed synergies previously noted in other cell lines with cisplatin and etoposide, but this effect was not found with the nitrogen mustard melphalan. The MCF-7 cell line has been noted to be relatively resistant to inhibition of proliferation by gefitinib compared with other cell lines (18). The nature of the DNA damage induced by these agents is well understood. The comet assay is a validated methodology for quantitating DNA damage and repair after exposure to these drugs (14, 15). As discussed above, the formation of strand breaks cannot be accounted for by induction of apoptosis. Initial experiments demonstrated striking inhibition of DNA repair by gefitinib of both DNA strand breaks and interstrand cross-links after exposure to etoposide and cisplatin, respectively. Interestingly, as with the results found in proliferation

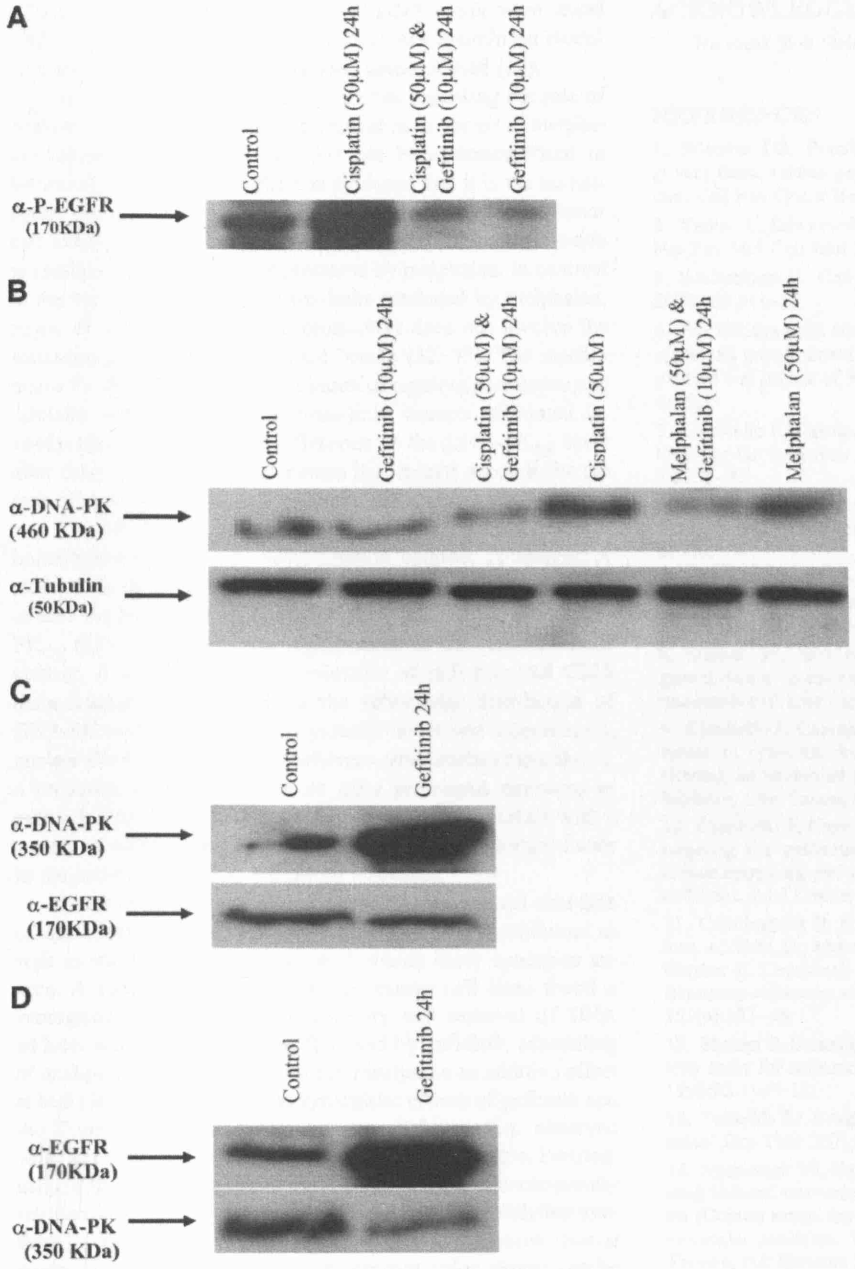

Fig. 7 A, tyrosine phosphorylation of EGFR in MCF-7 cells determined by immunoprecipitation with anti-EGFR and immunoblotted with anti-EGFR (phospho-Tyr^{845}) antibody. Cells were treated with cisplatin and gefitinib as described in the figure. *B*, immunoblotting with anti-DNA-PK_{CS} antibody on MCF-7 cell lysates. Cells were treated with cisplatin, melphalan, and gefitinib as described in the figure. *C*. Gefitinib induces association of EGFR with DNA-PK. *Top panel*. MCF-7 cells were treated with gefitinib (10 μmol/L), and lysates were immunoprecipitated with anti-EGFR and immunoblotted with anti-DNA-PK_{CS} antibody. *Bottom panel*. The blot was then stripped and reprobed with antibody to EGFR. *D*, treatment as in *C*. *Top panel*. Lysates were immunoprecipitated with anti-DNA-PK_{CS} and immunoblotted with anti-EGFR. *Bottom panel*. The blot was then stripped and reprobed with antibody to DNA-PK_{CS}.

assays, there was no modulation of the repair of DNA damage after treatment with melphalan.

To investigate these findings further, we focused on the DNA-PK pathway. DNA-PK is a critical component of the nonhomologous end rejoining nonhomologous end-joining recombination pathway, which has been shown to be responsible for repair of DNA double-strand breaks (26, 27). The DNA-PK complex consists of a heterodimer of the Ku70 and Ku80 proteins and DNA-PK_{CS}. The significance of this pathway in repair of drug-induced DNA damage has been shown for cells lacking nonhomologous end-joining recombination activity, which are hypersensitive to etoposide (28). The role of nonhomologous end-joining recombination in repair of DNA cross-links produced by cisplatin is unclear, but cellular sensitization to cisplatin has been found with other inhibitors of DNA-PK (29). Synergy of the effects of cisplatin on cell proliferation was found when cells were exposed to wortmannin and LY294002, which block the phosphatidylinositol 3′-kinase pathway. This was associated with inhibition of repair to a similar extent as that found with gefitinib; as with gefitinib, neither synergistic

effects on cytotoxicity nor effects on DNA repair were found with melphalan. An inhibitory effect of wortmannin on etoposide-induced DNA damage has been demonstrated (20).

There has been contrasting evidence regarding the role of nonhomologous end-joining recombination in repair of melphalan-induced lesions; although this has been demonstrated in hemopoietic cancer cells, there is evidence that it is the homologous recombination pathway that is critical in epithelial tumor cell lines (30, 31). The type and frequency of DNA lesions due to cisplatin differ from those produced by melphalan. In contrast to the repair of interstrand cross-links produced by melphalan, repair of cisplatin interstrand cross-links does not involve the formation of DNA double-strand breaks (32, 33). The mechanisms for the differences in inhibition of repair of melphalan and cisplatin-induced interstrand cross-links warrant additional investigation. There was no difference in the DNA-PK_{CS} level after drug treatment, and therefore this cannot account for the lack of synergy found with gefitinib and melphalan.

The mechanism by which gefitinib might inhibit the nonhomologous end-joining recombination pathway is unclear. A study with the antibody C225 directed against EGFR demonstrated a physical interaction between the EGFR and DNA-PK_{CS} (23). The functional significance of this interaction is unclear. A study using a combination of radiation and C225 demonstrated an alteration in the subcellular distribution of DNA-PK with an increase in cytosolic levels and a decrease in nuclear DNA-PK levels (34), whereas other studies have shown a reduction in DNA-PK levels after prolonged exposure to gefitinib (35). EGFR has been shown to directly interact with a variety of cellular proteins, and this may be an important factor in the activity of EGFR-inhibitory strategies.

There is an important need to define the optimal schedule of administration of anticancer drugs with EGFR inhibitors as well as identifying the agents with which these synergies are seen. A study of gefitinib in colon cancer cell lines found a synergistic effect on chemosensitivity and removal of DNA adducts when oxaliplatin was followed by gefitinib; scheduling of oxaliplatin followed by gefitinib resulted in an additive effect at best (36). Interestingly, the synergistic effects of gefitinib and the fluoropyrimidine derivative capecitabine were observed when gefitinib administration preceded drug exposure. Pretreatment with gefitinib reduced cell proliferation and consequently resulted in a 40-fold reduction in the enzyme thymidylate synthase, a key target of fluoropyrimidines (37). Recent clinical evidence suggests that irinotecan-resistant colon cancer can be successfully treated in a cohort of patients with a combination of the EGFR-inhibitory antibody C225 and irinotecan (11).

In conclusion, gefitinib modulates the activity of cisplatin and etoposide by a direct effect on the repair of chemotherapy-induced DNA lesions. These results provide a rationale for additional characterization of the mechanisms of these interactions to inform additional therapeutic trials of EGFR inhibitors. It will be critical to investigate these interactions in a variety of cancer cell lines. Understanding the mechanism of the interaction between EGFR inhibition and chemotherapy will be important in devising novel schedules and combinations for testing in the clinic.

ACKNOWLEDGMENTS

We thank Rob Stein for helpful discussions.

REFERENCES

1. Salomon DS, Brandt R, Ciardiello F, Normanno N. Epidermal growth factor-related peptides and their receptors in human malignancies. Crit Rev Oncol Hematol 1995;19:183–232.

2. Yarden Y, Sliwkowski MX. Untangling the erbB signaling network. Nat Rev Mol Cell Biol 2001;2:127–37.

3. Schlessinger J. Cell signaling by receptor tyrosine kinases. Cell 2000;103:211–25.

4. Fox SB, Smith K, Hollyer J, Greenall M, Hastrich D, Harris AL. The epidermal growth factor receptor as a prognostic marker: results of 370 patients and review of 3009 patients. Breast Cancer Res Treat 1994;29: 41–9.

5. Ciardiello F, Tortora G. A novel approach in the treatment of cancer: targeting the epidermal growth factor receptor. Clin Cancer Res 2001; 7:2958–70.

6. Slichenmyer WJ, Fry DW. Anticancer therapy targeting the erbB family of receptor tyrosine kinases. Semin Oncol 2001;28(Suppl 16): 67–79.

7. Morin MJ. From oncogene to drug: development of small molecule tyrosine kinase inhibitors as anti-tumor and anti-angiogenic agents. Oncogene 2000;19:6574–83.

8. Sridhar SS, Seymour L, Shepherd FA. Inhibitors of epidermal-growth-factor receptors: a review of clinical research with a focus on non-small-cell lung cancer. Lancet Oncol 2003;4:397–406.

9. Ciardiello F, Caputo R, Bianco R, et al. Antitumor effect and potentiation of cytotoxic drugs activity in human cancer cells by ZD1839 (Iressa), an epidermal growth factor receptor-selective tyrosine kinase inhibitor. Clin Cancer Res 2000;6:2053–63.

10. Ciardiello F, Caputo R, Troiani T, et al. Antisense oligonucleotides targeting the epidermal growth factor receptor inhibit proliferation, induce apoptosis, and cooperate with cytotoxic drugs in human cancer cell lines. Int J Cancer 2001;93:172–8.

11. Cunningham D, Humblet Y, Siena S, Khayat D, Bleiberg H, Santoro A, Bets D, Mueser M, Harstrick A, Verslype C, Chau, I, Van Cutsem E. Cetuximab monotherapy and cetuximab plus irinotecan in irinotecan-refractory metastatic colorectal cancer. N Engl J Med. 2004 351(4):337–45.

12. Skehan P, Storeng R, Scudiero D, et al. New colorimetric cytotoxicity assay for anticancer-drug screening. J Natl Cancer Inst (Bethesda) 1990;82:1107–12.

13. Tallarida RJ. Drug synergism: its detection and applications. J Pharmacol Exp Ther 2001;298:865–72.

14. Spanswick VJ, Hartley JM, Ward TH, Hartley JA. Measurement of drug-induced interstrand crosslinking using single-cell gel electrophoresis (Comet) assay. In: Brown R, Boger-Brown U, editors. Methods in molecular medicine. Vol 28. Cytotoxic drug resistance mechanisms. Totowa, NJ: Humana Press; 1999:143–54.

15. Hartley JM, Spanswick VJ, Gander M, et al. Measurement of DNA cross-linking in patients on ifosfamide therapy using the single cell gel electrophoresis (comet) assay. Clin Cancer Res 1999;5:507–12.

16. Olive PL, Banath JP, Durand RE. Heterogeneity in radiation-induced DNA damage and repair in tumour and normal cells measured using the "comet" assay. Radiat Res 1990;122:86–94.

17. Sirotnak FM, Zakowski MF, Miller VA, Scher HI, Kris MG. Efficacy of cytotoxic agents against human tumor xenografts is markedly enhanced by coadministration of ZD1839 (Iressa), an inhibitor of EGFR tyrosine kinase. Clin Cancer Res 2000;6:4885–92.

18. Moasser MM, Basso A, Averbuch SD, Rosen N. The tyrosine kinase inhibitor ZD1839 ("Iressa") inhibits HER2-driven signaling and suppresses the growth of HER2-overexpressing tumor cells. Cancer Res 2001;61:7184–8.

19. Zwelling LA, Anderson T, Kohn KW. DNA-protein and DNA interstrand cross-linking by cis- and trans-platinum(II) diamminedichloride in L1210 mouse leukemia cells and relation to cytotoxicity. Cancer Res 1979;39:365–9.

20. Boulton S, Kyle S, Durkacz BW. Mechanisms of enhancement of cytotoxicity in etoposide and ionising radiation-treated cells by the protein kinase inhibitor wortmannin. Eur J Cancer 2000;36:535–41.

21. Xu W, Liu L, Smith GC, Charles G. Nitric oxide upregulates expression of DNA-PKcs to protect cells from DNA-damaging antitumour agents. Nat Cell Biol. 2000; 2:339–45.

22. Benhar M, Engelberg D, Levitzki A. Cisplatin-induced activation of the EGF receptor. Oncogene 2002;21:8723–31.

23. Bandyopadhyay D, Mandal M, Adam L, Mendelsohn J, Kumar R. Physical interaction between epidermal growth factor receptor and DNA-dependent protein kinase in mammalian cells. J Biol Chem 1998; 273:1568–73.

24. Huang SM, Li J, Armstrong EA, Harari PM. Modulation of radiation response and tumor-induced angiogenesis after epidermal growth factor receptor inhibition by ZD1839 (Iressa) Cancer Res 2002;62: 4300–6.

25. Janmaat ML, Kruyt FA, Rodriguez JA, Giaccone G. Response to epidermal growth factor receptor inhibitors in non-small cell lung cancer cells: limited antiproliferative effects and absence of apoptosis associated with persistent activity of extracellular signal-regulated kinase or Akt kinase pathways Clin Cancer Res 2003;9:2316–26.

26. Critchlow SE, Jackson SP. DNA end-joining: from yeast to man. Trends Biochem Sci 1998;23:394–8.

27. Hoeijmakers JH. Genome maintenance mechanisms for preventing cancer. Nature 2001;411:366–74.

28. Adachi N, Suzuki H, Iiizumi S, Koyama H. Hypersensitivity of nonhomologous DNA end-joining mutants to VP-16 and ICRF-193: implications for the repair of topoisomerase II-mediated DNA damage. J Biol Chem 2003;278:35897–902.

29. Durant S, Karran P. Vanillins: a novel family of DNA-PK inhibitors. Nucleic Acids Res 2003;31:5501–12.

30. Wang ZM, Chen ZP, Xu ZY, et al. In vitro evidence for homologous recombinational repair in resistance to melphalan. J Natl Cancer Inst (Bethesda) 2001;93:1473–8.

31. Panasci L, Xu ZY, Bello V, Aloyz R. The role of DNA repair in nitrogen mustard drug resistance. Anticancer Drugs 2002;13:211–20.

32. De Silva IU, McHugh PJ, Clingen P, Hartley JA. Defining the roles of nucleotide excision repair and recombination in the repair of DNA interstrand cross-links in mammalian cells. Mol Cell Biol 2000;20: 7980–90.

33. McHugh PJ, Clingen P, Hartley JA, Inusha U, De Silva P. Defects in interstrand cross-link uncoupling do not account for the extreme sensitivity of ERCC1 and XPF cells to cisplatin. Nucleic Acids Res 2002;30:3848–56.

34. Huang S-M, Harari PM. Modulation of radiation response after epidermal growth factor receptor blockade in squamous cell carcinomas: inhibition of damage repair, cell cycle kinetics, and tumor angiogenesis. Clin Cancer Res 2000;6:2166–74.

35. Magne N, Fischel JL, Tiffon C, et al. Molecular mechanisms underlying the interaction between ZD1839 ('Iressa') and cisplatin/5-fluorouracil. Br J Cancer 2003;8:585–92.

36. Xu JM, Azzariti A, Severino M, Lu B, Colucci G, Paradiso A. Characterization of sequence-dependent synergy between ZD1839 ("Iressa") and oxaliplatin. Biochem Pharmacol 2003;66:551–63.

37. Magne N, Fischel JL, Dubreuil A, et al. ZD1839 (Iressa) modifies the activity of key enzymes linked to fluoropyrimidine activity: rational basis for a new combination therapy with capecitabine. Clin Cancer Res 2003;9:4735–42.